Chemical Biology as an Engineering Framework for Next-Generation Biomaterials

Ryan Gharios

A dissertation

submitted in partial fulfillment of the

requirements for the degree of

Doctor of Philosophy

University of Washington
2024

Reading Committee:

Cole DeForest, PhD, Chair

Elizabeth Nance, PhD

Jorge Marchand, PhD

Program Authorized to Offer Degree:

Department of Chemical Engineering

University of Washington

Abstract

Chemical Biology as an Engineering Framework for Next-Generation Biomaterials

Ryan Gharios

Chair of the Supervisory Committee:
Cole DeForest
Department of Chemical Engineering

Chemical biology-based frameworks integrate principles from chemistry and biology to develop a better understanding of and better control over biological systems. Advances in this space have revolutionized how pharmaceutical companies develop new therapeutics, or how basic researchers investigate the minute aberrances that cause disease. Chemical biology enables such directions because it imparts modularity and (re)configurability into what has historically been a descriptive science. In this thesis, I report the development of a semi-synthetic protein functionalization and purification scheme through atypically split inteins. The method allows the installation of virtually any synthetic cargo on the N-terminus of proteins-of-interest in a single step. Second, I introduce a novel framework for the engineering of an exhaustive set of 17 distinct YES/AND/OR logical operators, with three orthogonal proteases as input. By genetically encoding these topologies rather than synthetically assembling them, we can rapidly engineer bespoke architectures that correspond to sophisticated logical operators. This autonomous molecular compilation-based approach holds promise in applications such as controlled release

and biosensing. Third, I demonstrate an extension of the approach's applicability beyond model protein cargos by applying logical operators to a diverse class of proteins that span different functional categories. I also lay the groundwork for a diversified set of inputs that can be genetically encoded into our bespoke topologies. These advances showcase the promise of chemical biology as a highly enabling engineering framework for the synthesis and user-directed modification of next-generation biomaterials endowed with true biocomputational promise.

TABLE OF CONTENTS

TABLE OF FIGURES

ACKNOWLEDGEMENTS

Thank you to my committee for your mentorship, time, and energy. Your input was essential to the development and refinement of this thesis. Cole – you are an inspirational scientist and advisor; thank you for teaching me how to identify and conduct high-impact science with chutzpah, and how to balance that with a zest for life and the outdoors. Elizabeth – thank you for your generosity with your time and our chats on academia and management; I am grateful for your mentorship. Jorge – thank you for your unwavering intellectual curiosity, ideas, time, and, most of all, for your friendship. I am also equally indebted to my mentors outside of the lab and the confines of this document, specifically, Dr. John Berg, Dr. Tommy Wood, and Barry Wall. You taught me how to be a better researcher and teacher.

I have been blessed to work alongside incredibly talented undergraduate students – Annabella Li, Sarina Vafa, Abigail Garcia, and Francesca Abraham – whose energy and thirst for knowledge kept me inspired throughout my doctoral studies. I cannot wait to see what you accomplish throughout your careers.

I am also grateful for my endlessly supportive (and scientist extraordinaire) partner, my research collaborators, as well as all the amazing friends I met in graduate school (inside and outside of the lab). This experience would have been nowhere near as enriching had it not been for you.

Most of all, thank you to my parents for teaching me grace under pressure. You went through the most extenuating circumstances imaginable in the last five years and handled it with class. I would not have completed this thesis had it not been for your support and constant inspiration.

CHAPTER 1: INTRODUCTION AND BACKGROUND

Adapted from Gharios, R., Francis, R.M., DeForest, C.A. Chemical and biological engineering strategies to make and modify next-generation hydrogel biomaterials. *Matter* **6** (12), 4195-4244 (2023). DOI: 10.1016/j.matt.2023.10.012

Abstract

There is a growing interest in the development of technologies to probe and direct *in vitro* cellular function for fundamental organoid and stem cell biology, functional tissue and metabolic engineering, and biotherapeutic formulation. Recapitulating many critical aspects of the native cellular niche, hydrogel biomaterials have proved to be a defining platform technology in this space, catapulting biological investigation from traditional two-dimensional (2D) culture into the 3D world. Seeking to better emulate the dynamic heterogeneity characteristic of all living tissues, global efforts over the last several years have centered on upgrading hydrogel design from relatively simple and static architectures into stimuli-responsive and spatiotemporally evolvable niches. Toward this end, advances from traditionally disparate fields, including bioorthogonal click chemistry, chemoenzymatic synthesis, and DNA nanotechnology, have been co-opted and integrated to construct 4D-tunable systems that undergo preprogrammed functional changes in response to user-defined inputs. In this review, we highlight how advances in synthetic, semisynthetic, and bio-based chemistries have played a critical role in the triggered creation and customization of next-generation hydrogel biomaterials. We also chart how these advances stand to energize the translational pipeline of hydrogels from bench to market and close with an outlook on outstanding opportunities and challenges that lay ahead.

1.1. Introduction

Historically, cellular biology has been interrogated in the context of two-dimensional (2D) cell culture milieux, comprised primarily of aphysiologically stiff substrates (e.g., glass, polystyrene dishes). While potentially revealing, such environments fail to mimic many essential aspects of the native cellular niche (e.g., dimensionality, viscoelasticity). Now intuitively recognized, many insights garnered through such experiments translate poorly, if at all, when moved to downstream *in vivo* studies. A second generation of investigation sought to leapfrog these shortcomings by exploiting hydrogels—water-swollen polymeric networks—for 3D cell encapsulation.[1,2] Although these early efforts permitted extended cell culture in uniform materials with bulk characteristics closer to tissue than tissue-culture plastic, such constructs were static, monocellular, and isotropic. Recognizing that the tissue microenvironment is dynamically heterogeneous in its physicochemical composition, cellular makeup, and structured architecture, the third and current generation of cell culture platforms has focused on biomaterials whose properties can be customized on demand, often in both 3D space and time (i.e., 4D), across a variety of scales.[3] Toward this goal, materials scientists, chemists, and biologists have harnessed and driven diverse chemical and biological advances to engineer exquisitely modifiable and stimuli-responsive hydrogel biomaterials (**Figure 1.1**).

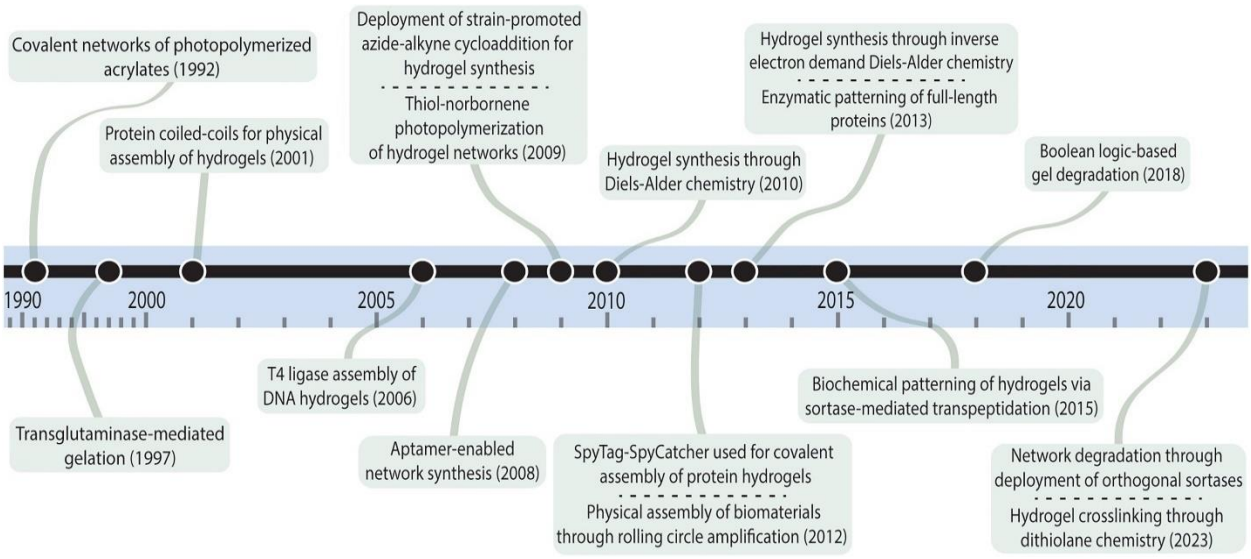

Figure 1.1*:* Key milestones in the deployment of new chemistries for hydrogel biomaterial synthesis

Key milestones marking the first instance of the deployment of a particular chemistry for the synthesis of a hydrogel biomaterial.

Beyond spatial and/or temporal initiation of gelation, systems can be endowed with defined macroarchitecture, shape memory, reversible mechanics/viscoelasticity, and anisotropic biochemical signaling, all of which enable spatiotemporal control of cell fate and behavior. Clearly, this encoded dynamism holds immense potential for different fields within biomedicine.[4,5] Importantly for biomaterial scientists and engineers, variable use cases call for dramatically different sets of properties. Within the same application space, developing a hydrogel matrix that seeks to capture bone tissue morphogenesis will require a resultant set of physicochemical properties that is qualitatively different than that geared for kidney or lung tissue engineering. Furthermore, moving our lens beyond tissue engineering proper, developing hydrogel matrices as therapeutic depots will also call for a substantially different set of design parameters; within this niche itself, whether a vehicle harbors synthetic drugs or living cells is another critical factor to consider.

As it stands, there is no shortage of problems to address, each requiring a bottom-up solution that is exquisitely tailored to meet it. (Bio)chemical advances—synthetic, semisynthetic, or biological in nature—are at the forefront of these exciting developments in biomaterials science. Through this review, we will discuss the most common, most promising, and recently emerging reaction schemes to make and modify hydrogel biomaterials—including both those that proceed spontaneously and those that can be exogenously triggered—from polymeric, small-molecule, protein, DNA, and other biomolecular precursors. In drafting this review, we found that charting the development of hydrogel biomaterial science and engineering was best tackled through the lens of understanding network crosslinking. By taking that as our starting point, we segmented the field into three main areas. Specifically, we looked at synthetic organic networks and define those as hydrogels that are crosslinked through routine organic-type reactions. We also ventured beyond the fume hood and elaborated upon protein- and peptide-enabled chemistries that are themselves gaining much more traction as viable crosslinking strategies. Lastly, we expanded upon DNA-enabled methods and discuss how these have also gone from an academic curiosity into a full-fledged engineering platform, both for hydrogels and other materials. We then frame this discussion within the context of translational promise for these platform technologies and expand upon the challenges faced by hydrogel biomaterials en route to the clinic. It is our hope that this work will encourage researchers to probe new questions enabled by truly next-generation biomaterials and impress the notion that different chemical and biochemical platforms can be tuned and optimized to very particular applications at hand.

A key challenge in providing a comprehensive review and perspective of the field lies in its variety. Given the breadth of the hydrogel biomaterials space and the numerous strategies that

have been developed for the creation and post-synthetic modification of networks, we categorize past efforts based on the nature of the assembly (i.e., covalent vs. non-covalent crosslinking) and the extent of user control that it affords (i.e., spontaneous vs. triggerable modulation). In so doing, we hope to systematically delineate the relative advantages and disadvantages of each platform in as mutually exclusive and collectively exhaustive a method as possible.

1.2. Chemical synthesis of hydrogel biomaterials

Biomaterials science has greatly benefitted from the co-opting of chemistries initially deployed for different applications and then re-purposed for materials development. These manifold reaction platforms have proved to be largely agnostic with respect to the nature of the underlying material, enabling assembly of networks from a wide variety of starting reactants. Broadly, hydrogel materials can be synthetic, naturally derived, or a hybrid of the two. Synthetic hydrogels are made up of polymer chains that are synthetic themselves, including poly(ethylene glycol) (PEG), poly(vinyl alcohol) (PVA), and poly(2-hydroxyethyl methacrylate) (PHEMA). Lacking in biological epitopes in their base form, such materials are bioinert at best, a feature that may or may not be advantageous depending on the use case being considered. Regardless, synthetic networks are readily modifiable, providing a "blank slate" upon which to engineer biological functionality.[6] Alternatively, naturally derived networks consist of biopolymers in the form of polysaccharides (e.g., hyaluronic acid, chitosan, dextran), proteins (e.g., fibrin, collagen, silk fibroin), or DNA. Innately endowed with biocompatibility, naturally derived networks can be sourced directly or recombinantly synthesized.[7] Such off-the-shelf networks (e.g., Matrigel, Geltrex) promote desirable cellular functions including adhesion, spreading, and dynamic matrix remodeling. However, batch-to-batch variability presents obstacles to widespread and

reproducible deployment. An alternative strategy to address this pitfall is to produce these networks in a pristine sequence-specific manner, such as is enabled through recombinant protein expression or DNA assembly via enzymatic, solid-phase, or biological replication-based methods.

Beyond the underlying material, an important design consideration—the focus of this review—is the reaction platform through which the hydrogel is formed, particularly whether the network is held intact through covalent or non-covalent bonds. Furthermore, some material-forming chemistries proceed spontaneously, leading to gelation upon simple mixing of the constituent macromers in solution. Other platforms undergo triggered formation, in that they typically require the action of an extraneous stimulus (e.g., temperature, pH, light) or a combination thereof to initiate the underlying gelation chemistry.

1.2.1. Spontaneous hydrogel formation

Given their simplicity and relative ease of onboarding, hydrogel formation chemistries that proceed spontaneously have become a cornerstone of recent biomaterials research. Classically, these platforms lead to network formation directly upon mixing of the constituent macromers in solution, proving most useful for applications such as cell or biomolecule encapsulation into scaffolds for tissue engineering and drug delivery.

1.2.1.1. Spontaneous gel formation via covalent reaction

1.2.1.1.1. Synthetic organic-based:

Owing to their high degree of tunability, crosslinking schemes that exploit synthetic organic reactions have propelled the field of hydrogel biomaterials forward to a largely unparalleled degree (**Table 1.1**). In fact, through rational modification of the starting macromers and employed gelation chemistry, reaction kinetics, network microarchitecture, and material mechanics/viscoelasticity can be exquisitely controlled. Since these chemistries have been profiled extensively in previous reviews,[8,9] we limit our survey to only the most broadly used and recently developed platforms.

Table 1.1 Comparison of chemical platforms for hydrogel synthesis
Widely used synthetic assembly schemes are compared based on their kinetic profile, biocompatibility, tractability, orthogonality, amenability to spatiotemporal control, and reversibility.

Chemistry	Mechanism	Kinetics	Bio-compatible	Synthetic Tractability	Orthogonality	Amenability to 4D Control	Reversibility	Other notes
SPAAC	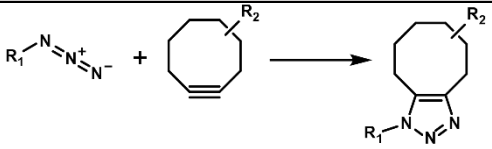	(+)(+)	(+)(+)	Moderate	Fair; may cross-react with thiols	Fair	Irreversible	Strained alkynes prone to dimerization
Diels-Alder	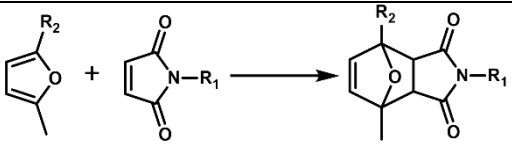	(+)	(+)(+)	Moderate	Fair; may cross-react with thiols	No	Reversible	Highly acid-sensitive until recent reagent optimization
Inverse-Electron Demand Diels-Alder	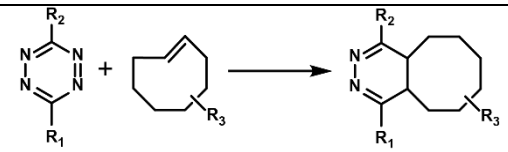	(+)(+)	(+)(+)	Moderate	Good	Fair	Irreversible	Highly acid-sensitive until recent reagent optimization
Oxime Ligation	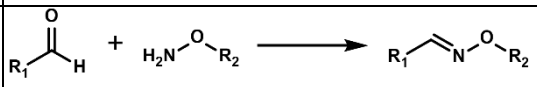	(+)(+)	(-)	Good	Good	Yes	Reversible	Base-catalyzed reaction until recent iterations
Thiol-Michael Addition		(+)(+)	(+)(+)	Good	Poor; cross-reacts with thiols	Yes	Reversible	Driving force for the reaction is dictated by the choice of vinyl group.
Native Chemical Ligation	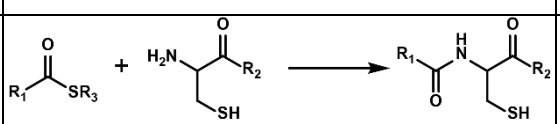	(-)	(-)	Moderate	Poor; cross-reacts with thiols	No	Reversible	Oxo-ester counterpart of this platform obviates the redox-dependency

								of the platform
CBT-Cys	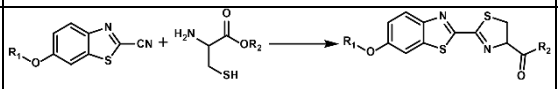	(+)(+)	(+)(+)	Moderate	Poor; cross-reacts with thiols	No	Irreversible	Recently engineered to be redox-activatable
KAT Ligation	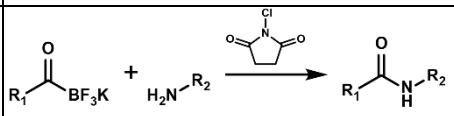	(+)(+)	(+)(+)	Good	Good	No	Reversible	Kinetics are strongly pH-dependent; reaction is much slower at physiological pH levels
Thiol-Halide	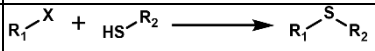	(+)(+)	(+)	Good	Poor; cross-reacts with thiols	No	Irreversible	Halide groups are easily synthetically tractable.
Thiol-Methylsulfone	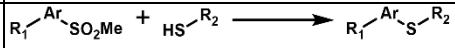	(+)	(+)(+)	Moderate	Poor; cross-reacts with thiols	No	Irreversible	Moderate and tunable platform kinetics render it a suitable intermediate between different thiol-Michael chemistries.

Step-growth polymerizations have become the most prominent synthetic crosslinking chemistries, whereby complementary reactive groups react specifically in a one-to-one manner. Directly contrasting most chain-growth chemistries in which reaction is propagated through active chemical radicals, such step-growth chemistries generally proceed in a radical-free manner and lead to a more uniform hydrogel microstructure (**Figure 1.2**). Not only does this hold immediate implications for the creation of more structurally sound therapeutic depots or extracellular matrix (ECM) mimics, it also translates directly to adjacent avenues such as bioprinting where ultimate network integrity is predicated on the platform chemistry deployed.[10] Lastly, many step-growth chemistries can be considered "click,"[11] a designation that is limited to reactions that are specific, high yielding, generate non-toxic products, and proceed in aqueous or otherwise benign solvents.

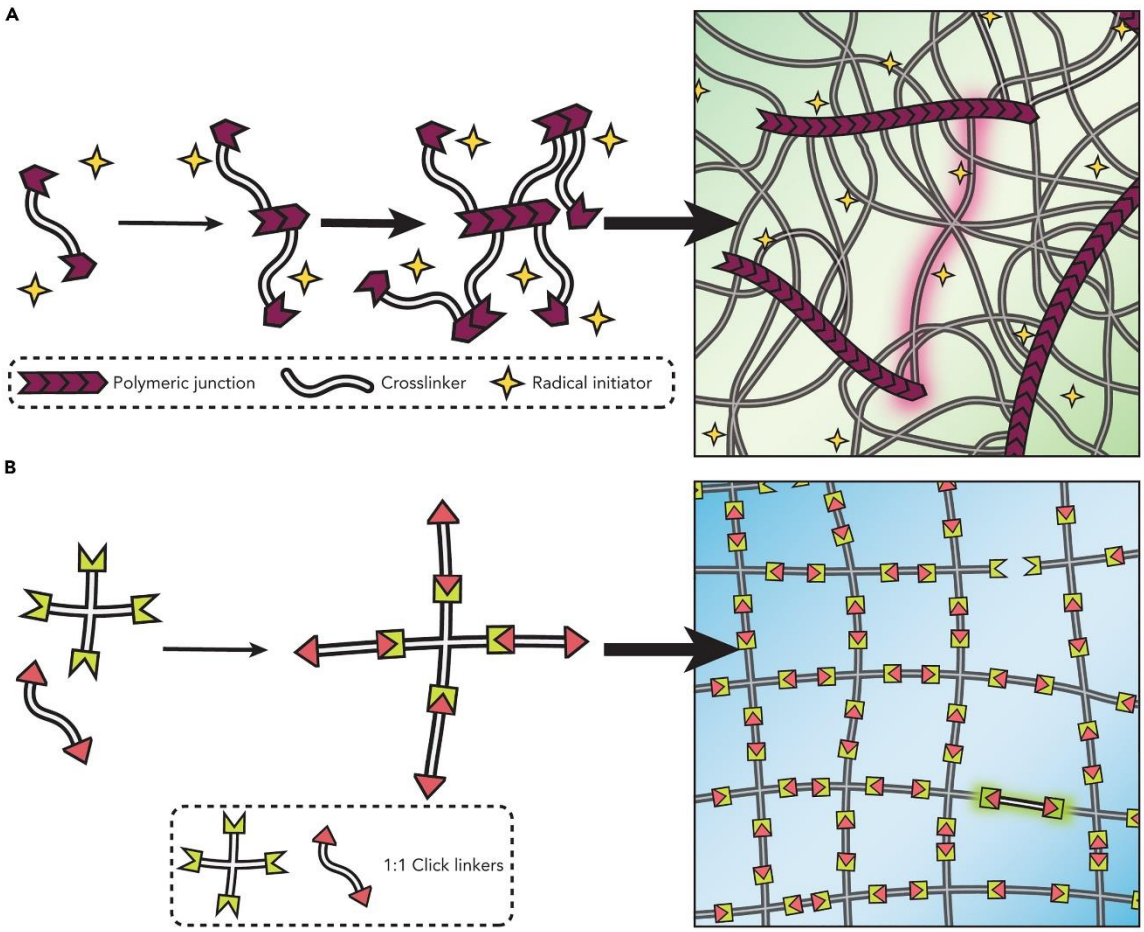

Figure 1.2: Chain-growth vs. step-growth chemistries for hydrogel network synthesis

(A) Radical-initiated chain-growth crosslinking results in a molecularly undefined and spatially heterogeneous network.
(B) Click chemistry-mediated step-growth networks spontaneously form more homogeneous and well-defined mesh structures, typically without the need for initiators.

Strain-promoted azide-alkyne cycloaddition (SPAAC) represents a now-classic example of a click platform that has been co-opted successfully for the generation of hydrogel networks. Developed by the Bertozzi group as a non-toxic alternative to the conventional copper-catalyzed cycloaddition (CuAAC),[12] ring-induced strain encoded within the alkyne moiety drives the reaction forward under physiological conditions and without the metal catalyst. Additionally, modifications to the strained-alkyne structure can directly modulate resultant kinetics and thereby accommodate use cases with different gelation time requirements. Owing to its limited

cross reaction with chemical moieties on natural biomolecules, the platform found use in and heralded an era of "bioorthogonal click chemistry".[13] Given its potential, it was subsequently co-opted for the cytocompatible synthesis of hydrogel biomaterials. Toward that end, DeForest and Anseth were the first to employ it for the synthesis of cell-laden hydrogels, using multi-armed PEG chains end-functionalized with azide groups and peptide chains capped with DIFO3 cyclooctyne moieties.[14] SPAAC is now broadly used for hydrogel synthesis for a range of applications; for instance, the Haag group harnessed this platform for engineering PEG-based networks crosslinked with acid-labile benzacetal groups, thereby enabling cell capture and subsequent triggered release over a cytocompatible pH range.[15] Additionally, SPAAC-based PEG networks have also shown promise as injectable embolic agents; for example, the Zhong group synthesized routine PEG-based matrices and successfully injected these in the auricular central artery of rabbits, enabling fast-flow blockage without the need for invasive surgical interventions.[16] Promisingly, these gels demonstrated good cytocompatibility and degraded over the span of 2 days, a timeframe that can be shortened or extended based on ultimate crosslinker design.

Similar to SPAAC, Diels-Alder (DA) is another widely used chemistry for cell encapsulation, but with additional avenues for modification afforded through its innate reversibility. DA platforms employ two starting groups—diene- and dienophile-modified macromers—that undergo a 1:1 cycloaddition upon mixing. Broad application of the chemistry was initially limited because of its reliance on acidic conditions to drive the DA reaction forward. Specifically, the first report by the Shoichet group that showcased this chemistry necessitated the reaction of furan- and maleimide-end-functionalized precursors at a pH of 5.5 to enable gelation

at reasonable timescales, precluding their use in cell encapsulation.[17] However, by replacing the furan diene with a more electron-rich methylfuran, the group successfully side-stepped such acid dependence to enable cytocompatible network assembly at a pH level of 7.4 on the order of minutes, and were able to encapsulate five different cancer cell lines, highlighting the portability of the system.[18] Since these foundational reports, the relative ease of onboarding this platform from a synthesis standpoint, coupled with its aforementioned reversibility, have made it a staple in different biomaterial labs looking to recreate near-native cellular environments[19] or develop new therapeutic delivery modalities.[20,21]

The inverse-electron-demand Diels-Alder (IEDDA) reaction has been gaining significant traction as a bioorthogonal crosslinking chemistry since the publication of foundational reports deploying it for *in vivo* cellular labeling[22] and endogenous epitope targeting.[23] First utilized for biomaterial formation by the Anseth group as a synthetically more tractable[24] platform than SPAAC,[25] its reaction involves a tetrazine and an appropriate dienophile group (e.g., norbornene, *trans*-cyclooctene). Specifically, the first proof of concept for this chemistry in a hydrogel context relied on the reaction of PEG macromers end-functionalized with a benzylamino tetrazine with a dinorbornene synthetic peptide, which showed that the approach is highly suitable for network formation, cellular encapsulation, and potential post-synthetic patterning. Stemming from its promising and tunable kinetics, which are readily modulated by rationally introduced modifications to either the tetrazine or the dienophile, the chemistry is rapidly gaining widespread use as a workhorse reaction in manifold chemical biology applications (reviewed elsewhere[26,27]) and as a viable hydrogel crosslinking strategy. Emblematic of the promise of the latter, the Vega group systematically investigated different ratios and multiple substitutions of

the starting tetrazine or norbornene end-functionalized groups and probed for downstream effects in their obtained hyaluronic acid networks. Their study showed direct and straightforward encoding of ultimate hydrogel mechanical properties through easily adjustable starting macromer concentrations, relative stoichiometry, and degree of substitution with photopatternable methacrylic anhydride moieties.[28] The tetrazine-norbornene chemistry was also employed for the creation of hydrolytically degradable alginate hydrogels, which was achieved through oxidation of the polymer backbone prior to gel crosslinking.[29] By controlling this initial extent of oxidation (e.g., unoxidized vs. 5% oxidized), mechanical properties and degradation timescales could be exquisitely controlled by the user.

Oxime ligation[30] is another commonly employed platform for the synthesis of hydrogel biomaterials. It involves the reaction of a hydroxylamine and a carbonyl (e.g., aldehyde, ketone), forming an oxime linkage and a water byproduct. Similar to DA, oxime ligation can be reversed with pH, making it suitable for the creation of dynamically switchable matrices. While early examples of this strategy were hampered by slow gelation times (on the order of hours) at physiological pH,[31] the Becker group found that tuning pH and the aniline catalyst concentration can yield gelation in seconds.[32] This newfound tunability enabled pristine control over network mesh size and modulus based on selected gelation parameters.[33] There are now multiple successful reports of oxime-crosslinked hydrogels, such as for the creation of hyaluronic acid (HA)-based vitreous substitutes[34] and the culture of tumor spheroids.[35]

Thiol-involved reactions also represent a very common route toward hydrogel biomaterial synthesis. In fact, thiols can react with a number of different chemical groups and are found

natively on proteins (i.e., cysteine amino acids), making thiol-based reactions uniquely suited for applications interfacing materials and polypeptides.[36] The most prominent example of such "thiol-X" reactions is the thiol-ene platform,[37] which involves the reaction of a thiol group with an alkene. Classically, the thiol-ene reaction is radical-mediated via photochemical or thermal initiation. While triggering gelation is important given the ensuant spatiotemporal control (a topic discussed at length in a subsequent section), propagating free radicals can be cytotoxic and non-specifically reactive, making such strategies much less attractive for applications that require interfacing with living cells. A powerful workaround is the adoption of a thiol-ene reaction that harnesses the reaction of a thiol with more electron-deficient alkenes (e.g., maleimides, vinyl-sulfones). Referred to as thiol-Michael additions,[38] these reactions are typically base- or nucleophile-catalyzed and progress through anion propagation rather than a free radical. Given these relative advantages, in addition to their powerful kinetics and resultant product stability, such reactions have been widely used for the creation of biomaterials for post-surgical implants,[39] stem cell encapsulation and maintenance,[40] lineage specification,[41] among others.

Less employed but still worthy of note as a synthetic crosslinking platform is "native chemical ligation",[42] which enabled the Messersmith group to generate PEG-based gels from multi-armed macromers functionalized with either an N-terminal cysteine or a thioester,[43] with follow-up work establishing the system's suitability for pancreatic islet cell encapsulation.[44] A subsequent report by the group sought to eliminate the crosslinking chemistry's dependence on reducing conditions, leading to an oxo-ester-mediated reaction rather than the more common thioester.[45]

Still more synthetic organic-based reaction schemes are being developed for spontaneous hydrogel formation, promisingly including the luciferin-inspired cyanobenzothiazole-cysteine (CBT-Cys) reaction,[46] potassium acyltrifluoroborate (KAT) ligation,[47] and alternative thiol-X reactions (e.g., thiol-halide,[48] thiol-epoxy,[49] thiol-methylsulfone[50]).

Summarily, multiple click-type platforms have now been developed for the covalent synthesis of gels. Since each has comparative advantages with regard to different metrics such as kinetics, reversibility, and temperature-dependence, the decision to deploy one or the other should ultimately be made on a use case basis.

1.2.1.1.2. Protein-based:

Protein-enabled chemistries harness platforms evolved by nature to genetically encode recognition and reactivity (**Table 2**). While protein-based interactions are predominantly non-covalent, there exist an increasing number of schemes enabling covalent network formation, most generally based on split-fragment reconstitution.[51] A quintessential example is the SpyTag-SpyCatcher system, developed by the Howarth lab through splitting the fibronectin-binding domain of *Streptococcus pyogenes* prior to rational fragment engineering.[52] Reconstitution is highly energetically favorable upon splitting; protein-protein ligation occurs rapidly through the formation of an isopeptide bond between the lysine 31 on the SpyCatcher protein and aspartate 230 on a short SpyTag peptide. In their seminal work, the Arnold and Tirrell groups exploited SpyTag/SpyCatcher repeating motifs interspaced by telechelic elastin-like polypeptides (ELPs) to engineer fully protein-based covalently assembled networks.[53] Subsequent work by Li employed the selfsame strategy to synthesize protein networks based on globular domains (GB) rather than the telechelic elastin, showcasing the versatility of fragment reconstitution-based

approaches with respect to different forms of protein folds.[54] Moreover, this system was also co-opted by the Niemeyer group to assemble flow biocatalysis hydrogel units; after expressing the two tetrameric enzymes *Lactobacillus brevis* alcohol dehydrogenase (LbADH) and glucose-1-dehydrogenase (GDH) as genetic fusions with either SpyTag or SpyCatcher, component mixing led to hydrogel bioreactor formation at near-quantitative yields without expensive co-factors.[55]

Table 1.2 Comparison of protein-enabled approaches for hydrogel synthesis
Widely used protein-enabled assembly schemes are compared based on their kinetic profile and reversibility. Additional notes regarding the platform are provided when appropriate.

Platform	Mechanism	Kinetics	Reversibility	Other notes
Fragment Reconstitution				
SpyTag – SpyCatcher Ligation	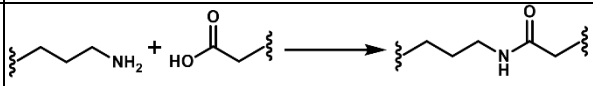	(+)(+)	Irreversible	Newer evolved SpyTag and SpyCatcher variants (e.g., 002 and 003 versions) exhibit enhanced kinetic profiles
SnoopTag – SnoopCatcher Ligation	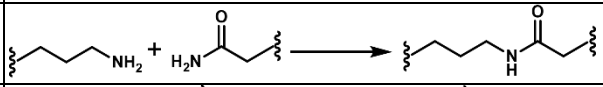	(+)	Irreversible	Challenging to bring the SnoopTag – SnoopCatcher ligation to full completion
GB Tag Ligation	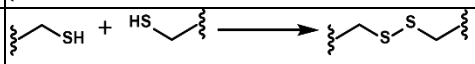	Fair	Reversible	GN and GC fragments may each homo-dimerize, limiting reaction efficiency.
Enzymatic Crosslinking				
Sortase-mediated	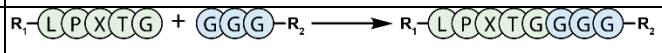	(+)(+)	Reversible	The existence of evolved sortases can enable different mode of reaction fully orthogonally.
Transglutaminase-mediated	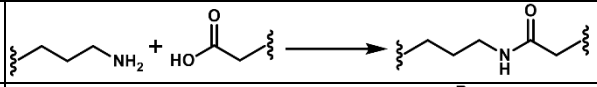	(+)	Irreversible	Reaction kinetics are ultimately dictated by the choice of peptide recognition sequence.
Tyrosinase-mediated	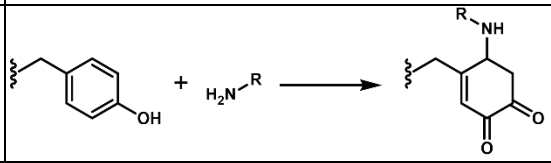	(+)(+)	Irreversible	Anecdotally reported to result in mechanically weak hydrogel networks.
Horseradish Peroxidase-mediated		(+)	Irreversible	Concerns remain over the cytotoxicity of H_2O_2 and the immunological response caused by trace amounts of enzyme.
Lysyl Oxidase-mediated	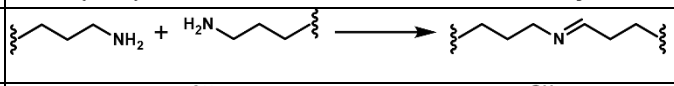	Fair	Irreversible	LOx is found endogenously, enabling straightforward *in situ* crosslinking if required.
Phosphopantetheinyl transferase-mediated	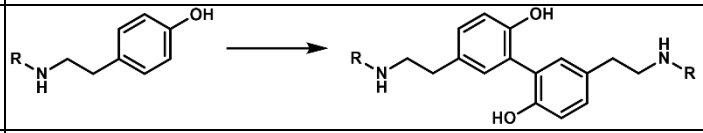	Poor	Irreversible	Requires Coenzyme A as cofactor for crosslinking.
Other Approaches				
Intein Trans-Splicing	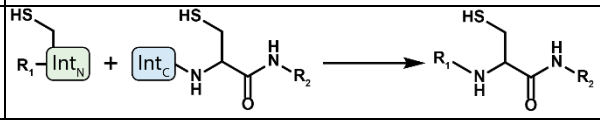	(+)(+)	Irreversible	Requires reducing conditions for splicing and crosslinking to occur; concerns also remain over the toxicity of splice products.

A related strategy uses proteins that are artificially split and maintain a high thermodynamic driving force for spontaneous reconstitution. A prominent example of this approach is demonstrated by the Sun group, who supplemented a SpyTag- and SpyCatcher-based strategy with split GFP reconstitution to create highly tunable protein-based networks, analogous to synthetic hydrogels formed via step-growth polymerization of multifunctional macromers (**Figure 1.3**).[56]

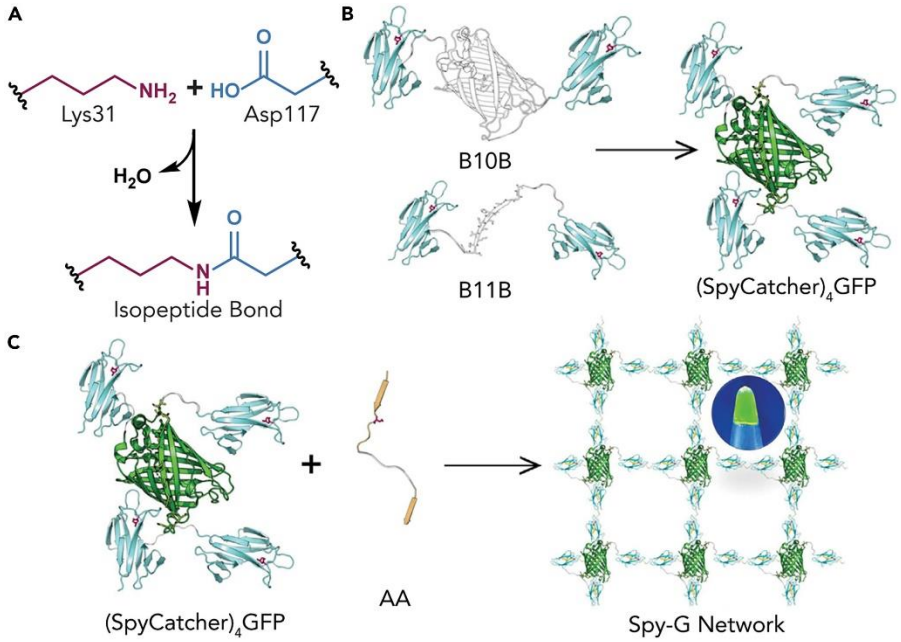

Figure 1.3: Hydrogel synthesis through SpyTag-SpyCatcher ligation and split GFP reconstitution

(A) SpyTag and SpyCatcher react spontaneously upon mixing and form an isopeptide bond between Lys31 on SpyCatcher and Asp117 on SpyTag.
(B) Star-like proteins bearing four reactive SpyCatchers physically assemble through spontaneous reconstitution of split GFP. Adapted with permission from Yang et al.[56] Copyright 2020, Elsevier.
(C) Covalent crosslinking of four-arm star-like protein macromers with difunctional SpyTag reagents yields a "Spy-G" hydrogel. Reproduced with permission from Yang et al.[56] Copyright 2020, Elsevier.

Moving forward, the main limiting factor in developing networks with added functionality lies in the availability of amenable split protein pairs. Indeed, newer splits are continuously being evolved to hold better kinetic and thermodynamic assembly profiles[57] or proceed through a

reaction that is orthogonal to existing systems.[58] However, as our understanding of protein design develops,[59] we anticipate that the development of computationally generated *de novo* proteins[60] will expand the palette of genetically encoded click-type chemistries that can induce gelation, both alone and in tandem with other orthogonal pairs.

Although relatively underexplored in biomaterials science, another potentially powerful approach exploits inteins to assemble protein-based networks. Inteins consist of autocatalytic protein processing domains that assemble, link their concomitant flanking "extein" proteins, and excise themselves out without the need for an exogenous cofactor or catalyst.[61] While harnessed extensively in the protein-protein ligation and semisynthesis sphere, inteins hold exciting potential toward the creation of entirely protein-based covalent materials. One example was demonstrated by the Chen group, who expressed trimeric CutA proteins as *Nostoc punctiforme* (Npu) intein fusions to rapidly generate pH- and temperature-stable networks for enzyme encapsulation.[62] A growing library of orthogonal and well-behaved intein pairs[63] with robust reaction profiles may enable hydrogel assembly with increasing levels of biological functionality.

1.2.1.2. Spontaneous gel formation via non-covalent reaction

1.2.1.2.1. Synthetic organic-based

While covalent linkage of macromolecular precursors yields stably persistent hydrogels, utilization of non-covalent reaction schemes to create hydrogel networks uniquely affords network dynamism; physically assembled gels can be formed and modified in a user-directed fashion, often including in response to applied shear.[64,65]

A widespread example of non-covalent synthetic reactions utilized for biomaterial formation is that of host-guest chemistries—a supramolecular chemistry in which structural relationships define the assembly of two species—best typified by a cyclodextrin host and a concomitant guest molecule. A notable early application of a host-guest gelation strategy was demonstrated by the Stoddard group, physically assembling a poly(acrylic acid) network through cyclodextrin/azobenzene interaction,[66] whereupon the *trans*-azobenzene isomer—but not the ultraviolet (UV) light-generated *cis* form—sets into the hydrophobic cyclodextrin cavitand. The Burdick group extensively characterized HA-based networks physically crosslinked through a cyclodextrin host and an adamantane guest (**Figures 1.4A and 1.4B**).[67] Variation in starting macromer concentration, chemical modifications to adamantane, as well as the host-to-guest molar ratio, enabled broad macroscopic tunability including erosion rate, shape memory, and gel stiffness. The group also exploited the effects of adamantane-cyclodextrin complexation on the affinity of HA toward encapsulated small molecules, enabling the tunable and sustained release of model small-molecule drugs.[68]

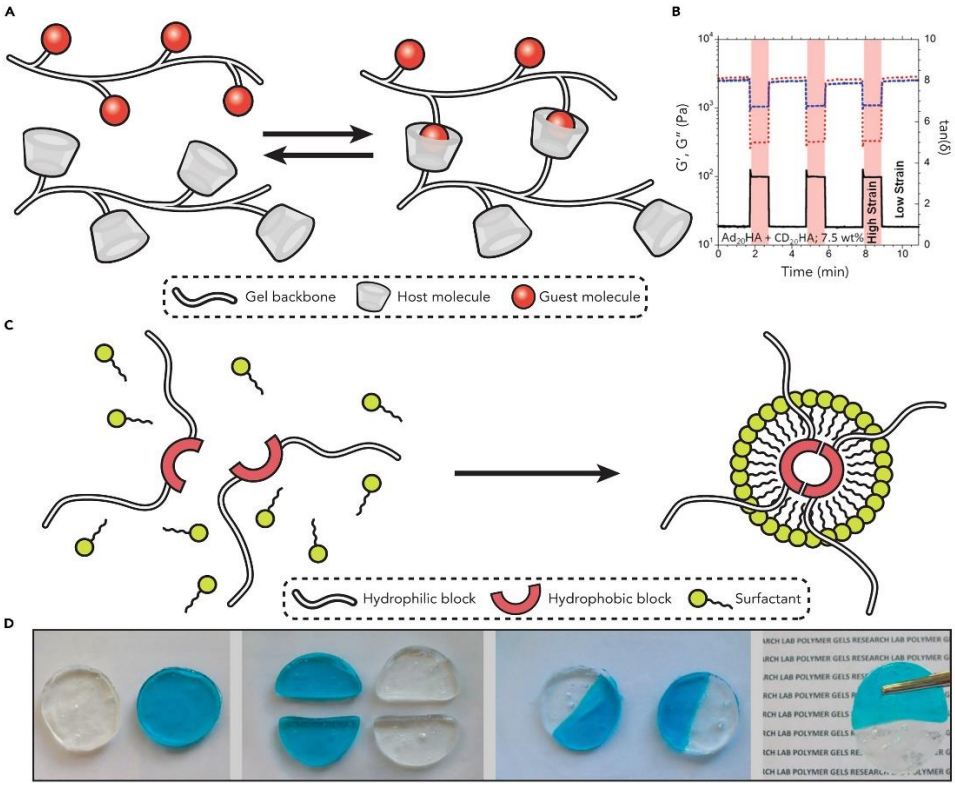

Figure 1.4: Assembly of non-covalently linked hydrogel networks through host-guest chemistry and hydrophobic-hydrophobic interactions

(A) Host-guest chemistries enable the formation of physically and reversibly crosslinked hydrogels.
(B) Demonstration of self-healing properties of a host-guest crosslinked hyaluronic acid-based hydrogel. White and red regions represent cyclic deformation at 0.5% and 250%, respectively. Storage and loss modulus are recovered after each cycle. Reproduced with permission from Rodell et al.[67] Copyright 2013, The American Chemical Society.
(C) Gel fragments formed by hydrophobic association undergo physical grafting when placed in direct contact. Reproduced with permission from Tuncaboylu et al.[69] Copyright 2011, The American Chemical Society.

Beyond cyclodextrin host-based physical networks, a newer generation of non-covalent gels exploits curcubit[n]uril (CB[n]) as host. While not yet as widespread as cyclodextrins in pharmaceutical formulations,[70] CB[n] hosts offer wider tunability and high affinities toward specific guest molecules, wherein binding usually occurs at or near the diffusion limit.[71] The Webber group extensively characterized CB[7] host-based PEG hydrogel formulations, where the expanded host-guest affinity range afforded orders-of-magnitude changes in macroscopic properties (e.g., stress relaxation, solute release).[72] These elevated affinities have made possible

the use of supramolecular chemical methods of hydrogel assembly to "home in" on a target location within the body to deliver a therapeutic payload. The Webber lab has successfully demonstrated that, provided spatial localization of a host-modified hydrogel in a specific tissue, intravenously delivered guest-functionalized therapeutics will preferentially accumulate at the host site and yield site-specific drug targeting.[73]

Hydrogels can also be physically assembled through hydrophobic-hydrophobic interactions. For example, the Okay group demonstrated the assembly of physically tough, highly stretchable, and self-healing hydrogels through copolymerization of large hydrophobic monomers (i.e., stearyl methacrylate, dodocyl acrylate) with a hydrophilic acrylamide monomer in a micellar solution of sodium dodecyl sulfate with sodium chloride (**Figures 1.4C and 1.4D**).[69] While the conditions necessary for network assembly (e.g., required surfactant, macromer interface hydrophobicity) are not the most suitable for bio-focused applications, the study highlighted the promise of tuning and optimizing hydrophobic-hydrophobic associations to control resultant macroscopic properties of physically crosslinked hydrogels. Specifically, alkyl side-chain length on the hydrophobic monomer and surfactant concentration were both found to crucially affect self-healing efficiency.[74]

Trends in non-covalent assembly schemes closely mirror those observed in chemical crosslinking methodologies, whereupon newer systems with increased breadth of tunability and applicability are continuously being developed.

1.2.1.2.2. Protein-based

Protein-enabled chemistries permitting non-covalent gelation are numerous and well characterized compared to their covalent counterparts. Many interactions proceed through biorecognition, wherein complementary polypeptide sequences recognize and assemble into a thermodynamically favorable structure that yields a physically stabilized network (**Figure 1.5A**).

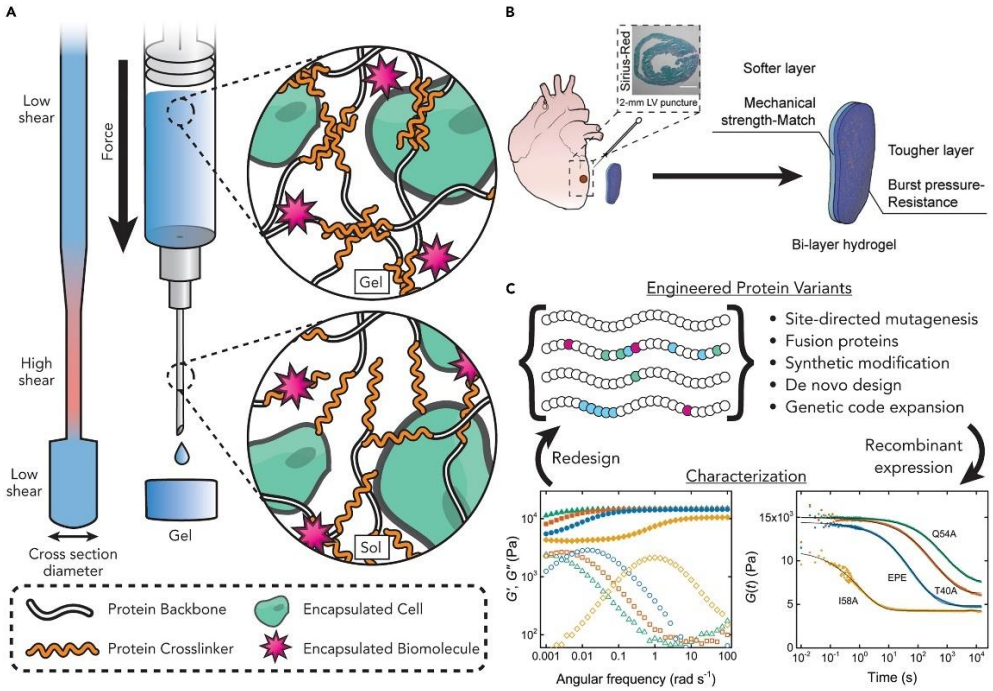

Figure 1.5: Injectable and printable recombinant protein hydrogels

(A) Shear-thinning behavior of the physical network and superior biocompatibility of many recombinant protein-based hydrogels make them attractive targets for injectable therapies and extrusion-based bioprinting applications. As these materials are pushed through narrow passages, increased shear stress causes reversible liquefication, carrying along any cellular or biochemical cargo.

(B) A burst-resistant bilayer patch uses two engineered variants of a shear-thinning leucine zipper-based hydrogel. The inner layer imitates the mechanical properties of softer native heart tissue, while the outer layer provides structural stability. Burst resistance was modulated by recombinant introduction of mussel foot protein domains Mefp3 and Mefp5 into the leucine zipper crosslinker, generating a chimeric set with an array of mechanical properties. Adapted with permission from Jiang et al.[75] Copyright 2022 Wiley-VCH.

(C) Recombinant protein hydrogels uniquely allow iterative and high-throughput screening of physicochemical and biological properties through classic and next-generation protein engineering techniques. Plots adapted from permission from Dooling and Tirrell.[76] Copyright 2016 The American Chemical Society.

Seminal work by the Tirrell and Kopeček groups established the coiled-coil motif as a widely used biorecognition module and crosslink of protein hydrogels[77] and hybrid synthetic-protein networks.[78] As their name implies, coiled coils are constituted of two or more α helix motifs that recognize and assemble into a supercoil maintained by hydrophobic interactions at the interface.[79] Coiled-coil-based networks constitute most protein-enabled physical assembly chemistries, with coil domains from distinct protein origins deployed for the design of a variety of networks. This prompted a suite of investigations into the molecular engineering principles underpinning coiled-coil folding to elucidate how systematic primary sequence variation scales and translates into macroscopic changes at the network scale.[76,80] Emblematic of the strategy, a recent study by the Zhong group makes use of a recombinantly produced coiled-coil crosslinked hydrogel to engineer bilayer cardiac patches capable of supporting cardiomyocyte proliferation, fibrosis reduction, and increased blood pumping capacity in two separate murine disease models (**Figure 1.5B**).[75]

Beyond coiled-coil biorecognition, the Heilshorn group introduced the mixing-induced, two-component hydrogel (MITCH) system for the creation of mechanically soft and fully recombinant scaffolds, originally to encapsulate, maintain, and differentiate neural stem cells.[81] MITCH systems are physically assembled from a seven-repeat WW domain from C43 (C7) and a cognate nine-repeat proline-rich sequence (P9), with heterologously expressed C7 and P9 reacting with 1:1 stoichiometry from liquid precursors to form a stable gel. In contrast to other protein-based biorecognition chemistries that either may not structurally hold under native physiological conditions or may cross-react with endogenous epitopes present on cell surfaces, the MITCH system deploys two sequences that are normally absent from the ECM. In spite of

their simplicity—containing both a tryptophan-rich WW sequence and a cognate proline peptide sequence—the two components assemble with good selectivity to enable gelation in the presence of living cells. Further molecular- and sequence-level characterization and understanding of this system[82] led to expanded uses in the stem cell culture niche, including delivery of adipocyte-derived stem cells[83] and as a gel-phase ink for bioprinting.[84]

The Burdick lab pioneered a hybrid synthetic-protein-based "dock-and-lock" (DnL) hydrogel consisting of two parts: (1) the RIIa subunit of cAMP-dependent kinase A, engineered heterologously as a telechelic protein (recombinant docking and dimerization domain, or rDDD), and (2) the anchoring domain of A-kinase anchoring protein (AD), achieved via solid-phase peptide synthesis and end-functionalized on a star-PEG macromer.[85] Upon mixing, the multivalent AD domains lock into the protein dimerization dock. The resultant physical crosslinks that form enable the construction of a self-healing, shear-thinning, and ultimately injectable construct. In a subsequent report, this system was used successfully as an injectable drug delivery vehicle for interleukin-10 to treat obstructive neuropathy in a mouse model.[86]
The Kiick group harnessed the heparin-binding capability of vascular endothelial growth factor (VEGF) proteins to non-covalently synthesize hydrogels.[87] Specifically, multi-arm PEG macromers end-functionalized with heparin motifs formed hydrogels when mixed with VEGF proteins. These networks only eroded when the VEGF protein was pulled down by a presented VEGF receptor. While there have not been many examples following up on this strategy, it does highlight the potential promise of protein-polysaccharide interactions (or other forms of molecular biorecognition) in the design of therapeutically relevant hydrogels, particularly in microenvironments with a rich set of different signaling factors present.

Physical networks stabilized through protein-protein interactions hold benefit for the encapsulation and maintenance of cells given their biocompatibility. Their mechanics also result in desirable properties such as self-healing and injectability. An often-underappreciated aspect, however, is their direct amenability to systematic interrogation and evolution through sequence optimization (**Figure 1.5C**). While previous efforts have mainly focused on site-directed mutagenesis, which has admittedly resulted in powerful gains in performance, we expect the field to be energized by the emergence and widespread adoption of *de novo* protein design[59] and genetic code expansion.[88] The former approach can generate large numbers of possible sequences to be tested for expression yields and bioactivity, and the latter can move outside of a purely biochemical space to access added degrees of functionality with a pristine regioselectivity beyond the capacity of stochastic modification. As these tools are codified, we predict many advances in biomaterial design and synthesis will become possible.

1.2.1.2.3. DNA-based

DNA biopolymers are being increasingly employed to enable new frontiers in nanotechnology and materials science.[89] Beyond its role as a genetic blueprint, DNA sequence encodes for rich structural and functional information driven through well-understood hydrogen-bond-driven base pairing that is readily co-opted for exquisitely user-definable and controllable material development. The effects of sequence variation often scale up and result in macroscopic changes, allowing tunable mechanics and stimulus responsiveness to be engineered through standard molecular biology methods. Moreover, the material stability of DNA in many biological contexts renders it highly useful as a crosslink in applications requiring long-term construct integrity. As a

result, DNA-crosslinked gels have matured within less than two decades from an academic curiosity into an established area of biomaterial development.[90]

Early landmark examples have successfully exploited the governing dynamics of DNA-DNA interaction to create materials. In an early report, the Liu group synthesized networks from tri-functional Y DNA starting reactants via formation of intermolecular i-motifs,[91] bypassing the need for an enzymatic trigger for the process but leading to networks that were not stable at physiological conditions. Follow-up work established DNA hybridization of compatible "sticky" ends as a viable and potentially highly versatile approach for network synthesis.[92] By mixing tri-functionalized Y DNA precursors and di-functionalized DNA linkers, the group engineered physical networks upon mixing endowed with enhanced stimulus responsiveness and mechanical stability. The Willner group also successfully harnessed DNA self-assembly for the creation of pH-responsive DNA-based networks endowed with robust shape memory by supplementing the i-motifs with DNA duplex units generated through the usage of adenosine-rich sequences. Their networks underwent preprogrammed and reversible sol-gel transitions, whereby gelation would occur at a pH level of 5 and network dissociation at a level of 8.[93]

1.2.2. Triggered hydrogel formation

As described earlier, the biomaterials field is benefitting from an expanding armamentarium of spontaneous assembly schemes for network creation. While important in a host of application spaces, these platforms often become inadequate when more nuanced control over hydrogel formation is necessary. For instance, hydrogel implants stand to benefit from spatiotemporal control over network formation. Building triggerability into gelation allows for these problems to

be addressed and stands to buttress the immediate bench-to-bedside translatability of hydrogel biomaterials.[94]

Broadly, creating triggerable systems can proceed by two different methods: through the engineering of gating mechanisms (e.g., molecular "cages") into reactions that otherwise would proceed spontaneously, or alternatively deploying a reaction scheme that *a priori* requires an exogenously delivered catalyst. These stratagems will be expounded upon in detail and applications where they have proved a strong fit highlighted.

1.2.2.1. Triggered gel formation via covalent reaction

1.2.2.1.1. Synthetic organic-based

Engineering gating mechanisms is of broad interest to chemists, biologists, and material scientists given the potentially afforded spatial and/or temporal control over reaction initiation and extent.[95] While click chemistries have proved essential in the engineering of new networks, reactions typically proceed rapidly upon mixing, hampering more nuanced use cases where added control over the spatiotemporal aspects of gelation is essential. As such, efforts have been poured into taking otherwise-spontaneous step-growth chemistries and engineering gating mechanisms to control their initiation and/or progression through different triggers. Potential engineered stimuli are manifold and ultimately depend on the context of the application.

A common trigger is redox-based initiation, whereupon introduced oxidants or reductants can actuate hydrogel formation from redox-sensitive macromers.[96] Thermally triggered gelation is also a viable strategy[97]; while non-ideal for a number of biological applications involving temperature-intolerant mammalian cells, thermal actuation of gelation is useful for drug delivery platform creation. Lastly, pH can serve as a hydrogelation stimulus but is again typically

precluded from applications involving live cell encapsulation.[98] Although these stimuli can afford temporal control over network formation, as well as a route to uniformly modulate hydrogel properties post synthesis, their ability to be controlled in space is limited.[99] Moreover, their applicability is hampered when minimal cellular interference is required.

Photoreactions, which can spatiotemporally dictate gelation based on when/where light is shone onto a sample, offer exciting advances in targeted hydrogel formation. This partially explains the earlier widespread adoption of photoradical-mediated chain-growth systems (e.g., acrylates, methacrylates) (**Figure 1.2A**). While now less employed for cell encapsulation stemming from concerns over formation of cytotoxic free radicals[100] and heterogeneous network structures,[101] their reagent availability, ease of preparation and use, along with the control they afford in both triggering gelation and modifying formed networks makes photopolymerization a suitable candidate for the creation of permissive 3D scaffolds. Specifically, the combination of this chain-growth platform with a gelatin methacryloyl (GelMA) starting material was highly synergistic, as it led to the creation of networks that were amenable to cellular encapsulation and maintenance[102] as well as relatively easy photo-enabled post-synthetic modification. This galvanized reports generating hybrid-gelatin networks from methacrylated starting macromers, such gelatin-gellan gum, -PEG, -HA, and -silk fibroin.

Another popular photochemistry is the radical-mediated thiol-norbornene platform, initially developed by the Anseth group[103] for the step-growth polymerization of PEG-based hydrogels. The reaction takes place between norbornene end-functionalized macromers and thiol-terminated crosslinkers. Requiring a lower initiator and active radical concentration than typical vinyl-based

chain-growth chemistries, the reaction minimizes radical-induced damage to encapsulated cells or tethered biological moieties such as proteins. Additionally, it can proceed orders of magnitude faster than a chain-growth-driven reaction and is not susceptible to oxygen inhibition. The platform was co-opted by multiple groups who applied it successfully to different base materials such as HA and gelatin.[104]

In looking to move photocrosslinking beyond radical-mediated chemistries, many labs have identified innovative ways to take step-growth chemistries previously considered uncontrollable and engineer photo-gating mechanisms into them, side-stepping radical-related cytotoxicity concerns. Toward this end, SPAAC was successfully rendered two- and three-photon activatable by the Popik and Bjerknes groups through inactivation of its strained-alkyne group with a photocaging cyclopropenone group,[105] paving the way for SPAAC hydrogel formation and biomolecule derivatization in deep tissue. Upon photo-uncaging with near-infrared light, the alkyne group is liberated from its cyclopropenone cage to enable SPAAC reactivity. Oxime ligation was also successfully gated through photochemistry: our lab previously caged the alkoxyamine with a cytocompatible UV-light-labile 2-(2-nitrophenyl)propyloxycarbonyl (NPPOC) group, such that the photo-liberated alkoxyamine could react with a cognate aldehyde and enable photocrosslinking for hydrogel formation and patterned biomolecule immobilization.[106] The Barner-Kowollik group also recently red-shifted photocaged oxime ligation (λ = 625 nm) through generation of an aldehyde from a furan precursor molecule in the presence of a photosensitizer, enabling transdermal initiation of photocrosslinking through a 0.5-cm-thick phantom mimic.[107]

Lastly, harnessing the [4 + 4]-photodimerization of anthracene has been shown by the Forsythe group to be a viable method to trigger network formation in the presence of cells.[108] Eliminating the need for two distinct reagents typical to click-based platforms, the group end-functionalized PEG macromers with anthracene moieties and induced network gelation via cytocompatible visible-light (λ = 400–500 nm) illumination. While earlier reports had demonstrated network formation using anthracene dimerization, requisite cytotoxic UV light was not suitable for cell encapsulation. To overcome this limitation, the group installed electron-rich substituents (e.g., triazole, benzyltriazole) to red shift anthracene absorbance, resulting in a synthetically tractable (one form of macromer required rather than two) and cytocompatible network synthesis scheme. Owing to the powerful synergies proffered by incorporating photoresponsiveness into bioorthogonal crosslinking chemistries, there has been a remarkable recent uptick in novel platforms that are phototriggerable.[109,110] While not all of these have yet been deployed in the context of hydrogel assembly, they are uniquely suited for many applications.

1.2.2.1.2. Protein-based

Beyond recognition and assembly of cognate pairs, protein-based platforms can act as enzymatic catalysts for the crosslinking of network precursors bearing the appropriate peptide substrate sequences. In fact, while thermal, redox, or light initiation triggers are well suited for certain applications, their usage can be sub-optimal when full bioorthogonality is desired. Given the prevalence of enzymes in all living organisms, their use as a highly bioorthogonal crosslinking reagent is potentially a powerful strategy (**Table 1.2**).

The Griffith lab first pioneered the use of transglutaminase to crosslink synthetic networks with macromers bearing appropriate recognition sequences.[111] Transglutaminase, a Ca^{2+}-dependent

enzyme, catalyzes a transamidation reaction between the carboxamide side chain of glutamine and the amine group found on lysines, releasing ammonia as a byproduct. This early work demonstrated network formation within a couple of hours from PEG macromers functionalized with either a glutamine residue or a lysine-phenylalanine dipeptide sequence. While highly promising, the relatively slow gelation placed limitations on encapsulation efficiency and uniformity. This strategy, however, laid the groundwork for a slew of follow-up research broadening the enzymatic toolset and optimizing reaction parameters (e.g., substrate recognition, crosslinking kinetics). The Messersmith group, for instance, rationally designed substrates with high transglutaminase specificity to enable faster gel assembly kinetics.[112] Subsequent work from different groups expanded the palette of available crosslinking enzymes with substrate recognition sequences of their own: these include horseradish peroxidase (HRP), phosphopantetheinyltransferase (PPTase), tyrosinase, lysyl oxidase, and sortase A.[113] Highlighting the promise of bioorthogonal enzymatic crosslinking, the Hwang group recently employed a tyrosinase-mediated reaction to form protective nanofilm hydrogels from monophenol-modified glycol chitosan and HA in the presence of pancreatic β cells to regulate blood glucose in a type 1 diabetes mouse model.[114]

Enzymatic crosslinking has also proved to be particularly well suited in the design and engineering of DNA-based hydrogel materials. In fact, routine enzymes in molecular biology applications have been co-opted to create hydrogels and other material structures from branched-chain DNA. This was first exemplified by the Luo group, who harnessed T4 ligase to covalently assemble branched DNA structures (X, Y, and T motifs) into hydrogels.[115] Combining enzymatic crosslinking with DNA as starting material has made possible the design of wholly novel

topologies and network structures. An interesting example is the generation of hydrogels solely from pristine plasmid DNA rather than more complicated branched DNA structures. After digestion by appropriate restriction enzymes and generation of sticky ends, crosslinking through the action of a ligase leads to gelation, and in so doing solves many issues associated with material costs, synthetic intractability, and severe stoichiometric dependence.[116] Building on enzymatic synthesis even further, the Walther group[117] deployed a strategy whereby two antagonistic enzymes (i.e., urease, esterase) act in an autonomous feedback loop to regenerate a DNA hydrogel from sol to gel continuously, driven by ambient pH levels. This enabled biomaterial creation with a distinct lag-time and lifetime under closed system conditions.

1.2.2.1.3. DNA-based

While the molecular engineering of DNA has enabled spontaneous gelation from nucleotide-modified polymeric macromers, relatively simple modification to the involved reaction motifs can turn DNA-enabled platforms into chemically triggerable systems (**Figure 1.6A**). Emblematic of this approach is the use of aptamers, which are short nucleic acid sequences that are designed and engineered to bind to a particular target or family of targets. They can best be conceptualized as the nucleic acid-counterpart to protein-based antibodies, and their deployment as a material chemistry can confer several benefits. For instance, in the case of DNA aptamers, constructs can be readily synthesized through routine and economical solid-phase synthesis. Moreover, aptamers are often endowed with robust stability under different solution conditions, rendering them particularly useful as base material for material crosslinks and tethers for different cargos. Lastly, it is theoretically both straightforward and rapid to generate aptamers for a wide variety of targets spanning different biochemical classes through a now-optimized combinatorial method known as systematic evolution of ligands by exponential enrichment (SELEX).[118] A foundational

example of harnessing aptamers as a material chemistry for hydrogels was demonstrated by the Tan group, where starting polyacrylamide-based macromers were end-modified with linear strands of nucleic acids and yielded network formation upon introduction of an exogenous DNA molecule, termed LinkerAdap.[119] While this was engineered to hybridize both strands of the starting macromers, it also includes an aptamer sequence for adenosine. Subsequently, introducing LinkerAdap into solution kickstarts a sol-gel transition, whereas adding adenosine will destabilize and degrade the network. This foundational example led to a flurry of downstream work that sought to apply DNA crosslink engineering for highly sensitive therapeutic delivery and biosensing applications.[120] For instance, the Wang group exploited the straightforward engineering of an anti-platelet-derived growth factor (PDGF) and incorporated it into routinely synthesized PEG-diacrylate hydrogel matrices.[121] When gelation occurs in the presence of encapsulated PDGF, this platform can serve as a robust and synthetically tractable drug release strategy that uses affinity interactions rather than bulk material degradation to deliver its payload. Promisingly, the kinetics of the release can be dictated by controlling the degree of aptamer incorporation, wherein higher-affinity networks containing more anti-PDGF aptamers led to a slower release, while lower aptamer content led to faster release.

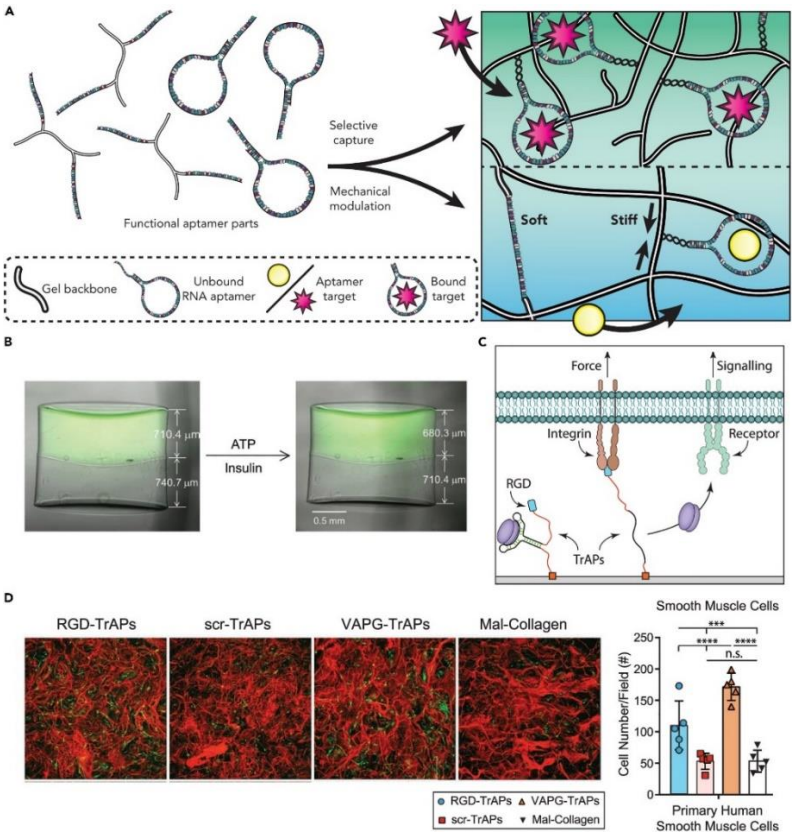

Figure 1.6: Engineering dynamic biomaterials through aptamer biology

(A) When incorporated into a hydrogel backbone, aptamers in an extended initial state can lead to macroscopic-level changes in network mechanical properties through basic biorecognition and cognate target capture.

(B) *Layered hydrogels are synthesized such that the top hydrogel (fluorescent green) is crosslinked through ATP-binding extended-state aptamers and the bottom hydrogel is crosslinked through insulin-binding extended-state aptamers. When exposed to the appropriate cognate molecule (ATP in the top and insulin in the bottom network), conformational changes in the aptamer crosslink lead to significant network volume decrease. Image reproduced with permission from Bae et al.*[122] Copyright 2018, Wiley-CVH.

(C) Aptamers can be engineered as force-mediated release systems. Traction-force-activated payloads (TrAPs) are designed such that an aptamer bound to a target molecule is also linked to an RGD motif that recognizes force-responsive integrin motifs. Upon local mechanosensing or application of a force stimulus, unfolding of the aptamer leads to target molecule release.

(D) TrAPs enable selective activation of growth factors in 3D collagen scaffolds by primary human smooth muscle cells. Extent of release and variation between different cell types is due to the relative expression of different adhesion receptors. Images for © and (D) reproduced with permission from Strejskalova et al.[123] Copyright 2019, Wiley-CVH.

Aptamers can be deployed for applications that go beyond triggered payload release. One recent example of this was in fact demonstrated by the Murphy group[122]; cDNA-bound (thus initially extended) aptamers were incorporated as network crosslinks in a synthetic gel backbone, and the

target motif binding capacity of these was co-opted to effect substantial volume decreases in the hydrogel (**Figure 1.6B**). They were able to show the applicability of this system both with ATP- and insulin-binding aptamers: up to a 40% volume decrease could be obtained in the case of the former and 15% in the case of the latter. This strategy is exciting as it can theoretically go much farther beyond these proofs of concept, limited only by the development of appropriate aptamer motifs that recognize relevant targets. Another powerful example by the Almquist lab showcased the deployment of aptamers as a force-responsive motif for the release of target payloads, rather than the usual scheme of "bind to release."[123] Specifically, the group developed traction-force-activated payloads (TrAPs) such that an aptamer motif was linked to both a cargo of interest (e.g., different growth factors) and an arginine-glycine-aspartic acid (RGD) cell adhesion motif that binds to cell membrane integrins. Deployment of an integrin-binding motif imparts force responsiveness to the construct, such that local applied forces lead to payload release (**Figures 1.6C and 1.6D**). This biomimetic approach was inspired by the large latent complex that natively controls the release of the transforming growth factor family. Excitingly, it bypasses the need for any exogenous trigger and relies on the nuances of cellular communication within the matrix to guide growth factor delivery.

1.2.2.2. Triggered gel formation via non-covalent reaction

1.2.2.2.1. Synthetic organic-based

Early examples of triggerable gelation of physical networks have relied on small-molecule introduction. For example, alginate polymers have historically lent themselves well to physical network assembly,[124] as the introduction of divalent cation—most typically Ca^{2+}—leads to the formation of ionic bridges between different chains and subsequent gelation. However, given the

crucial role calcium plays in biological signaling and cell-cell communication, this method falls short of creating truly bioorthogonal systems.

Beyond the now-classic calcium-alginate gels, recent reports outlining triggered assembly of physically crosslinked networks have been relatively few, albeit powerful given the dynamism that they can encode for and the relative ease with which desired downstream properties can be achieved. For example, the Rowan group demonstrated that the thermal gelation of polyisocyanopeptide chains can yield non-covalent network formation.[125] Polyisocyanopeptides rely on a non-traditional β-helical architecture stabilized by a supportive hydrogen-bonded network. Upon heating to 37°C, the polymer fibers bundle into a stiff hydrogel, which can be further stress-stiffened—a highly desirable property that is almost always beyond the capacity of synthetic networks—in the presence of living cells in order to closely mimic cytoskeletal viscoelasticity over time. Moreover, the synthetic nature of these chains allows for the routine introduction of different epitopes for biochemical signal presentation, or alternatively modification of starting materials to enable pristine user control over downstream properties such as ultimate stiffness and stress relaxation. A more recent example by the Zhu and He groups outlines the use of the Hofmeister effect in order to trigger PVA network formation and modulate its properties.[126] By varying ion type and concentration (thereby dictating whether salting in or salting out is occurring), the team induced hydrogelation through systematic control of PVA aggregation state, as well as encoding for the hydrogel's starting mechanics. Moreover, the ions only trigger gelation and do not play a role in maintaining network integrity, which means they can be dialyzed out post assembly and do not stand to hamper applications that require subsequent interfacing with living cells.

1.2.2.2.2. Protein-based

Most triggerable protein-enabled stratagems result in the formation of covalent networks, as seen when applying traditional enzyme-assembly methodologies or photocrosslinking of constituent residues. There are, however, some interesting examples of protein-based physical network assembly. An enzyme otherwise routinely used in molecular biology—phi29 polymerase—has been successfully applied for the physical assembly of DNA-based networks in a process termed rolling circle amplification (RCA).[127] Best conceptualized as an isothermal alternative to polymerase chain reactions (PCRs), RCA avoids the damage caused to biomolecules induced by cyclical heating and cooling, which are otherwise necessary in the case of routine PCRs. It does so by starting with a small (25–35 nucleotides) circular strand of DNA as starting material for subsequent amplification. Moreover, given that RCAs can occur at physiological temperatures, they can be deployed in the presence of living systems. This makes them ideal for the non-covalent assembly of a variety of networks through DNA chain entanglement or sequence hybridizations.[128,129]

1.2.2.2.3. DNA-based

While most DNA-crosslinked hydrogels have been limited to synthetic schemes that proceed spontaneously in a relatively uncontrollable manner, recent efforts have sought to gate or guide DNA self-assembly into macroscopic networks. Early attempts to trigger gelation were primarily focused on the introduction of Ag^+ ions to form duplex bridges between DNA chains.[130] However, other have sought to bypass the use of cytotoxic Ag^+ triggers and engineer more sophisticated spatiotemporal control into the process. Toward that end, the Willner and Fan groups reported a DNA hydrogel synthesis that is triggered by the introduction of a DNA initiator in a method they termed a “clamped” hybridization chain reaction.[131] As its name

indicates, the stratagem relies on introducing a clamp into a DNA hybridization chain reaction, a process through which stable DNA fragments assemble only upon exposure to an initiator molecule. This kickstarts a series of amplification events, with ultimate amplicon size varying inversely with the size of the initiator used, in an isothermal and enzyme-free fashion.[132] Classical hybridization chain reactions occur with two starting hairpin structures and an initiator molecule to kickstart successive assembly and amplification events. In a powerful example showcasing the promise of DNA molecular engineering, simple modification of one of the starting hairpins to incorporate a repeat palindromic sequence leads to a cyclical self-assembly scheme with intermediate three- and four-arm junctions to ultimately form a DNA hydrogel, with the small initiator linker operating as stimulus for the ensuing sol-gel transition. A subsequent report by the Li and Zuo labs harnessed this system for the capture of circulating tumor cells (**Figure 1.7**).[133] Keeping the main setup of the system relatively unchanged, the groups engineered a biblock initiator-aptamer molecule that recognizes specific receptors on tumor cell surfaces. Upon aptamer-receptor binding, the initiator strand is revealed, leading to hydrogelation in the presence of the circulating hairpin structures. This “cloaks” tumor cells with minimal damage, allowing for subsequent quantification and potential single-cell analysis.

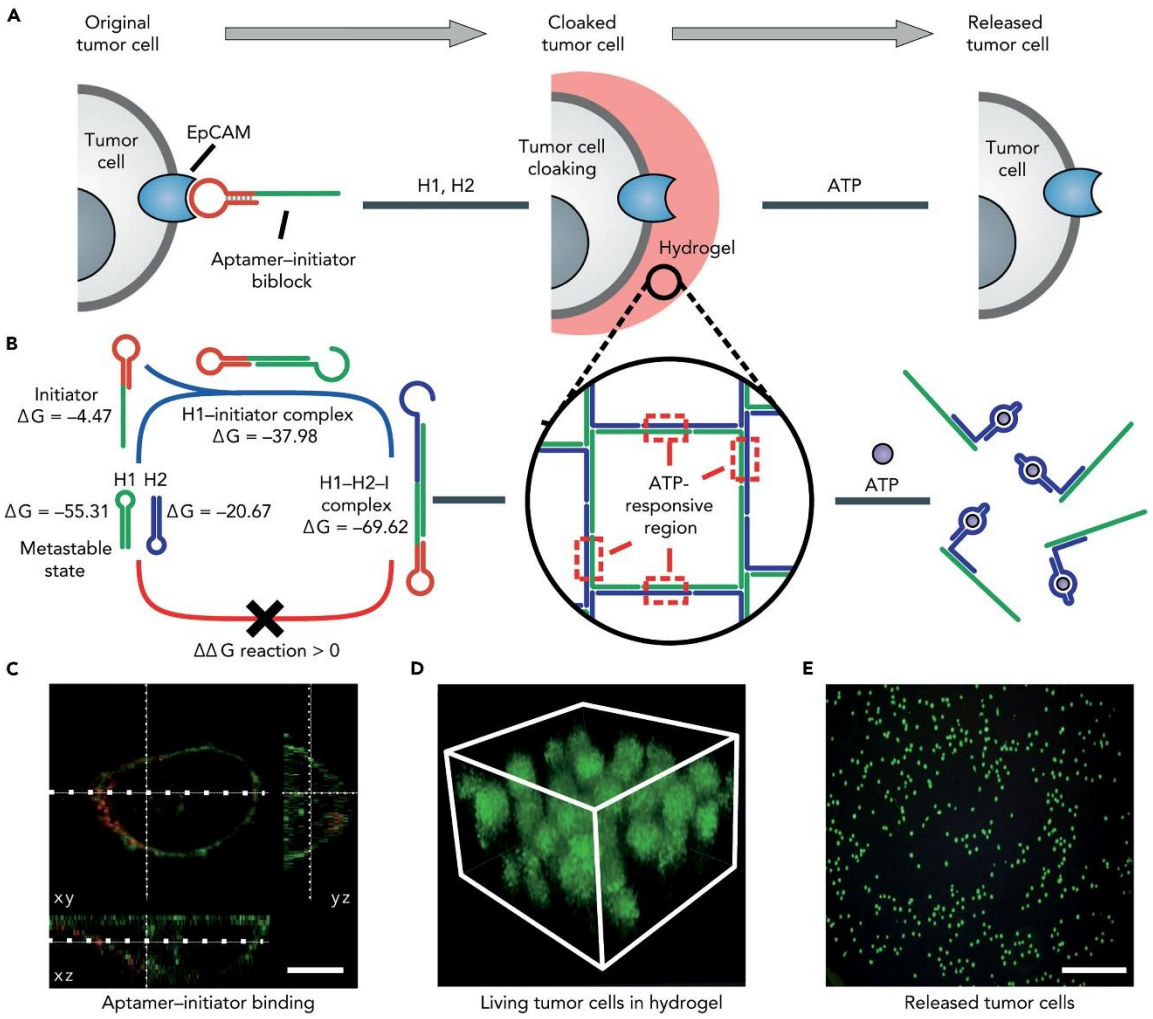

Figure 1.7: Aptamer-enabled targeting and capture of circulating tumor cells

(A) Aptamer-initiator biblock constructs are designed to specifically bind to epithelial cell adhesion molecules (epCAMs), which are highly expressed on the membranes of tumor cells. Following binding, biblocks containing an initiator trigger the formation of an encapsulating DNA hydrogel. Post encapsulation, ATP can be used to effect a conformational change within the ATP-responsive aptamer to destroy the gel, leading to tumor cell release.

(B) H1 and H2, which are step-look structured, are in a metastable state because of the protective effects of long stems in their secondary structures. In the presence of the initiator, the hybridization reaction is triggered leading to hydrogel assembly.

(C) Confocal microscopic imaging showing aptamer-initiator biblock binding to the cell surface membrane. Scale bar, 10 μm.

(D) Multi-layered cells can be found encapsulated within the DNA hydrogel when stained with FDA dyes. Stack height, 40 μm.

(E) Cells disperse in solution upon ATP-triggered release. Scale bar, 100 μm. Image reproduced with permission from Ye et al.[133] Copyright 2020, Springer Nature.

1.3. Post-synthetic modification of hydrogel biomaterials

As highlighted above, a growing toolbox of externally triggered and spontaneously proceeding reactions has birthed a wide method collection to fabricate hydrogel biomaterials. An equally if not more important thrust focuses on developing chemical methodologies that post-synthetically modulate hydrogel properties. This would enable the field to go beyond encoding an initial set of biochemical and biomechanical parameters for a hydrogel matrix and to create constructs that can be customized on demand, potentially even in 4D. Engineering controllable dynamism into such systems would make possible longitudinal interrogation and/or control of biology, ideally in ways that capture all possible timescales of interest throughout space. In the ensuing section, we will survey different modalities that have been used to post-synthetically modify networks, with an eye toward rendering these chemistries more user controllable.

1.3.1. Spontaneous hydrogel modification

Key to engineering evolvable networks is the identification and deployment of methodologies that modify hydrogels post assembly.

1.3.1.1. Spontaneous gel modification via covalent reaction

1.3.1.1.1. Synthetic organic-based

Synthetic schemes offer different avenues for spontaneous modification post assembly. A first category to that effect adopts off-stoichiometric ratios during the initial network formation step; by maintaining an excess of a particular reactant, biological epitopes functionalized with the appropriate handle could later be immobilized with temporal (and sometimes spatial) control. This presents a very straightforward approach that minimizes biomaterial design complexity; most often, a “mixed-mode” approach can be adopted whereby one chemistry is used for network formation and another for post-synthetic modification. As one illustrative use case,

networks formed by a tetrazine-norbornene platform, for instance, can routinely be assembled such that excess norbornene groups are presented throughout the hydrogel. Biological epitopes harboring reactive thiols can then be introduced and photo-clicked in through an orthogonal thiol-ene chemistry.[25] Another example along the same line of thought was presented by the Chen group; in this report, the base platform used for network assembly was DA chemistry, and excess maleimide was left unreacted for post-synthetic patterning.[134] It is important to note that such mixed-mode methods do not necessarily always hinge on stoichiometric manipulation of starting reactants, elegant as this approach may be. Orthogonal chemical handles can be introduced into the starting macromers such that they do not influence initial network synthesis but instead present avenues for later biochemical modification. An example of this method was presented by DeForest and Anseth;[135] in that report, SPAAC was used to assemble PEG hydrogels with chemically orthogonal vinyl moieties incorporated into the starting materials and subsequently presented throughout the network. These reactive ene groups served as pendants for the later introduction and patterning of different classes of biological epitopes including small molecules and bioactive peptides through thiol-ene photochemistry. As can be seen from the examples above, owing to the diversity of chemical approaches developed for hydrogel synthesis and modification, there exist no shortage of platforms that can prove amenable to mixed approaches, where one chemistry is geared toward assembly and another tailored toward biochemical or biomechanical modification.

Another exciting development in evolvable hydrogel networks is the deployment of covalent-adaptable networks, which combine the mechanical integrity and stability of chemically crosslinked systems with the stress relaxation and enhanced viscoelasticity of physical

assemblies.[136,137,138] By occupying this intermediate niche between the two modes of crosslinking, biomaterial scientists have been able to tap into synergies unobtainable from either strategy alone and turn the reversibility of some of these base reactions (e.g., the previously touched upon DA and oxime ligation schemes)—typically thought to be a potential weakness—into an exploitable property. Nevertheless, early iterations of these reconfigurable networks were not suited to the needs of the biomaterials science and engineering community; in fact, the landmark report outlining the use of DA chemistry (with furan and maleimide as starting macromers) for the generation of a "re-mendable" material only did so at a transition temperature of 120°C,[139] which was the only transition point at which the adaptability of the chemistry could be accessed. A similar early landmark paper deploying hydrazone chemistry for the generation of adaptable polyethylene oxide (PEO) matrices only showed network reconfiguration within reasonable timescales at a transition pH level of 4, well below the useful range for cell studies; the linkages would break at apparent pH levels less than 4 and would reform when above that cutoff.[140] While powerful proofs of concept, rational changes had to be incorporated into the base chemistries used if this approach was to prove useful for pursuits in tissue engineering.[141] Toward that end, the first report detailing the use of a covalent-adaptable network for the encapsulation and maintenance of a cell population was presented by the Anseth group, who did so through the deployment of a hydrazone transimination platform.[142] A rapid screen of reactivities of two different aldehydes—one aliphatic and the other an arylaldehyde—with a methylhydrazine partner showed that both approaches could be viable candidates. In fact, both reaction pairs led to gelation and response profiles within reasonable timescales, and both approaches enabled the encapsulation of C2C12 myoblast cells. Since then, multiple dynamic covalent methodologies have proved useful in addition to the traditional DA[143,144] and oxime

ligation[145] workhorses; among these chemistries are hydrazone,[146] thioester exchange,[147] hindered urea bond,[148] boronate transesterification,[149] among others still. Interestingly, dynamic covalent chemistries can also be used in mixed-mode approaches provided their reaction profiles and necessary solution conditions are compatible and amenable to multiplexability. One method to effect this was presented by the Anderson group, whose report used diol exchange of two kinetically distinct phenylboronic acid derivatives, 4-carboxyphenylboronic acid and *o*-aminomethylphenylboronic acid. In so doing, the authors were able to access highly nuanced mechanical and viscoelastic property ranges by mere tuning of the starting concentrations of either acid, and achieved response profiles beyond the reach of either acid alone.[150] Another method is to deploy two dynamic platforms that are fully orthogonal; a recent example of this is provided by Fustin group, who in an interpenetrating network setting were able to combine Schiff base chemistry in one hydrogel and metal-ligand coordination in another.[151]

1.3.1.1.2. Protein-based

The advent of orthogonal protein pairs has been highly enabling for the covalent post-synthetic modification of hydrogels consisting of different base materials. The fragment reconstitution-based toolkits mentioned previously have been deployed to great effect for network modulation across many synthetic platforms. To implement this strategy, the Li group photochemically crosslinked SpyCatcher-containing motifs into an underlying tandem elastomeric protein network. With these moieties in place, different SpyTagged fusions were swollen in to covalently decorate the gel with a host of proteins (i.e., fluorescent proteins, as well as cell-adhesive TNfn3 domain derived from type III fibronectin).[152] The Sun group also harnessed this approach successfully to decorate mussel foot protein-3 (Mfp-3) hydrogels displaying

SpyCatcher motifs, enabling post-gelation incorporation of SpyTagged protein.[153] The West group took this blueprint further: by photochemically crosslinking different amounts of SpyTag within PEG-diacrylate hydrogels, they could specify the concentration of tethered SpyCatcher fusion proteins.[154]

Beyond fragment reconstitution, enzymes can also be co-opted for the post-synthetic modification of networks, particularly in cases where bioorthogonality and maintenance of native bioactivity levels are essential. The Griffith lab pioneered the use of sortase-mediated transpeptidation to post-synthetically decorate hydrogel matrices. Specifically, a PEG hydrogel assembled through Michael-type chemistry was decorated with epidermal growth factor (EGF) via sortase (**Figure 1.8A**).[155] Beyond biochemical immobilization, their group also demonstrated sortase-enabled degradation of PEG networks, demonstrating gains in biocompatibility of the enzyme to the encapsulated cells when compared to more standard proteolytic gel degradation methods.[156] In the same vein, the Lin group also employed sortase to control network crosslinking density.[157] In order to do so, they exploited the inherent reversibility of sortase reactions to impart cyclical stiffening or unidirectional softening, based on the design of the constituent crosslinkers. Moreover, taking advantage of recently engineered sortases that were evolved to recognize orthogonal peptide substrates, our lab recently demonstrated the ability to spatially control degradation and cell recovery from multi-material biomaterials[158] (**Figures 1.8B and 1.8C**). Applications such as these highlight the extent to which genetic encodability can result in highly nuanced material responsiveness.

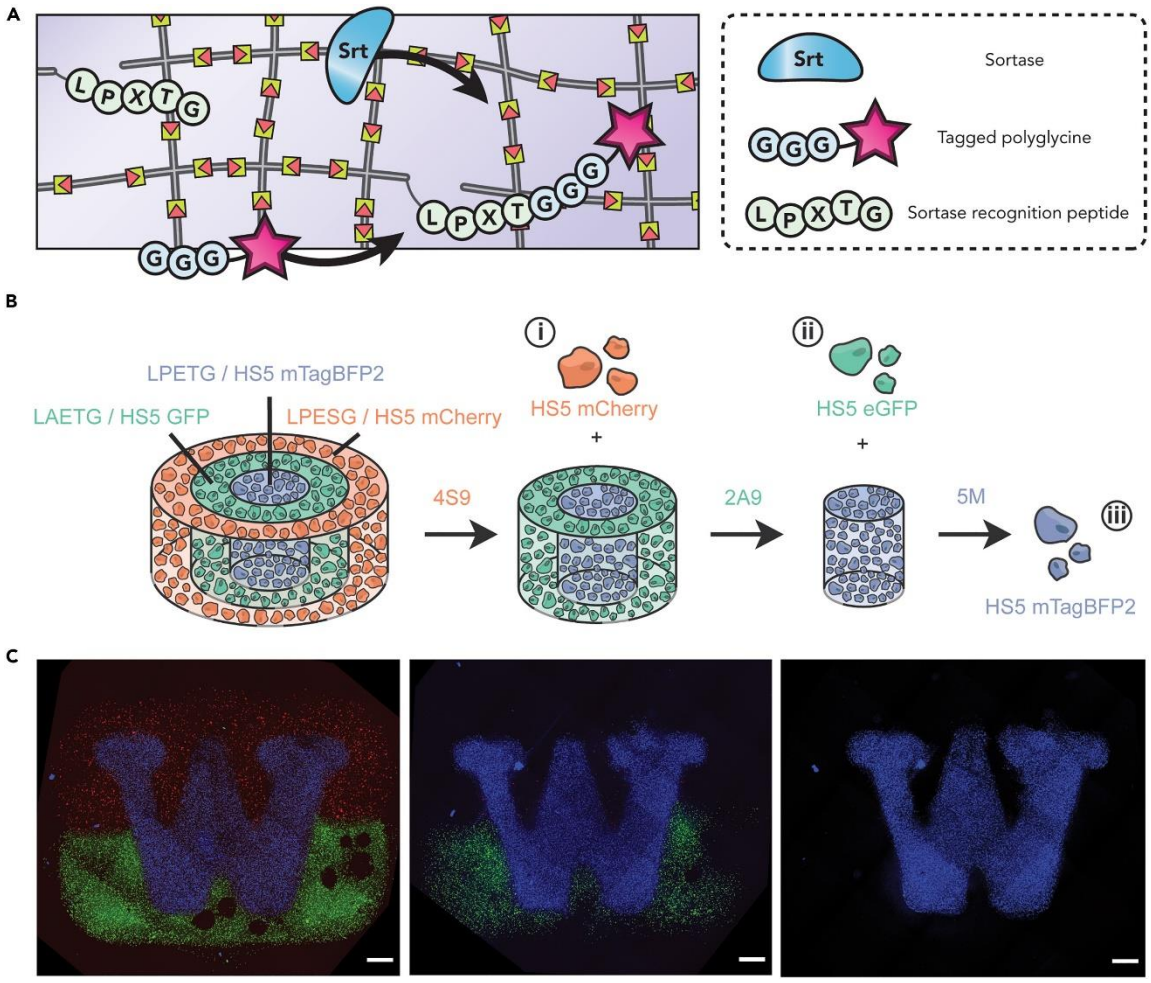

Figure 1.8: Sortase-mediated gel functionalization and multi-material degradation

(A) Sortase selectively ligates polyglycine-tagged cargo onto LPXTG-containing peptide sequences covalently bound to the polymer network.

(B) Harnessing evolved sortases' ability to recognize orthogonal peptide motifs found within crosslinkers comprising different gel regions, staged material degradation and accompanying cellular release can be achieved; for example, with eSrtA(4S9), then eSrtA(2A9), then eSrtA-5M. Adapted with permission from Bretherton et al.[158] Copyright 2023, Wiley-VCH.

(C) Sequential sortase treatment enables user-defined control over cell-laden multi-material degradation. Maximum intensity projections of the University of Washington logo, comprising cells constitutively expressing one of three fluorescent proteins, are shown prior to degradation (left), following treatment with eSrtA(4S9) treatment (center), and following eSrtA(2A9) treatment (right). Scale bars, 1 mm. Reproduced with permission from Bretherton et al.[158] Copyright 2023, Wiley-VCH.

In a non-classical example showcasing protein-enabled network modification, the Collins group have engineered hydrogel networks with integrated nucleic acid crosslinks that cleave in response to the action of Cas12a nuclease proteins (**Figure 1.9**).[159,160] Based on the material design adopted, the group successfully demonstrated release of cargo tethered to the network through pendant DNA, bulk degradation of the network when crosslinked through appropriate DNA substrates, actuation of an electronic fuse, as well as co-opting the material for paper diagnostics endowed with remote signaling capacities. We expect recent advances in triggering CRISPR activity to further next-generation responsive materials development.

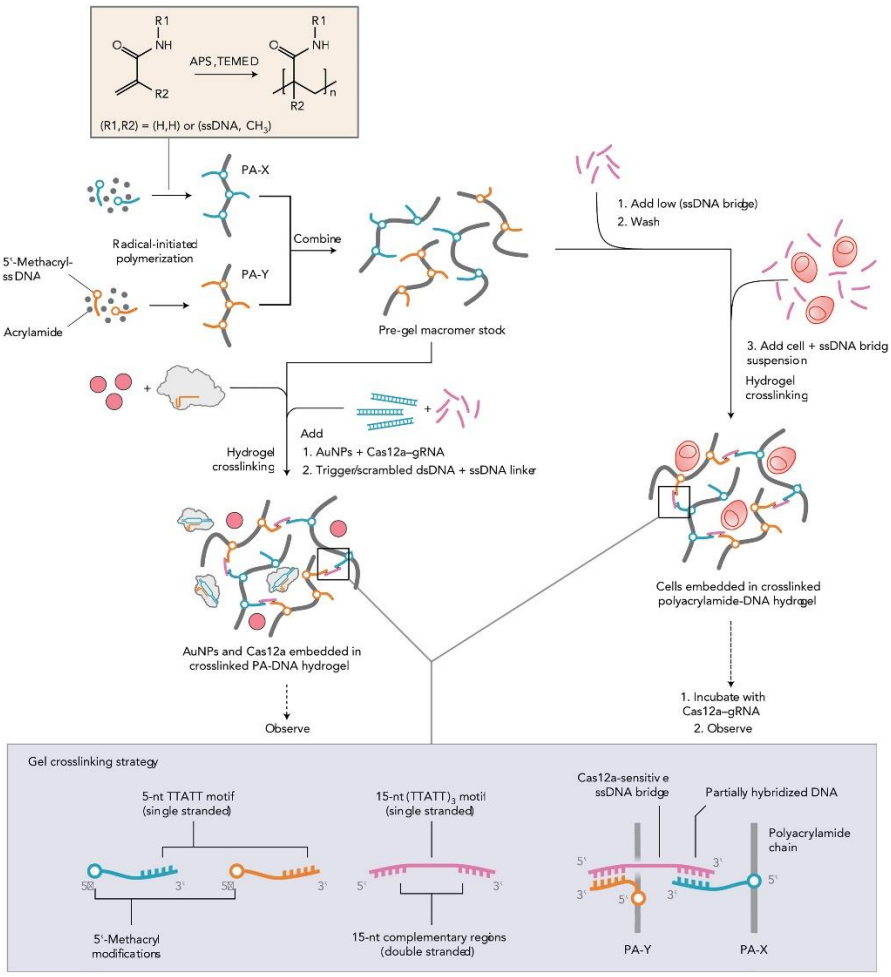

Figure 1.9: Design and synthesis of Cas-responsive hydrogel networks

Methacryl-functionalized DNA is incorporated into polyacrylamide chains (PA-X, PA-Y) during starting macromer polymerization. This enables different routes to gel actuation and response modes. In one example, shown on the left, the Cas12a-gRNA is added to the gel precursor with the nanoparticle cargo, before the addition of double-stranded DNA (dsDNA) cues and single-stranded DNA (ssDNA) crosslinker. In another example, shown on the right, cell encapsulation is triggered through the addition of a small amount of ssDNA bridge crosslinker to the macromers mixed in solution. This thickens the pre-gel solution and minimizes losses incurred during the washing step. More ssDNA linker is then added at the same time as the cells to fully crosslink the hydrogels. Finally, the experiment is initiated by exposing the gels to gRNA-complexed Cas12a and dsDNA. Additional details of the crosslinking strategy (bottom of the panel): the two ends of the DNA bridge hybridize with distinct ssDNA anchors incorporated into polyacrylamide macromers, while the central AT-rich portion remains single stranded and sensitive to Cas12a collateral activity. Reproduced with permission from Gayet et al.[160] Copyright 2020, Springer Nature.

1.3.1.2. Spontaneous gel modification via non-covalent reaction

1.3.1.2.1. Synthetic organic-based

The earliest and arguably most robust example of a non-covalent method to confer modifiability into hydrogels is heparin, either chemically tethered via synthetic coupling, encapsulated, or included as a network crosslink.[161] Heparin is a linear polysaccharide group that was initially deployed to reduce biomaterial-induced thrombogenesis following blood contact given its anticoagulant activity. However, it was soon discovered to preferentially bind to a wide host of growth factors,[162] rendering it particularly useful for controlled the release of protein therapeutics and regenerative medicine applications.[163,164] However, in spite of its relative simplicity, routine usage of heparin has been hampered by its broad binding capabilities; its biorecognition is not limited to a singular cognate partner. Instead, it recognizes a wide family of growth factors that harbor a heparin-binding motif, which would likely complicate its use *in vivo*.

Moving beyond the broad recognition capacity of chemically immobilized/encapsulated heparin would require more judicious design or identification of target-specific docking sites that can enable the stimulus-responsive and precise release of encapsulated drugs upon analyte sensing (i.e., a more precise form of molecular biorecognition). An early example of this is the coumermycin-inducible release of drugs in loaded polyacrylamide hydrogels presented by the Weber group.[165] In fact, the group chemically conjugated a bacterially produced gyrase B protein subunit—which harbors a very strong affinity to coumermycin—to nitrolotriacetic acid-modified polyacrylamide via Ni^{2+} chelation. Introducing the coumarin-based antibiotic coumermycin leads to gyrase B homodimerization, polymer crosslinking, and subsequent network assembly. Subsequent addition of the competitive antibiotic novobiocin, however, leads to dimer

dissociation and resultant network degradation. This was used successfully for the encapsulation of a VEGF protein during encapsulation and controlled release, which could be tuned by varying the relative concentrations of the different parameters at play. Given the simplicity of the platform as well as its reliance on commonly used and US Food and Drug Administration (FDA)-approved antibiotics (rendering potential downstream translation all the more promising), the group built upon their strategy further by porting it into a more bioinert PEG-based network crosslinked through Michael-type chemistry,[166] applying it for the release of a hepatitis B vaccine,[167] and exploiting its amenability for pharmacological regulation to build a cell-growth-supporting matrix.[168,169]

1.3.1.2.2. Protein-based

Analogously to covalent schemes for the post-synthetic modification of networks via proteins, non-covalent chemistries also hold significant promise for the reversible modulation of network properties, be they mechanical or biochemical in nature. Early examples were provided by the Li group, who incorporated what they termed a mutually exclusive protein (MEP) to act as a redox-controlled crosslink that can switch between folding and unfolding.[170] After initial photochemical crosslinking, the MEP—a GL5CC-I27 domain—can exhibit an unfolded state when exposed to a reductant (i.e., DTT) and refolded when re-oxidized (with H_2O_2). This translates to direct changes in resultant stress-strain curves, whereby different patterns can be cycled through reversibly based on environmental redox activity. Through these, the group also showcased the granular-level changes in properties such as the network Young's modulus, resilience, and swelling ratio. While modulating redox activity may not be a promising bioorthogonal avenue, it does lend itself well to insightful investigations of gelation and hydrogel architecture; promisingly, the deployment of this stimulus is not limited to the modulation of

properties at the macro scale but can also at the nano scale. Specifically, the Dougan group co-opted the aforementioned strategy and applied it to photochemically crosslinked bovine serum albumin (BSA) networks, which are tied together further by disulfide-bonded "nanostaples." The existence of this secondary crosslink enabled the group to harness a diverse array of protein characterization techniques—most notably circular dichroism (CD) and small-angle scattering (SAS)—to identify the formation of self-similar (i.e., fractal) nanoclusters upon local unfolding, leading to force-labile crosslinks.[171] Going beyond modulating redox activity to control downstream network properties, another robust strategy to cycle through different network profiles consists of reversibly folding-unfolding protein crosslinks through denaturing agents. In a representative example, the Li group showcased a hydrogel consisting of the highly folded globular GB1 or a *de novo*-designed FL domain.[172] Harnessing the reversible folding-unfolding of folded domains upon exposure to a denaturant (guanidine hydrochloride in this report), the group demonstrated solid shape memory and, impressively, were able to construct different multi-material geometries.

Physically dynamic systems can also be codified into fragment reconstitution-type chemical platforms. Although covalent schemes such as isopeptide bond formation between SpyTag and SpyCatcher are irreversible, those based on non-covalent reconstitution such as the GL5CC region of GB1 are dynamic by nature.[173] Splitting the aforementioned GL5CC domain leads to two fragments, termed GN and GC, that predictably assemble non-covalently in solution.[174] Owing to the redox dependency of such a linkage material dynamism can again be imparted by cycling through different redox states, with oxidative environments and low temperatures (approximately 4°C) leading to disulfide bond formation and reduction (coupled

with temperatures above 37°C) yielding a more dynamic physical network amenable to subsequent re-patterning. This remains the only example of a dual-component non-covalent protein-based modification that is controlled via a redox mechanism, and it was applied with success for the repeatable tethering and release of an enhanced cyan fluorescent protein (ECFP) and the Tnf3 protein from the tenascin domain. We envision that the identification of similar motifs—either inspired by nature or developed *de novo*—stands to energize work in this space by providing more robust tether-and-release profiles as well as removing the necessity for rather stark temperature changes.

1.3.1.2.3. DNA-based

Owing to well-established paradigms governing DNA interactions, DNA crosslinks are well suited for modification through different modalities (e.g., heat, pH, enzyme) without extensive redesign of starting macromers. Beyond unidirectional modification, shape memory is a feature implicit to many DNA-based networks, allowing reversible state switching based on underlying gel conditions.

In addition, aptamer technologies have proved uniquely enabling for creating dynamic physically assembled networks that recognize highly specific molecules (e.g., signaling factors, metabolites, toxins). Harnessing aptamers as DNA antibodies, various groups have successfully built hydrogel vehicles for either therapeutic delivery or alternatively biosafety and bio-detection units. Unlike conventional antibodies, however, aptamers hold the added benefit of construct stability across harsh physicochemical conditions. Beyond aptamer-based technologies, there exist examples of groups who have harnessed the complementarity of designed nucleic acids to impart modifiability into networks. A powerful example of this is provided by the Mooney lab,

who exploited nucleic acid complementarity to create a refillable drug depot for extended therapeutic release *in vivo*.[175] As DNA synthesis continues to gain in speed and efficiency, high-throughput screening of aptamer libraries will enable the identification of newer aptamer-target pairs.

1.3.2. Triggered hydrogel modification

Moving beyond spontaneous reaction schemes for hydrogel modification, triggerable platforms enable temporally and/or spatially controllable avenues for network modulation. Most often, these advances are made possible through photochemical methods, which enable dose-dependent responses and reaction specification in both space and time.

1.3.2.1. Triggered gel modification via covalent reaction

1.3.2.1.1. Synthetic organic-based

User-triggered modification of network properties post assembly is a necessary precondition for gaining 4D control. To achieve this capability, stimulus responsiveness is engineered into the hydrogel during assembly in the form of stimuli-responsive crosslinks or, alternatively, stimuli-responsive excess moieties for post-synthetic epitope patterning and biochemical/biomechanical modulation.

Representative of the first strategy, our group engineered a PEG-based hydrogel that could flexibly exercise Boolean logical response,[176] whereby preprogrammed combinations of environmental cues would yield specific downstream outputs (e.g., gel dissolution, therapeutic delivery) (**Figure 1.10A**). Showcasing all possible YES/OR/AND logical outputs for a three-input system (i.e., enzyme, light, reductant), 17 distinct stimuli-responsive materials were

synthesized, wherein differences in linker structure translated into different material outputs. This logic-predicated response strategy was then extended by our group for release of living cells,[176] proteins,[177] and small-molecule payloads.[178]

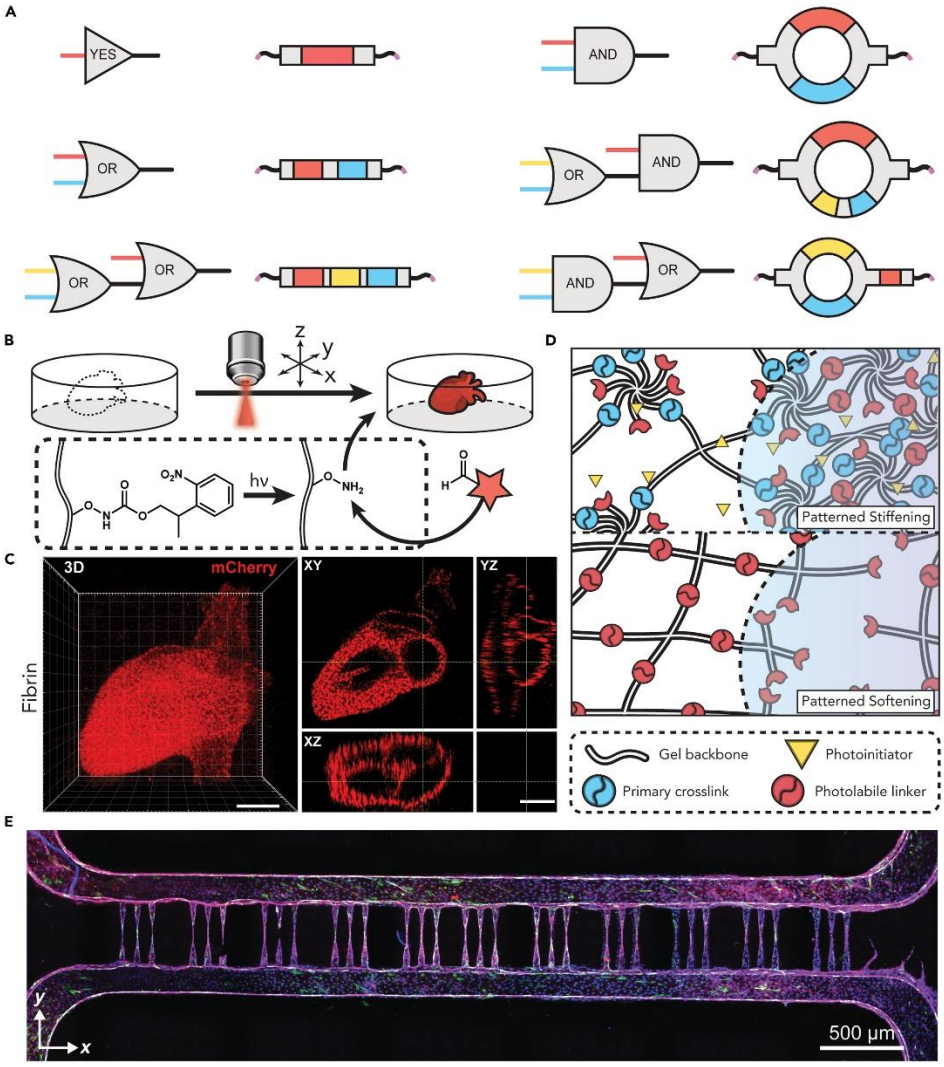

Figure 1.10: User-engineered and directed biomaterial responsiveness

(A) Material inputs such as light, enzyme, and reductant responsiveness can be codified as Boolean logic crosslinkers. Adapted with permission from Badeau et al.[176] Copyright 2018, the authors.
(B) Biological epitopes can be photo-patterned with pristine spatiotemporal control in order to recapitulate native physiological structures ex vivo *(reaction platform shown here is a photomediated oxime ligation).*
(C) Three-dimensional patterning of an anatomical heart is achieved in a fibrin-based hydrogel network through photomediated oxime ligation, showcased with 3D and cross-sectional cut views (mCherry-CHO is shown in red). (Scale bar, 50 μm).
(D) Hydrogel networks can be engineered to reversibly photostiffen/photosoften through judicious engineering of a secondary photolabile linker.

(E) Photodegradation of hydrogel networks can yield shapes and geometries with pristinely conserved features such as endothelialized 3D vascular networks. Adapted with permission from Arakawa et al.[179] Copyright 2020, the authors.

For the triggerable introduction of biological signaling factors, our group also harnessed a photocaged oxime ligation strategy to post-synthetically modify PEG-,[180] collagen-, and fibrin-based networks.[181] Post network formation, user-directed light exposure liberates NPPOC-caged alkoxyamines, enabling the tethering of aldehyde-functionalized proteins and anisotropic biological signaling to take place within the network. This strategy is encouraging given the tunability it has afforded photopatterning of natural protein-based gels, typically thought to be more limited in their configurability than their purely synthetic counterparts (**Figures 1.10B and 1.10C**).

Photocontrolled reaction schemes are also a viable strategy for the modulation of networks, enabling either stiffening or softening based on the underlying design (**Figure 1.10D**). For softening matrices, an early example was presented by Kloxin and Anseth, who designed photocleavable crosslinks and network tethers based on an *ortho*-nitrobenzyl group moiety, enabling post-gelation modification of the hydrogel in the form of either softening or biomolecule release.[182] Our group also coupled this photochemistry with multiphoton lithography, enabling the creation of pristine microvoid geometries at the capillary scale and beyond (**Figure 1.10E**).[179,183] Given the broad interest that photomodulation chemistries have garnered, and their limitations with regard to tissue penetration, recent efforts have poured into the development of more red-shifted and more photolabile groups. An example of this was recently demonstrated by our group, wherein, through the design of novel ruthenium-based crosslinks and tethers, hydrogel modulation was successfully effected up to several centimeters deep in tissue.[184]

For stiffening networks, a recent study by the Anseth group details the use of an SPAAC-based network for the study of injury-mediated stiffening environments.[185] Strained alkynes can undergo secondary photocrosslinking in the presence of a suitable photoinitiator, enabling matrix stiffening on demand from a commonly employed reaction scheme. Another example of this strategy is the reversible [2 + 2] photocycloaddition reaction of pyrenes.[186] First harnessed by the Forsythe group to engineer PEG networks using styrylpyrene groups, the light-triggerable nature of the reaction permitted a bidirectional modulation of resultant mechanical properties by controlling the number of formed crosslinks.[187] Additionally, its reversible nature allowed for a potential network disassembly upon exposure to 340-nm light. Subsequent work substituted the styrylpyrene groups for acrylamidylpyrenes,[188] a substitution that enabled the decoupling of light wavelength needed for network formation and network stiffening. The Anseth group also built upon anthracene-enabled [4 + 4]-photodimerization—previously demonstrated as a viable network synthesis strategy[108]—to construct a longitudinally modifiable hydrogel well suited for the interrogation of cellular behavior in stiffening environments.[189] Illumination with cytocompatible 365-nm light induces gelation, and further exposure to the same wavelength leads to progressive network stiffening, resulting in a compositionally simple single-starting reagent tool to study mechanobiology in 4D.

A step beyond one-shot network functionalization would enable repeatable biomolecule patterning in order to fully recapture ECM dynamism and biochemical heterogeneity. An example of this, previously demonstrated by DeForest and Anseth, employs orthogonal photochemistries, with one—the thiol-ene reaction—deployed for biomolecule tethering and another—the photocleavage of an incorporated *ortho*-nitrobenzyl group—toward subsequent

release.[190] While robust, such approaches are ultimately limited by cycle repeatability. Toward that end, the Anseth group developed an allyl sulfide-based platform for the theoretically repeatable introduction, exchange, and removal of different biochemical epitopes,[191,192] all of which can occur while retaining the synthetic tether functionality. Taking inspiration from reversible addition-fragmentation chain transfer (RAFT)-based polymerizations,[193] during which the main transfer agent can be natively regenerated, allyl sulfide functional moieties can enable the reversible addition and removal of virtually any reactive thiol-containing compound. This platform has also made possible the amplified photodegradation of hydrogels at light intensities much more attenuated than those used for typical degradations.[194] However, free radicals are prone to degrade proximal proteins over time,[195] and concerns remain over their potentially cytotoxic effects on encapsulated cells, which may limit more widespread use of this platform in spite of its promise. In addition, theoretical cyclability in the aforementioned system is harshly limited because of ligand exchange with the underlying network anchor motif, leading to the degradation and release of the reactive allyl sulfide moieties over time.

1.3.2.1.2. Protein-based

While spontaneous protein-based chemistries have proved useful in generating networks decorated with different polypeptide moieties, biological interrogation at multiple timescales can be greatly enhanced with triggerable platforms. Protein-enabled chemistries, particularly “smart” constructs with well-established input-output responses, are suited to that goal.

In the same vein, enzymatic modification workflows can also be engineered such that they present avenues for user-directed photocontrol. A prominent early example of this was demonstrated by the Lutolf group. Building on their prior work showing uniform gel protein patterning with transglutaminase,[196] the group then installed an Nvoc lysine photocage on its

cognate peptide substrate such that the ensuing enzymatic ligation reaction is fully abrogated until cage photorelease.[197] This enabled the group to successfully guide protein patterning to user-defined sub-volumes of the network, showcasing arguably the first controllable and fully bioorthogonal hydrogel functionalization strategy targeting full-length proteins such as VEGF and a fibronectin domain. Inspired by this strategy, our group has also looked to control protein presentation in hydrogels through methodologies that preserve native-level bioactivity.[198] Prior to protein immobilization onto gels, sortase-enhanced protein ligation (STEPL) was employed to install a variety of synthetic tethers onto a protein library. These synthetic tethers can be engineered to enable clicking onto virtually any network chemistry. A caged alkoxyamine, for instance, can be used to guide protein patterning to user-definable matrix sub-volumes via a photomediated oxime ligation. Moreover, judicious installation of stimuli-responsive chemical groups, such as photoscissile moieties, can enable spatiotemporally guided protein release within the network.

Beyond enzymes, tools derived from non-opsin optogenetics have proved to be well suited for photoresponsive material development. A prominent example of this is the photocleavable protein (PhoCl), which is the first fully genetically encoded polypeptide with a photoconversion mechanism that leads to backbone scission.[199,200] Derived from the photoconvertible protein mMaple,[201] PhoCl harbors a Kaede green-to-red chromophore within its backbone that undergoes beta-elimination upon illumination with 400-nm light. Rather than photoconvert, as is the case with its predecessor protein, PhoCl was evolved to cleave instead, leaving behind an empty barrel that is no longer fluorescent and a small peptide scar. Moreover, its main value proposition lies in its amenability to expression as a chimera with a wide host of C-terminal

fusion partners, which partially explains its widespread adoption both within the optogenetics community and beyond. By recombinantly expressing PhoCl with a suite of C-terminal proteins and N-terminally tagging PhoCl with an azide handle, our group generated SPAAC networks uniformly decorated with photoreleasable proteins.[202] The West lab also harnessed the photoresponsiveness of PhoCl to extend their prior work tethering SpyCatcher fusion proteins into PEG-diacrylate networks, enabling post-synthetic tethering of biological moieties and their subsequent photorelease.[203] Given the versatility of PhoCl as a fusion partner, it has found a prominent application space within hydrogel biomaterials, where it has also been co-opted for the design of networks with tunable mechanical properties[204] and the creation of a solid-phase protein display system.[205]

Beyond the release of bioactive molecules, recapturing the native cellular niche at different scales of spatiotemporal resolution would stand to benefit from full user control over protein activation. Toward that end, our group recently established a versatile method to photocontrol protein ligation via a light-activated SpyLigation (LASL).[206] This method relies on the use of amber codon suppression to introduce an *ortho*-nitrobenzyl photocaged lysine at the critical residue within the SpyCatcher protein, preventing ligation until photo-uncaging. When used to photoassemble otherwise inactive split protein fragment pairs, this method can re-confer bioactivity onto the stably reassembled protein product. While a promising avenue for future work in protein-protein complementation, especially when considered in tandem with elegant computational approaches for the generation of split proteins from full-length precursors,[207,208] this approach is limited by the following constraints: (1) the parent protein should be amenable to splitting at a site such that both fragments are separately inactive; (2) its

split fragments should not spontaneously reassemble; (3) each split fragment should be amenable to expression as either a SpyTag or a SpyCatcher fusion, and lastly (4) it may still prove refractory to systems that collapse into an unfavorable orientation upon complementation, preventing the recapture of native-level bioactivity. Ongoing efforts in our lab seek to sidestep these existing limitations while permitting direct photoactivation of many diverse protein classes in solution, throughout biomaterials, and within living cells.

1.3.2.2. Triggered gel modification via non-covalent reaction

The application of an exogenous stimulus to direct network modification—ideally in a fully bidirectional manner—is a highly desirable feature to engineer into next-generation hydrogels. Triggerable non-covalent reactions can potentially afford this desired reversibility in hydrogel customization.

1.3.2.2.1. Synthetic organic-based

In the context of host-guest chemistry-based gels, light responsiveness can be engineered in a straightforward way by having the guest molecule be a stimulus-responsive construct rather than a simple aliphatic chain. For instance, the Stoddart group used an azobenzene as guest within a cyclodextrin host. After spontaneous gelation, they were able to photocontrol reversible sol-gel transitions based on the wavelength of light delivered.[66] In fact, azobenzene in its *trans* conformation docks into the cyclodextrin cavitand, resulting in gelation; upon illumination with 350-nm UV light, the azobenzene adopts a *cis* conformation and results in disassociation from the cyclodextrin core, leading to a gel-sol transition. Subsequent exposure to 450-nm visible light results in a reversion to a *trans* configuration and docking, thereby recapturing the gel state and showcasing the reversibility of the procedure. Engineering

photoresponsive host-guest systems has led to the conceptualization of smarter therapeutic delivery vehicles. For example, the Anseth lab has developed a PEG-based azobenzene-cyclodextrin hydrogel for the encapsulation of a model fluorophore-tagged peptide.[209] Inducing a *trans-cis* isomerization by 450-nm light exposure leads to an accelerated rate of peptide release, motivating the potential and possibility for on-site therapeutic release using relatively simple formulations.

1.3.2.2.2. Protein-based

Controllable protein-based modulation of hydrogel networks is rendered possible primarily by optogenetics-derived dimers that assemble and/or disassemble upon directed light exposure.[210] Given the tunability of these constructs and their amenability to rational optimization, multiple groups have recently sought to co-opt them as hydrogel crosslinks to modify network properties on demand. A report by the Weber group, for example, covalently coupled a monocysteine-containing bacterial phytochrome (Cph1)[211] to a multi-arm PEG through a routine vinyl sulfone reaction.[212,213] Illumination of the protein-PEG conjugates with 660-nm light led to Cph1 dimerization, increasing gel crosslink density and stiffening; 740-nm light shifts the protein construct back to a monomeric state, leading to softening. These changes in the underlying network mechanics—as shown by changes in hydrogel storage and loss moduli—depend on illumination wavelength, light dosage, as well as the amount of incorporated Cph1 dimers. Illustrating the power of this approach, the storage modulus of an example network with 70 mg/mL of incorporated Cph1 dimers can drop by approximately 40% (from a starting point of approximately 2,500 Pa down to 1,500 Pa) when exposed to 740-nm light (at which most Cph1 components turn monomeric), and regains its initial value upon re-exposure to 660-nm light and subsequent network stiffening. This method is powerful owing to its reversibility—hydrogels can

be cyclically stiffened and softened on demand—and the wavelength of light delivered is red shifted, obviating any cytotoxicity concerns. Moreover, it is a compositionally simple platform requiring one protein to be generated and purified. Recent work has extended the dynamic range achievable by this initial iteration—termed CyPhyGel by the group—through the introduction of a single amino acid mutation R472A identified by benchmarking against other phytochrome variants.[214] While a simple mutation, this change increased the dynamic range of achievable stiffness states—measured through the network storage modulus—by approximately 12%. While powerful, both reports fell short of achieving reversible sol-gel transitions, a staple of non-covalent synthetic- and DNA-based crosslinking approaches and often beyond the reach of protein-enabled platforms. Most recently, the group successfully showcased reversible sol-gel transitions by introducing judicious changes to their starting macromers.[215] Eight-armed PEG macromers were deployed (instead of four-armed, as in the earlier reports), and the system was predicated on the heterodimerization of the red/far-red light photoreceptor phytochrome B (PhyB) and phytochrome interacting factor 6 (PIF6). The starting reactants do not gel upon mixing; rather, it is illumination with 660-nm light that leads to heterodimerization and subsequent gelation. Exposure to 740-nm light then reverts the system back to a sol state, with a storage modulus dynamic range of 0–800 Pa.

Another example of reversible modulation of network mechanical properties was showcased by our group. By incorporating either a photoresponsive LOV2-Jα[216] or calcium-responsive calmodulin-M13[217] fusion motif as a material crosslink, we were able to effect cyclic stiffening/softening of PEG-protein gels, respectively blue light or calcium ion exposure.[218] Other strategies looking to achieve similar reversible modulation outcomes have

used other optogenetic constructs such as Dronpa145N[219] and UVR8.[220] Many of these non-opsin optogenetic pairs can be scanned for performance and appearance in prior reports in a regularly updated community database named OptoBase (https://www.optobase.org/).[221] While evolved both in nature and at the lab bench with drastically different use cases envisioned, these opto-proteins hold great promise as material-forming chemistries and will likely continue to serve as inspiration for biomaterial scientists looking to create more user-controllable cellular niches.

1.3.2.2.3. DNA-based

While a relatively new frontier, triggered modification schemes for DNA-based networks are gaining traction in the field. The governing dynamics of DNA stimulus responsiveness are getting increasingly elucidated and codified. Applying these rules to material design may result in constructs with switchable properties such as dynamic ligand presentation and cyclical stiffness states. In arguably the most powerful example showcasing the potential tunability of DNA-crosslinked networks, the Willner group introduced a multi-triggered supramolecular DNA/bipyridinium dithienylethene (DTE) that can be modulated reversibly over time through light, redox switching, or introduction of a crown-ether molecule.[222] This network can be in one of two states depending on the photoisomerization of the DTE group: a closed state in which it acts as an electron acceptor and an open state in which it loses its electron-acceptor properties. Practically, this entails that control of DTE isomerization dictates the downstream triggerability and modifiability of the network through photochemistry, redox changes, or introduction of a crown-ether molecule for electron transfer. Given the ease of cycling through different DTE states through illumination with UV-visible light, the system can enable near-effortless cycling through different stiffness states while remaining endowed with robust shape memory. Another

report by the group showcased photochemical or small-molecule control over a polyacrylamide-based network cooperatively bridged by stimuli-responsive DNA chains.[223] While technically consisting of boronate ester-crosslinked polyacrylamide, the initial hydrogel matrix is cooperatively bridged by nucleic acid sequences that serve as the launchpad for further stimulus responsiveness. In one design, an azobenzene motif is incorporated into the intercalator unit. As discussed previously, azobenzene exhibits robust optical switching properties, basically operating as a robust optical gear to switch the system from higher (60 Pa in storage modulus at wavelengths beyond 420 nm) to lower (20 Pa at a wavelength of 365 nm) stiffness states. In another design, G-quadruplex units stabilized by K+ ions serve as further cooperative crosslinkers instead of the azobenzene intercalator. This allows the group to then cycle through the same high- and low-stiffness states by repeated introduction or removal of a crown-ether small molecule. Another recent example by the Di Michele group deploys G-quadruplex units to physically crosslink hydrogel networks—which the group terms quad-stars—in a one-pot, isothermal, and enzyme-free manner.[224] The G-quadruplex units can then serve as cation-responsive (e.g., K+) crosslinks enabling the cyclical assembly or disassembly of the hydrogel. Alternatively, UV-light exposure in the presence of a porphyrin photosensitizer can also lead to matrix photocleavage.

1.4. Translational considerations in biomaterial development

We hope our above discussion has successfully highlighted the diverse array of chemical and biological platforms that can be deployed to assemble and subsequently modify hydrogel biomaterials. However, we also want to switch our lens and critically assess the translational promise and actual market traction that these bioengineering advances have successfully driven.

While all nascent technological (and specifically biotechnological) platforms should be given time to develop at pilot scales before getting stress tested on the market, the time is ripe for hydrogel biomaterials to mature and transition from bench to bedside. Hydrogels first came to the fore as a market reality more than six decades ago in the form of contact lenses,[225] and, promisingly, have since witnessed consecutive foundational landmarks in their study that have promised to expand their use cases far beyond their beachhead application. Among these is the initial Langer and Folkman proof of concept for the deployment of amphipathic and/or hydrophilic polymer matrices for the release of macromolecular drugs (arguably the origin of controlled release as a field proper)[226] and the critical extension and formalization of the space as well as supplementation with predictive mathematical modeling[227,228] put forth by Peppas. In addition, the foundational theoretical-experimental work developed by Bissell in the early 1980s highlighted the importance of the extracellular niche as a critical regulator of gene expression[229] and cellular differentiation and tissue development[230]; in so doing, her work catalyzed the framing and deployment of hydrogel biomaterials as powerful scaffolds for the recreation of the native cellular niche, what we now broadly refer to as tissue engineering.[231,232] The advances we have surveyed throughout the core of this review expand upon how rational deployment of novel chemical and biological crosslinking platforms stand to sharpen and optimize the use of hydrogel matrices as controlled release depots, implants, and tissue engineering scaffolds, among other adjacent applications. However, despite a burgeoning palette of seemingly promising crosslinking platforms, comparatively very few hydrogel-based therapies have made it to the clinic; tellingly, in searching for clinical trials (clinicaltrials.gov) that mention “hydrogel,” approximately 50% of search results point to contact lenses or variations on ocular implants. Understandably, this leaky translational pipeline has led to much debate and

discussion, with an increasing number of manuscripts now dedicated to discussing platforms with concrete translational promise[233] or charting the development of hydrogels in the clinic.[4] In an effort to fix this leaky pipeline, biomaterial scientists and engineers need to first understand the regulatory hurdles that they will face in looking to transport their technologies to the clinic. Following this exposé, we hope to highlight some market applications and promising technologies for next-generation hydrogel biomaterial deployment.

1.4.1. Regulatory approval constraints and approval hurdle

A challenging regulatory landscape is the predominant reason for a leaky translational pipeline. Hydrogels are considered a medical device as per section 201(g) of the Federal Food, Drug, and Cosmetic Act, with ultimate product class (i.e., class I, II, or III) dictated by the number and type of payload and additives within the formulation. When a hydrogel biomaterial is designed to be delivered as a standalone construct, as is usually the case for wound healing or anti-inflammation therapies, product champions contend with a development timeline on the order of 1–5 years, as the product is categorized as a less risky class I or II device. The existence of safety predicates owing to older hydrogel products on the market accelerate this regulatory navigation substantially as a result. However, newer-generation hydrogels are typically co-opted for the delivery of therapeutic cargos (e.g., nucleic acids, proteins, living cells, or combinations thereof). For these indications, cases for safety predicates become considerably weaker; as a result, these biomaterials are marketed as class III devices and considered "combination products" in FDA parlance. Practically, this engenders the need for a 510(k) Pre-Market Notification Submission for legal marketing rights within the US, entails a development timeline on the order of 7–10 years, and results in drug development costs that range from $50 million up to $800–900 million, often on the upper end. For perspective, Medtronic's INFUSE—typically considered the

landmark hydrogel biomaterial in the clinic—peaked at $750 million in sales in 2011, with revenue levels varying substantially year on year since. Such high development costs severely compromise the translational potential of otherwise promising technologies that may have a pressing clinical need but no substantial market to allow them to recoup initial development costs, as is often the case with many orphan indications.[234]

1.4.2. Translational potential beyond injectable therapies

While earlier discussion centered on injectable therapies is likely the most broadly relevant, the translational promise of hydrogels should not remain entirely predicated on controlled release and directly adjacent application spaces. Many of the chemistries touched upon throughout this review stand to impart higher-order stimulus responsiveness than that required for smart drug delivery systems, which may render newer constructs over-engineered for controlled release but otherwise uniquely suited for the recreation of pristine ECM niches *ex vivo* for avenues such as disease modeling, value-added chemical bioproduction, and bioprinting. For instance, one of the most pressing hurdles to clear in modern biomedicine is the path toward regulatory approval, which currently stands at a 2023 approval rate of 7.9%.[235] Even when successful, navigating through all requisite phases through to FDA clearance is a decade-long procedure that routinely incurs multiple hundred millions of dollars in development costs. Clearly, this is a large pain point in the engineering of new therapies, and one to clear rapidly if healthcare innovation is to keep its requisite momentum. A powerful solution to this quandary lies in the development and engineering of organoid models—ideally in a massively parallel manner—that would sidestep the need for lengthy clinical trials by providing an avenue to collecting the same (if not higher) quality clinical data from reproducible tissue biology models.[236,237] A key advantage to well-

engineered organoid models is the generation of patient-specific clinical insights based on the recapitulation of near-native tissue signature, which promises to catapult personalized medicine from an academic dream to a market reality.[238] Galvanized by a foundational manuscript showcasing the engineering of a lung "organ on a chip" that successfully mimicked key physiological markers of native lung tissue,[239] multiple startups have emerged and ventured into organ-on-a-chip and organoid model engineering, including Emulate Bio, Herophilus, Chinook Therapeutics (now acquired by Novartis), Organoid Therapeutics, among many others still, each with a slightly different base platform chemistry and/or organoid portfolio in development. Large-cap pharmaceutical companies have also looked to infiltrate and grow organically within this niche; for example, the Institute for Human Biology (IHB) was started at Roche to engineer reproducible disease models at scale for faster drug lead identification. The number of players competing within this space highlights its market promise. Importantly for our discussion in this review, enabling technologies such as controllable bioorthogonal chemistries coupled with pristine biochemical and biomechanical patterning will prove crucial to the development of these technologies, where precise user 4D control and reproducible findings emblematic of native tissue biology are of the highest order.[240,241] Beyond disease model engineering, hydrogels have also proved to be powerful scaffolds for the encapsulation of a wide range of microorganisms, rendering them uniquely suited for biomanufacturing pursuits. Common use cases involve the freeze-drying of hydrogel constructs that harbor a target expression strain, abrogating the need for stringent cold chains in their transport, followed by rehydration and reconstitution at the site of interest. This then enables biomanufacturing at target locations of a variety of value-added chemicals (predominantly hard-to-transport pharmaceuticals) all while bypassing otherwise limiting supply chain constraints.[242,243] Advances in the sourcing of gel materials and the impact

of different crosslinking chemistries on encapsulated culture viability and long-term maintenance can then directly translate into more powerful hydrogels-as-living materials for bioproduction.[244]

1.4.3. Hydrogel biomaterials in the market

Previous reviews have presented significantly valuable contributions in surveying biomaterials that have progressed to the clinic and/or market. Prominent examples of these include a broad landscape of injectable therapies[4,245] as well as relatively recent deep dives into hydrogel biomaterials geared toward musculoskeletal therapy,[246] orthopedic implants,[247] skin-tissue wound healing,[248] and cardiac tissue engineering.[249] Herein, we provide a focused survey of some of the most prominent hydrogel biomaterials that have been marketed across as wide a range of indications and mechanisms of action. We also highlight some promising recent technologies in various stages of development. Beyond listing the platform name and developer, we look to provide some clarity with regard to material composition and crosslinking chemistry wherever possible. Prominent injectable therapies that have been broadly marketed are surveyed in **Table 1.3**, and we call out the nuances of the delivery method or underlying mechanism where appropriate.

Table 1.3 Survey of representative hydrogel injectable therapies
Representative hydrogel-based injectable therapies are surveyed and platform specifics such as source material, base chemistry, and delivery method are discussed where appropriate. BMP, bone-morphogenic protein; AMD, age-related macular degeneration.

Platform	Company	FDA Approval Status / Year if Marketed	Approved Indications	Source Material	Base Chemistry	Delivery Method	Mechanism	Other notes
INFUSE®	Medtronic	2002 (for first indication in spinal fusion)	Spinal fusion, orthopedic trauma surgeries, maxillofacial correction, and currently in clinical trials for further indication.	Collagen	Non-covalent interaction between base collagen and encapsulated bone-morphogenic protein-2 (BMP-2)	Spinal injection	Passive and diffusion-controlled delivery of BMP-2	Commercial market leader in hydrogel drug delivery systems, achieving peak sales of 750M$.

Vantas®	Endo Pharmaceuticals	2004 (for first indication in palliative prostate cancer treatment)	Palliative advanced prostate cancer treatment, treatment for early-onset puberty.	Poly(hydroxyethyl-methacrylate) and poly(2-hydroxypropyl-methacrylate)	Methacrylate chemistry for initial crosslinking with passive non-covalent encapsulation of histrelin acetate (a gonadotropin-release hormone agonist)	Subcutaneous injection (at inner aspect of upper arm)	Passive and diffusion-controlled delivery of histrelin acetate.	Discontinued indefinitely as of September 2021 because of manufacturing issues.
Bukamid®	Searchlight Pharma	2006	Injected to aid in treating female stress urinary incontinence.	Polyacrylamide	Chemically crosslinked polyacrylamide with no further additives or delivered cargo.	Transurtheral injection	Acts as a bulking agent when injected. Procedure is a series of injections (3-4), no incisions are necessary, and treatment is long-lasting (order of years).	One of two female stress urinary incontinence hydrogel therapies on the market on the market, wit the other (Coaptite®) based on a cellulose matrix.
Belotero Balance®	Merz Pharmaceuticals	2011	Injected to aid in the correction of moderate-to-severe facial wrinkles.	Hyaluronic acid (HA)	Chemically crosslinked hyaluronic acid with no further additives or delivered cargo.	Dermal injection	Acts as a filler designed to integrate into facial skin tissue.	First approved in the EU in 2004 making it the first marketed HA-based therapy. Other therapies marketed since have used a similar starting formula or supplemented HA with lidocaine for local anesthesia.
TraceIT®	Augmenix, Inc. (now acquired by Boston Scientific)	2013	Installed to improve tissue alignment to streamline image-guided therapy.	PEG	Chemically crosslinked PEG with no further additives or delivered cargo.	Percutaneous injection	Acts as a filler; improves tissue alignment for image-guided therapy.	
SpaceOAR®	Augmenix, Inc. (now acquired by Boston Scientific)	2015	Installed as a rectal spacer designed to minimize the side effects of radiation therapy for prostate cancer.	PEG	Chemically crosslinked PEG with no further additives or delivered cargo.	Rectal injection	Acts as a rectal spacer; no payload to deliver	Remains at the injection site for approximately 3 months post-injection.
OTX-TKI	Ocular Therapeutix	*Currently in Phase II*	Injected to treat wet age-related macular degeneration (AMD).	PEG	Chemically crosslinked PEG with incorporated axitinib, a small tyrosine kinase inhibitor.	Intra-vitreal injection	Acts as a delivery agent for the sustained (6 month+) release of axitinib.	There currently exists no sustained release platform for the treatment of wet AMD.
Neo-Kidney Augment (NKA)	InRegen (now acquired by ProKidney)	*Currently in Phase II*	Injected as a Type 2 diabetes	Gelatin	Chemically crosslinked gelatin with	Kidney injection	Acts a cell therapy scaffold for kidney tissue regeneration.	InRegen has also deployed a similar cell

			treatment as well as kidney disease treatment (both indications are currently pursued).		encapsulated renal cells.			therapy strategy for the treatment of chronic kidney disease.
VentriGel	Ventrix	*Currently preparing for Phase II*	Injected as a repair treatment after myocardial damage.	Native myocardial ECM	Unmodified, porcine-sourced native myocardial ECM	Cardiac injection	Acts as a repair scaffold for damaged myocardium microenvironments.	

As can be seen from the highlighted injectable therapies above, a disproportionate number are simple and very often uni-compositional (e.g., hydrogels as fillers, bulking agents, or spacers). Recently, more groups have designed more complex injectables harboring protein, oligonucleotide, or cellular therapies with varying rates of success. Anecdotes of costly and high-profile failures (e.g., recently, FX-322 from Frequency Therapeutics) often deter hopeful entrants with similar material platforms, especially when the target pathophysiology is located at a challenging injection site. This harsh regulatory landscape has contributed to an unsurprising trend whereby relatively simple injectable hydrogels that have already gained FDA clearance for a specific indication get tested for as broad a palette of indications as possible. For instance, Bulkamid, initially developed as a treatment for female stress urinary incontinence, is now undergoing regulatory tests for multiple incontinence indications. In the same vein, TraceIT, first approved for bladder tumor image guiding, is now being tested for a variety of tumors such as pancreatic, rectal, and oropharyngeal.

Going beyond injectable therapies, we also provide an overview into some of the most promising organoid and organ-on-a-chip companies (**Table 1.4**), as we believe this niche to be an often-overlooked killer application when looking at hydrogel biomaterial commercial promise. As part

of our survey, we highlighted therapeutic focus areas and close with thoughts on the path forward for the field.

Table 1.4 Survey of organoid and organ-on-a-chip companies

Notable organoid and organ-on-a-chip companies are surveyed, and platform nuances are highlighted where appropriate. PDMS, polydimethysiloxane; NA, not available.

Company	Year Founded	Tissue Model Portfolio	Brief Description of Platform Technology	Notes
Chinook Therapeutics	2011 (now acquired by Novartis)	Focused on kidney organoid preclinical models for lead generation	Primary kidney cells are induced into organoids when grown in a Matrigel® 3D support.	Chinook's kidney models have proven immediately fruitful as they have led to 6 possible drug leads that have cleared Phase 1.
Emulate Bio	2013	Brain-chip, colon-intestine chip, duodenum-intestine chip, kidney chip, lung-chip, liver-chip	Microfludiic polydimethysiloxane (PDMS) harboring tissue-mimicking hydrogel culture. Source hydrogel material and crosslinking specifics varies chip-to-chip, although most likely relies on either Matrigel® or a proprietary form of decellularized ECM.	Chips for further tissue models are underway; first mover in disease modeling
Sengine Precision Medicine	2015	Proprietary PARIS® test is theoretically applicable to all solid tumors	Primary cancer cells are grown in a Matrigel® network to recapture native and patient-specific solid tumor intricacies. Cells are then assayed for particular genotypic and phenotypic markers through bioinformatics analyses.	CLIA-certified platform for identification of optimal chemotherapy drugs or drug combinations for therapeutic intervention.
Organoid Therapeutics	2019	Focused on the engineering of: 1) glandular organoids for clinical implantation as an alternative to pharmacological therapy, and 2) organoids as clinical models	Primary cells are grown on a first-of-its-kind ECM substrate sourced from pancreatic ECM, with advantages being a more familiar and natural microenvironment for encapsulated cellular populations compared to Matrigel®.	Organoid Therapeutics is one of very organoid engineering las that have side-stepped the use of Matrigel® as supporting scaffold.
Herophilus (previously System1 Biosciences)	2021	Focused on the development of primary-cell derived brain organoids for the modeling of neurodevelopmental, neurodegenerative, and neuropsychiatric diseases	Patient-derived neuronal populations are induced into organoids when grown in a Matrigel® scaffold.	Most leads are still in development across different indications, with a promising candidate for Rett syndrome furthest in development.
Institute of Human Biology (IHB) – Roche	2023	NA	NA	This represents the first greenfield investment by a large pharmaceutical company looking to develop in-house tissue models.

What stands out in the case of most organoid platforms has been their historical over-reliance on off-the-shelf source material as the underlying matrix, with Matrigel being the most prominent.[250] While highly enabling because of sourcing simplicity and relative

straightforwardness in work-up and preparation, such materials can be limiting across many different aspects. Most prominently, they suffer from severe batch-to-batch variation, leading to a reproducibility crisis in cell culture experiments that routinely deploy them. Moreover, they are not readily amenable to downstream modification, rendering them practically refractory to many of the chemistries and related platforms that can be engineered to create dynamic cell culture environments and, in the process, generate actionable biological insight.[251] We hope to impress the notion that the field stands to benefit greatly from a steady migration from sourced ECM alternatives to "blank-slate"-like starting materials that are amenable to downstream biochemical and biomechanical modulation. The explosion in chemistries that are uniquely suited for spatiotemporal modulation promises to energize the field by imparting both more confident and reproducible results, as well as the possibility to fully recapture the nuances of the extracellular niche *in vitro*.[252] Naturally, aspects such as synthetic tractability and ease of use will come to the forefront of discussion as these chemistries look to achieve market traction.

1.5. Challenges and future outlook

As highlighted in this review, advances in materials chemistry have catapulted hydrogel biomaterials well beyond static frameworks for the simple encapsulation of cells and therapeutics and into the world of 4D customization. Central to this shift has been the enabling power of emerging click, bioorthogonal, and chemoenzymatic reactions that have allowed researchers a much-increased breadth of properties such as tunability of kinetics, biocompatibility, triggerability, and multiplexability. The palette of assembly and post-synthetic modification schemes available for use are manifold, and we hope that this work galvanizes the necessary form of convergent science that bridges different areas of expertise together.

However, we do want to highlight the multiple challenges standing in the way of broad commercial adoption of modern biomaterial systems. While the past decades of research have made possible dozens of novel chemical platforms encoding expanded biomaterial functionalities, the pipeline from bench to market has proved to be problematically leaky. In large part, this can be explained by first-order constraints—defined here as the near-inevitable engineering design problems and necessary nuanced tradeoffs—such as the difficulty of achieving an optimal set of mechanical properties (e.g., in the case of injectable therapies, exquisitely tuned shape memory has to be engineered *a priori* into the material) or showing good biocompatibility and avoiding unwanted immune responses (particularly important in the case of implants or drug delivery depots). Second-order constraints, however, are also highly important in the broader context of hydrogel biomaterials achieving their commercial promise; we define these as more general problems and perhaps non-obvious concerns that should be on the minds of scientists and engineers looking to push their materials into broader commercial applicability. These constraints include, but are not limited to, (1) limitations of the underlying material platform with regard to breadth of applicability, generally due to over-engineering; (2) the particularly challenging regulatory landscape that hydrogel biomaterials have to navigate en route to approval; and (3) the difficulty of achieving meaningful scale-up of materials with many chemistries in academic laboratories.

1.5.1. Complexity versus simplicity in biomaterial design

The increased dynamism and stimulus responsiveness engineered into newer hydrogel networks has necessitated a steady concomitant increase in their design complexity. While highly enabling of biological interrogation, such systems have often fallen beyond the reach of labs that would

make the most use of them and have inadvertently dimmed their own translational potential. As it stands, many next-generation constructs are powerful but over-engineered, necessitating a near-perfect confluence of artificial experimental conditions or parameters, beyond which they do not hold much value. Debates have ensued over whether complexity as a design principle should be embraced in biomaterial engineering[253] or whether efforts should be put into creating systems that are simpler and more tractable by comparison instead.[254] The answer most likely falls somewhere in the middle: researchers should note how enabling newer and more "complex" platforms—either operating alone or in tandem with other chemistries—have been for different use cases. However, new developments in the space should also be evaluated on their portability and ease of use across different contexts for a more holistic assessment of true translational promise.

1.5.2. Regulatory landscape for hydrogel biomaterials

A key roadblock for hydrogel biomaterials is the particularly complicated regulatory landscape they are required to navigate. With frustratingly few exceptions, all hydrogel-based products are categorized as devices in the eyes of the FDA, as mentioned earlier. When used as depots for drug or cell therapies, they are designated as combination products. Practically, this implies that any potential hydrogel-encapsulated therapies have to undergo an additional 510(k) Pre-Market Notification submission and are looking at close to a decade prior to approval for their indications, severely hampering any commercial viability. The solution to this goes beyond the bench and should take the form of lobbying for faster approvals, particularly in cases where promising precedents have been established with regard to safety, efficacy, and biocompatibility.

1.5.3. Achieving material scale-up

Should an enabling chemical platform for the synthesis of evolvable networks show promise beyond the lab bench, an immediate consideration should be whether achieving meaningful material scale-up is possible in the first place. Highly costly materials will likely not find much traction in the marketplace, and many biomaterials, while elegant on paper and in particular killer applications, are severely compromised with regard to translational promise when their synthetic intractability or other adjacent caveats (e.g., shelf life, ease of use) are brought to the fore. Ready material availability and overall portability thus should be critical factors when evaluating the promise of novel chemistries used for biomaterial engineering.

1.5.4. Parting thoughts

Biology is a dynamic discipline at every level, from singular signaling pathways to broader systems-level views of organismal development. Proper interrogation of such a complex and multi-layered environment necessitates a convergence of disciplines and areas of expertise to guide the design and engineering of environments that enable proper design, sensing, and interrogation of biology in 4D. We believe the selfsame multi-disciplinarity that initially conceptualized and defined the field of hydrogel biomaterials will provide it its requisite impetus to pose and answer the next generation of questions and develop newer theranostic modalities. Specifically, we envision the next frontier of biomaterials science and engineering to be enabled by disciplines previously thought to be fully orthogonal, such as optogenetics, *de novo* protein design, high-throughput materials discovery, and advanced analytics tools. While challenging to bridge together all these sets of expertise within the umbrella of a singular lab, it will become all the more

necessary in the medium to long term for these synergies to be captured if the field is to converge onto solutions to its longest standing problems.

Acknowledgements

This work was supported by a Faculty Early Career Development CAREER Award (DMR 1652141, C.A.D.), a grant (DMR 1807398, C.A.D.) from the National Science Foundation, and a Maximizing Investigators' Research Award (R35GM138036, C.A.D.) from the National Institutes of Health. R.G. was supported by a John C. Berg Endowed Fellowship, and R.M.F. was supported by an ITHS-TL1 Fellowship.

Author contributions

R.G. and C.A.D. discussed and wrote this review with feedback from R.M.F. Figures were prepared by R.M.F. with input from R.G. and C.A.D.

References

1. Peppas, N. A., Hilt, J. Z., Khademhosseini, A. & Langer, R. Hydrogels in Biology and Medicine: From Molecular Principles to Bionanotechnology. *Adv. Mater.* **18**, 1345–1360 (2006).
2. Hoffman, A. S. Hydrogels for biomedical applications. *Adv. Drug Deliv. Rev.* **64**, 18–23 (2012).
3. Qazi, T. H. *et al.* Programming hydrogels to probe spatiotemporal cell biology. *Cell Stem Cell* **29**, 678–691 (2022).
4. Mandal, A., Clegg, J. R., Anselmo, A. C. & Mitragotri, S. Hydrogels in the clinic. *Bioeng. Transl. Med.* **5**, e10158 (2020).
5. Correa, S. *et al.* Translational Applications of Hydrogels. *Chem. Rev.* **121**, 11385–11457 (2021).

6. Unal, A. Z. & West, J. L. Synthetic ECM: Bioactive Synthetic Hydrogels for 3D Tissue Engineering. *Bioconjug. Chem.* **31**, 2253–2271 (2020).

7. Muir, V. G. & Burdick, J. A. Chemically Modified Biopolymers for the Formation of Biomedical Hydrogels. *Chem. Rev.* **121**, 10908–10949 (2021).

8. Gao, Y., Peng, K. & Mitragotri, S. Covalently Crosslinked Hydrogels via Step-Growth Reactions: Crosslinking Chemistries, Polymers, and Clinical Impact. *Adv. Mater.* **33**, (2021).

9. Nimmo, C. M. & Shoichet, M. S. Regenerative biomaterials that 'click': Simple, aqueous-based protocols for hydrogel synthesis, surface immobilization, and 3D patterning. *Bioconjug. Chem.* **22**, 2199–2209 (2011).

10. Zhang, W., Ye, W. & Yan, Y. Advances in Photocrosslinkable Materials for 3D Bioprinting. *Adv. Eng. Mater.* **24**, 2100663 (2022).

11. Kolb, H. C., Finn, M. G. & Sharpless, K. B. Click Chemistry: Diverse Chemical Function from a Few Good Reactions. *Angew. Chem. Int. Ed.* **40**, 2004–2021 (2001).

12. Agard, N. J., Prescher, J. A. & Bertozzi, C. R. A strain-promoted [3 + 2] azide-alkyne cycloaddition for covalent modification of biomolecules in living systems. *J. Am. Chem. Soc.* **126**, 15046–15047 (2004).

13. McKay, C. S. & Finn, M. G. Click Chemistry in Complex Mixtures: Bioorthogonal Bioconjugation. *Chem. Biol.* **21**, 1075–1101 (2014).

14. DeForest, C. A., Polizzotti, B. D. & Anseth, K. S. Sequential click reactions for synthesizing and patterning three-dimensional cell microenvironments. *Nat. Mater.* **8**, 659–664 (2009).

15. Steinhilber, D. *et al.* A Microgel Construction Kit for Bioorthogonal Encapsulation and pH-Controlled Release of Living Cells. *Angew. Chem. Int. Ed.* **52**, 13538–13543 (2013).

16. Su, X. *et al.* An injectable PEG-based hydrogel synthesized by strain-promoted alkyne–azide cycloaddition for use as an embolic agent. *RSC Adv.* **6**, 2904–2909 (2016).

17. Nimmo, C. M., Owen, S. C. & Shoichet, M. S. Diels-Alder Click Cross-Linked Hyaluronic Acid Hydrogels for Tissue Engineering. *Biomacromolecules* **12**, 824–830 (2011).

18. Smith, L. J. *et al.* Diels-Alder Click-Cross-Linked Hydrogels with Increased Reactivity Enable 3D Cell Encapsulation. *Biomacromolecules* **19**, 926–935 (2018).

19. Bailey, S. J. *et al.* Rational mechanochemical design of Diels–Alder crosslinked biocompatible hydrogels with enhanced properties. *Mater. Horiz.* **9**, 1947–1953 (2022).

20. Yan, J. *et al.* Injectable Diels–Alder cycloaddition hydrogels with tuneable gelation, stiffness and degradation for the sustained release of T-lymphocytes. *J. Mater. Chem. B* **10**, 3329–3343 (2022).

21. Ilochonwu, B. C. *et al.* Thermo-responsive Diels-Alder stabilized hydrogels for ocular drug delivery of a corticosteroid and an anti-VEGF fab fragment. *J. Controlled Release* **361**, 334–349 (2023).

22. Devaraj, N. K., Weissleder, R. & Hilderbrand, S. A. Tetrazine-Based Cycloadditions: Application to Pretargeted Live Cell Imaging. *Bioconjug. Chem.* **19**, 2297–2299 (2008).

23. Devaraj, N. K., Thurber, G. M., Keliher, E. J., Marinelli, B. & Weissleder, R. Reactive polymer enables efficient in vivo bioorthogonal chemistry. *Proc. Natl. Acad. Sci.* **109**, 4762–4767 (2012).

24. Karver, M. R., Weissleder, R. & Hilderbrand, S. A. Bioorthogonal Reaction Pairs Enable Simultaneous, Selective, Multi-Target Imaging. *Angew. Chem. Int. Ed.* **51**, 920–922 (2012).

25. Alge, D. L., Azagarsamy, M. A., Donohue, D. F. & Anseth, K. S. Synthetically tractable click hydrogels for three-dimensional cell culture formed using tetrazine-norbornene chemistry. *Biomacromolecules* **14**, 949–953 (2013).

26. Šečkutė, J. & Devaraj, N. K. Expanding room for tetrazine ligations in the in vivo chemistry toolbox. *Curr. Opin. Chem. Biol.* **17**, 761–767 (2013).

27. L. Oliveira, B., Guo, Z. & L. Bernardes, G. J. Inverse electron demand Diels–Alder reactions in chemical biology. *Chem. Soc. Rev.* **46**, 4895–4950 (2017).

28. Gultian, K. A., Gandhi, R., Kim, T. W. B. & Vega, S. L. Self-Forming Norbornene-Tetrazine Hydrogels with Independently Tunable Properties. *Macromol. Biosci.* **23**, 2200425 (2023).

29. Lueckgen, A. *et al.* Hydrolytically-degradable click-crosslinked alginate hydrogels. *Biomaterials* **181**, 189–198 (2018).

30. Collins, J., Xiao, Z., Müllner, M. & A. Connal, L. The emergence of oxime click chemistry and its utility in polymer science. *Polym. Chem.* **7**, 3812–3826 (2016).

31. Grover, G. N., Lam, J., Nguyen, T. H., Segura, T. & Maynard, H. D. Biocompatible Hydrogels by Oxime Click Chemistry. *Biomacromolecules* **13**, 3013–3017 (2012).

32. Lin, F. *et al.* Peptide-Functionalized Oxime Hydrogels with Tunable Mechanical Properties and Gelation Behavior. *Biomacromolecules* **14**, 3749–3758 (2013).

33. Zander, Z. K., Hua, G., Wiener, C. G., Vogt, B. D. & Becker, M. L. Control of Mesh Size and Modulus by Kinetically Dependent Cross-Linking in Hydrogels. *Adv. Mater.* **27**, 6283–6288 (2015).

34. Baker, A. E. G. *et al.* Stable oxime-crosslinked hyaluronan-based hydrogel as a biomimetic vitreous substitute. *Biomaterials* **271**, 120750–120750 (2021).

35. Baker, A. E. G., Tam, R. Y. & Shoichet, M. S. Independently Tuning the Biochemical and Mechanical Properties of 3D Hyaluronan-Based Hydrogels with Oxime and Diels–Alder Chemistry to Culture Breast Cancer Spheroids. *Biomacromolecules* **18**, 4373–4384 (2017).

36. Hoyle, C. E., Lowe, A. B. & Bowman, C. N. Thiol-click chemistry: A multifaceted toolbox for small molecule and polymer synthesis. *Chem. Soc. Rev.* **39**, 1355–1387 (2010).

37. Hoyle, C. E. & Bowman, C. N. Thiol–Ene Click Chemistry. *Angew. Chem. Int. Ed.* **49**, 1540–1573 (2010).

38. Nair, D. P. *et al.* The Thiol-Michael Addition Click Reaction: A Powerful and Widely Used Tool in Materials Chemistry. *Chem. Mater.* **26**, 724–744 (2014).

39. Khan, Z. M., Wilts, E., Vlaisavljevich, E., Long, T. E. & Verbridge, S. S. Characterization and structure-property relationships of an injectable thiol-Michael addition hydrogel toward compatibility with glioblastoma therapy. *Acta Biomater.* **144**, 266–278 (2022).

40. Gilchrist, A. E. *et al.* Encapsulation of murine hematopoietic stem and progenitor cells in a thiol-crosslinked maleimide-functionalized gelatin hydrogel. *Acta Biomater.* **131**, 138–148 (2021).

41. Xue, B. *et al.* Engineering hydrogels with homogeneous mechanical properties for controlling stem cell lineage specification. *Proc. Natl. Acad. Sci. U. S. A.* **118**, (2021).

42. Agouridas, V. *et al.* Native Chemical Ligation and Extended Methods: Mechanisms, Catalysis, Scope, and Limitations. *Chem. Rev.* **119**, 7328–7443 (2019).

43. Hu, B. H., Su, J. & Messersmith, P. B. Hydrogels cross-linked by native chemical ligation. *Biomacromolecules* **10**, 2194–2200 (2009).

44. Su, J., Hu, B. H., Lowe, W. L., Kaufman, D. B. & Messersmith, P. B. Anti-inflammatory peptide-functionalized hydrogels for insulin-secreting cell encapsulation. *Biomaterials* **31**, 308–314 (2010).

45. Strehin, I., Gourevitch, D., Zhang, Y., Heber-Katz, E. & Messersmith, P. B. Hydrogels formed by oxo-ester mediated native chemical ligation. *Biomater. Sci.* **1**, 603–613 (2013).

46. Jin, M., Koçer, G. & Paez, J. I. Luciferin-Bioinspired Click Ligation Enables Hydrogel Platforms with Fine-Tunable Properties for 3D Cell Culture. *ACS Appl. Mater. Interfaces* **14**, 5017–5032 (2022).

47. Schauenburg, D., Osuna Gálvez, A. & Bode, J. W. Covalently functionalized amide cross-linked hydrogels from primary amines and polyethylene glycol acyltrifluoroborates (PEG-KATs). *J. Mater. Chem. B* **6**, 4775–4782 (2018).

48. Truong, V. X., Donderwinkel, I. & Frith, J. E. Bioorthogonal hydrogels by thiol–halide click crosslinking with fast gelation time and tunable stability in aqueous media. *J. Polym. Sci. Part Polym. Chem.* **57**, 1872–1876 (2019).

49. Huynh, C. T., Liu, F., Cheng, Y., Coughlin, K. A. & Alsberg, E. Thiol-Epoxy 'click' Chemistry to Engineer Cytocompatible PEG-Based Hydrogel for siRNA-Mediated Osteogenesis of hMSCs. *ACS Appl. Mater. Interfaces* **10**, 25936–25942 (2018).

50. Paez, J. I., Farrukh, A., Valbuena-Mendoza, R., Włodarczyk-Biegun, M. K. & Del Campo, A. Thiol-Methylsulfone-Based Hydrogels for 3D Cell Encapsulation. *ACS Appl. Mater. Interfaces* **12**, 8062–8072 (2020).

51. Kong, N. & Li, H. Protein Fragment Reconstitution as a Driving Force for Self-Assembling Reversible Protein Hydrogels. *Adv. Funct. Mater.* **25**, 5593–5601 (2015).

52. Zakeri, B. *et al.* Peptide tag forming a rapid covalent bond to a protein, through engineering a bacterial adhesin. *Proc. Natl. Acad. Sci. U. S. A.* **109**, E690–E697 (2012).

53. Sun, F., Zhang, W. B., Mahdavi, A., Arnold, F. H. & Tirrell, D. A. Synthesis of bioactive protein hydrogels by genetically encoded SpyTag-SpyCatcher chemistry. *Proc. Natl. Acad. Sci. U. S. A.* **111**, 11269–11274 (2014).

54. Gao, X., Fang, J., Xue, B., Fu, L. & Li, H. Engineering Protein Hydrogels Using SpyCatcher-SpyTag Chemistry. *Biomacromolecules* **17**, 2812–2819 (2016).

55. Peschke, T. *et al.* Self-Assembling All-Enzyme Hydrogels for Flow Biocatalysis. *Angew. Chem. - Int. Ed.* **57**, 17028–17032 (2018).

56. Yang, Z. *et al.* Dynamically Tunable, Macroscopic Molecular Networks Enabled by Cellular Synthesis of 4-Arm Star-like Proteins. *Matter* **2**, 233–249 (2020).

57. Keeble, A. H. *et al.* Approaching infinite affinity through engineering of peptide-protein interaction. *Proc. Natl. Acad. Sci. U. S. A.* **116**, 26523–26533 (2019).

58. Veggiani, G. *et al.* Programmable polyproteams built using twin peptide superglues. *Proc. Natl. Acad. Sci. U. S. A.* **113**, 1202–1207 (2016).

59. Huang, P. S., Boyken, S. E. & Baker, D. The coming of age of de novo protein design. *Nature* **537**, 320–327 (2016).

60. Chen, Z. *et al.* Programmable design of orthogonal protein heterodimers. *Nature* **565**, 106–111 (2019).

61. Shah, N. H. & Muir, T. W. Inteins: Nature's gift to protein chemists. *Chem. Sci.* **5**, 446–461 (2014).

62. Ramirez, M., Guan, D., Ugaz, V. & Chen, Z. Intein-triggered artificial protein hydrogels that support the immobilization of bioactive proteins. *J. Am. Chem. Soc.* **135**, 5290–5293 (2013).

63. Pinto, F., Thornton, E. L. & Wang, B. An expanded library of orthogonal split inteins enables modular multi-peptide assemblies. *Nat. Commun. 2020 111* **11**, 1–15 (2020).

64. Mantooth, S. M., Munoz-Robles, B. G. & Webber, M. J. Dynamic Hydrogels from Host–Guest Supramolecular Interactions. *Macromol. Biosci.* **19**, 1–12 (2019).

65. Xiao, T. *et al.* Dynamic hydrogels mediated by macrocyclic host-guest interactions. *J. Mater. Chem. B* **7**, 1526–1540 (2019).

66. Zhao, Y. L. & Fraser Stoddart, J. Azobenzene-based light-responsive hydrogel system. *Langmuir* **25**, 8442–8446 (2009).

67. Rodell, C. B., Kaminski, A. L. & Burdick, J. A. Rational design of network properties in guest-host assembled and shear-thinning hyaluronic acid hydrogels. *Biomacromolecules* **14**, 4125–4134 (2013).

68. Mealy, J. E., Rodell, C. B. & Burdick, J. A. Sustained small molecule delivery from injectable hyaluronic acid hydrogels through host-guest mediated retention. *J. Mater. Chem. B* **3**, 8010–8019 (2015).

69. Webber, M. J. & Langer, R. Drug delivery by supramolecular design. *Chem. Soc. Rev.* **46**, 6600–6620 (2017).

70. Cao, L. *et al.* Cucurbit[7]uril·Guest Pair with an Attomolar Dissociation Constant. *Angew. Chem. Int. Ed.* **53**, 988–993 (2014).

71. Zou, L., Braegelman, A. S. & Webber, M. J. Dynamic Supramolecular Hydrogels Spanning an Unprecedented Range of Host-Guest Affinity. *ACS Appl. Mater. Interfaces* 8–13 (2019).

72. Zou, L., Braegelman, A. S. & Webber, M. J. Spatially Defined Drug Targeting by in Situ Host-Guest Chemistry in a Living Animal. *ACS Cent. Sci.* **5**, 1035–1043 (2019).

73. Tuncaboylu, D. C., Sari, M., Oppermann, W. & Okay, O. Tough and self-healing hydrogels formed via hydrophobic interactions. *Macromolecules* **44**, 4997–5005 (2011).

74. Tuncaboylu, D. C., Argun, A., Sahin, M., Sari, M. & Okay, O. Structure optimization of self-healing hydrogels formed via hydrophobic interactions. *Polymer* **53**, 5513–5522 (2012).

75. Petka, W. A., Harden, J. L., McGrath, K. P., Wirtz, D. & Tirrell, D. A. Reversible hydrogels from self-assembling artificial proteins. *Science* **281**, 389–392 (1998).

76. Wang, C., Stewart, R. J. & Kopeček, J. Hybrid hydrogels assembled from synthetic polymers and coiled-coil protein domains. *Nature* **397**, 417–420 (1999).

77. Jorgensen, M. D. & Chmielewski, J. Recent advances in coiled-coil peptide materials and their biomedical applications. *Chem. Commun.* **58**, 11625–11636 (2022).

78. Shen, W., Kornfield, J. A. & Tirrell, D. A. Dynamic Properties of Artificial Protein Hydrogels Assembled through Aggregation of Leucine Zipper Peptide Domains. *Macromolecules* **40**, 689–692 (2007).

79. Dooling, L. J. & Tirrell, D. A. Engineering the Dynamic Properties of Protein Networks through Sequence Variation. *ACS Cent. Sci.* **2**, 812–819 (2016).

80. Jiang, X. *et al.* A Bi-Layer Hydrogel Cardiac Patch Made of Recombinant Functional Proteins. *Adv. Mater.* **34**, 2201411–2201411 (2022).

81. Wong Po Foo, C. T. S., Lee, J. S., Mulyasasmita, W., Parisi-Amon, A. & Heilshorn, S. C. Two-component protein-engineered physical hydrogels for cell encapsulation. *Proc. Natl. Acad. Sci. U. S. A.* **106**, 22067–22072 (2009).

82. Mulyasasmita, W., Lee, J. S. & Heilshorn, S. C. Molecular-level engineering of protein physical hydrogels for predictive sol-gel phase behavior. *Biomacromolecules* **12**, 3406–3411 (2011).

83. Parisi-Amon, A., Mulyasasmita, W., Chung, C. & Heilshorn, S. C. Protein-Engineered Injectable Hydrogel to Improve Retention of Transplanted Adipose-Derived Stem Cells. *Adv. Healthc. Mater.* **2**, 428–432 (2013).

84. Dubbin, K. *et al.* Dual-Stage Crosslinking of a Gel-Phase Bioink Improves Cell Viability and Homogeneity for 3D Bioprinting. *Adv. Healthc. Mater.* **5**, 2488–2492 (2016).

85. Lu, H. D., Charati, M. B., Kim, I. L. & Burdick, J. A. Injectable shear-thinning hydrogels engineered with a self-assembling Dock-and-Lock mechanism. *Biomaterials* **33**, 2145–2153 (2012).

86. Soranno, D. E., Lu, H. D., Weber, H. M., Rai, R. & Burdick, J. A. Immunotherapy with injectable hydrogels to treat obstructive nephropathy. *J. Biomed. Mater. Res. A* **102**, 2173–2180 (2014).

87. Yamaguchi, N. *et al.* Growth factor mediated assembly of cell receptor-responsive hydrogels. *J. Am. Chem. Soc.* **129**, 3040–3041 (2007).

88. de la Torre, D. & Chin, J. W. Reprogramming the genetic code. *Nat. Rev. Genet.* **22**, 169–184 (2021).

89. Seeman, N. C. & Sleiman, H. F. DNA nanotechnology. *Nat. Rev. Mater.* **3**, (2017).

90. Shahbazi, M.-A., Bauleth-Ramos, T. & Santos, H. A. DNA Hydrogel Assemblies: Bridging Synthesis Principles to Biomedical Applications. *Adv. Ther.* **1**, 1800042 (2018).

91. Cheng, E. *et al.* A pH-Triggered, Fast-Responding DNA Hydrogel. *Angew. Chem. Int. Ed.* **48**, 7660–7663 (2009).

92. Xing, Y. *et al.* Self-assembled DNA hydrogels with designable thermal and enzymatic responsiveness. *Adv. Mater.* **23**, 1117–1121 (2011).

93. Guo, W. *et al.* pH-stimulated DNA hydrogels exhibiting shape-memory properties. *Adv. Mater.* **27**, 73–78 (2014).

94. Nele, V., Wojciechowski, J. P., Armstrong, J. P. K. & Stevens, M. M. Tailoring Gelation Mechanisms for Advanced Hydrogel Applications. *Adv. Funct. Mater.* **30**, 2002759 (2020).

95. Aubert, S., Bezagu, M., Spivey, A. C. & Arseniyadis, S. Spatial and temporal control of chemical processes. *Nat. Rev. Chem.* **3**, 706–722 (2019).

96. Fadeev, M. *et al.* Redox-triggered hydrogels revealing switchable stiffness properties and shape-memory functions. *Polym. Chem.* **9**, 2905–2912 (2018).

97. Prasannan, A., Tsai, H.-C., Chen, Y.-S. & Hsiue, G.-H. A thermally triggered in situ hydrogel from poly(acrylic acid-co-N-isopropylacrylamide) for controlled release of anti-glaucoma drugs. *J. Mater. Chem. B* **2**, 1988–1997 (2014).

98. Zhao, L. *et al.* pH triggered injectable amphiphilic hydrogel containing doxorubicin and paclitaxel. *Int. J. Pharm.* **410**, 83–91 (2011).

99. Koetting, M. C., Peters, J. T., Steichen, S. D. & Peppas, N. A. Stimulus-responsive hydrogels: Theory, modern advances, and applications. *Mater. Sci. Eng. R Rep.* **93**, 1–49 (2015).

100. Williams, C. G., Malik, A. N., Kim, T. K., Manson, P. N. & Elisseeff, J. H. Variable cytocompatibility of six cell lines with photoinitiators used for polymerizing hydrogels and cell encapsulation. *Biomaterials* **26**, 1211–1218 (2005).

101. Bowman, C. N. & Kloxin, C. J. Toward an enhanced understanding and implementation of photopolymerization reactions. *AIChE J.* **54**, 2775–2795 (2008).

102. Benton, J. A., DeForest, C. A., Vivekanandan, V. & Anseth, K. S. Photocrosslinking of Gelatin Macromers to Synthesize Porous Hydrogels That Promote Valvular Interstitial Cell Function. *Tissue Eng. Part A* **15**, 3221–3230 (2009).

103. Fairbanks, B. D. *et al.* A versatile synthetic extracellular matrix mimic via thiol-norbornene photopolymerization. *Adv. Mater.* **21**, 5005–5010 (2009).

104. Lin, C. C., Ki, C. S. & Shih, H. Thiol-norbornene photoclick hydrogels for tissue engineering applications. *J. Appl. Polym. Sci.* **132**, (2015).

105. McNitt, C. D., Cheng, H., Ullrich, S., Popik, V. V. & Bjerknes, M. Multiphoton Activation of Photo-Strain-Promoted Azide Alkyne Cycloaddition 'click' Reagents Enables in Situ Labeling with Submicrometer Resolution. *J. Am. Chem. Soc.* **139**, 14029–14032 (2017).

106. Farahani, P. E., Adelmund, S. M., Shadish, J. A. & DeForest, C. A. Photomediated oxime ligation as a bioorthogonal tool for spatiotemporally-controlled hydrogel formation and modification. *J. Mater. Chem. B* **5**, 4435–4442 (2017).

107. Truong, V. X. & Barner-Kowollik, C. Red-Light Driven Photocatalytic Oxime Ligation for Bioorthogonal Hydrogel Design. *ACS Macro Lett.* **10**, 78–83 (2021).

108. Truong, V. X., Li, F. & Forsythe, J. S. Versatile Bioorthogonal Hydrogel Platform by Catalyst-Free Visible Light Initiated Photodimerization of Anthracene. *ACS Macro Lett.* **6**, 657–662 (2017).

109. Mayer, S. V., Murnauer, A., von Wrisberg, M.-K., Jokisch, M.-L. & Lang, K. Photo-induced and Rapid Labeling of Tetrazine-Bearing Proteins via Cyclopropenone-Caged Bicyclononynes. *Angew. Chem. Int. Ed.* **58**, 15876–15882 (2019).

110. Jiang, S. *et al.* Ring-Strain-Promoted Ultrafast Diaryltetrazole–Alkyne Photoclick Reactions Triggered by Visible Light. *ChemPhotoChem* **4**, 327–331 (2020).

111. Sperinde, J. J. & Griffith, L. G. Synthesis and Characterization of Enzymatically-Cross-Linked Poly(ethylene glycol) Hydrogels. *Macromolecules* **30**, 5255–5264 (1997).

112. Hu, B. H. & Messersmith, P. B. Rational Design of Transglutaminase Substrate Peptides for Rapid Enzymatic Formation of Hydrogels. *J. Am. Chem. Soc.* **125**, 14298–14299 (2003).

113. Moreira Teixeira, L. S., Feijen, J., van Blitterswijk, C. A., Dijkstra, P. J. & Karperien, M. Enzyme-catalyzed crosslinkable hydrogels: Emerging strategies for tissue engineering. *Biomaterials* **33**, 1281–1290 (2012).

114. Kim, M. *et al.* Novel enzymatic cross-linking–based hydrogel nanofilm caging system on pancreatic β cell spheroid for long-term blood glucose regulation. *Sci. Adv.* **7**, 7832–7855 (2021).

115. Um, S. H. *et al.* Enzyme-catalysed assembly of DNA hydrogel. *Nat. Mater.* **5**, 797–801 (2006).

116. Nöll, T., Wenderhold-Reeb, S., Schönherr, H. & Nöll, G. Pristine DNA Hydrogels from Biotechnologically Derived Plasmid DNA. *Angew. Chem. - Int. Ed.* **56**, 12004–12008 (2017).

117. Heinen, L., Heuser, T., Steinschulte, A. & Walther, A. Antagonistic Enzymes in a Biocatalytic pH Feedback System Program Autonomous DNA Hydrogel Life Cycles. *Nano Lett.* **17**, 4989–4995 (2017).

118. Stoltenburg, R., Reinemann, C. & Strehlitz, B. SELEX—A (r)evolutionary method to generate high-affinity nucleic acid ligands. *Biomol. Eng.* **24**, 381–403 (2007).

119. Yang, H., Liu, H., Kang, H. & Tan, W. Engineering Target-Responsive Hydrogels Based on Aptamer-Target Interactions. *J. Am. Chem. Soc.* **130**, 6320–6321 (2008).

120. Li, F., Lyu, D., Liu, S. & Guo, W. DNA Hydrogels and Microgels for Biosensing and Biomedical Applications. *Adv. Mater.* **32**, 1–9 (2020).

121. Soontornworajit, B., Zhou, J., Shaw, M. T., Fan, T. H. & Wang, Y. Hydrogel functionalization with DNA aptamers for sustained PDGF-BB release. *Chem. Commun.* **46**, 1857–1859 (2010).

122. Bae, S. W., Lee, J. S., Harms, V. M. & Murphy, W. L. Dynamic, Bioresponsive Hydrogels via Changes in DNA Aptamer Conformation. *Macromol. Biosci.* **19**, 1–6 (2019).

123. Stejskalová, A., Oliva, N., England, F. J. & Almquist, B. D. Biologically Inspired, Cell-Selective Release of Aptamer-Trapped Growth Factors by Traction Forces. *Adv. Mater.* **31**, 1806380 (2019).

124. Augst, A. D., Kong, H. J. & Mooney, D. J. Alginate Hydrogels as Biomaterials. *Macromol. Biosci.* **6**, 623–633 (2006).

125. Kouwer, P. H. J. *et al.* Responsive biomimetic networks from polyisocyanopeptide hydrogels. *Nature* **493**, 651–655 (2013).

126. Wu, S. *et al.* Poly(vinyl alcohol) Hydrogels with Broad-Range Tunable Mechanical Properties via the Hofmeister Effect. *Adv. Mater.* **33**, 1–9 (2021).

127. Ali, M. M. *et al.* Rolling circle amplification: A versatile tool for chemical biology, materials science and medicine. *Chem. Soc. Rev.* **43**, 3324–3341 (2014).

128. Yao, C. *et al.* Double Rolling Circle Amplification Generates Physically Cross-Linked DNA Network for Stem Cell Fishing. *J. Am. Chem. Soc.* **142**, 3422–3429 (2020).

129. Yao, C., Zhang, R., Tang, J. & Yang, D. Rolling circle amplification (RCA)-based DNA hydrogel. *Nat. Protoc.* **16**, 5460–5483 (2021).

130. Guo, W. *et al.* Switchable Bifunctional Stimuli-Triggered Poly-N-Isopropylacrylamide/DNA Hydrogels. *Angew. Chem. Int. Ed.* **53**, 10134–10138 (2014).

131. Wang, J. *et al.* Clamped Hybridization Chain Reactions for the Self-Assembly of Patterned DNA Hydrogels. *Angew. Chem. - Int. Ed.* **56**, 2171–2175 (2017).

132. Bi, S., Yue, S. & Zhang, S. Hybridization chain reaction: a versatile molecular tool for biosensing, bioimaging, and biomedicine. *Chem. Soc. Rev.* **46**, 4281–4298 (2017).

133. Ye, D. *et al.* Encapsulation and release of living tumor cells using hydrogels with the hybridization chain reaction. *Nat. Protoc.* **15**, 2163–2185 (2020).

134. Yu, F., Cao, X., Li, Y. & Chen, X. Diels-Alder Click-Based Hydrogels for Direct Spatiotemporal Postpatterning via Photoclick Chemistry. *ACS Macro Lett.* **4**, 289–292 (2015).

135. DeForest, C. A. & Anseth, K. S. Cytocompatible click-based hydrogels with dynamically tunable properties through orthogonal photoconjugation and photocleavage reactions. *Nat. Chem.* **3**, 925–931 (2011).

136. Kloxin, C. J. & Bowman, C. N. Covalent adaptable networks: Smart, reconfigurable and responsive network systems. *Chem. Soc. Rev.* **42**, 7161–7173 (2013).

137. McBride, M. K. *et al.* Enabling Applications of Covalent Adaptable Networks. *Annu. Rev. Chem. Biomol. Eng.* **10**, 175–198 (2019).

138. Rizwan, M., Baker, A. E. G. & Shoichet, M. S. Designing Hydrogels for 3D Cell Culture Using Dynamic Covalent Crosslinking. *Adv. Healthc. Mater.* **10**, 1–23 (2021).

139. Chen, X. *et al.* A Thermally Re-mendable Cross-Linked Polymeric Material. *Science* **295**, 1698–1702 (2002).

140. Deng, G., Tang, C., Li, F., Jiang, H. & Chen, Y. Covalent Cross-Linked Polymer Gels with Reversible Sol−Gel Transition and Self-Healing Properties. *Macromolecules* **43**, 1191–1194 (2010).

141. Wang, H. & Heilshorn, S. C. Adaptable Hydrogel Networks with Reversible Linkages for Tissue Engineering. *Adv. Mater.* **27**, 3717–3736 (2015).

142. McKinnon, D. D., Domaille, D. W., Cha, J. N. & Anseth, K. S. Biophysically defined and cytocompatible covalently adaptable networks as viscoelastic 3D cell culture systems. *Adv. Mater.* **26**, 865–872 (2014).

143. Wei, Z. *et al.* Dextran-Based Self-Healing Hydrogels Formed by Reversible Diels–Alder Reaction under Physiological Conditions. *Macromol. Rapid Commun.* **34**, 1464–1470 (2013).

144. Kirchhof, S., Brandl, F. P., Hammer, N. & Goepferich, A. M. Investigation of the Diels–Alder reaction as a cross-linking mechanism for degradable poly(ethylene glycol) based hydrogels. *J. Mater. Chem. B* **1**, 4855–4864 (2013).

145. Grover, G. N., Braden, R. L. & Christman, K. L. Oxime Cross-Linked Injectable Hydrogels for Catheter Delivery. *Adv. Mater.* **25**, 2937–2942 (2013).

146. Richardson, B. M. *et al.* Viscoelasticity of hydrazone crosslinked poly(ethylene glycol) hydrogels directs chondrocyte morphology during mechanical deformation. *Biomater. Sci.* **8**, 3804–3811 (2020).

147. Brown, T. E. *et al.* Photopolymerized dynamic hydrogels with tunable viscoelastic properties through thioester exchange. *Biomaterials* **178**, 496–503 (2018).

148. Ying, H., Zhang, Y. & Cheng, J. Dynamic urea bond for the design of reversible and self-healing polymers. *Nat. Commun.* **5**, 3218 (2014).

149. Cromwell, O. R., Chung, J. & Guan, Z. Malleable and Self-Healing Covalent Polymer Networks through Tunable Dynamic Boronic Ester Bonds. *J. Am. Chem. Soc.* **137**, 6492–6495 (2015).

150. Yesilyurt, V. *et al.* Mixed Reversible Covalent Crosslink Kinetics Enable Precise, Hierarchical Mechanical Tuning of Hydrogel Networks. *Adv. Mater.* **29**, 1–6 (2017).

151. Yang, H., Ghiassinejad, S., van Ruymbeke, E. & Fustin, C.-A. Tunable Interpenetrating Polymer Network Hydrogels Based on Dynamic Covalent Bonds and Metal–Ligand Bonds. *Macromolecules* **53**, 6956–6967 (2020).

152. Gao, X., Lyu, S. & Li, H. Decorating a Blank Slate Protein Hydrogel: A General and Robust Approach for Functionalizing Protein Hydrogels. *Biomacromolecules* **18**, 3726–3732 (2017).

153. Luo, J., Liu, X., Yang, Z. & Sun, F. Synthesis of Entirely Protein-Based Hydrogels by Enzymatic Oxidation Enabling Water-Resistant Bioadhesion and Stem Cell Encapsulation. *ACS Appl. Bio Mater.* **1**, 1735–1740 (2018).

154. Hammer, J. A., Ruta, A., Therien, A. M. & West, J. L. Cell-Compatible, Site-Specific Covalent Modification of Hydrogel Scaffolds Enables User-Defined Control over Cell-Material Interactions. *Biomacromolecules* **20**, 2486–2493 (2019).

155. Cambria, E. *et al.* Covalent Modification of Synthetic Hydrogels with Bioactive Proteins via Sortase-Mediated Ligation. *Biomacromolecules* **16**, 2316–2326 (2015).

156. Valdez, J. *et al.* On-demand dissolution of modular, synthetic extracellular matrix reveals local epithelial-stromal communication networks. *Biomaterials* **130**, 90–103 (2017).

157. Arkenberg, M. R., Moore, D. M. & Lin, C. C. Dynamic control of hydrogel crosslinking via sortase-mediated reversible transpeptidation. *Acta Biomater.* **83**, 83–95 (2019).

158. Bretherton, R. C. *et al.* User-Controlled 4D Biomaterial Degradation with Substrate-Selective Sortase Transpeptidases for Single-Cell Biology. *Adv. Mater.* **35**, 2209904 (2023).

159. English, M. A. *et al.* Programmable CRISPR-responsive smart materials. *Science* **785**, 780–785 (2019).

160. Gayet, R. V. *et al.* Creating CRISPR-responsive smart materials for diagnostics and programmable cargo release. *Nat. Protoc.* **15**, (2020).

161. Sakiyama-Elbert, S. E. Incorporation of heparin into biomaterials. *Acta Biomater.* **10**, 1581–1587 (2014).

162. Burgess, W. H. & Maciag, T. The Heparin-Binding (fibroblast) Growth Factor Family of Proteins. *Annu. Rev. Biochem.* **58**, 575–602 (1989).

163. Hudalla, G. A. & Murphy, W. L. Biomaterials that Regulate Growth Factor Activity via Bioinspired Interactions. *Adv. Funct. Mater.* **21**, 1754–1768 (2011).

164. Liang, Y. & Kiick, K. L. Heparin-functionalized polymeric biomaterials in tissue engineering and drug delivery applications. *Acta Biomater.* **10**, 1588–1600 (2014).

165. Ehrbar, M., Schoenmakers, R., Christen, E. H., Fussenegger, M. & Weber, W. Drug-sensing hydrogels for the inducible release of biopharmaceuticals. *Nat. Mater.* **7**, 800–804 (2008).

166. Gübeli, R. J., Ehrbar, M., Fussenegger, M., Friedrich, C. & Weber, W. Synthesis and Characterization of PEG-Based Drug-Responsive Biohybrid Hydrogels. *Macromol. Rapid Commun.* **33**, 1280–1285 (2012).

167. Gübeli, R. J. *et al.* Pharmacologically Triggered Hydrogel for Scheduling Hepatitis B Vaccine Administration. *Sci. Rep.* **3**, 2610 (2013).

168. Gübeli, R. J. *et al.* Pharmacologically tunable polyethylene-glycol-based cell growth substrate. *Acta Biomater.* **9**, 8272–8278 (2013).

169. Wu, K.-L., Bretherton, R. C., Davis, J. & DeForest, C. A. Pharmacological regulation of protein-polymer hydrogel stiffness. *RSC Adv.* **13**, 24487–24490 (2023).

170. Kong, N., Peng, Q. & Li, H. Rationally designed dynamic protein hydrogels with reversibly tunable mechanical properties. *Adv. Funct. Mater.* **24**, 7310–7317 (2014).

171. Hughes, M. D. G. *et al.* Control of Nanoscale In Situ Protein Unfolding Defines Network Architecture and Mechanics of Protein Hydrogels. *ACS Nano* **15**, 11296–11308 (2021).

172. Bian, Q., Fu, L. & Li, H. Engineering shape memory and morphing protein hydrogels based on protein unfolding and folding. *Nat. Commun.* **13**, 1–8 (2022).

173. Wang, R., Liu, M., Wang, H., Xia, J. & Li, H. GB Tags: Small Covalent Peptide Tags Based on Protein Fragment Reconstitution. *Bioconjug. Chem.* **32**, 1926–1934 (2021).

174. Wang, R., Fu, L., Liu, J. & Li, H. Decorating protein hydrogels reversibly enables dynamic presentation and release of functional protein ligands on protein hydrogels. *Chem. Commun.* **55**, 12703–12706 (2019).

175. Brudno, Y. *et al.* Refilling drug delivery depots through the blood. *Proc. Natl. Acad. Sci.* **111**, 12722–12727 (2014).

176. Badeau, B. A., Comerford, M. P., Arakawa, C. K., Shadish, J. A. & DeForest, C. A. Engineered modular biomaterial logic gates for environmentally triggered therapeutic delivery. *Nat. Chem.* **10**, 251–258 (2018).

177. Gawade, P. M., Shadish, J. A., Badeau, B. A. & DeForest, C. A. Logic-Based Delivery of Site-Specifically Modified Proteins from Environmentally Responsive Hydrogel Biomaterials. *Adv. Mater.* **31**, 1–6 (2019).

178. Ruskowitz, E. R., Comerford, M. P., Badeau, B. A. & DeForest, C. A. Logical stimuli-triggered delivery of small molecules from hydrogel biomaterials. *Biomater. Sci.* **7**, 542–546 (2019).

179. Arakawa, C.K., Gunnarsson, C., Bernabeu, M., Howard, C., Phong, K., Yang, E., DeForest, C.A., Smith, J. & Zheng, Y. Biophysical and Biomolecular Interactions of Malaria-Infected Erythrocytes in Engineered Human Capillaries. *Sci. Adv.* **6**, (2020).

180. DeForest, C. A. & Tirrell, D. A. A photoreversible protein-patterning approach for guiding stem cell fate in three-dimensional gels. *Nat. Mater.* **14**, 523–531 (2015).

181. Batalov, I., Stevens, K. R. & DeForest, C. A. Photopatterned biomolecule immobilization to guide three-dimensional cell fate in natural protein-based hydrogels. *Proc. Natl. Acad. Sci. U. S. A.* **118**, (2021).

182. Kloxin, A. M., Kasko, A. M., Salinas, C. N. & Anseth, K. S. Photodegradable Hydrogels for Dynamic Tuning of Physical and Chemical Properties. *Science* **324**, 59–63 (2009).

183. Arakawa, C. K., Badeau, B. A., Zheng, Y. & DeForest, C. A. Multicellular Vascularized Engineered Tissues through User-Programmable Biomaterial Photodegradation. *Adv. Mater.* **29**, 1703156 (2017).

184. Rapp, T. & DeForest, C. Tricolor Visible Wavelength-selective Photodegradable Hydrogel Biomaterials. *Nat. Commun.* **14**, 5250 (2023).

185. Silver, J. S. *et al.* Injury-mediated stiffening persistently activates muscle stem cells through YAP and TAZ mechanotransduction. *Sci. Adv.* **7**, 1–14 (2021).

186. Marschner, D. E. *et al.* Visible Light [2 + 2] Cycloadditions for Reversible Polymer Ligation. *Macromolecules* **51**, 3802–3807 (2018).

187. Truong, V. X., Li, F., Ercole, F. & Forsythe, J. S. Wavelength-Selective Coupling and Decoupling of Polymer Chains via Reversible [2 + 2] Photocycloaddition of Styrylpyrene for Construction of Cytocompatible Photodynamic Hydrogels. *ACS Macro Lett.* **7**, 464–469 (2018).

188. Kalayci, K., Frisch, H., Barner-Kowollik, C. & Truong, V. X. Wavelength-Dependent Stiffening of Hydrogel Matrices via Redshifted [2+2] Photocycloadditions. *Adv. Funct. Mater.* **30**, 1–9 (2020).

189. Günay, K. A. *et al.* PEG–Anthracene Hydrogels as an On-Demand Stiffening Matrix To Study Mechanobiology. *Angew. Chem. - Int. Ed.* **58**, 9912–9916 (2019).

190. DeForest, C. A. & Anseth, K. S. Photoreversible patterning of biomolecules within click-based hydrogels. *Angew. Chem. - Int. Ed.* **51**, 1816–1819 (2012).

191. Gandavarapu, N. R., Azagarsamy, M. A. & Anseth, K. S. Photo-click living strategy for controlled, reversible exchange of biochemical ligands. *Adv. Mater.* **26**, 2521–2526 (2014).

192. Grim, J. C. *et al.* A Reversible and Repeatable Thiol-Ene Bioconjugation for Dynamic Patterning of Signaling Proteins in Hydrogels. *ACS Cent. Sci.* **4**, 909–916 (2018).

193. Boyer, C. *et al.* Bioapplications of RAFT Polymerization. *Chem. Rev.* **109**, 5402–5436 (2009).

194. Brown, T. E., Marozas, I. A. & Anseth, K. S. Amplified Photodegradation of Cell-Laden Hydrogels via an Addition–Fragmentation Chain Transfer Reaction. *Adv. Mater.* **29**, (2017).

195. Salvi, A., Carrupt, P., Tillement, J. & Testa, B. Structural damage to proteins caused by free radicals: asessment, protection by antioxidants, and influence of protein binding. *Biochem. Pharmacol.* **61**, 1237–1242 (2001).

196. Ehrbar, M. *et al.* Enzymatic formation of modular cell-instructive fibrin analogs for tissue engineering. *Biomaterials* **28**, 3856–3866 (2007).

197. Mosiewicz, K. A. *et al.* In situ cell manipulation through enzymatic hydrogel photopatterning. *Nat. Mater.* **12**, 1072–1078 (2013).

198. Shadish, J. A., Benuska, G. M. & DeForest, C. A. Bioactive site-specifically modified proteins for 4D patterning of gel biomaterials. *Nat. Mater.* **18**, 1005–1014 (2019).

199. Zhang, W. *et al.* Optogenetic control with a photocleavable protein, PhoCl. *Nat. Methods* **14**, 391–394 (2017).

200. Lu, X. *et al.* Photocleavable proteins that undergo fast and efficient dissociation. *Chem. Sci.* **12**, 9658–9672 (2021).

201. McEvoy, A. L. *et al.* mMaple: A Photoconvertible Fluorescent Protein for Use in Multiple Imaging Modalities. *PLOS ONE* **7**, e51314 (2012).

202. Shadish, J. A., Strange, A. C. & DeForest, C. A. Genetically Encoded Photocleavable Linkers for Patterned Protein Release from Biomaterials. *J. Am. Chem. Soc.* **141**, 15619–15625 (2019).

203. Chapla, R., Hammer, J. A. & West, J. L. Adding Dynamic Biomolecule Signaling to Hydrogel Systems via Tethered Photolabile Cell-Adhesive Proteins. *ACS Biomater. Sci. Eng.* **8**, 208–217 (2022).

204. Xiang, D. *et al.* Hydrogels With Tunable Mechanical Properties Based on Photocleavable Proteins. *Front. Chem.* **8**, (2020).

205. Fryer, T. *et al.* Gigavalent Display of Proteins on Monodisperse Polyacrylamide Hydrogels as a Versatile Modular Platform for Functional Assays and Protein Engineering. *ACS Cent. Sci.* **8**, 1182–1195 (2022).

206. Ruskowitz, E. R. *et al.* Spatiotemporal functional assembly of split protein pairs through a light-activated SpyLigation. *Nat. Chem.* **15**, 694–704 (2023).

207. Dagliyan, O. *et al.* Computational design of chemogenetic and optogenetic split proteins. *Nat. Commun.* **9**, 4042 (2018).

208. Dolberg, T. B. *et al.* Computation-guided optimization of split protein systems. *Nat. Chem. Biol.* **17**, 531–539 (2021).

209. Nehls, E. M., Rosales, A. M. & Anseth, K. S. Enhanced user-control of small molecule drug release from a poly(ethylene glycol) hydrogel via azobenzene/cyclodextrin complex tethers. *J. Mater. Chem. B* **4**, 1035–1039 (2016).

210. Klewer, L. & Wu, Y.-W. Light-Induced Dimerization Approaches to Control Cellular Processes. *Chem. – Eur. J.* **25**, 12452–12463 (2019).

211. Lamparter, T., Esteban, B. & Hughes, J. Phytochrome Cph1 from the cyanobacterium Synechocystis PCC6803. *Eur. J. Biochem.* **268**, 4720–4730 (2001).

212. Hörner, M. *et al.* Phytochrome-Based Extracellular Matrix with Reversibly Tunable Mechanical Properties. *Adv. Mater.* **31**, 1–11 (2019).

213. Hörner, M., Hoess, P., Emig, R., Rebmann, B. & Weber, W. Synthesis of a Light-Controlled Phytochrome-Based Extracellular MatrixExtracellular matrices with Reversibly Adjustable Mechanical Properties. in *Photoswitching Proteins : Methods and Protocols* (ed. Niopek, D.) 217–231 (Springer US, 2020). doi:10.1007/978-1-0716-0755-8_15.

214. Emig, R. *et al.* Benchmarking of Cph1 Mutants and DrBphP for Light-Responsive Phytochrome-Based Hydrogels with Reversibly Adjustable Mechanical Properties. *Adv. Biol.* **6**, 2000337–2000337 (2022).

215. Hörner, M. *et al.* A Photoreceptor-Based Hydrogel with Red Light-Responsive Reversible Sol-Gel Transition as Transient Cellular Matrix. *Adv. Mater. Technol.* **8**, 2300195 (2023).

216. Kennis, J. T. M. *et al.* The LOV2 Domain of Phototropin: A Reversible Photochromic Switch. *J. Am. Chem. Soc.* **126**, 4512–4513 (2004).

217. Chin, D. & Means, A. R. Calmodulin: a prototypical calcium sensor. *Trends Cell Biol.* **10**, 322–328 (2000).

218. Liu, L. *et al.* Cyclic Stiffness Modulation of Cell-Laden Protein–Polymer Hydrogels in Response to User-Specified Stimuli Including Light. *Adv. Biosyst.* **2**, 1–9 (2018).

219. Wu, X. *et al.* Reversible hydrogels with tunable mechanical properties for optically controlling cell migration. *Nano Res. 2017 1110* **11**, 5556–5565 (2018).

220. Zhang, X. *et al.* Rational design of a photo-responsive UVR8-derived protein and a self-assembling peptide–protein conjugate for responsive hydrogel formation. *Nanoscale* **7**, 16666–16670 (2015).

221. Kolar, K., Knobloch, C., Stork, H., Žnidarič, M. & Weber, W. OptoBase: A Web Platform for Molecular Optogenetics. *ACS Synth. Biol.* **7**, 1825–1828 (2018).

222. Li, Z. *et al.* Multi-triggered Supramolecular DNA/Bipyridinium Dithienylethene Hydrogels Driven by Light, Redox, and Chemical Stimuli for Shape-Memory and Self-Healing Applications. *J. Am. Chem. Soc.* **140**, 17691–17701 (2018).

223. Liu, X. *et al.* Chemical and photochemical DNA "gears" reversibly control stiffness, shape-memory, self-healing and controlled release properties of polyacrylamide hydrogels. *Chem. Sci.* **10**, 1008–1016 (2019).

224. Fabrini, G., Minard, A., Brady, R. A., Di Antonio, M. & Di Michele, L. Cation-Responsive and Photocleavable Hydrogels from Noncanonical Amphiphilic DNA Nanostructures. *Nano Lett.* **22**, 602–611 (2022).

225. Wichterle, O. & Lím, D. Hydrophilic Gels for Biological Use. *Nature* **185**, 117–118 (1960).

226. Langer, R. & Folkman, J. Polymers for the sustained release of proteins and other macromolecules. *Nature* **263**, 797–800 (1976).

227. Korsmeyer, R. W. & Peppas, N. A. Effect of the morphology of hydrophilic polymeric matrices on the diffusion and release of water soluble drugs. *J. Membr. Sci.* **9**, 211–227 (1981).

228. Korsmeyer, R. W. & Peppas, N. A. Solute and penetrant diffusion in swellable polymers. III. Drug release from glassy poly(HEMA-co-NVP) copolymers. *J. Controlled Release* **1**, 89–98 (1984).

229. Bissell, M. J., Hall, H. G. & Parry, G. How does the extracellular matrix direct gene expression? *J. Theor. Biol.* **99**, 31–68 (1982).

230. Lin, C. Q. & Bissell, M. J. Multi-faceted regulation of cell differentiation by extracellular matrix. *FASEB J.* **7**, 737–743 (1993).

231. Langer, R. & Vacanti, J. P. Tissue Engineering. *Science* **260**, 920–926 (1993).

232. Langer, R. *et al.* Tissue Engineering: Biomedical Applications. *Tissue Eng.* **1**, 151–161 (1995).

233. Xue, K. *et al.* Hydrogels as Emerging Materials for Translational Biomedicine. *Adv. Ther.* **2**, 1800088 (2019).

234. Hunziker, E. *et al.* Translation from Research to Applications. *Tissue Eng.* **12**, 3341–64 (2007).

235. Kim, E., Yang, J., Park, S. & Shin, K. Factors Affecting Success of New Drug Clinical Trials. *Ther. Innov. Regul. Sci.* **57**, 737–750 (2023).

236. Clevers, H. Modeling Development and Disease with Organoids. *Cell* **165**, 1586–1597 (2016).

237. Hofer, M. & Lutolf, M. P. Engineering organoids. *Nat. Rev. Mater.* **6**, 402–420 (2021).

238. Takahashi, T. Organoids for Drug Discovery and Personalized Medicine. *Annu. Rev. Pharmacol. Toxicol.* **59**, 447–462 (2019).

239. Huh, D. *et al.* Reconstituting Organ-Level Lung Functions on a Chip. *Science* **328**, 1662–1668 (2010).

240. Takebe, T., Wells, J. M., Helmrath, M. A. & Zorn, A. M. Organoid Center Strategies for Accelerating Clinical Translation. *Cell Stem Cell* **22**, 806–809 (2018).

241. Choudhury, D., Ashok, A. & Naing, M. W. Commercialization of Organoids. *Trends Mol. Med.* **26**, 245–249 (2020).

242. Johnston, T. G. *et al.* Compartmentalized microbes and co-cultures in hydrogels for on-demand bioproduction and preservation. *Nat. Commun.* **11**, 563 (2020).

243. Yuan, S.-F. *et al.* Bioproduced Proteins On Demand (Bio-POD) in hydrogels using Pichia pastoris. *Bioact. Mater.* **6**, 2390–2399 (2021).

244. Liu, X., Inda, M. E., Lai, Y., Lu, T. K. & Zhao, X. Engineered Living Hydrogels. *Adv. Mater.* **34**, 2201326 (2022).

245. Vargason, A. M., Anselmo, A. C. & Mitragotri, S. The evolution of commercial drug delivery technologies. *Nat. Biomed. Eng.* **5**, 951–967 (2021).

246. Øvrebø, Ø. *et al.* Design and clinical application of injectable hydrogels for musculoskeletal therapy. *Bioeng. Transl. Med.* **7**, e10295 (2022).

247. Garg, D., Matai, I. & Sachdev, A. Toward Designing of Anti-infective Hydrogels for Orthopedic Implants: From Lab to Clinic. *ACS Biomater. Sci. Eng.* **7**, 1933–1961 (2021).

248. Kaur, G., Narayanan, G., Garg, D., Sachdev, A. & Matai, I. Biomaterials-Based Regenerative Strategies for Skin Tissue Wound Healing. *ACS Appl. Bio Mater.* **5**, 2069–2106 (2022).

249. Peña, B. *et al.* Injectable Hydrogels for Cardiac Tissue Engineering. *Macromol. Biosci.* **18**, 1800079 (2018).

250. Hughes, C. S., Postovit, L. M. & Lajoie, G. A. Matrigel: A complex protein mixture required for optimal growth of cell culture. *PROTEOMICS* **10**, 1886–1890 (2010).

251. Aisenbrey, E. A. & Murphy, W. L. Synthetic alternatives to Matrigel. *Nat. Rev. Mater.* **5**, 539–551 (2020).

252. Moura, B. S. *et al.* Advancing Tissue Decellularized Hydrogels for Engineering Human Organoids. *Adv. Funct. Mater.* **32**, 2202825 (2022).

253. Azevedo, H. S. & Mata, A. Embracing complexity in biomaterials design. *Biomater. Biosyst.* **6**, 100039 (2022).

254. Webber, M. J. Embracing simplicity in biomaterials design. *Biomater. Biosyst.* **6**, 100043 (2022).

CHAPTER 2: ENGINEERING COMPUTABILITY IN BIOMATERIALS AND BIOLOGICAL SYSTEMS

Adapted from Gharios, R. & DeForest, C.A. Engineering Computability in Biomaterials and Biological Systems. *(in preparation)*

Abstract

In less than a quarter-century, synthetic biology has galvanized research and enabled advances previously thought unattainable in fields such as biomanufacturing and biosensing. In near-record speed, the space has co-opted learnings from different disciplines and has matured from an academic curiosity into a full-fledged engineering framework with true translational promise. In parallel, developments in soft matter design and post-synthetic modulation have made possible the engineering of user-programmable biomaterials, which have enabled new frontiers in the realms of drug/cell delivery and tissue engineering, with some marketplace success. We argue that these paradigm-changing developments in both spaces take root in a refinement of our understanding of and a proper formalization of how stimulus-responsiveness is engineered into both biological systems on the one hand and biomaterials on the other. Going further, we posit that these parallel developments not only superficially cross-pollinate, but that they will soon enable truly synergistic research emanating from a convergence of the two disciplines. We

envision that this coming century of biology has much to gain from concerted efforts towards engineering truly programmable living materials that enable modulation both from the outside-in and the inside-out. In this Chapter, we highlight the key approaches that have upgraded biocomputational potential in both biological systems and biomaterials. We then shift our discussion to address the promise of design through Boolean frameworks, ending with a forward-looking perspective on the engineering of bespoke living materials.

2.1. Introduction

Synthetic biology broadly refers to methods through which native biological function can be augmented, or wholly novel function can be engineered into microorganisms.[1] This new engineering paradigm holds far-reaching consequences in bioengineering applications such as improving agricultural efficiency,[2,3] maintaining environmental sustainability,[4] and designing living therapeutics.[5–7] Promisingly, in spite of its young age, it is gaining significant traction and holds imminent market promise, with many synthetic biology-derived constructs already converted into full-fledged commercial products across different industries.[8,9]

Biomaterials science and engineering well-predates formal synthetic biology, going back to more than 2,000 years ago when precious metals constituted the material of choice in dentistry and rudimentary glass globes were used to magnify text.[10] Spurred by great strides in macromolecular theory pioneered by Staudinger,[11] the field steadily underwent a dramatic shift from a near-exclusive focus on metals as medical materials to an increasing emphasis on soft matter, which could now be rationally designed and exquisitely tuned through the then-nascent science of polymer chemistry.[12] Seminal work by Langer cemented the use of polymeric materials to engineer controlled release.[13] Bissell formalized the importance of understanding the

extracellular matrix, in addition to cell biology proper, as a pre-requisite to engineering tissues mimics *ex vivo*.[14] In parallel, steady advances made in chemical and biochemical reaction schemes led to the development and refinement of programmable biomaterials that could be modulated in time and space.[15,16] Today, the field has reached a point of maturity such that organoids can be engineered reliably *ex vivo*,[17,18] and organ physiology and pathophysiology can be faithfully recapitulated on microfluidic chips,[19] bringing much of the early hype around nanomedicine and tissue engineering closer to becoming a technological reality.

While the two fields emanate from divergent histories, both stand to benefit greatly from a unifying framework through which we could approach how a novel biological organism, material, or biohybrid construct can be engineered. Different research reports have started to blur the line between the two disciplines, with the "biologization of material science" through synthetic biology becoming increasingly prevalent.[20–22] In the same vein, extrinsic biochemical and biomechanical cues cell directly impact encapsulated cells, and the control of this niche can directly modulate encapsulated cell programs and functions.[23] It follows that thinking of advances that can bridge the two spaces holds the potential for powerful synergies.

At the heart of both efforts lies the concept of biocomputation. A forward-looking perspective on molecular logic by de Silva and Uchimaya formalized a framework in which molecular substrates can be viewed as stand-alone computational devices, sensing and actuating upon specific sets of inputs.[24] The authors posited that such a framework can find a host of killer applications in the life sciences, where the small size of biomolecules relative to semiconductors and their information richness stand out as powerful advantages. While the concept met with

some initial skepticism, it soon gained more widespread adoption as a unifying theory through which to approach design problems in biology and biomaterials. Unsurprisingly, pioneering work has since been conducted using synthetic building blocks,[25] DNA,[26] RNA,[27] and proteins[28] as computing elements, with the ultimate goal of achieving whole-cell based computations that can excel in cases where semiconductor-based computers remain inadequate.[29,30] Thus, in order to provide conceptual parallels charting the development of both fields, we could think of no better lens than biocomputation. In looking to provide a mutually exclusive and collectively exhaustive segmentation of avenues through which this computability has been engineered into living organisms and into biomaterials, we deep-dive into four main categories, or types of "circuitry": synthetic, DNA, RNA, and protein. Throughout this Chapter, we hope to bring out the relative advantages and disadvantages of each framework, with an eye towards identifying the most promising methodologies that can bridge the gap between biological systems and biomaterials.

2.2. Computability in biological systems

Computability and methods to engineer it into prokaryotes and eukaryotes has been at the center of biological research for decades. While more routine use of the term is a fairly recent phenomenon, it can be argued that "computability" in biological systems goes back fundamentally to the discovery of the *lac operon* in *Escherichia coli*,[31] and the elucidation of its role in effecting a predictably inducible metabolic switch. While rudimentary, this model could be construed as a Boolean circuit.[29]

In its most classical sense, synthetic biology – now approaching its first quarter-century – refers to the reprogramming of different microorganisms (originally bacteria) to either impart novel function or augment existing ones.[1,32] Heralded formally in 2000 with the creation of a genetic toggle-switch[33] and repressilator[34], it led to a new dawn in biological research where new functionalities now followed the design rules and terminologies of electronic circuitry and computer science. For example, recombinases could now be deployed in a targeted manner to implement DNA-encoded "memory units" into mammalian cells.[35] Autoinhibited proteases could amplify molecular queues generated by a receptor unit, effectively acting as a biological signal amplifiers.[36] Cells broadly were now referred to as "wetware", guided by synthetic circuits often built using computer-aided design. There exist multiple methods to engineer these novel functionalities, which we review and discuss below based on the type of molecular circuitry involved.

2.2.1. Synthetic circuitry

Synthetic approaches to engineering computability remain few and far between within the realm of biological organisms, at least relative to other approaches. Most often, these interventions occur from the outside-in, wherein synthetic molecules that are routinely deployed to control gene expression are modified to allow for an added degree of triggerability or tunability. For instance, in the quintessential lac operon example, Isopropyl ß-D-1-thiogalactopyranoside (IPTG) – a synthetic analog of allolactose – acts the fundamental circuit-switch in T7-RNA Polymerase-dependent expression systems; controlling and titrating the extent to which IPTG (or equivalent inducer) actuates a cell would enable robust and simple control over gene expression and downstream protein production. While soluble addition of IPTG affords temporal control over gene expression, gaining spatial control of such activation remains of interest. In this

regard, the Deiters group successfully photocaged IPTG in a single-step reaction and demonstrated spatial and temporal control over gene expression in *E. Coli* following photochemical unmasking of the native inducer,[37] with follow-up work by different groups extending this approach to different prokaryotic strains[38,39]. Similar reports demonstrated that gene expression in *E. Coli* could be photo-modulated through engineering of photocaged analogues for an array of small-molecule inducers such as erythromycin,[40] arabinose,[41] as well as carbohydrates like glucose, galactose, rhamnose, and lactose.[42] Functionally, these reports all result in light-gated logic gates and bandpass filters. In spite of their irreversibility, they allow for the titration of products generated by microbial factories, and thus hold significant biotechnological relevance. Analogous studies have been conducted in eukaryotes, where the same strategy was deployed for the photocontrol of small-molecules involved in inducible gene expression systems, such as doxycycline[43] and cyclofen,[44] among others.[45,46]

2.2.1. DNA circuitry

Using DNA as base computing element is at the cornerstone of most paradigmatic advances that have spurred synthetic biology as an engineering discipline.[47] In his famous "There's plenty of room at the bottom" lecture, Feynman posited that DNA, which by that point had a solved structure, could be used as a computing element in its own right via mechanisms such as strand displacement. Outside of this lecture's immediate relevance to the then-nascent field of nanotechnology, it was also one of the first public mentions of alternative modes of computation beyond semiconductors. Four decades later, the first synthetic gene network (in the form of bistable toggle switch) was constructed in *E. Coli*, resulting in cells that held two "memory states" that could be alternated between by controlling which repressor was getting induced.[33] The field rapidly progressed in sophistication from this origin-point, as more sophisticated

synthetic gene networks could now be constructed with relative ease. Soon thereafter, efforts shifted to building the most sophisticated synthetic networks possible equipped with true biocomputational promise. In an early landmark report outlining the similarities between synthetic gene circuits and their silicon-based counterparts, the Voigt group developed a CAD software that enables users to construct DNA circuits outfitted with 37 3-input possible Boolean logic gates in a fully automated manner.[50]

2.2.1. Protein circuitry

The targeting precision of protein-based circuitry goes beyond that of genetic or transcriptional-level modules, as these often suffer from an actuation "lag-time" and a relative lack of user control over final translated products. Another key advantage to protein-based circuitries is their direct interaction with cellular pathways without having to cause genomic modifications in the host cell. These methods remain more challenging to implement than their nucleic acid-based counterparts; however, they constitute the modality of choice when approaching problems that require fine-tuned control over protein signal presentation and dosage, such as in cell-cell communication[51] or intracellular phase separation.[52]

Perhaps the most promising form of this circuitry is protease-based signaling networks.[53–55] Proteases catalyze the irreversible hydrolysis of peptide bonds, and this ability to (in)activate proteins directly makes them promising therapeutic candidates,[56] potential activators for prodrugs,[57] or valuable reagents in preparative biochemistry.[58] Moreover, many proteases, particularly those from potyviral origins, display stringent substrate specificity, endowing them with a high degree of precision not commonly present in other input types such as light irradiation or redox state modulation. Because such proteases recognize and cleave amino acid

sequences 5-7 residues long,[58] the probability of encountering such specific sequences endogenously is low, rendering them effectively invisible to natively present proteins. Given these advantages, protease-based methods have been deployed to great effect to modulate mammalian biology, as each protease could be deployed as either an activator or repressor based on construct design.[59] A landmark example was demonstrated by the Elowitz group, who developed circuits of hacked orthogonal modular proteases (CHOMP).[60] This was the first report that used multiple orthogonal proteases (e.g., TEV, TVMV, and HCVP) *in tandem* and as composable elements to build numerous biocomputational functions into mammalian cell lines. In this tour de force, reporters are expressed in either a protease-activatable manner if a degron module (which, as the name implies, tags a biomolecule for degradation[61]) is expressed accessibly in-frame with the reporter molecule, or a protease-repressible manner if the degron is shielded upon expression until proteolytic cleavage. Moreover, by modifying reporter architecture (i.e., whether protease cleavage sequences are engineered accessibly in series, in parallel, or alternatively shielded until activation), the team successfully engineered a suite of Boolean logical operators that sense and actuate upon two orthogonal protease inputs. Additional successes reported in the manuscript include the development of an analog signal filtering modality through the engineering of an incoherent feed-forward loop motif, wherein a protease plays a signal repressor role and another, orthogonal, protease doubles as a signal activator. Excitingly, these proteases could be modified and re-deployed such that they are conditioned by an external stimulus themselves. For instance, HCVP activity could be further conditioned by the small-molecule asunaprevir,[62] and TEV could be implemented in a split and inactive conformation that only regains function upon addition of rapamycin.[63] Practically, this results in synthetic protein circuits that can be controlled through small-molecule actuation as well. One

relative disadvantage to CHOMP, however, lies in its reliance on innate cellular degradation machinery, which may result in output delay. In the same spirit as CHOMP, the Jerala group co-opted a mutually orthogonal set 4 of split proteases (TEV, PPV, SbMV, SuMMV) that re-assemble through orthogonal coiled-coil dimerization.[64] This split-protease-cleavable orthogonal coiled-coil (SPOC)-based circuit enables another powerful route for the engineering of Boolean computability into mammalian cell populations or the engineering of designer signaling cascades.

Since these two landmark reports,[65] a suite of powerful proofs-of-concept that use the same frameworks have been published. These achieve novel cellular functions or programs by combining orthogonal protease inputs (which may themselves be conditionally activated[66,67]) with motifs that allow for the creation of bespoke logic operations. For example, the Gao group developed the RELEASE (Retained Endoplasmic Cleavable Secretion) platform that can control protein secretion from the endoplasmic reticulum through two-input OR/AND type-operations or through a protease signaling cascade.[68] The Elowitz group was able to elucidate some of dynamics underlying morphogen signaling and ligand shuttling through the engineering of different extracellular protein circuits.[69] *De novo* protein design[70–72] is also poised to imminently change the synthetic circuit landscape by outfitting researchers with a dramatically expanded set of heterodimeric proteins that can act as composable elements themselves to recreate a suite of logic operations.[73] Moreover, newer proteases are continuously being developed that act orthogonally to those in current circulation or hold comparatively better reaction profiles. For instance, improved variants for TEV have been generated successfully through directed evolution[74] or through sequestration screening in yeast.[75,76] AI-driven design approaches are also

imminently promising; for example, the Baker lab recently deployed its ProteinMPNN neural network to generate TEV designs with improved catalytic reaction profiles over previous variants, setting the stage for similar work across different biotechnologically relevant proteases.[77,78]

Biocomputation through proteins extends well beyond synthetic protein circuits, however. Opsin-based optogenetics enabled a new wave of mechanistic investigations into different populations of excitable cells, such as neurons or cardiac cells.[79,80] The field originated from a foundational report published 2 decades ago, where the Deisseroth lab successfully re-purposed a light-sensitive cation channel algal protein – Channelrhodopsin-2 – to photostimulate mammalian neuronal populations. This photoswitch was stably and safely incorporated into neurons through lentiviral transduction.[81] The relative simplicity of its experimental set-up and portability lab-to-lab ushered in a highly productive era of investigations into neuro- and cardiac biology. Perhaps most impressive has been the rapid adoption of this technique by different labs and its inexorable march towards the clinic.[82] One of the chief objectives of this space is the seamless interrogation of different cell types; however, targeting viral vectors to specific cell populations remains a significant challenge. This motivates the importance of supplementing this approach with viral vectors that can autonomously identify their target prior using multiple features such as specific promoter activity, cellular location, and connectivity, and use these markers in turn to effect payload release. The Deisseroth has conducted pioneering work on this front; by engineering an array of introns with multiplexed recombinases (e.g. Cre and Flp), cell-specific features capable of AND-type Boolean logic can be genetically encoded to guide transgene delivery with substantially improved precision. This method – termed INTRSECT –

has been deployed to great effect to target highly specific neuronal populations that were "intersectionally" pre-specified through up to two different anatomic and genomic features.[83,84] More recently, the group was able to upgrade their INTRSECT modality by dramatically increasing the library of cellular features that can be read to effect payload release. Moreover, they successfully reported the first single-vector virus (Triplesect) capable of transgene delivery to triply defined cell types.[85]

Equally as important for our discussion, non-opsin optogenetics has been a great resource for light-responsive modules that enable user-control over different aspects of cellular biology, beyond excitable cell populations.[86] PhoCl was developed through directed evolution from a photoconvertible precursor protein, mMaple,[87,88] and is the first fully genetically encodable protein endowed with photocleavability. It soon found a host of applications in controlling biomolecule presentation and localization within living cells.[89] For instance, PhoCl was used successfully for the light-triggered formation of biomolecular condensates in a method called SPLIT.[90] In the same vein, it was incorporated within E-cadherin motifs to control mechanotransduction through the photocleavage of cell-cell junctions.[91] Lastly, it was also used to develop an optogenetic genome engineering platform based on Cre recombinase by controlling its translocation through induced sequestration and subsequent photo-liberation.[92] Similar to PhoCl, a recently developed enzymatically and photochemically controlled protein release system is LAUNCHER. It holds the benefit of being an AND-type release mechanism, which requires both proteolytic cleavage by a TEV protease and irradiation with 400nm light to release its cargo.[93]

While photoresponsive proteins enable the modulation of biology in 3D space and time, light as an actuator faces significant challenges in moving from bench to bedside. For instance, extensive scattering limits the depths to which light can penetrate skin and other tissues.[94] While there have been attempts to address these limitations through identifying and characterizing innately red-shifted constructs[95] or engineering more red-shifted versions of photoresponsive modules,[96–98] most clinical interventions would still require highly invasive surgical procedures, which motivates the need for different stimuli that can bypass this targeting problem. One such stimulus is ultrasound,[99] which is gaining traction as a viable alternative actuator. While the repertoire of reporter genes and bioswitches remains slim compared to those established for optogenetics (where modules and components are archived in community databases[100]), sonogenetics is gaining traction as a powerful modality in its own right. Recent successes include the use of magneto-gas vesicles as contrast agents for the non-invasive imaging of tissues[101] and the controlled release of a chemotherapeutic through biocompatible ultrasound.[102]

Lastly, a highly enabling platform is inteins, which are protein domains that assemble in solution and splice themselves out in a near-scarless manner, enabling the assembly of a diversity of architectures.[103,104] Given their versatility, they can be used in diverse synthetic biology applications.[105] While initially limited in scope because of poor splicing yields as well as sub-par expression and folding, the discovery of well-behaved and ultrafast splicing inteins from cyanobacteria (Npu DnaE from *Nostoc punctiforme*)[106] re-energized efforts in tagless protein purification,[107] expressed protein ligation,[108] and polypeptide cyclization.[109] This then led the discovery and/or development of evolved variants of Npu DnaE,[110] and to the evolution of alternative evolved versions through consensus alignment[111] and rational design.[112] Given their

scarless nature and robust reaction profiles, inteins hold tremendous promise in synthetic biology.

2.3. Computability in biomaterials

As touched upon prior, biomaterials are now pre-programmable constructs. Different research groups have developed a rich library of "smart" biomaterials,[113,114] capable of degrading, triggering payload release, shape-morphing, and other outputs.

2.3.1. Synthetic circuitry

Synthetic chemistry has been the main driver behind engineering advanced computability in biomaterial platforms. In early reports from the field, most material assembly methods consisted of chain-growth chemistry platforms that allowed for initial synthesis and subsequent spatiotemporal modulation of construct properties.[115] In more recent years, these have given way for step-growth-based, click-type, chemistries that offered pathways to more uniform networks with minimal structural irregularities.[116] While previously branded as "uncontrollable", recent landmark reports have sought to engineer triggerability into many of these step-growth platforms,[117] making them the modality of choice for the preparation of different biomaterials. The core benefits afforded by synthetic approaches are versatility and pristine control over material properties imparted by rational molecular design over linker/crosslink wiring, which is difficult to match when using equivalent approaches predicated on nucleic acids or proteins. In looking to develop a truly generalizable strategy for Boolean-type control over material properties,[25] our group resorted to exercising molecular control over material crosslinks.[118] By engineering bespoke crosslink structures, we were able to recapture all 17 possible operators

emanating from YES/AND/OR combinations of three inputs: light, redox state modulation, and protease cleavage. Using this framework, we demonstrated the successful release of an encapsulated doxorubicin in response to sensing a matrix metalloproteinase and a reductant. We then expanded this approach to enable the control of tethered protein[119] and small-molecule release[120] from hydrogel networks.

2.3.1. DNA circuitry

DNA-based approaches have proven trailblazing in the engineering of new dynamic hydrogel biomaterials. In much the same way as the control of DNA nanostructures had enabled key advances for the control of synthetic biology, more nuanced understanding of the design rules of DNA upgraded it from a genetic blueprint into a *bona fide* engineering approach, capable of holding rich information in its sequence. Using DNA as an engineering building block developed rapidly from an early theoretical curiosity, e.g., for the creation of lattices and junction-points[121] and was co-opted to assemble a wide-variety of geometries, such as cubes[122] and octahedrons.[123] While not directly linked to their use as material assembly platforms, with hindsight we can now see clearly how the origins of DNA nanotechnology were first laid out.[124]

2.3.1. Protein circuitry

Not unexpectedly, protein-enabled approaches have enabled increasingly more sophisticated approaches to controlling biomaterial properties. Deploying recombinant expression to engineer sequence-specific materials with programmable properties is now quickly becoming a straightforward endeavor. One example is fragment reconstitution-based approaches;[125] seminal work by the Howarth lab led to the discovery of the SpyTag/SpyCatcher chemistry,[126] an uncommon platform in which a smaller peptide – the Tag – recognizes a larger protein partner –

its cognate Catcher – and in the process forms a covalent isopeptide bond. SpyTag/SpyCatcher has been co-opted to great success in protein cyclization,[127] chromatographic purification,[128] and antibody engineering.[129] Soon after initial publication of the system, pioneering work by Arnold and Tirrell incorporated the Tag/Catcher motifs into telechelic ELP chains resulting in the covalent synthesis of bioactive and fully genetically encoded hydrogels.[130] Follow-up work then extended this strategy to globularly folded polypeptide backbones as well.[131]

2.4. The interface of biomaterials and biological systems

A particularly exciting frontier which we touch upon throughout the Chapter is that of "living" materials.[132] While no formal definition of the term exists yet, living materials most generally refer to materials that integrate both biological components (e.g., encapsulated microorganisms) and an abiotic yet stimulus-responsive material support into their design.

An evolving theme among synthetic bioengineers is that of collective intelligence,[133,134] which refers to the capacity of distinct yet nested cellular compartments to make decisions necessitating cooperation to reach target outcomes or states. This collective intelligence is not solely constrained to individual cell populations, but can scale to the level of tissues, organs, and whole organisms. Such a framework, and others like it derived from systems biology, can be applied towards modeling the crosstalk between encapsulated co-cultures, as well as between those and their surrounding smart material scaffold. This holds tremendous potential for the design of bespoke "living" materials. One powerful example of such crosstalk is provided by Lu and Ellis, who demonstrate a symbiotic and stable co-culture of *S. Cerevisiae* (engineered to secrete enzymes into bacterial cellulose), and *K. rhaeticus* (engineered to produce bacterial cellulose).[135]

This sense-and-respond type of biomaterial, which is also amenable to spatial and temporal patterning, can be readily deployed in biocatalysis and bioremediation applications where autonomous decision-making is an integral material feature.

2.5. Looking Forward

We now stand at a remarkable nexus of chemical engineering innovation. On the one hand, synthetic biology has enabled the metabolic engineering of value-added chemicals that span different industries. On the other, biomaterials can now be tailored and modified on-demand with a level of precision that has rendered the engineering of many nuanced physiological structures *ex vivo* possible.

By basing the design of next-generation biological systems and biomaterials on biocomputation-predicated frameworks, chemical engineers are now able to draw on a rich and multi-level (genetic, transcriptional, translational, as well as synthetic) set of tools and motifs to build bespoke functional circuits and programs. By integrating both cellular populations and materials into these design problems, the space looks ripe for disruption; frontiers such as living materials with co-evolvable components and *ex vivo* tissue constructs capable of bidirectional crosstalk become less of an academic curiosity and more of a technological reality.

Summarily, we envision a future ripe with innovation provided synergies between the two disciplines can be captured. At the core of this is the realization that it is the same biocomputation framework that has galvanized and guided innovation in both areas. As with any major chemical engineering undertaking, a convergence of disciplines that bridge concepts from genome sciences, electronic circuits, protein design, among others, will be necessary to drive the field forward. We look forward to seeing how we can engineer truly co-evolvable biological

systems and biomaterials, and where this next decade takes us in addressing the most pressing challenges in therapeutics, manufacturing, and sustainability.

References

1. Ausländer, S., Ausländer, D. & Fussenegger, M. Synthetic Biology—The Synthesis of Biology. *Angew. Chem. Int. Ed.* **56**, 6396–6419 (2017).
2. Roell, M.-S. & Zurbriggen, M. D. The impact of synthetic biology for future agriculture and nutrition. *Curr. Opin. Biotechnol.* **61**, 102–109 (2020).
3. Sargent, D., Conaty, W. C., Tissue, D. T. & Sharwood, R. E. Synthetic biology and opportunities within agricultural crops. *J. Sustain. Agric. Environ.* **1**, 89–107 (2022).
4. Jones, E. M., Marken, J. P. & Silver, P. A. Synthetic microbiology in sustainability applications. *Nat. Rev. Microbiol.* **22**, 345–359 (2024).
5. Cubillos-Ruiz, A. *et al.* Engineering living therapeutics with synthetic biology. *Nat. Rev. Drug Discov.* **20**, 941–960 (2021).
6. Tan, X., Letendre, J. H., Collins, J. J. & Wong, W. W. Synthetic biology in the clinic: engineering vaccines, diagnostics, and therapeutics. *Cell* **184**, 881–898 (2021).
7. Hahn, J. *et al.* Bacterial therapies at the interface of synthetic biology and nanomedicine. *Nat. Rev. Bioeng.* **2**, 120–135 (2024).
8. Voigt, C. A. Synthetic biology 2020–2030: six commercially-available products that are changing our world. *Nat. Commun.* **11**, 6379 (2020).
9. Brooks, S. M. & Alper, H. S. Applications, challenges, and needs for employing synthetic biology beyond the lab. *Nat. Commun.* **12**, 1390 (2021).
10. Ratner, B. D. & Zhang, G. 1.1.2 - A History of Biomaterials. in *Biomaterials Science (Fourth Edition)* (eds. Wagner, W. R., Sakiyama-Elbert, S. E., Zhang, G. & Yaszemski, M. J.) 21–34 (Academic Press, 2020). doi:10.1016/B978-0-12-816137-1.00002-7.
11. Mülhaupt, R. Hermann Staudinger and the Origin of Macromolecular Chemistry. *Angew. Chem. Int. Ed.* **43**, 1054–1063 (2004).
12. Langer, R. & Tirrell, D. A. Designing materials for biology and medicine. *Nature* **428**, 487–492 (2004).
13. Langer, R. & Folkman, J. Polymers for the sustained release of proteins and other macromolecules. *Nature* **263**, 797–800 (1976).
14. Bissell, M. J., Hall, H. G. & Parry, G. How does the extracellular matrix direct gene expression? *J. Theor. Biol.* **99**, 31–68 (1982).
15. Francis, R. M. & DeForest, C. A. 4D Biochemical Photocustomization of Hydrogel Scaffolds for Biomimetic Tissue Engineering. *Acc. Mater. Res.* **4**, 704–715 (2023).
16. Gharios, R., Francis, R. M. & DeForest, C. A. Chemical and biological engineering strategies to make and modify next-generation hydrogel biomaterials. *Matter* **6**, 4195–4244 (2023).
17. Gjorevski, N. *et al.* Tissue geometry drives deterministic organoid patterning. *Science* **375**, eaaw9021 (2022).
18. Lorenzo-Martín, L. F. *et al.* Spatiotemporally resolved colorectal oncogenesis in mini-colons ex vivo. *Nature* **629**, 450–457 (2024).

19. Ingber, D. E. Human organs-on-chips for disease modelling, drug development and personalized medicine. *Nat. Rev. Genet.* **23**, 467–491 (2022).

20. Le Feuvre, R. A. & Scrutton, N. S. A living foundry for Synthetic Biological Materials: A synthetic biology roadmap to new advanced materials. *Synth. Syst. Biotechnol.* **3**, 105–112 (2018).

21. Burgos-Morales, O. *et al.* Synthetic biology as driver for the biologization of materials sciences. *Mater. Today Bio* **11**, 100115 (2021).

22. Liu, A. P. *et al.* The living interface between synthetic biology and biomaterial design. *Nat. Mater.* **21**, 390–397 (2022).

23. Shariati, K. *et al.* Hylozoic by Design: Converging Material and Biological Complexities for Cell-Driven Living Materials with 4D Behaviors. *Adv. Funct. Mater.* **32**, 2108057 (2022).

24. de Silva, A. P. & Uchiyama, S. Molecular logic and computing. *Nat. Nanotechnol.* **2**, 399–410 (2007).

25. Badeau, B. A. & DeForest, C. A. Programming Stimuli-Responsive Behavior into Biomaterials. *Annu. Rev. Biomed. Eng.* **21**, 241–265 (2019).

26. Mao, X., Liu, M., Li, Q., Fan, C. & Zuo, X. DNA-Based Molecular Machines. *JACS Au* **2**, 2381–2399 (2022).

27. Qiu, M. *et al.* RNA nanotechnology for computer design and in vivo computation. *Philos. Trans. R. Soc. Math. Phys. Eng. Sci.* **371**, 20120310 (2013).

28. Katz, E. Biocomputing — tools, aims, perspectives. *Curr. Opin. Biotechnol.* **34**, 202–208 (2015).

29. Grozinger, L. *et al.* Pathways to cellular supremacy in biocomputing. *Nat. Commun.* **10**, 5250 (2019).

30. Goñi-Moreno, Á. Biocomputation: Moving Beyond Turing with Living Cellular Computers. *Commun. ACM* (2024) doi:10.1145/3635470.

31. Jacob, F. & Monod, J. Genetic regulatory mechanisms in the synthesis of proteins. *J. Mol. Biol.* **3**, 318–356 (1961).

32. Khalil, A. S. & Collins, J. J. Synthetic biology: applications come of age. *Nat. Rev. Genet.* **11**, 367–379 (2010).

33. Gardner, T. S., Cantor, C. R. & Collins, J. J. Construction of a genetic toggle switch in Escherichia coli. *Nature* **403**, 339–342 (2000).

34. Elowitz, M. B. & Leibler, S. A synthetic oscillatory network of transcriptional regulators. *Nature* **403**, 335–338 (2000).

35. Siuti, P., Yazbek, J. & Lu, T. K. Synthetic circuits integrating logic and memory in living cells. *Nat. Biotechnol.* **31**, 448–452 (2013).

36. Stein, V. & Alexandrov, K. Protease-based synthetic sensing and signal amplification. *Proc. Natl. Acad. Sci.* **111**, 15934–15939 (2014).

37. Young, D. D. & Deiters, A. Photochemical Activation of Protein Expression in Bacterial Cells. *Angew. Chem. Int. Ed.* **46**, 4290–4292 (2007).

38. Binder, D. *et al.* Light-Controlled Cell Factories: Employing Photocaged Isopropyl-β-d-Thiogalactopyranoside for Light-Mediated Optimization of lac Promoter-Based Gene Expression and (+)-Valencene Biosynthesis in Corynebacterium glutamicum. *Appl. Environ. Microbiol.* **82**, 6141–6149 (2016).

39. Hogenkamp, F. *et al.* Effect of Photocaged Isopropyl β-d-1-thiogalactopyranoside Solubility on the Light Responsiveness of LacI-controlled Expression Systems in Different Bacteria. *ChemBioChem* **22**, 539–547 (2021).

40. Gardner, L., Zou, Y., Mara, A., Cropp, T. A. & Deiters, A. Photochemical control of bacterial signal processing using a light-activated erythromycin. *Mol. Biosyst.* **7**, 2554–2557 (2011).

41. Binder, D. *et al.* Photocaged Arabinose: A Novel Optogenetic Switch for Rapid and Gradual Control of Microbial Gene Expression. *ChemBioChem* **17**, 296–299 (2016).

42. Bier, C. *et al.* Photocaged Carbohydrates: Versatile Tools for Controlling Gene Expression by Light. *Synthesis* **49**, 42–52 (2017).

43. Sauers, D. J. *et al.* Light-Activated Gene Expression Directs Segregation of Co-cultured Cells in Vitro. *ACS Chem. Biol.* **5**, 313–320 (2010).

44. Gorka, A. P., Yamamoto, T., Zhu, J. & Schnermann, M. J. Cyanine Photocages Enable Spatial Control of Inducible Cre-Mediated Recombination. *ChemBioChem* **19**, 1239–1243 (2018).

45. Kusen, P. M. *et al.* Light-controlled gene expression in yeast using photocaged Cu2+. *J. Biotechnol.* **258**, 117–125 (2017).

46. Wong, P. T. *et al.* Control of an Unusual Photo-Claisen Rearrangement in Coumarin Caged Tamoxifen through an Extended Spacer. *ACS Chem. Biol.* **12**, 1001–1010 (2017).

47. Lv, H., Li, Q., Shi, J., Fan, C. & Wang, F. Biocomputing Based on DNA Strand Displacement Reactions. *ChemPhysChem* **22**, 1151–1166 (2021).

48. Gao, Y., Wang, L. & Wang, B. Customizing cellular signal processing by synthetic multi-level regulatory circuits. *Nat. Commun.* **14**, 8415 (2023).

49. Feynman, R.P. There's Plenty of Room at the Botom. *Engineering and Science* **23**, 22-36 (1960).

50. Nielsen, A. A. K. *et al.* Genetic circuit design automation. *Science* **352**, aac7341 (2016).

51. Toda, S., Frankel, N. W. & Lim, W. A. Engineering cell–cell communication networks: programming multicellular behaviors. *Curr. Opin. Chem. Biol.* **52**, 31–38 (2019).

52. Dai, Y., You, L. & Chilkoti, A. Engineering synthetic biomolecular condensates. *Nat. Rev. Bioeng.* **1**, 466–480 (2023).

53. Chen, Z. & Elowitz, M. B. Programmable protein circuit design. *Cell* **184**, 2284–2301 (2021).

54. Fink, T. & Jerala, R. Designed protease-based signaling networks. *Curr. Opin. Chem. Biol.* **68**, 102146 (2022).

55. Klumpe, H. E., Garcia-Ojalvo, J., Elowitz, M. B. & Antebi, Y. E. The computational capabilities of many-to-many protein interaction networks. *Cell Syst.* **14**, 430–446 (2023).

56. Craik, C. S., Page, M. J. & Madison, E. L. Proteases as therapeutics. *Biochem. J.* **435**, 1–16 (2011).

57. Poreba, M. Protease-activated prodrugs: strategies, challenges, and future directions. *FEBS J.* **287**, 1936–1969 (2020).

58. Waugh, D. S. An overview of enzymatic reagents for the removal of affinity tags. *Protein Expr. Purif.* **80**, 283–293 (2011).

59. Fernandez-Rodriguez, J. & Voigt, C. A. Post-translational control of genetic circuits using Potyvirus proteases. *Nucleic Acids Res.* **44**, 6493–6502 (2016).

60. Gao, X. J., Chong, L. S., Kim, M. S. & Elowitz, M. B. Programmable protein circuits in living cells. *Science* **361**, 1252–1258 (2018).
61. Varshavsky, A. N-degron and C-degron pathways of protein degradation. *Proc. Natl. Acad. Sci.* **116**, 358–366 (2019).
62. Chung, H. K. *et al.* Tunable and reversible drug control of protein production via a self-excising degron. *Nat. Chem. Biol.* **11**, 713–720 (2015).
63. Wehr, M. C. *et al.* Monitoring regulated protein-protein interactions using split TEV. *Nat. Methods* **3**, 985–993 (2006).
64. Fink, T. *et al.* Design of fast proteolysis-based signaling and logic circuits in mammalian cells. *Nat. Chem. Biol.* **15**, 115–122 (2019).
65. Wu, Y. & Wang, Y. Protein circuits reprogram cells. *Nat. Chem. Biol.* **15**, 96–97 (2019).
66. Scheller, L., Strittmatter, T., Fuchs, D., Bojar, D. & Fussenegger, M. Generalized extracellular molecule sensor platform for programming cellular behavior. *Nat. Chem. Biol.* **14**, 723–729 (2018).
67. Djannatian, M. S., Galinski, S., Fischer, T. M. & Rossner, M. J. Studying G protein-coupled receptor activation using split-tobacco etch virus assays. *Anal. Biochem.* **412**, 141–152 (2011).
68. Vlahos, A. E. *et al.* Protease-controlled secretion and display of intercellular signals. *Nat. Commun.* **13**, 912 (2022).
69. Zhu, R. *et al.* Reconstitution of morphogen shuttling circuits. *Sci. Adv.* **9**, eadf9336 (2023).
70. Huang, P.-S., Boyken, S. E. & Baker, D. The coming of age of de novo protein design. *Nature* **537**, 320–327 (2016).
71. Korendovych, I. V. & DeGrado, W. F. De novo protein design, a retrospective. *Q. Rev. Biophys.* **53**, e3 (2020).
72. Pan, X. & Kortemme, T. Recent advances in de novo protein design: Principles, methods, and applications. *J. Biol. Chem.* **296**, (2021).
73. Chen, Z. *et al.* De novo design of protein logic gates. *Science* **368**, 78–84 (2020).
74. Sanchez, M. I. & Ting, A. Y. Directed evolution improves the catalytic efficiency of TEV protease. *Nat. Methods* **17**, 167–174 (2020).
75. Yi, L. *et al.* Engineering of TEV protease variants by yeast ER sequestration screening (YESS) of combinatorial libraries. *Proc. Natl. Acad. Sci.* **110**, 7229–7234 (2013).
76. Denard, C. A. *et al.* YESS 2.0, a Tunable Platform for Enzyme Evolution, Yields Highly Active TEV Protease Variants. *ACS Synth. Biol.* **10**, 63–71 (2021).
77. Dauparas, J. *et al.* Robust deep learning–based protein sequence design using ProteinMPNN. *Science* **378**, 49–56 (2022).
78. Sumida, K. H. *et al.* Improving Protein Expression, Stability, and Function with ProteinMPNN. *J. Am. Chem. Soc.* **146**, 2054–2061 (2024).
79. Entcheva, E. & Kay, M. W. Cardiac optogenetics: a decade of enlightenment. *Nat. Rev. Cardiol.* **18**, 349–367 (2021).
80. Gao, T. T. *et al.* The clinical potential of optogenetic interrogation of pathogenesis. *Clin. Transl. Med.* **13**, e1243 (2023).
81. Boyden, E. S., Zhang, F., Bamberg, E., Nagel, G. & Deisseroth, K. Millisecond-timescale, genetically targeted optical control of neural activity. *Nat. Neurosci.* **8**, 1263–1268 (2005).

82. Bansal, A., Shikha, S. & Zhang, Y. Towards translational optogenetics. *Nat. Biomed. Eng.* **7**, 349–369 (2023).

83. Fenno, L. E. *et al.* Targeting cells with single vectors using multiple-feature Boolean logic. *Nat. Methods* **11**, 763–772 (2014).

84. Fenno, L. E., Mattis, J., Ramakrishnan, C. & Deisseroth, K. A Guide to Creating and Testing New INTRSECT Constructs. *Curr. Protoc. Neurosci.* **80**, 4.39.1-4.39.24 (2017).

85. Fenno, L. E. *et al.* Comprehensive Dual- and Triple-Feature Intersectional Single-Vector Delivery of Diverse Functional Payloads to Cells of Behaving Mammals. *Neuron* **107**, 836-853.e11 (2020).

86. Lu, X., Shen, Y. & Campbell, R. E. Engineering Photosensory Modules of Non-Opsin-Based Optogenetic Actuators. *Int. J. Mol. Sci.* **21**, 6522 (2020).

87. Zhang, W. *et al.* Optogenetic control with a photocleavable protein, PhoCl. *Nat. Methods* **14**, 391–394 (2017).

88. Lu, X. *et al.* Photocleavable proteins that undergo fast and efficient dissociation. *Chem. Sci.* **12**, 9658–9672 (2021).

89. Kashyap, P. *et al.* An optogenetic method for the controlled release of single molecules. *Nat. Methods* **21**, 666–672 (2024).

90. Reed, E. H., Schuster, B. S., Good, M. C. & Hammer, D. A. SPLIT: Stable Protein Coacervation Using a Light Induced Transition. *ACS Synth. Biol.* **9**, 500–507 (2020).

91. Endo, M., Iwawaki, T., Yoshimura, H. & Ozawa, T. Photocleavable Cadherin Inhibits Cell-to-Cell Mechanotransduction by Light. *ACS Chem. Biol.* **14**, 2206–2214 (2019).

92. Vizoso, M. *et al.* A doxycycline- and light-inducible Cre recombinase mouse model for optogenetic genome editing. *Nat. Commun.* **13**, (2022).

93. Cui, M. *et al.* A single-component, light-assisted uncaging switch for endoproteolytic release. *Nat. Chem. Biol.* **20**, 353–364 (2024).

94. Tao, Y., Chan, H. F., Shi, B., Li, M. & Leong, K. W. Light: A Magical Tool for Controlled Drug Delivery. *Adv. Funct. Mater.* **30**, 2005029 (2020).

95. Mager, T. *et al.* High frequency neural spiking and auditory signaling by ultrafast red-shifted optogenetics. *Nat. Commun.* **9**, 1750 (2018).

96. Lin, J. Y., Knutsen, P. M., Muller, A., Kleinfeld, D. & Tsien, R. Y. ReaChR: a red-shifted variant of channelrhodopsin enables deep transcranial optogenetic excitation. *Nat. Neurosci.* **16**, 1499–1508 (2013).

97. Alachouzos, G., Schulte, A. M., Mondal, A., Szymanski, W. & Feringa, B. L. Computational Design, Synthesis, and Photochemistry of Cy7-PPG, an Efficient NIR-Activated Photolabile Protecting Group for Therapeutic Applications**. *Angew. Chem. Int. Ed.* **61**, e202201308 (2022).

98. Rapp, T. L. & DeForest, C. A. Tricolor visible wavelength-selective photodegradable hydrogel biomaterials. *Nat. Commun.* **14**, 5250 (2023).

99. Maresca, D. *et al.* Biomolecular Ultrasound and Sonogenetics. *Annu. Rev. Chem. Biomol. Eng.* **9**, 229–252 (2018).

100. Kolar, K., Knobloch, C., Stork, H., Žnidarič, M. & Weber, W. OptoBase: A Web Platform for Molecular Optogenetics. *ACS Synth. Biol.* **7**, 1825–1828 (2018).

101. Kim, W.-S. *et al.* Magneto-acoustic protein nanostructures for non-invasive imaging of tissue mechanics in vivo. *Nat. Mater.* **23**, 290–300 (2024).

102. Yao, Y. *et al.* Remote control of mechanochemical reactions under physiological conditions using biocompatible focused ultrasound. *Proc. Natl. Acad. Sci.* **120**, e2309822120 (2023).
103. Shah, N. H. & Muir, T. W. Inteins: Nature's gift to protein chemists. *Chem. Sci.* **5**, 446–461 (2014).
104. Wood, D. W., Belfort, M. & Lennon, C. W. Inteins—mechanism of protein splicing, emerging regulatory roles, and applications in protein engineering. *Front. Microbiol.* **14**, (2023).
105. Anastassov, S., Filo, M. & Khammash, M. Inteins: A Swiss army knife for synthetic biology. *Biotechnol. Adv.* **73**, 108349 (2024).
106. Zettler, J., Schütz, V. & Mootz, H. D. The naturally split *Npu* DnaE intein exhibits an extraordinarily high rate in the protein *trans*-splicing reaction. *FEBS Lett.* **583**, 909–914 (2009).
107. Ramirez, M., Valdes, N., Guan, D. & Chen, Z. Engineering split intein DnaE from Nostoc punctiforme for rapid protein purification. *Protein Eng. Des. Sel.* **26**, 215–223 (2013).
108. Vila-Perelló, M. *et al.* Streamlined Expressed Protein Ligation Using Split Inteins. *J. Am. Chem. Soc.* **135**, 286–292 (2013).
109. Townend, J. E. & Tavassoli, A. Traceless Production of Cyclic Peptide Libraries in E. coli. *ACS Chem. Biol.* **11**, 1624–1630 (2016).
110. Shah, N. H., Dann, G. P., Vila-Perelló, M., Liu, Z. & Muir, T. W. Ultrafast Protein Splicing is Common among Cyanobacterial Split Inteins: Implications for Protein Engineering. *J. Am. Chem. Soc.* **134**, 11338–11341 (2012).
111. Stevens, A. J. *et al.* Design of a Split Intein with Exceptional Protein Splicing Activity. *J. Am. Chem. Soc.* **138**, 2162–2165 (2016).
112. Stevens, A. J. *et al.* A promiscuous split intein with expanded protein engineering applications. *Proc. Natl. Acad. Sci.* **114**, 8538–8543 (2017).
113. Furth, M. E., Atala, A. & Van Dyke, M. E. Smart biomaterials design for tissue engineering and regenerative medicine. *Biomaterials* **28**, 5068–5073 (2007).
114. Cecen, B., Hassan, S., Li, X. & Zhang, Y. S. Smart Biomaterials in Biomedical Applications: Current Advances and Possible Future Directions. *Macromol. Biosci.* **24**, 2200550 (2024).
115. West, J. L. & Hubbell, J. A. Photopolymerized hydrogel materials for drug delivery applications. *React. Polym.* **25**, 139–147 (1995).
116. Gao, Y., Peng, K. & Mitragotri, S. Covalently Crosslinked Hydrogels via Step-Growth Reactions: Crosslinking Chemistries, Polymers, and Clinical Impact. *Adv. Mater.* **33**, (2021).
117. Kumar, G. & Lin, Q. Light-Triggered Click Chemistry. *Chem. Rev.* **121**, 6991–7031 (2021).
118. Badeau, B. A. & Deforest, C. A. Programming Stimuli-Responsive Behavior into Biomaterials. *Annu. Rev. Biomed. Eng.* **21**, 241–265 (2019).
119. Gawade, P. M., Shadish, J. A., Badeau, B. A. & DeForest, C. A. Logic-Based Delivery of Site-Specifically Modified Proteins from Environmentally Responsive Hydrogel Biomaterials. *Adv. Mater.* **31**, 1902462 (2019).
120. Ruskowitz, E. R., Comerford, M. P., Badeau, B. A. & Deforest, C. A. Logical stimuli-triggered delivery of small molecules from hydrogel biomaterials. *Biomater. Sci.* **7**, 542–546 (2019).

121. Seeman, N. C. Nucleic acid junctions and lattices. *J. Theor. Biol.* **99**, 237–247 (1982).

122. Chen, J. & Seeman, N. C. Synthesis from DNA of a molecule with the connectivity of a cube. *Nature* **350**, 631–633 (1991).

123. Zhang, Y. & Seeman, N. C. Construction of a DNA-Truncated Octahedron. *J. Am. Chem. Soc.* **116**, 1661–1669 (1994).

124. Seeman, N. C. & Sleiman, H. F. DNA nanotechnology. *Nat. Rev. Mater.* **3**, 1–23 (2017).

125. Fan, R. & Aranko, A. S. Catcher/Tag Toolbox: Biomolecular Click-Reactions For Protein Engineering Beyond Genetics. *ChemBioChem* **25**, e202300600 (2024).

126. Zakeri, B. *et al.* Peptide tag forming a rapid covalent bond to a protein, through engineering a bacterial adhesin. *Proc. Natl. Acad. Sci. U. S. A.* **109**, E690–E697 (2012).

127. Schoene, C., Fierer, J. O., Bennett, S. P. & Howarth, M. SpyTag/SpyCatcher Cyclization Confers Resilience to Boiling on a Mesophilic Enzyme. *Angew. Chem. Int. Ed.* **53**, 6101–6104 (2014).

128. Khairil Anuar, I. N. A. *et al.* Spy&Go purification of SpyTag-proteins using pseudo-SpyCatcher to access an oligomerization toolbox. *Nat. Commun.* **10**, 1734 (2019).

129. Driscoll, C. L., Keeble, A. H. & Howarth, M. R. SpyMask enables combinatorial assembly of bispecific binders. *Nat. Commun.* **15**, 2403 (2024).

130. Sun, F., Zhang, W. B., Mahdavi, A., Arnold, F. H. & Tirrell, D. A. Synthesis of bioactive protein hydrogels by genetically encoded SpyTag-SpyCatcher chemistry. *Proc. Natl. Acad. Sci. U. S. A.* **111**, 11269–11274 (2014).

131. Gao, X., Fang, J., Xue, B., Fu, L. & Li, H. Engineering Protein Hydrogels Using SpyCatcher-SpyTag Chemistry. *Biomacromolecules* **17**, 2812–2819 (2016).

132. Liu, X., Inda, M. E., Lai, Y., Lu, T. K. & Zhao, X. Engineered Living Hydrogels. *Adv. Mater.* **34**, 2201326 (2022).

133. Solé, R. *et al.* Synthetic collective intelligence. *Biosystems* **148**, 47–61 (2016).

134. McMillen, P. & Levin, M. Collective intelligence: A unifying concept for integrating biology across scales and substrates. *Commun. Biol.* **7**, 1–17 (2024).

135. Gilbert, C. *et al.* Living materials with programmable functionalities grown from engineered microbial co-cultures. *Nat. Mater.* **20**, 691–700 (2021).

CHAPTER 3: DISSERTATION AIMS

The bioeconomy is at an inflection point; we are now operating in a century where the rules of multiple industries are undergoing a paradigm shift spurred predominantly by advances in our understanding of biology and the development of different methods to modulate it. For instance, therapeutic design is no longer subject to the same heuristics that had curtailed it for decades. In the same vein, synthetic biology is undergoing a robust upgrade into the realm of mammalian biology, offering multiple exciting directions for the biomanufacturing of value-added chemicals and therapeutics. Central to this switch has been the enabling power of chemical biology, which has allowed us to not only understand mechanistically how biomolecules interact, but also provided a route to co-opt these design rules and codify them into methods to assemble new protein architectures and program their activation and presentation in both space and time. Broadly, this dissertation aims to demonstrate new ways in which chemical biology, far from being a siloed academic discipline, can be co-opted to engineer next-generation biomaterials. Specifically, I focus on the creation of hybrid polymer-polypeptide-based materials, with an eye towards engineering ever-more advanced bio-functional materials.

In **Chapter 1**, I provided a broad overview into how "programmability" has guided the development of newer generations of hydrogel biomaterials, and what the next frontier looks like for the field as it tackles the pressing questions of translatability and ease-of-access.

In **Chapter 2**, I presented a focused discussion on how biomaterial engineering can learn from advances in synthetic biology, and how developments in both fields can cross-pollinate and synergize to unlock completely novel capabilities.

Building on this rich landscape and looking to push the envelope further still, my original research work is detailed as follows:

In **Chapter 4**, I will describe the first strategy enabling the N-terminal functionalization and purification of recombinant proteins in a single step. Based on intein trans-splicing, this method, VidaL-tagged Expression and Protein Ligation (VEPL), allows for the installation of virtually any synthetic cargo on the N-terminus of a protein-of-interest, all while preserving native-level bioactivity.

In **Chapter 5**, I will showcase how spontaneous intramolecular ligations derived from different realms of chemical biology can be combined to recombinantly assemble advanced logical operators for controlled protein presentations. This method – which we refer to as autonomous molecular compilation – holds vast implications for disciplines such as tissue engineering and biosensing, among others.

In **Chapter 6**, I will describe ongoing work that seeks to grow this molecular compilation-based approach to control the presentation of a wide array of bio-epitopes, spanning different protein categories. I also posit that this approach, far from being limited to protease-driven actuation, can also harness light and small-molecules as potential inputs.

In **Chapter 7**, I will be providing a survey of more downstream work that has spun off from the autonomous molecular compilation thrust. This will be exemplified by highlighting two main tracks: one that aims to re-engineer our previously validated tether topologies as material

crosslinks to gain Boolean control over network-scale degradation, and another that demonstrates the use of these manifold chemistries to build next-generation biosensors in a facile manner. Lastly, in **Chapter 8,** I will be providing a summary of key aspects of the work presented throughout this thesis, as well as a forward-looking perspective on the engineering of truly smart biomaterials and biohybrid constructs.

CHAPTER 4: ONE-STEP PURIFICATION AND N-TERMINAL FUNCTIONALIZATION OF BIOACTIVE PROTEINS VIA ATYPICALLY SPLIT INTEINS

Adapted from Gharios, R., Li, A., Kopyeva, I., Francis, R.M., DeForest, C.A. One-Step Purification and N-terminal Functionalization of Bioactive Proteins via Atypically Split Inteins. *Bioconjugate Chemistry (In press)* (2024). DOI: 10.1021/acs.bioconjchem.4c00223

Abstract

Site-specific installation of non-natural functionality onto proteins has enabled countless applications in biotechnology, chemical biology, and biomaterials science. Though the N-terminus is an attractive target for derivatization, prior methodologies targeting this site have suffered from low selectivity, a limited selection of potential chemical modifications, and/or challenges associated with divergent protein purification/modification steps. In this work, we harness the atypically split VidaL intein to simultaneously N-functionalize and purify homogeneous protein populations in a single step. Our method – referred to as VidaL-tagged expression and protein ligation (VEPL) – enables modular and scalable production of N-terminally modified proteins with native bioactivity. Demonstrating its flexibility and ease of use, we employ VEPL to combinatorially install 4 distinct (multi)functional handles (e.g., biotin, alkyne, fluorophores) to the N-terminus of 4 proteins that span three different classes: fluorescent

(Enhanced Green Fluorescent Protein, mCherry), enzymatic (β-lactamase), and growth factor (epidermal growth factor). Moving forward, we anticipate that VEPL's ability to rapidly generate and isolate N-modified proteins will prove useful across the growing fields of applied chemical biology.

4.1. Introduction

The creation of well-defined protein conjugates, whether wholly genetically encoded or semisynthetic in nature, is crucial for studies in chemical biology and beyond.[1] The expression and assembly of different protein chimeras has, in fact, led to advances in spaces as diverse as biomolecule localization and tracking[2] and the creation of well-defined antibody-drug conjugates for therapeutic targeting.[3] Beyond these applications, site-specific protein modification is also key for the creation of functional biomaterials.[4–7] In recent years, researchers in this space have steadily moved away from stochastic modification methodologies (e.g., based on activated esters), which while convenient, often lead to heterogeneous protein populations and significant batch-to-batch variability. To address this issue, multiple semisynthetic methods have been developed in order to afford a rich armamentarium of site-specific protein modification techniques.[8–11]

In particular, N-terminal modification of proteins has been a long-standing goal for the field partly to recapture the diversity of proteoforms that result from diverse N-terminal modifications.[12,13] Moreover, N-termini are also typically solvent-exposed and fall outside of the final fold, implying that modifications incorporated at this site preserve protein bioactivity better

than those installed at internal residues.[14] As such, the N-terminus is particularly suitable for installing synthetic handles onto protein constructs that are otherwise fragile. Hampering this end-goal is the lack of broad applicability of typical N-terminal modification strategies, as these usually suffer from overall sub-optimal selectivity and propensity towards multiple side-reactions, the need for multiple sequential purification and derivatization steps, and/or a constriction to a limited sub-set of installable cargos. For example, a seminal early report by the Francis group outlined a powerful transamination-based strategy to install reactive carbonyls at protein N-termini through the use of a pyridoxal-5-phosphate (PLP) reagent; however, this strategy is constricted to N-terminal residues that do not react with aldehydes.[15] Another method developed by the group deployed potassium ferricyanide-based coupling of oxidized o-phenols or o-catechols to N-terminally functionalize proteins, potentially in a single step; this method, however, relies heavily on the presence of an N-terminal proline when applied to full-length proteins, which may limit its scope of applicability.[16] Another approach developed by the Bordusa group engineered a "trypsiligase" as a ligase derived from trypsin to modify proteins at their N-termini. While robust, it holds the risk of context-specific hydrolysis side-reactions, hampering straightforward off-the-shelf use for different proteins.[17] Analogously, the Wells group pioneered the deployment of subtiligase-based peptide ligation to target protein N-termini.[18,19] However, this methodology, given its targeting of reactive amines, is also liable to inadvertently functionalize lysines throughout the target polypeptide chain non-specifically, limiting its potential achievement of pristine regioselectivity. Lastly, a reliable suite of methods includes relatively recent fragment-reconstitution-based approaches such as the SpyTag-SpyCatcher chemistry and related platforms that rely on isopeptide bond formation between split pairs. While these may be convenient for protein-protein ligation at termini, such strategies

typically result in the formation of bulky protein assemblies at the ligation site, thereby hampering native protein reconstitution, and require the sequential expression and purification of multiple constructs separately prior to assembly.[20–25]

In an effort to overcome these limitations, we identified split inteins as a uniquely powerful platform for protein-protein ligation.[26,27] Split inteins are protein elements that are able to recognize themselves with high affinity and assemble in solution upon mixing, ligating their fused polypeptides (termed exteins) with a native amide bond while "splicing" themselves out of the final fold in a series of highly choreographed reaction steps (**Figure 4.1**).[28] In comparison to other systems, inteins hold the benefit of being a virtually scarless modality, theoretically leaving as little as a single amino acid scar (typically cysteine or serine) in the final product depending on the specific intein adopted. Moreover, split inteins are categorized as either canonical splits – wherein the N-terminal intein is larger than its corresponding C-intein – or atypical splits, where the reverse is true. This relative difference in sizes affords a powerful benefit to the incorporation of synthetic handles onto proteins; the larger fragment (N or C, depending on the type of split intein) can be expressed heterologously, while the shorter fragment may be accessible to solid-phase peptide synthesis, obviating the limitations of metabolic incorporation of non-natural groups and making possible the installation of virtually any synthetic handle(s) or probe post-translationally.[29] Owing to these powerful advantages, split inteins can be harnessed as a base platform towards the purification and functionalization of diverse proteins.[30,31] Specifically, early pioneering work by the Wood group led to the development of a pH-activatable intein cleavage system (a miniaturized *Mtu-recA* with a deleted endonuclease domain) for the purification of tag-free proteins,[32] a thrust which has since improved substantially in scope and reaction profile with

the discovery and evolution of newer and better-behaved canonically split intein systems (e.g., *Npu*).[33,34] In the same vein, such systems have also lent themselves well to a growing body of work targeting for the C-terminal modification of different protein cargos with manifold handles, either through regular splicing[35] or controlled cleavage through expressed protein ligation.[36,37] Summarily, while the literature is now rich in intein-based methods that enable the tagless purification and/or C-terminal modification of protein cargos, no such robust methodology has been developed for the single-step purification and N-terminal functionalization of proteins. This is an essential unmet need for cases where the C-terminus is necessary for protein function (e.g., Ubiquitin,[38] Interferon-gamma,[39] among others) or proves persistently refractory to post-translational modification.

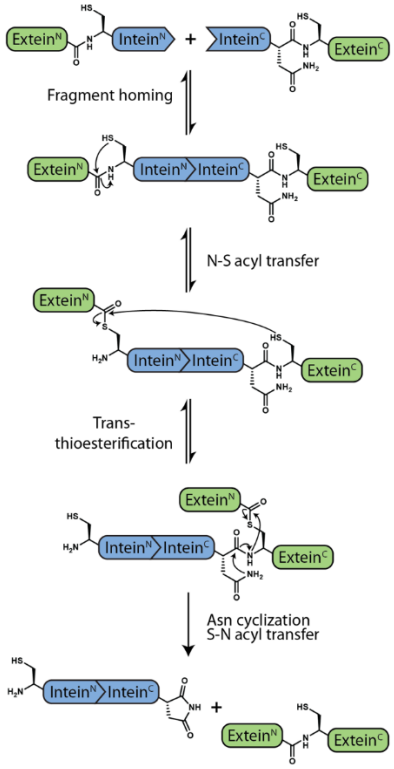

Figure 11: Intein trans-splicing reaction cascade

Intein fragments assemble in solution, ligating their concomitant protein cargos – exteins – in a series of highly choreographed reaction steps.

4.2. Results and Discussion

In looking to develop a generalizable and modular method for the single-step N-terminal modification of proteins, we were encouraged by a recent report by the Muir lab characterizing an atypical split intein isolated from Lake Vida in Antarctica, termed VidaL.[40] It holds the benefit of being a very short naturally occurring split intein; the N fragment of VidaL (Vid^N) has only 16 residues, rendering it readily accessible to solid-phase peptide synthesis in good yield. Moreover, it is among the fastest splicing intein systems discovered to date, with a reported reaction half-life of approximately a minute. The requisite extein load for VidaL is also an advantage compared to other intein systems and semisynthesis approaches more broadly: its N-terminal extein sequence is an E-S-G tripeptide and its corresponding C-terminal sequence is S-G-K. Functionally, this results in a final splicing "scar" that is a flexible serine-glycine linker, often adopted in the design of fusion chimeras as an innocuous spacer motif.[41] Lastly, while broader use of atypically split inteins has thus far been limited by their increased propensity towards C-terminal cleavage,[42] we were drawn to VidaL for its reported negligible tendency to undergo this side-reaction.

Specifically, we sought to exploit VidaL's splicing efficiency to both generate and purify homogeneous populations of monofunctionalized proteins in a single step. Our method – referred to as VidaL-tagged expression and protein ligation (VEPL) – relies on expressing proteins of interest as C-terminal fusions to a polyhistidine-tagged and SUMO-fused C-fragment of VidaL (Vid^C) protein and binding these onto immobilized metal affinity chromatography supports (in this case, a Ni-NTA matrix) (**Figure 4.2**). Introduction of the synthetic N-fragment modified with a cargo of interest then "cleaves" the target modified protein off the matrix via trans-

splicing, thereby enabling clean retrieval of pure and modified product from the column flow-through and subsequent washes. The highly folded structure of Vid^C makes it a suitable fusion partner to different proteins-of-interest. Additionally, the small size of Vid^N (1,783.2 Da) paves the way for virtually any synthetic handle to be installed through routine peptide synthesis. As proposed, VEPL should prove broadly applicable regardless of the specific affinity chromatography system being used.

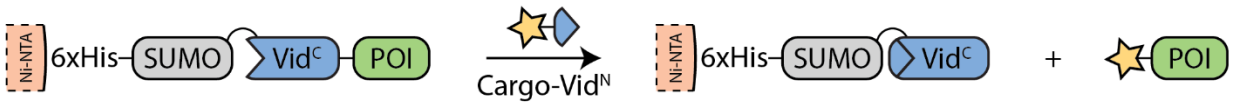

Figure 12: One-step protein biofunctionalization and purification of N-modified bioconjugates via VEPL

In VidaL-tagged expression and protein ligation (VEPL), proteins of interest (POI) are expressed as a C-fusion with Vid^C, SUMO, and a 6xHis tag. After chromatographic isolation on the Ni-NTA resin, a functionalized Vid^N peptide promotes trans-splicing, concomitantly N-functionalizing the POI while displacing it from the resin.

A known shortcoming of intein systems generally and atypically split inteins in particular is their varying propensity towards non-specific N- and/or C-terminal cleavage over splicing. To assess whether VidaL fragment assembly and splicing occur with minimal C-terminal cleavage, we applied two different approaches. The first entailed the expression of a Vid^C-fused EGFP protein (**Supplementary Method S4.1**), which was then incubated with Ni-NTA and bound to a fritted column. No cleaved protein is obtained after 2 hours on-resin, demonstrating complete absence of C-terminal cleavage (**Supplementary Figure S4.1**). Going further, and in order to ensure that cleavage of the system is not caused by a recapture of the intein domain fold,[43] we expressed a Maltose-binding Protein (MBP)-fused Vid^N and purified it using amylose chromatography (**Supplementary Method S4.2**). After expression of a Vid^C-EGFP fusion and incubation on

column with Ni-NTA, we introduced the MBP-Vid^{N} protein and allowed the system to react for 2 hours with varied temperatures prior to collecting reaction products in the column flow-through. Encouragingly, no C-terminally cleaved product could be discriminated via sodium dodecyl sulfate-polyacrylamide gel electrophoresis (SDS-PAGE), proving that no C-terminal cleavage takes place even after formation of the assembled intein domain under three different temperature conditions (i.e., 4°C, 25°C, 37°C) (**Supplementary Figure S4.2**).

Heartened by these results, and as a prelude to establishing the versatility of the VEPL platform, we aimed to characterize its efficiency under various other reaction conditions: namely, by investigating splicing kinetics, temperature-dependence, and sensitivity to excess peptide stoichiometric ratios (**Figure 4.3**). Using EGFP as our model protein and an amine-Vid^{N} (**Supplementary Methods S4.3-S4.6**) as cognate peptide cargo for proof-of-concept characterization studies, we first conducted a trans-splicing time-course analysis, using a 10X excess of Vid^{N} under 25°C ambient temperature. Encouragingly, despite the steric hindrances potentially introduced by protein-resin binding, the splicing reaction proceeded to completion within 2 hours. Next, we investigated VEPL's temperature-dependence by running a splicing time-course for 2 hours and a 10X excess of Vid^{N} to Vid^{C} at different temperatures (4°C, 25°C, 37°C). We found that optimal splicing yield occurs at 37 °C but that meaningful extents of on-resin functionalization (i.e., 50% that of optimal yield) was achieved at 4 °C, highly encouraging for the system's use for thermal-sensitive proteins. Lastly, the effect of peptide excess was interrogated by varying the relative molar ratios of peptide-to-protein (1X, 5X, 10X) while keeping a constant reaction time of 2 hours at 25°C. While typical enzymatic routes to protein modification often require large excesses of the nucleophilic peptide substrate, VidaL can

achieve high splicing yields even under equimolar conditions. Optimal stoichiometry is a 10X ratio of Vid^N peptide to the Vid^C-tagged protein, but maintaining as low as a 1:1 ratio still enables roughly 50% yield, which can prove fruitful for more esoteric peptide cargos or those in short supply. Uncropped gels showcasing these assays are provided in **Supplementary Figure S3**.

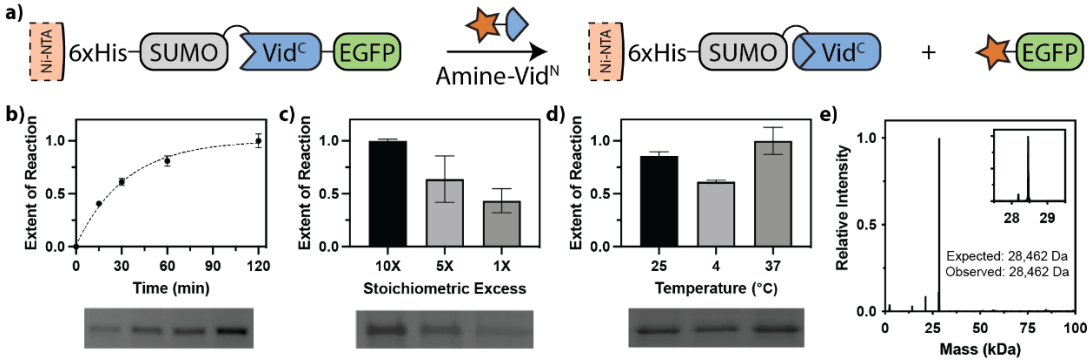

Figure 13: VEPL modification kinetics depend on stoichiometry and temperature.

a) EGFP was modified with an amine-functionalized Vid^N peptide via VEPL.
b) Trans-splicing proceeds quickly on resin, here at 25 °C with 10X stoichiometric excess of the amine-Vid^N peptide, as quantified through SDS-PAGE densitometry. Representative Coomassie-stained gel outlining reaction progress (15, 30, 60, 120 min from left to right).
c) Holding reaction time (120 min) and temperature (25 °C) constant, extent of trans-splicing scales with amine-Vid^N peptide excess. Representative Coomassie-stained gel depicts 10X, 5X, 1X excess from left to right.
d) With constant peptide excess (10X) and trans-splicing time (120 min), extent of trans-splicing varied with temperature. Coomassie-stained gel depicts 25, 5, and 37 °C from left to right.
e) N-terminal amine-tagged EGFP was obtained in high purity and with the expected molecular weight.

To further establish and demonstrate VEPL's broad utility, we next expressed four proteins spanning three different categories: Enhanced Green Fluorescent Protein (EGFP) and mCherry fluorescent proteins, β-lactamase (bla) enzyme, and epidermal growth factor (EGF), each as Vid^C fusions **(Figure 4.4, Supplementary Method S4.3)**. Additionally, we exploited solid-phase peptide synthesis to prepare four peptides harboring different N-terminal cargos: a primary amine, a biotin affinity ligand, an alkyne click handle, and a dual cargo modified with both biotin

and fluoresceine (FAM), each fused to Vid^N (**Supplementary Methods S4.3-S4.6**). Using broadly optimal on-resin splicing conditions identified with Vid^C-EGFP and amine-Vid^N, we found that each protein proved amenable to VEPL with our introduced library of synthetic handles; correctly modified species were obtained in each case and verified via mass spectrometry and Coomassie-stained SDS-PAGE (**Supplementary Tables S4.1 and S4.2, Supplementary Figures S4.4-S4.5**). Importantly, all SUMO-Vid^C-POI constructs were expressed directly in soluble form in aqueous buffers, in good purity, and without harsh denaturing agents and subsequent refolding steps, which had proven to be key impediments to more widespread use of prior split intein-based systems. Functionalized proteins were also purified and isolated in good yield; EGFP, mCherry and bla-based species were obtained at approximately 10 mgs/L of culture, and EGF-based species were obtained at 1-2 mgs/L of culture.

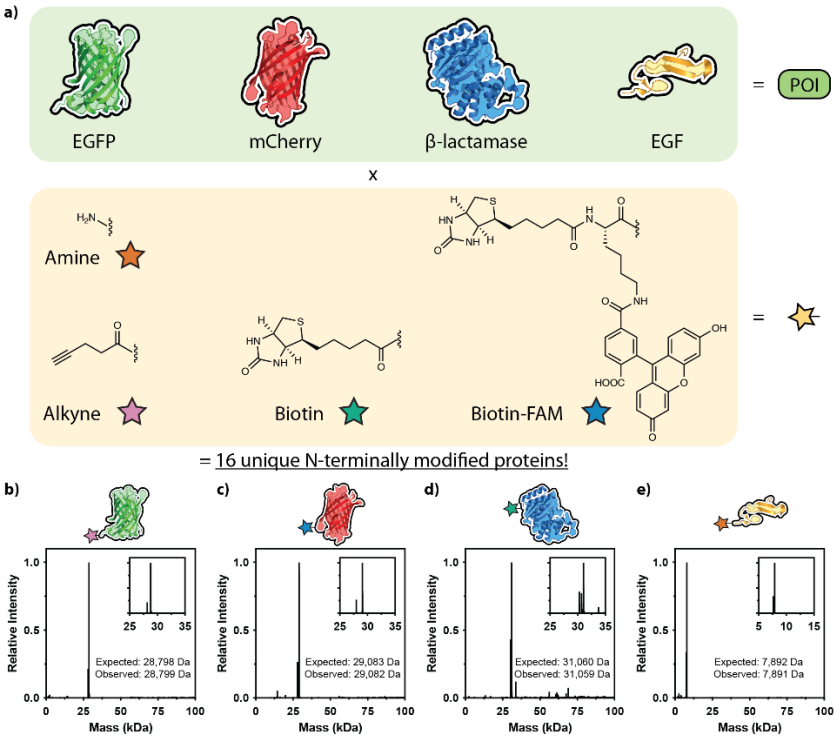

Figure 14: VEPL is compatible with a wide range of proteins and cargos.

a) VEPL was demonstrated using 4 different proteins (i.e., EGFP, mCherry, bla, EGF) and 4 distinctly functionalized Vid^N peptide cargos, yielding 16 unique N-terminal modified proteins. Species were obtained in high purity and with the expected molecular weight, with mass spectrometry analysis shown for:
b) alkyne-EGFP
c) biotin-FAM-mCherry
d) biotin-bla
e) amine-EGF.

With the full library of N-modified proteins in hand, we next sought to assess their bioactivity. For EGFP and mCherry, we quantified fluorescence as a surrogate measure of bioactivity for the amine-, alkyne-, and biotin-modified constructs; studies involving Biotin-FAM modification of EGFP and mCherry were excluded due to fluorescence crosstalk (**Figure 4.5a-b**). EGFP fluorescence was assessed using $\lambda_{excitation}$ = 490 nm, and $\lambda_{emission}$ = 525 nm. Similarly, mCherry fluorescence was determined with $\lambda_{excitation}$ = 575 nm, and $\lambda_{emission}$ = 610 nm. Encouragingly, each

of the distinctly N-functionalized proteins displayed statistically indistinguishable fluorescence, consistent with our starting hypothesis.

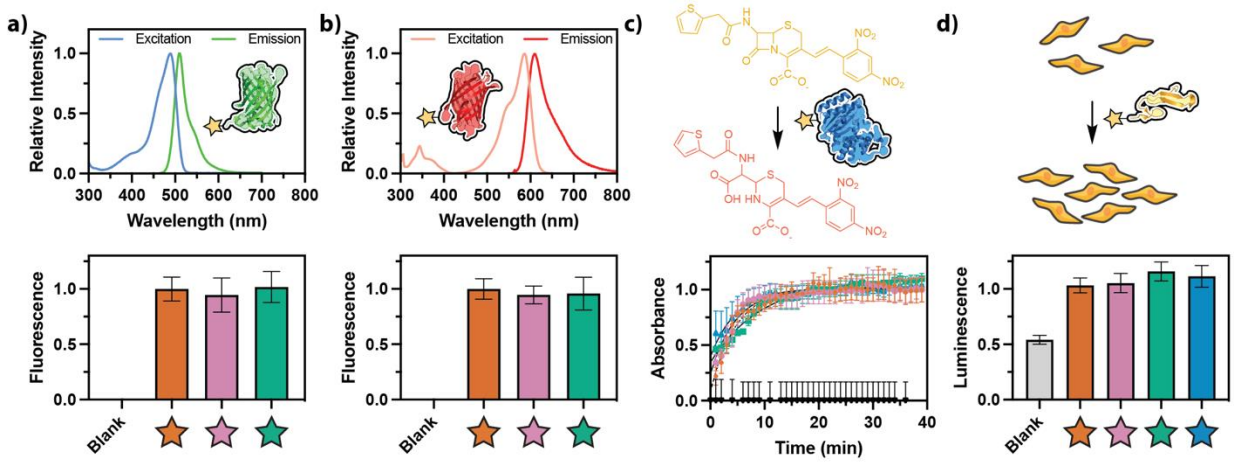

Figure 15: VEPL-modified proteins exhibit native bioactivity.

The activity of proteins N-modified via VEPL with amine, alkyne, biotin, or biotin-FAM was assessed (denoted respectively with orange, pink, green, and blue stars and/or individual data point).
a-b) EGFP and mCherry fluorescence was used as a surrogate of their respective activity.
c) Bla activity was determined by its ability to degrade a chromogenic nitrocefin substrate, whereby β-lactam cleavage yields a yellow-to-red color change.
d) EGF activity was assayed by its ability to stimulate HeLa cell proliferation, quantified using a RealTime-Glo™ MT cell viability assay. In all cases, N-modified protein bioactivity was statistically indistinguishable from native levels. Studies involving Biotin-FAM modification of EGFP and mCherry were excluded due to fluorescence crosstalk. Error bars correspond to the s.e.m. about the mean for biological replicate experiments (n = 3 for EGFP, mCherry, and Bla studies; n = 5 for EGF).

Having observed unaltered activity in fluorescent proteins, we then shifted our attention to the more sensitive bio-constructs. Since VEPL does not require harsh denaturants or other additives, we reasoned that this method could be readily extended to any polypeptide class with no loss of translational promise, particularly those that often prove refractory to functionalization.

For bla, taken as model enzyme, we applied a colorimetric assay based on the hydrolysis of nitrocefin (**Supplementary Method S4.7**), a chromogenic substrate which changes color from yellow to red upon cleavage of its beta-lactam bond (**Figure 4.5c**). Time-course colorimetric

read-outs established that statistically indistinguishable bla activity was retained regardless of the N-terminal cargo installed (**Figure 4.5c**).

Lastly, we applied VEPL to the model growth factor EGF, as growth factors are often both of prime interest and challenging to functionalize and post-translationally modify. EGF bioactivity was assessed based on its capacity to stimulate the proliferation of HeLa cells through the RealTime-Glo^{TM} MT Cell Viability Assay (Promega ®) (**Supplementary Methods S4.8 and S4.9**), which provides a metabolism-based count of viable cells through a bioluminescent assay. Bioactivity of the N-terminally modified EGFs proved unchanged, which is highly encouraging given its relative fragility (**Figure 4.5d**). We note that the "blank" treatment displays roughly half the luminescence of the EGF-treated samples, reflecting a smaller number of metabolically active cells present in this condition.

4.3. Conclusion

In this study, we have introduced the VEPL platform to generate and purify a suite of N-terminally modified proteins in a single step. Taking advantage of the atypically split VidaL intein whose N-fragment is readily accessible to solid-phase synthesis, VEPL permits diverse and multifunctional cargos to be N-terminally installed on a wide range of proteins all while maintaining native levels of bioactivity. Provided a protein-of-interest can be expressed as a Vid^{C} fusion, VEPL may N-terminally functionalize any POI regardless of the specific amino acid sequence present at the N-terminus. As such, we expect this method to prove broadly useful in

the creation of semisynthetic protein chimeras for a host of applications that interface materials and polypeptide-based assemblies.

References

1. Tamura, T.; Hamachi, I. Chemistry for Covalent Modification of Endogenous/Native Proteins: From Test Tubes to Complex Biological Systems. *J. Am. Chem. Soc.* **2019**, *141* (7), 2782–2799. https://doi.org/10.1021/jacs.8b11747.
2. Peng, T.; Hang, H. C. Site-Specific Bioorthogonal Labeling for Fluorescence Imaging of Intracellular Proteins in Living Cells. *J. Am. Chem. Soc.* **2016**, *138* (43), 14423–14433. https://doi.org/10.1021/jacs.6b08733.
3. Freedy, A. M.; Matos, M. J.; Boutureira, O.; Corzana, F.; Guerreiro, A.; Akkapeddi, P.; Somovilla, V. J.; Rodrigues, T.; Nicholls, K.; Xie, B.; Jiménez-Osés, G.; Brindle, K. M.; Neves, A. A.; Bernardes, G. J. L. Chemoselective Installation of Amine Bonds on Proteins through Aza-Michael Ligation. *J. Am. Chem. Soc.* **2017**, *139* (50), 18365–18375. https://doi.org/10.1021/jacs.7b10702.
4. Fisher, S. A.; Baker, A. E. G.; Shoichet, M. S. Designing Peptide and Protein Modified Hydrogels: Selecting the Optimal Conjugation Strategy. *J. Am. Chem. Soc.* **2017**, *139* (22), 7416–7427. https://doi.org/10.1021/jacs.7b00513.
5. Spicer, C. D.; Pashuck, E. T.; Stevens, M. M. Achieving Controlled Biomolecule–Biomaterial Conjugation. *Chem. Rev.* **2018**, *118* (16), 7702–7743. https://doi.org/10.1021/acs.chemrev.8b00253.
6. Shadish, J. A.; DeForest, C. A. Site-Selective Protein Modification: From Functionalized Proteins to Functional Biomaterials. *Matter* **2020**, *2* (1), 50–77. https://doi.org/10.1016/j.matt.2019.11.011.
7. Gharios, R.; Francis, R. M.; DeForest, C. A. Chemical and Biological Engineering Strategies to Make and Modify Next-Generation Hydrogel Biomaterials. *Matter* **2023**, *6* (12), 4195–4244. https://doi.org/10.1016/j.matt.2023.10.012.
8. Thompson, R. E.; Muir, T. W. Chemoenzymatic Semisynthesis of Proteins. *Chem. Rev.* **2020**, *120* (6), 3051–3126. https://doi.org/10.1021/acs.chemrev.9b00450.
9. Taylor, R. J.; Geeson, M. B.; Journeaux, T.; Bernardes, G. J. L. Chemical and Enzymatic Methods for Post-Translational Protein-Protein Conjugation. *J. Am. Chem. Soc.* **2022**, *144* (32), 14404–14419. https://doi.org/10.1021/jacs.2c00129.
10. Warden-Rothman, R.; Caturegli, I.; Popik, V.; Tsourkas, A. Sortase-Tag Expressed Protein Ligation: Combining Protein Purification and Site-Specific Bioconjugation into a Single Step. *Anal. Chem.* **2013**, *85* (22), 11090–11097. https://doi.org/10.1021/ac402871k.
11. Shadish, J. A.; Benuska, G. M.; DeForest, C. A. Bioactive Site-Specifically Modified Proteins for 4D Patterning of Gel Biomaterials. *Nat. Mater.* **2019**, *18* (9), 1005–1014. https://doi.org/10.1038/s41563-019-0367-7.
12. Marino, G.; Eckhard, U.; Overall, C. M. Protein Termini and Their Modifications Revealed by Positional Proteomics. *ACS Chem. Biol.* **2015**, *10* (8), 1754–1764. https://doi.org/10.1021/acschembio.5b00189.

13. Rosen, C. B.; Francis, M. B. Targeting the N Terminus for Site-Selective Protein Modification. *Nat. Chem. Biol.* **2017**, *13* (7), 697–705. https://doi.org/10.1038/nchembio.2416.

14. Jacob, E.; Unger, R. A Tale of Two Tails: Why Are Terminal Residues of Proteins Exposed? *Bioinformatics* **2007**, *23* (2), e225–e230. https://doi.org/10.1093/bioinformatics/btl318.

15. Gilmore, J. M.; Scheck, R. A.; Esser-Kahn, A. P.; Joshi, N. S.; Francis, M. B. N-Terminal Protein Modification through a Biomimetic Transamination Reaction. *Angew. Chem. Int. Ed.* **2006**, *45* (32), 5307–5311. https://doi.org/10.1002/anie.200600368.

16. Obermeyer, A. C.; Jarman, J. B.; Francis, M. B. N-Terminal Modification of Proteins with o-Aminophenols. *J. Am. Chem. Soc.* **2014**, *136* (27), 9572–9579. https://doi.org/10.1021/ja500728c.

17. Liebscher, S.; Schöpfel, M.; Aumüller, T.; Sharkhuukhen, A.; Pech, A.; Höss, E.; Parthier, C.; Jahreis, G.; Stubbs, M. T.; Bordusa, F. N-Terminal Protein Modification by Substrate-Activated Reverse Proteolysis. *Angew. Chem. Int. Ed.* **2014**, *53* (11), 3024–3028. https://doi.org/10.1002/anie.201307736.

18. Weeks, A. M.; Wells, J. A. Subtiligase-Catalyzed Peptide Ligation. *Chem. Rev.* **2020**, *120* (6), 3127–3160. https://doi.org/10.1021/acs.chemrev.9b00372.

19. Weeks, A. M.; Wells, J. A. N-Terminal Modification of Proteins with Subtiligase Specificity Variants. *Curr. Protoc. Chem. Biol.* **2020**, *12* (1), e79. https://doi.org/10.1002/cpch.79.

20. Zakeri, B.; Fierer, J. O.; Celik, E.; Chittock, E. C.; Schwarz-Linek, U.; Moy, V. T.; Howarth, M. Peptide Tag Forming a Rapid Covalent Bond to a Protein, through Engineering a Bacterial Adhesin. *Proc. Natl. Acad. Sci. U. S. A.* **2012**, *109* (12), E690–E697. https://doi.org/10.1073/PNAS.1115485109/SUPPL_FILE/APPENDIX.PDF.

21. Veggiani, G.; Nakamura, T.; Brenner, M. D.; Gayet, R. V.; Yan, J.; Robinson, C. V.; Howarth, M. Programmable Polyproteams Built Using Twin Peptide Superglues. *Proc. Natl. Acad. Sci. U. S. A.* **2016**, *113* (5), 1202–1207. https://doi.org/10.1073/PNAS.1519214113/SUPPL_FILE/PNAS.201519214SI.PDF.

22. Keeble, A. H.; Banerjee, A.; Ferla, M. P.; Reddington, S. C.; Anuar, I. N. A. K.; Howarth, M. Evolving Accelerated Amidation by SpyTag/SpyCatcher to Analyze Membrane Dynamics. *Angew. Chem. Int. Ed.* **2017**, *56* (52), 16521–16525. https://doi.org/10.1002/ANIE.201707623.

23. Keeble, A. H.; Turkki, P.; Stokes, S.; Anuar, I. N. A. K.; Rahikainen, R.; Hytönen, V. P.; Howarth, M. Approaching Infinite Affinity through Engineering of Peptide-Protein Interaction. *Proc. Natl. Acad. Sci. U. S. A.* **2019**, *116* (52), 26523–26533. https://doi.org/10.1073/PNAS.1909653116/SUPPL_FILE/PNAS.1909653116.SAPP.PDF.

24. Buldun, C. M.; Jean, J. X.; Bedford, M. R.; Howarth, M. SnoopLigase Catalyzes Peptide–Peptide Locking and Enables Solid-Phase Conjugate Isolation. *J. Am. Chem. Soc.* **2018**, *140* (8), 3008–3018. https://doi.org/10.1021/jacs.7b13237.

25. Keeble, A. H.; Yadav, V. K.; Ferla, M. P.; Bauer, C. C.; Chuntharpursat-Bon, E.; Huang, J.; Bon, R. S.; Howarth, M. DogCatcher Allows Loop-Friendly Protein-Protein Ligation. *Cell Chem. Biol.* **2022**, *29* (2), 339-350.e10. https://doi.org/10.1016/j.chembiol.2021.07.005.

26. Shah, N. H.; Muir, T. W. Split Inteins: Nature's Protein Ligases. *Isr. J. Chem.* **2011**, *51* (8–9), 854–861. https://doi.org/10.1002/ijch.201100094.

27. Shah, N. H.; Muir, T. W. Inteins: Nature's Gift to Protein Chemists. *Chem. Sci.* **2014**, *5* (2), 446–461. https://doi.org/10.1039/c3sc52951g.

28. Mootz, H. D. Split Inteins as Versatile Tools for Protein Semisynthesis. *ChemBioChem* **2009**, *10* (16), 2579–2589. https://doi.org/10.1002/CBIC.200900370.

29. Thiel, I. V.; Volkmann, G.; Pietrokovski, S.; Mootz, H. D. An Atypical Naturally Split Intein Engineered for Highly Efficient Protein Labeling. *Angew. Chem. - Int. Ed.* **2014**, *53* (5), 1306–1310. https://doi.org/10.1002/anie.201307969.

30. Prabhala, S. V.; Gierach, I.; Wood, D. W. The Evolution of Intein-Based Affinity Methods as Reflected in 30 Years of Patent History. *Front. Mol. Biosci.* **2022**, *9*. https://doi.org/10.3389/fmolb.2022.857566.

31. Wood, D. W.; Belfort, M.; Lennon, C. W. Inteins—Mechanism of Protein Splicing, Emerging Regulatory Roles, and Applications in Protein Engineering. *Front. Microbiol.* **2023**, *14*. https://doi.org/10.3389/fmicb.2023.1305848.

32. Wood, D. W.; Wu, W.; Belfort, G.; Derbyshire, V.; Belfort, M. A Genetic System Yields Self-Cleaving Inteins for Bioseparations. *Nat. Biotechnol.* **1999**, *17* (9), 889–892. https://doi.org/10.1038/12879.

33. Guan, D.; Ramirez, M.; Chen, Z. Split Intein Mediated Ultra-Rapid Purification of Tagless Protein (SIRP). *Biotechnol. Bioeng.* **2013**, *110* (9), 2471–2481. https://doi.org/10.1002/bit.24913.

34. Xia, H.-F.; Zhou, T.-J.; Du, Y.-X.; Wang, Y.-J.; Shi, C.-H.; Wood, D. W. Improved Protein Purification System Based on C-Terminal Cleavage of Npu DnaE Split Intein. *Bioprocess Biosyst. Eng.* **2020**, *43* (11), 1931–1941. https://doi.org/10.1007/s00449-020-02382-w.

35. Volkmann, G.; Liu, X.-Q. Protein C-Terminal Labeling and Biotinylation Using Synthetic Peptide and Split-Intein. *PLOS ONE* **2009**, *4* (12), e8381. https://doi.org/10.1371/journal.pone.0008381.

36. Graulus, G.-J.; Ta, D. T.; Tran, H.; Hansen, R.; Billen, B.; Royackers, E.; Noben, J.-P.; Devoogdt, N.; Muyldermans, S.; Guedens, W.; Adriaensens, P. Site-Selective Functionalization of Nanobodies Using Intein-Mediated Protein Ligation for Innovative Bioconjugation. In *Bioconjugation: Methods and Protocols*; Massa, S., Devoogdt, N., Eds.; Springer: New York, NY, 2019; pp 117–130. https://doi.org/10.1007/978-1-4939-9654-4_9.

37. Roller, R. F.; Malik, A.; Carillo, M. A.; Garg, M.; Rella, A.; Raulf, M.-K.; Lepenies, B.; Seeberger, P. H.; Varón Silva, D. Semisynthesis of Functional Glycosylphosphatidylinositol-Anchored Proteins. *Angew. Chem. Int. Ed.* **2020**, *59* (29), 12035–12040. https://doi.org/10.1002/anie.202002479.

38. Reyes-Turcu, F. E.; Horton, J. R.; Mullally, J. E.; Heroux, A.; Cheng, X.; Wilkinson, K. D. The Ubiquitin Binding Domain ZnF UBP Recognizes the C-Terminal Diglycine Motif of Unanchored Ubiquitin. *Cell* **2006**, *124* (6), 1197–1208. https://doi.org/10.1016/j.cell.2006.02.038.

39. Szente, B. E.; Soos, J. M.; Johnson, H. M. The C-Terminus of IFN-γ Is Sufficient for Intracellular Function. *Biochem. Biophys. Res. Commun.* **1994**, *203* (3), 1645–1654. https://doi.org/10.1006/bbrc.1994.2375.

40. Burton, A. J.; Haugbro, M.; Parisi, E.; Muir, T. W. Live-Cell Protein Engineering with an Ultra-Short Split Intein. *Proc. Natl. Acad. Sci. U. S. A.* **2020**, *117* (22), 12041–12049. https://doi.org/10.1073/pnas.2003613117.

41. Ceballos-Alcantarilla, E.; Merkx, M. Chapter One - Understanding and Applications of Ser/Gly Linkers in Protein Engineering. In *Methods in Enzymology*; Merkx, M., Ed.; Linkers in Biomacromolecules; Academic Press, 2021; Vol. 647, pp 1–22. https://doi.org/10.1016/bs.mie.2020.12.001.

42. Friedel, K.; A. Popp, M.; J. Matern, J. C.; M. Gazdag, E.; V. Thiel, I.; Volkmann, G.; Blankenfeldt, W.; D. Mootz, H. A Functional Interplay between Intein and Extein Sequences

in Protein Splicing Compensates for the Essential Block B Histidine. *Chem. Sci.* **2019**, *10* (1), 239–251. https://doi.org/10.1039/C8SC01074A.

43. Ludwig, C.; Schwarzer, D.; Zettler, J.; Garbe, D.; Janning, P.; Czeslik, C.; Mootz, H. D. Chapter 4 Semisynthesis of Proteins Using Split Inteins. In *Methods in Enzymology*; Muir, T. W., Abelson, J. N., Eds.; Non-Natural Amino Acids; Academic Press, 2009; Vol. 462, pp 77–96. https://doi.org/10.1016/S0076-6879(09)62004-8.

Acknowledgements

The authors would like to thank Prof. Tom Muir and Dr. Anthony Burton for helpful discussions on intein chemistry and for providing us with different intein plasmid constructs. We would also like to thank Dr. Drew Sellers for expert guidance on peptide synthesis and modification. This work was supported by a Faculty Early Career Development CAREER Award (DMR 1652141, C.A.D.) a grant (DMR 1807398, C.A.D.) from the National Science Foundation, and a Maximizing Investigators' Research Award (R35GM138036, C.A.D.) from the National Institutes of Health. Student support was further provided through a John C. Berg Endowed Fellowship (R.G.), an NSF Graduate Student Research Fellowship (DGE 1762114, I.K.), and an ITHS-TL1 Fellowship (R.M.F.).

Methods

General Synthetic Information

Chemical reagents and solvents were purchased and used as indicated from either Sigma-Aldrich or Fisher Scientific. Peptide synthesis reagents were purchased from ChemPep or Chem-Impex and used as received. Deionized water (DH 2 O) was obtained from departmental sources and generated from a U.S. Filter Corporation Reverse Osmosis system equipped with a Desal membrane. Peptide synthesis was performed on a CEM Liberty One peptide synthesizer. Semi-preparative reverse-phase high-pressure liquid chromatography (RP HPLC) was accomplished using a Dionex Ultimate 3000 equipped with a variable multiple wavelength detector, automated fraction collector, and a Thermo 5 μm Syncronis silica 250 x 21.2 mm C18 column. Peaks were collected based on absorption at 220 nm. Fractions were collected and analyzed via electro-spray ionization mass spectrometry (ESI-MS) on an AB Sciex 5600 mass spectrometer. Fractions were directly injected onto the instrument and were analyzed in a 100% Acetonitrile (+ 0.1% formic acid) solution for 2 minutes. Fractions determined to be the desired product were frozen and lyophilized on a LABCONCO FreeZone 2.5 Plus freeze-dryer equipped with a LABCONCO rotary vane 117 vacuum pump. Cells were lysed using a Fisher Scientific Model 505 Sonic Dismembrator with a 1.27 cm diameter probe. Mammalian cell culture was performed in a NuAire LabGard ES NU-437 Class II Type A2 Biosafety Cabinet. Cells were maintained in a Sanyo inCu saFe® MCO-17AC incubator at 37 °C and 5% CO_2.

Method S4.1 General methods for protein expression

E. coli SHuffle cells were transformed with the appropriate construct and grown at 37°C and 220 rpm agitation to an OD of 0.6-0.8 in LB broth supplemented with kanamycin. Isopropyl β-D-1-thiogalactopyranoside (IPTG) was used to induce protein expression, at which point the cultures were moved to a reduced temperature (18 °C) for 18 hours. Cells were then harvested via centrifugation (4,000g, 20 minutes, 4 °C) and pellets were re-suspended in lysis buffer (50 mM Tris, 150 mM NaCl, 1 mM PMSF, 2 mM DTT, pH 7.5) and sonicated on ice (6 cycles, each for 3 minutes at 30% amplitude, 33% duty cycle, and 3 minutes resting). The soluble fraction was then isolated by centrifugation (7,500g, 45 minutes, 4 °C) and incubated with INDIGO Ni-NTA resin (Cube Biotech) (2 mL slurry/L of culture) under mild agitation (2 hours, 4 °C). Flow-through was discarded and the resin was washed with lysis buffer (10x column volume) until full removal of soluble aggregates and impurities.

Method S4.2 Purification of MBP-Vid^{N} through amylose chromatography

E. coli cell pellets were re-suspended in lysis buffer (50 mM Tris, 150 mM NaCl, 1 mM PMSF, 2 mM DTT, pH 7.5) and sonicated on ice (6 cycles, each for 3 minutes at 30% amplitude, 33% duty cycle, and 3 minutes resting). The soluble fraction was then isolated by centrifugation (7,500g, 45 minutes, 4°C) and incubated with Amylose Resin (New England Biolabs) (2 mL slurry/L of culture) under mild agitation (2 hours, 4°C). Flow-through was discarded and the resin was washed with lysis buffer (10x column volume) until full removal of impurities. The MBP-Vid^{N} target protein was obtained at high yields and high purity when eluted off the column with elution buffer (lysis buffer + 10 mM maltose).

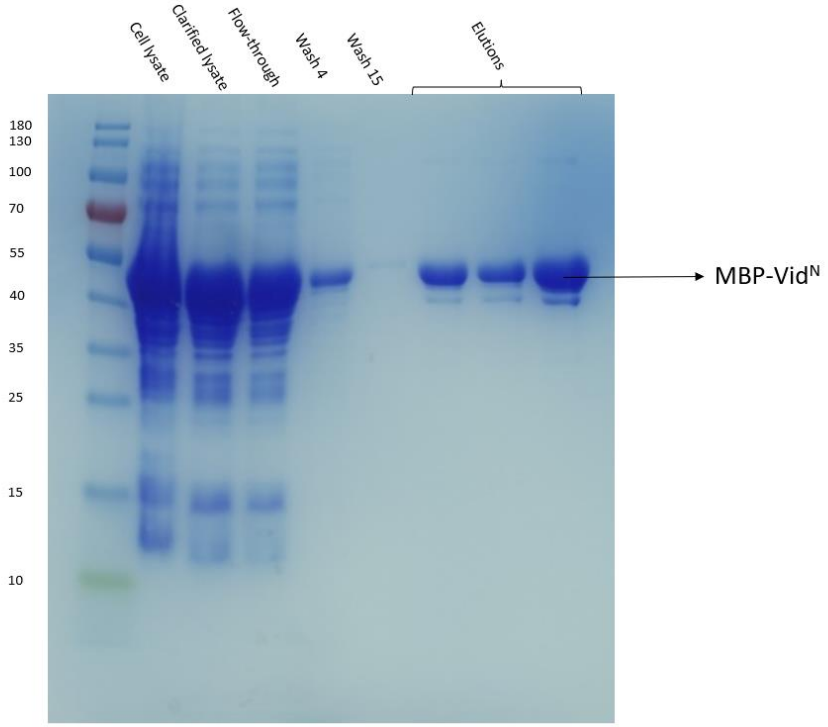

MBP-Vid^{N} can be recombinantly expressed at high purity and in good yield.

Method S4.3 Plasmid construction for protein expression

For the streamlined construction of plasmids used in this study, gBlocks harboring a 6xHis-SUMO-Vid^{C}-POI-FLAG chimera were ordered from Integrated DNA Technologies (IDT). Gibson Assembly was used to ligate ordered genes into a pET-21 vector for EGF and bla constructs and pET-29 for EGFP and mCherry.

The open reading frames (ORFs) for the reported constructs are given below:

GSS-6xHis-SUMO-Vid^{C}-EGFP-FLAG:

GGCAGCAGCCATCATCATCATCATCACGGCAGCGGCCTGGTGCCGCGCGGCAGCGCTAGCATGT
CGGACTCAGAAGTCAATCAAGAAGCTAAGCCAGAGGTCAAGCCAGAAGTCAAGCCTGAGACTCA
CATCAATTTAAAGGTGTCCGATGGATCTTCAGAGATCTTCTTCAAGATCAAAAAGACCACTCCT
TTAAGAAGGCTGATGGAAGCGTTCGCTAAAAGACAGGGTAAGGAAATGGACTCCTTAAGATTCT
TGTACGACGGTATTAGAATTCAAGCTGATCAGACCCCTGAAGATTTGGACATGGAGGATAACGA
TATTATTGAGGCTCACAGAGAACAGATTGGTGGTATGATTGAGGAGAAAAAGGTCACCGTGCAG
GAGCTGAGAGAATTGTATCTGTCTGGAGAGTACACGATCGAAATAGATACCCCCGACGGATACC
AGACCATTGGGAAATGGTTTGATAAGGGCGTCTTATCAATGGTACGGGTCGCGACTGCTACATA
CGAGACAGTTTGCGCATTCAACCATATGATCCAACTCGCCGACAATACCTGGGTGCAAGCATGC
GAACTGGACGTAGGTGTTGATATTCAGACAGCCGCCGGGATCCAGCCAGTGATGCTTGTGGAGG
ACACTAGTGATGCTGAATGTTATGATTTCGAAGTGATGCACCCTAATCACAGGTACTATGGCGA
CGGTATCGTGAGCCATAACTCCGGCAAGATGGTGAGCAAGGGCGAGGAGCTGTTCACCGGGGTG
GTGCCCATCCTGGTCGAGCTGGACGGCGACGTAAACGGCCACAAGTTCAGCGTGTCCGGCGAGG
GCGAGGGCGATGCCACCTACGGCAAGCTGACCCTGAAGTTCATCTGCACCACCGGCAAGCTGCC
CGTGCCCTGGCCCACCCTCGTGACCACCCTGACCTACGGCGTGCAGTGCTTCAGCCGCTACCCC
GACCACATGAAGCAGCACGACTTCTTCAAGTCCGCCATGCCCGAAGGCTACGTCCAGGAGCGCA
CCATCTTCTTCAAGGACGACGGCAACTACAAGACCCGCGCCGAGGTGAAGTTCGAGGGCGACAC
CCTGGTGAACCGCATCGAGCTGAAGGGCATCGACTTCAAGGAGGACGGCAACATCCTGGGGCAC
AAGCTGGAGTACAACTACAACAGCCACAACGTCTATATCATGGCCGACAAGCAGAAGAACGGCA
TCAAGGTGAACTTCAAGATCCGCCACAACATCGAGGACGGCAGCGTGCAGCTCGCCGACCACTA
CCAGCAGAACACCCCCATCGGCGACGGCCCCGTGCTGCTGCCCGACAACCACTACCTGAGCACC
CAGTCCGCCCTGAGCAAAGACCCCAACGAGAAGCGCGATCACATGGTCCTGCTGGAGTTCGTGA
CCGCCGCCGGGATCACTCTCGGCATGGACGAGCTGTACAAGGACTACAAGGACGACGACGACAA
G

GSS-6xHis-SUMO-Vid^{C}-mCherry-FLAG:

GGCAGCAGCCATCATCATCATCATCACGGCAGCGGCCTGGTGCCGCGCGGCAGCGCTAGCATGT
CGGACTCAGAAGTCAATCAAGAAGCTAAGCCAGAGGTCAAGCCAGAAGTCAAGCCTGAGACTCA
CATCAATTTAAAGGTGTCCGATGGATCTTCAGAGATCTTCTTCAAGATCAAAAAGACCACTCCT
TTAAGAAGGCTGATGGAAGCGTTCGCTAAAAGACAGGGTAAGGAAATGGACTCCTTAAGATTCT
TGTACGACGGTATTAGAATTCAAGCTGATCAGACCCCTGAAGATTTGGACATGGAGGATAACGA

TATTATTGAGGCTCACAGAGAACAGATTGGTGGTATGATTGAGGAGAAAAAGGTCACCGTGCAG
GAGCTGAGAGAATTGTATCTGTCTGGAGAGTACACGATCGAAATAGATACCCCCGACGGATACC
AGACCATTGGGAAATGGTTTGATAAGGGCGTCTTATCAATGGTACGGGTCGCGACTGCTACATA
CGAGACAGTTTGCGCATTCAACCATATGATCCAACTCGCCGACAATACCTGGGTGCAAGCATGC
GAACTGGACGTAGGTGTTGATATTCAGACAGCCGCCGGGATCCAGCCAGTGATGCTTGTGGAGG
ACACTAGTGATGCTGAATGTTATGATTTCGAAGTGATGCACCCTAATCACAGGTACTATGGCGA
CGGTATCGTGAGCCATAACTCCGGCAAGGACTACAAGGACGACGACGACAAG

GSS-6xHis-SUMO-Vid^{C}-EGF-FLAG:
GGCAGCAGCCATCATCATCATCATCACGGCAGCGGCCTGGTGCCGCGCGGCAGCGCTAGCATGT
CGGACTCAGAAGTCAATCAAGAAGCTAAGCCAGAGGTCAAGCCAGAAGTCAAGCCTGAGACTCA
CATCAATTTAAAGGTGTCCGATGGATCTTCAGAGATCTTCTTCAAGATCAAAAAGACCACTCCT
TTAAGAAGGCTGATGGAAGCGTTCGCTAAAAGACAGGGTAAGGAAATGGACTCCTTAAGATTCT
TGTACGACGGTATTAGAATTCAAGCTGATCAGACCCCTGAAGATTTGGACATGGAGGATAACGA
TATTATTGAGGCTCACAGAGAACAGATTGGTGGTATGATTGAGGAGAAAAAGGTCACCGTGCAG
GAGCTGAGAGAATTGTATCTGTCTGGAGAGTACACGATCGAAATAGATACCCCCGACGGATACC
AGACCATTGGGAAATGGTTTGATAAGGGCGTCTTATCAATGGTACGGGTCGCGACTGCTACATA
CGAGACAGTTTGCGCATTCAACCATATGATCCAACTCGCCGACAATACCTGGGTGCAAGCATGC
GAACTGGACGTAGGTGTTGATATTCAGACAGCCGCCGGGATCCAGCCAGTGATGCTTGTGGAGG
ACACTAGTGATGCTGAATGTTATGATTTCGAAGTGATGCACCCTAATCACAGGTACTATGGCGA
CGGTATCGTGAGCCATAACTCCGGCAAGAACAGTGATTCGGAATGTCCGTTGAGCCATGATGGT
TATTGCCTGCACGACGGGGTTTGCATGTACATCGAAGCGCTGGACAAATACGCCTGTAATTGCG
TCGTGGGCTATATTGGCGAACGGTGTCAGTATCGTGATTTAAAATGGTGGGAGCTTCGCGACTA
CAAGGACGACGACGACAAG

GSS-6xHis-SUMO-Vid^{C}-bla-FLAG:
GGCAGCAGCCATCATCATCATCATCACGGCAGCGGCCTGGTGCCGCGCGGCAGCGCTAGCATGT
CGGACTCAGAAGTCAATCAAGAAGCTAAGCCAGAGGTCAAGCCAGAAGTCAAGCCTGAGACTCA
CATCAATTTAAAGGTGTCCGATGGATCTTCAGAGATCTTCTTCAAGATCAAAAAGACCACTCCT
TTAAGAAGGCTGATGGAAGCGTTCGCTAAAAGACAGGGTAAGGAAATGGACTCCTTAAGATTCT
TGTACGACGGTATTAGAATTCAAGCTGATCAGACCCCTGAAGATTTGGACATGGAGGATAACGA
TATTATTGAGGCTCACAGAGAACAGATTGGTGGTATGATTGAGGAGAAAAAGGTCACCGTGCAG
GAGCTGAGAGAATTGTATCTGTCTGGAGAGTACACGATCGAAATAGATACCCCCGACGGATACC
AGACCATTGGGAAATGGTTTGATAAGGGCGTCTTATCAATGGTACGGGTCGCGACTGCTACATA
CGAGACAGTTTGCGCATTCAACCATATGATCCAACTCGCCGACAATACCTGGGTGCAAGCATGC
GAACTGGACGTAGGTGTTGATATTCAGACAGCCGCCGGGATCCAGCCAGTGATGCTTGTGGAGG
ACACTAGTGATGCTGAATGTTATGATTTCGAAGTGATGCACCCTAATCACAGGTACTATGGCGA
CGGTATCGTGAGCCATAACTCCGGCAAGATGCACCCGGAAACCCTGGTTAAAGTTAAAGACGCT
GAAGACCAGCTGGGTGCTCGTGTTGGTTACATCGAACTGGACCTGAACTCTGGTAAAATCCTGG
AATCTTTCCGTCCGGAAGAACGTTTCCCGATGATGTCTACCTTCAAAGTTCTGCTGTGCGGTGC
TGTTCTGTCTCGTGTTGACGCTGGTCAGGAACAGCTGGGTCGTCGTATCCACTACTCTCAGAAC
GACCTGGTTGAATACTCTCCGGTTACCGAAAAACACCTGACCGACGGTATGACCGTTCGTGAAC
TGTGCTCTGCTGCTATCACCATGTCTGACAACACCGCTGCTAACCTGCTGCTGACCACCATCGG
TGGTCCGAAAGAACTGACCGCTTTCCTGCACAACATGGGTGACCACGTTACCCGTCTGGACCGT
TGGGAACCGGAACTGAACGAAGCTATCCCGAACGACGAACGTGACACCACCATGCCGGCTGCTA

TGGCTACCACCCTGCGTAAACTGCTGACCGGTGAACTGCTGACCCTGGCTTCTCGTCAGCAGCT
GATCGACTGGATGGAAGCTGACAAAGTTGCTGGTCCGCTGCTGCGTTCTGCTCTGCCGGCTGGT
TGGTTCATCGCTGACAAATCTGGTGCTGGTGAACGTGGTTCTCGTGGTATCATCGCTGCTCTGG
GTCCGGACGGTAAACCGTCTCGTATCGTTGTTATCTACACCACCGGTTCTCAGGCTACCATGGA
CGAACGTAACCGTCAGATCGCTGAAATCGGTGCTTCTCTGATCAAACACTGGGACTACAAGGAC
GACGACGACAAG

MBP-Vid^{N}:

ATGAAGACAGAAGAAGGCAAACTCGTTATCTGGATCAATGGGGACAAGGGCTACAATGGCCTGG
CGGAAGTCGGCAAGAAATTTGAAAAAGATACCGGGATCAAAGTGACCGTTGAACACCCGGATAA
ATTGGAGGAAAAGTTCCCGCAAGTGGCCGCGACCGGAGATGGTCCTGACATAATTTTTTGGGCG
CACGATCGGTTTGGTGGGTACGCTCAATCGGGCCTTCTAGCAGAAATTACGCCGGACAAAGCGT
TTCAGGATAAACTCTATCCGTTTACCTGGGACGCGGTACGCTATAATGGAAAACTGATTGCATA
TCCGATTGCAGTGGAAGCGCTGAGCCTTATTTACAATAAAGATCTGCTTCCTAATCCGCCCAAG
ACCTGGGAAGAAATTCCGGCACTGGACAAAGAACTGAAAGCCAAAGGTAAAAGCGCACTTATGT
TCAATCTGCAGGAGCCGTATTTCACCTGGCCGCTAATCGCGGCCGACGGCGGTTATGCCTTTAA
ATATGAAAACGGCAAGTATGATATCAAAGATGTTGGTGTAGACAACGCCGGTGCCAAAGCTGGC
TTGACCTTCTTGGTGGATTTAATTAAAAACAAACACATGAACGCAGATACGGATTATTCAATTG
CGGAGGCCGCGTTCAACAAGGGCGAGACTGCAATGACTATTAACGGTCCATGGGCGTGGTCAAA
CATCGACACTTCTAAAGTGAACTACGGTGTCACTGTGCTCCCGACGTTTAAAGGTCAGCCGTCC
AAACCGTTTGTGGGCGTGCTGAGTGCAGGAATCAACGCGGCGAGTCCGAATAAAGAATTAGCGA
AAGAATTTTTAGAAAACTATCTGTTAACGGATGAGGGTCTGGAAGCTGTCAACAAAGACAAGCC
TTTGGGGGCCGTGGCACTGAAATCATATGAGGAAGAGTTAGCAAAGGATCCCCGCATCGCTGCG
ACCATGGAAAATGCCCAAAAAGGCGAAATTATGCCAAATATCCCCCAGATGAGCGCTTTCTGGT
ACGCTGTCAGGACAGCCGTCATTAACGCCGCGTCCGGCCGTCAAACTGTTGATGAAGCTTTGAA
AGATGCACAGACTAATTCCTCGAGCAATAATAACAACAATAACAACAATAATAACCTGGGAATC
GAGGGGCGTGAAAGCGGCTGCCTGCCGAAAGAAGCGGTGGTGCAGATTCGCCTGACCAAAAAAG
GC

Method S4.4 Synthesis of non-canonical amino acids

Method S4.4.1 Synthesis of N^2-[(9H-Fluoren-9-ylmethoxy)carbonyl]-N^6-(1-oxo-4-pentyn-1-yl)-L-lysine (Fmoc-Lys(alkyne)-OH)

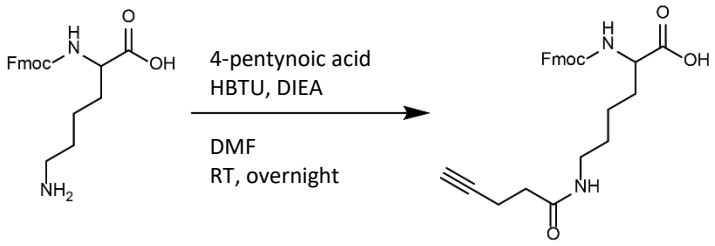

4-pentynoic acid (250 mg, 2.5 mmol), HBTU (950 mg, 2.5 mmol), and *N,N'*-diisopropylethylamine (640 mg, 5.0 mmol) were reacted in 6 mL of *N,N'*-dimethylformamide for 5 minutes at room temperature. N_α-Fmoc-L-lysine hydrochloride (1.0 g, 2.5 mmol) was added, and the reaction continued overnight at room temperature. Solvent was removed *in vacuo*, leaving an orange syrup that was purified by preparatory C18 HPLC using a gradient of 40-100% acetonitrile in water containing 0.1% trifluoroacetic acid. Purified fractions were lyophilized to yield 803 mg (1.8 mmol, 72%) of Fmoc-Lys(alkyne)-OH, a colorless powder. ^{1}H NMR (500 MHz, MeOD): δ = 1.38-1.62 (m, 4 H), 1.64-1.76 (m, 1 H), 1.81-1.91 (m, 1 H), 2.23-2.27 (t, J = 2.6 Hz, 1 H), 2.32-2.40 (t, J = 6.9 Hz, 2 H), 2.42-2.49 (td, J = 7.0 Hz, 2.4 Hz, 2 H), 3.15-3.23 (t, J = 6.9 Hz, 2 H), 4.10-4.17 (m, 1 H), 4.20-4.27 (t, J = 7.0 Hz, 1 H), 4.30-4.41 (m, 2 H), 7.29-7.34 (td, J = 7.4 Hz, 1.1 Hz, 2 H), 7.36-7.42 (t, J = 7.5 Hz, 2 H), 7.65-7.71 (t, J = 7.5 Hz, 2 H), 7.77-7.82 (d, J = 7.5 Hz, 2 H), consistent with previous literature[1]. MS (ESI-MS): calculated for $C_{26}H_{29}N_2O_5$ ($[M+H]^+$): 449.208; found: 449.208.

Method S4.4.2 Synthesis of N^2-[(9H-Fluoren-9-ylmethoxy)carbonyl]-N^6-[5-[(3aS,4S,6aR)-hexahydro-2-oxo-1H-thieno[3,4-d]imidazol-4-yl]-1-oxopentyl]-L-lysine (Fmoc-Lys(biotin)-OH)

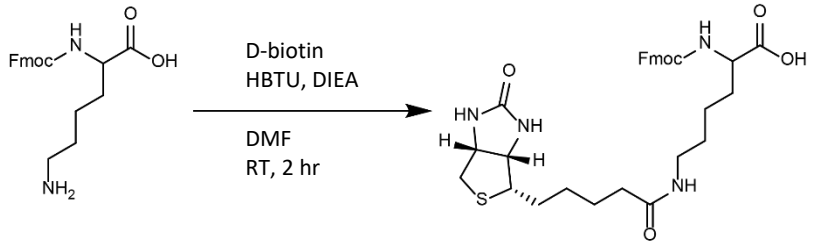

Fmoc-Lys(biotin)-OH was synthesized as previously reported[2]. D-biotin (610 mg, 2.5 mmol), HBTU (950 mg, 2.5 mmol) and *N,N'*-diisopropylethylamine (650 mg, 5.0 mmol) were reacted in 15 mL of *N,N'*-dimethylformamide for 5 minutes at room temperature. N_α-Fmoc-L-lysine hydrochloride (1.00 g, 2.5 mmol) was added, and the reaction continued at room temperature for 2 hours. Solvent was removed *in vacuo*, and the resulting residue was resuspended in 80 mL of saturated sodium bicarbonate under vigorous stirring for 1 hour. The precipitate was collected by vacuum filtration, then washed with water and ice-cold methanol. Remaining solids were resuspended in 50 mL of water and acidified with 50 mL of saturated citric acid solution. The precipitate was collected by vacuum filtration and washed with water and cold methanol, then recrystallized from methanol and minimal *N,N'*-dimethylformamide. The crystals were dried *in vacuo* at 70 °C to yield 685 mg (1.2 mmol, 46%) of Fmoc-Lys(biotin)-OH, a colorless powder. ^{1}H NMR (500 MHz, DMSO-d_6): δ = 1.16-1.75 (m, 12 H), 1.99-2.09 (q, 2 H, J = 6.0 Hz), 2.53-2.60 (d, J = 12.5 Hz, 1 H), 2.76-2.84 (dt, J = 12.5, 5.2 Hz, 1 H), 2.93-3.10 (m, 3 H), 3.86-3.95 (m, 1 H), 4.17-4.33 (m, 5 H), 6.32-6.37 (s, 1 H), 6.38-6.43 (s, 1 H), 7.27-7.36 (m, 2 H), 7.37-7.45 (m, 2 H), 7.58-7.64 (d, J = 8.1 Hz, 1 H), 7.68-7.76 (m, 2 H), 7.84-7.92 (m, 2 H). MS (ESI-MS): calculated for $C_{31}H_{39}N_4O_6S$ ($[M+H]^+$): 595.259; found: 595.259.

Method S4.5 Fmoc solid-phase peptide synthesis

A CEM Liberty 1 was used to perform microwave-assisted Fmoc solid-phase peptide synthesis (SPPS, 0.25 mmol scale). Fmoc deprotection was performed in 20% piperidine (v/v) in dimethylformamide (DMF) with 1-hydroxybenzotriazole (HOBt, 0.1 M, 90 °C, 90 sec). Amino acids were coupled to resin-bound peptides upon treatment (75 °C, 5 min) with Fmoc-protected amino acid (2 mmol, 4x), 2-(1H-benzotriazol-1-yl)-1,1,3,3-tetramethyluronium hexafluorophosphate (HBTU, 2 mmol, 4x), and *N*,*N*-diisopropylethylamine (DIEA, 2 mmol, 4x) in a mixture of DMF (9 mL) and *N*-Methyl-2-pyrrolidone (NMP, 2 mL). Room-temperature couplings were performed without microwave assistance (1 hr).

Method S4.5.1 Synthesis of Amine-Vid^{N}

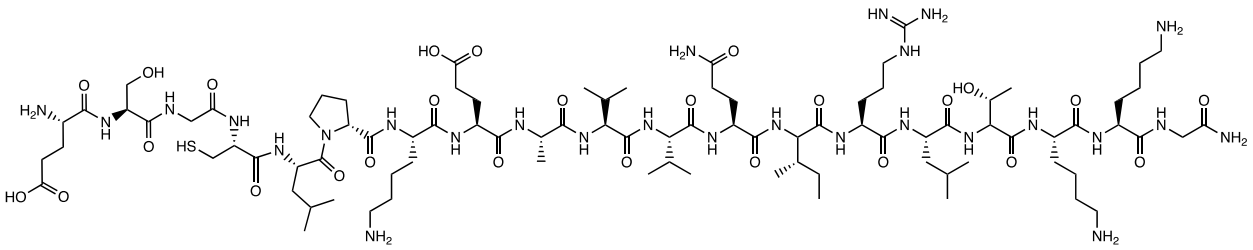

The resin-bound peptide H-ESGCLPKEAVVQIRLTKKG-NH_2 was synthesized by Fmoc SPPS by GenScript (>95% purity).

Method S4.5.2 Synthesis of Alkyne-Vid^{N}

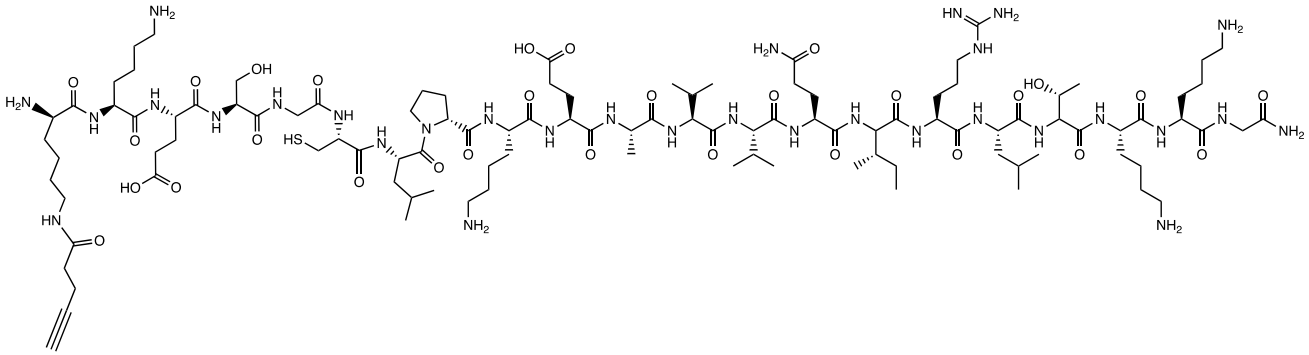

The resin-bound peptide H-K(alkyne)KESGCLPKEAVVQIRLTKKG-NH_2 was synthesized by Fmoc SPPS on Rink Amide Pro-Tide resin (CEM Corporation) (0.1 mmol scale). Fmoc-Lys(Alkyne)-OH was synthesized as described in Method S1.1 and included as a specialty amino acid on the peptide synthesizer. The peptide was deprotected and simultaneously cleaved under nitrogen by treatment with a TFA/DH_2O/EDT/TIS (94%/2.5%/2.5%/1%) cocktail (15 mL) for 4 hours and precipitated and washed in ice-cold diethyl ether (2x). The crude peptide was stored under nitrogen until further use. Prior to purification via RP-HPLC, the peptide was resuspended in a mixture of acetonitrile and water (50%/50%) and lyophilized to yield a powder. Each aliquot of the crude powder was resuspended in 1 mL DMSO and 4 mL of 20% acetonitrile in water (+0.1% TFA) and subsequently purified via RP-HPLC operating with a 60 min linear gradient (20-100%) of acetonitrile in water (+0.1% TFA). Lyophilization yielded the final product (41.4 mgs, 0.017 mmol, 17% yield) as a white powder (denoted Alkyne-Vid^{N}). The peptide was resuspended in 10% glacial acetic acid in DH_2O, aliquoted, and then lyophilized. Peptide purity was assessed via ESI-MS; calculated $C_{106}H_{187}N_{31}O_{29}S$ = 2391.91 g/mol, observed $C_{106}H_{187}N_{31}O_{29}S$ $[M + 1H]^+$ = 2392.410 g/mol.

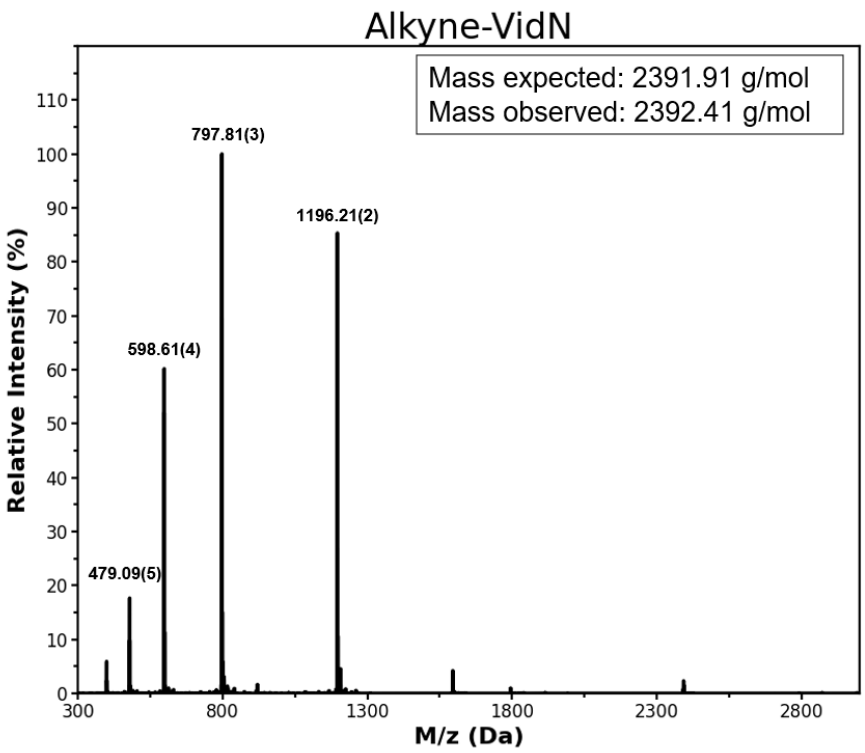
Alkyne-VidN
Mass expected: 2391.91 g/mol
Mass observed: 2392.41 g/mol
797.81(3)
1196.21(2)
598.61(4)
479.09(5)
Relative Intensity (%)
M/z (Da)
0
10
20
30
40
50
60
70
80
90
100
110
300
800
1300
1800
2300
2800

Method S4.5.3 Synthesis of Biotin-Vid^{N}

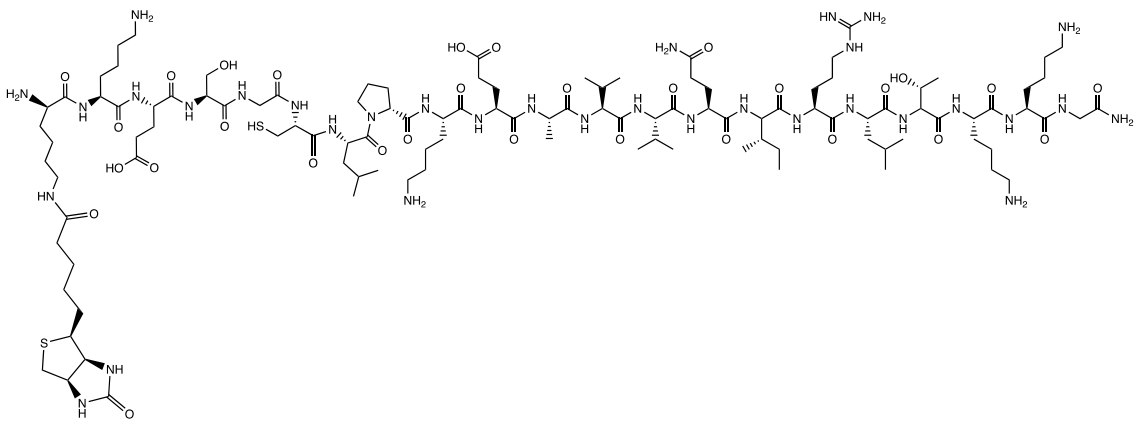

The resin-bound peptide H-K(biotin)KESGCLPKEAVVQIRLTKKG-NH_2 was synthesized by Fmoc SPPS on Rink Amide Pro-Tide resin (CEM Corporation) (0.1 mmol scale). Fmoc-Lys(Biotin)-OH was synthesized as described in Method S1.2 and included as a specialty amino acid on the peptide synthesizer. The peptide was deprotected and simultaneously cleaved under nitrogen by treatment with a TFA/DH_2O/EDT/TIS (94%/2.5%/2.5%/1%) cocktail (15 mL) for 4 hours and precipitated and washed in ice-cold diethyl ether (2x). The crude peptide was stored under nitrogen until further use. Prior to purification via RP-HPLC, the peptide was resuspended in a mixture of acetonitrile and water (50%/50%) and lyophilized to yield a powder. Each aliquot of the crude powder was resuspended in 1 mL DMSO and 4 mL of 20% acetonitrile in water (+0.1% TFA) and subsequently purified via RP-HPLC operating with a 60 min linear gradient (20-100%) of acetonitrile in water (+0.1% TFA). Lyophilization yielded the final product (23 mgs, 0.009 mmol, 9% yield) as a white powder (denoted Biotin-Vid^{N}). The peptide was resuspended in 10% glacial acetic acid in DH_2O, aliquoted, and then lyophilized. Peptide purity was assessed via ESI-MS; calculated $C_{94}H_{162}N_{26}O_{28}S$ = 2536.43 g/mol, observed $C_{94}H_{162}N_{26}O_{28}S$ $[M + 2H]^+$ = 2538.47 g/mol.

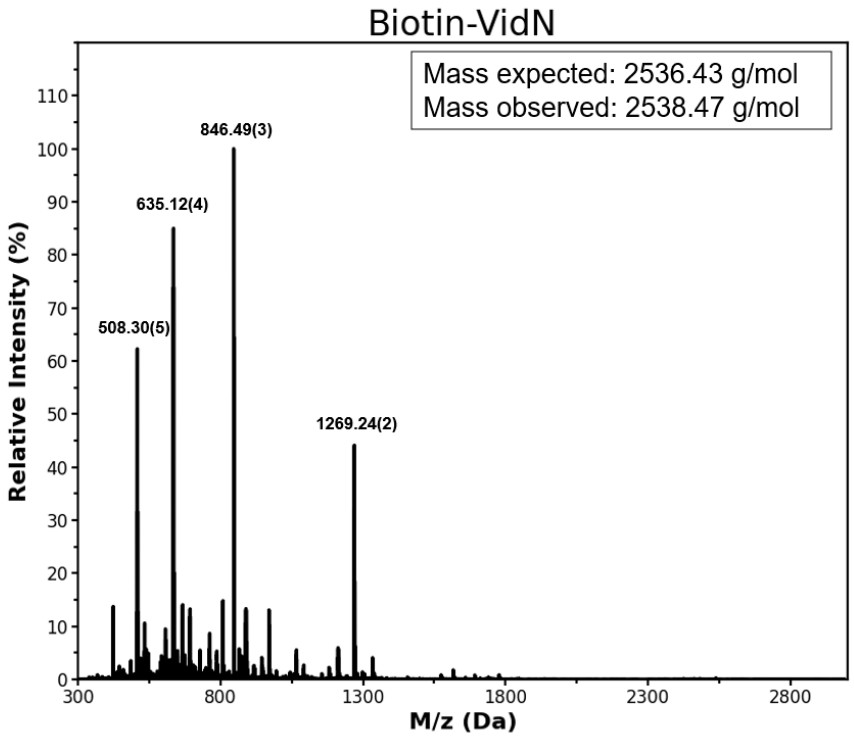
Biotin-VidN
Mass expected: 2536.43 g/mol
Mass observed: 2538.47 g/mol
846.49(3)
635.12(4)
508.30(5)
1269.24(2)
Relative Intensity (%)
M/z (Da)
0
10
20
30
40
50
60
70
80
90
100
110
300
800
1300
1800
2300
2800

Method S4.5.4 Synthesis of FAM-Biotin-Vid^{N}

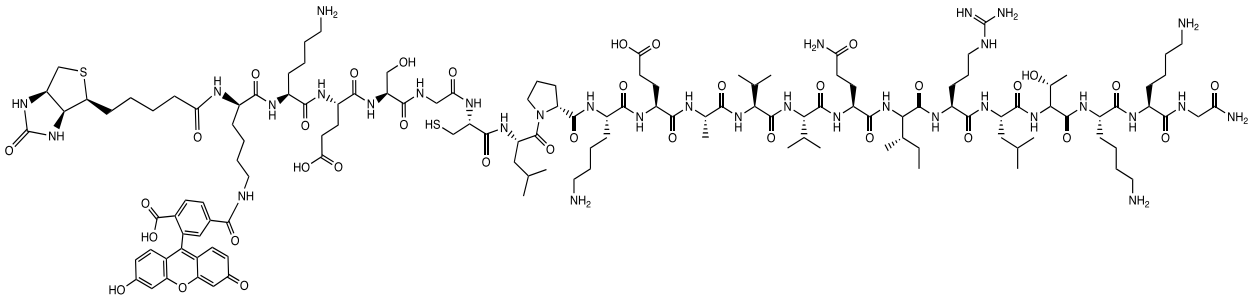

The resin-bound peptide H-K(Dde)KESGCLPKEAVVQIRLTKKG-NH_2 was synthesized by Fmoc solid-phase, microwave assisted peptide synthesis (SPPS) on Rink Amide Pro-Tide resin (CEM Corporation) (0.1 mmol scale). Biotin (CombiBlocks, San Diego, 244.31mgs, 1mmol, 4x) was pre-reacted with 1-[Bis(dimethylamino)methylene]-1H-1,2,3-triazolo[4,5-b]pyridinium 3-oxide hexafluorophosphate (HATU, 375 mgs, 0.9875 mmol, 3.95x) and DIEA (0.517 g, 4 mmol, 16x) in 5 mL of DMF for 5 minutes and then reacted with the resin overnight, under nitrogen, to functionalize the N-terminus of the peptide. The resin was then treated with hydrazine monohydrate (2%) in DMF (3 x 10 mins) to remove the N-(1-(4,4-dimethyl-2,6-dioxocyclohexylidene)ethyl) (Dde) protecting group on the N-terminal Lysine. Subsequently, 5(6)-carboxyfluorescein (FAM, ACROS organics, 376.31 mgs, 1 mmol, 4x) was pre-reacted with HATU (375 mgs, 0.9875 mmol, 3.95x) and DIEA (0.517 g, 4mmol, 16x) in 5 mLs of DMF for 5 minutes and then reacted with the resin overnight in a nitrogenous atmosphere to functionalize the e-amino group of the Lysine. The peptide was then deprotected and simultaneously cleaved under nitrogen by treatment with a trifluoroacetic acid (TFA)/DH_2O/ethane-1,2-dithiol (EDT)/triisopropylsilane (TIS) (94%/2.5%/2.5%/1%) cocktail for 4 hrs at room temperature. The crude peptide was precipitated and washed in ice-cold diethyl ether (2x) and stored under nitrogen until further use. Prior to purification, the crude peptide was resuspended in a water and acetonitrile mixture (50%/50%) and lyophilized to yield powder that could more easily be resuspended before

purification. The crude peptide powder was resuspended in 1 mL DMSO and 4 mL of a mixture of acetonitrile (20%) in water (+ 0.1% TFA) and purified using RP-HPLC operating with a 60-minute linear gradient (20-100%) acetonitrile in water (+ 0.1% TFA). Lyophilization yielded the final product Biotin-FAM-Vid^{N} (18 mgs, 0.006 mmol, 6% yield) as a lemon-yellow solid. The peptide was dissolved in 10% glacial acetic acid in water and aliquoted, and then lyophilized again. Peptide purity was verified via ESI-MS; calculated $C_{132}H_{207}N_{33}O_{36}S_2$ = 2894.48 g/mol, observed $C_{132}H_{207}N_{33}O_{36}S_2$ $[M + 2H]^+$ = 2896.509 g/mol.

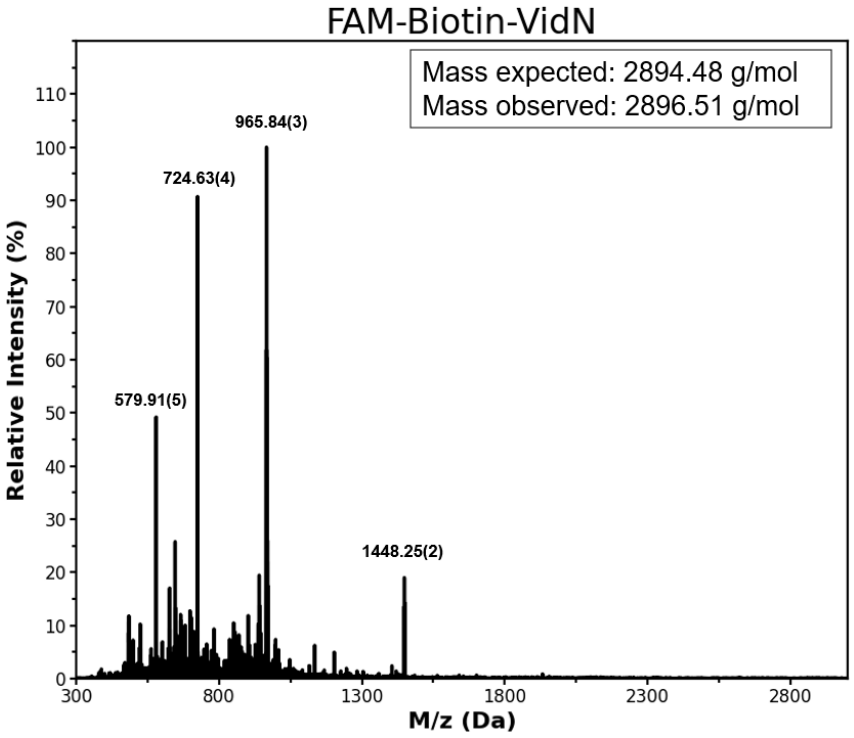

Method S4.6 Protein expression and purification by VEPL

E. coli SHuffle cells were transformed with the proper 6xHis-SUMO-VidC construct and grown at 37°C and 220 rpm agitation to an OD of 0.6-0.8 in LB broth supplemented with kanamycin (6xHis-SUMO-VidC-EGFP-FLAG; 6xHis-SUMO-VidC-mCherry-FLAG) or carbenicillin (6xHis-SUMO-VidC-Bla-FLAG; 6xHis-SUMO-VidC-EGF-FLAG). Isopropyl β-D-1-thiogalactopyranoside (IPTG) was used to induce protein expression, at which point the cultures were moved to a reduced temperature (18°C) for 18 hours. Cells were then harvested via centrifugation (4,000g, 20 minutes, 4°C) and either flash-frozen and stored at -80°C or used directly.

E. coli cell pellets were re-suspended in lysis buffer (50 mM Tris, 150 mM NaCl, 1 mM PMSF, 2 mM DTT, pH 7.5) and sonicated on ice (6 cycles, each for 3 minutes at 30% amplitude, 33% duty cycle, and 3 minutes resting). The soluble fraction was then isolated by centrifugation (7,500g, 45 minutes, 4°C) and incubated with INDIGO Ni-NTA resin (Cube Biotech) (2 mL slurry/L of culture) under mild agitation (2 hours, 4°C). Flow-through was discarded and the resin was washed with lysis buffer (10x column volume) until full removal of soluble aggregates and impurities.

The Vid^N peptide (10X molar excess, unless otherwise specified) was reconstituted in splicing buffer (50 mM Tris, 150 mM NaCl, 10% Glycerol, 1 mM EDTA, pH 7.2) prior to on-resin splicing experiments.

With 4 base proteins and 4 different Vid^N probes, a total of 16 N-terminally tagged proteins were generated. Identification codes denoting VEPL-modified species identity are given in Table S1.

Method S4.7 Assessing beta-lactamase activity

The enzymatic activity of Bla was monitored through a chromogenic assay involving nitrocefin hydrolysis. 20 ng per protein (Amine-bla, Biotin-bla Alkyne-bla) was added to nitrocefin (2 mM in PBS, 100 µL, pH of 7.4). The solution sample absorbance (λ_{abs} = 486 nm) was measured over a 40-minute timespan at 37 °C.

Method S4.8 Cell culture conditions for HeLa maintenance and passaging

For passaging and growth prior to EGF treatment, HeLa cells were maintained at 37 °C and 5% CO_2 in Dulbecco's Modified Eagle Medium (DMEM) (Life Technologies), additionally supplemented with 10% Fetal Bovine Serum (FBS) and 1% Penicillin/Streptomycin (P/S). Media was replaced every 3 days.

Cells were passaged using Trypsin-EDTA (0.05%, Thermo-Fisher), pelleted at 125 x g for 5 minutes, and resuspended (2 x 10^7 cells/mL) in DMEM supplemented with 10% FBS and 1% P/S.

Method S4.9 Determining EGF activity

EGF activity was monitored through its ability to drive HeLa cell proliferation as quantified by the endpoint cell reducing potential. HeLa cells were plated in 96-well plates (2,000 cells / well) and allowed to attach overnight. The media was then swapped for serum-free medium (DMEM containing 1% P/S and 0.1% BSA) to starve the cells. Different N-terminally modified EGF proteins (i.e., Amine-EGF, Alkyne-EGF, Biotin-EGF, FAM-Biotin-EGF) were individually added to each well (1 µg/mL of final EGF concentration). No proteins were added to the blank. Cells were then cultured for 2 days under each condition before assaying the number of viable cells through the RealTime-Glo™ MT Cell Viability Assay (Promega) according to the manufacturer's instructions.

Supplementary Figures

Figure S4.1 Assessing on-column C-terminal cleavage

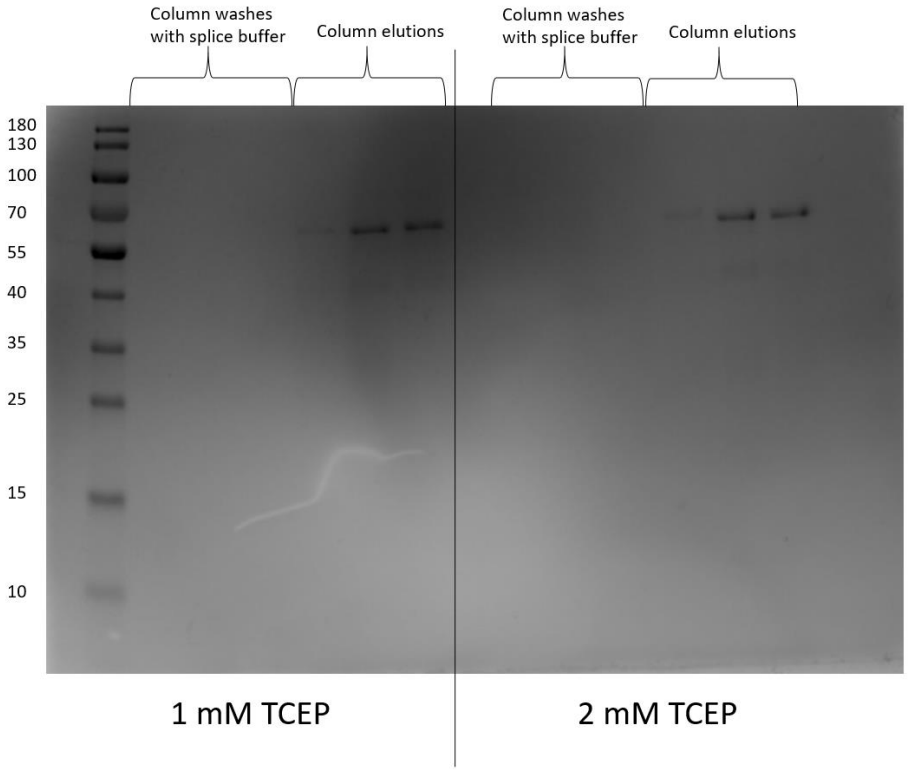

Vid^{C}-EGFP bound to a Ni-NTA column does not undergo C-terminal cleavage. Two concentrations of reducing agent were tested (1 and 2 mM TCEP) and neither yielded any cleavage of the EGFP cargo.

Figure S4.2 Assessing C-terminal cleavage during on-column splicing

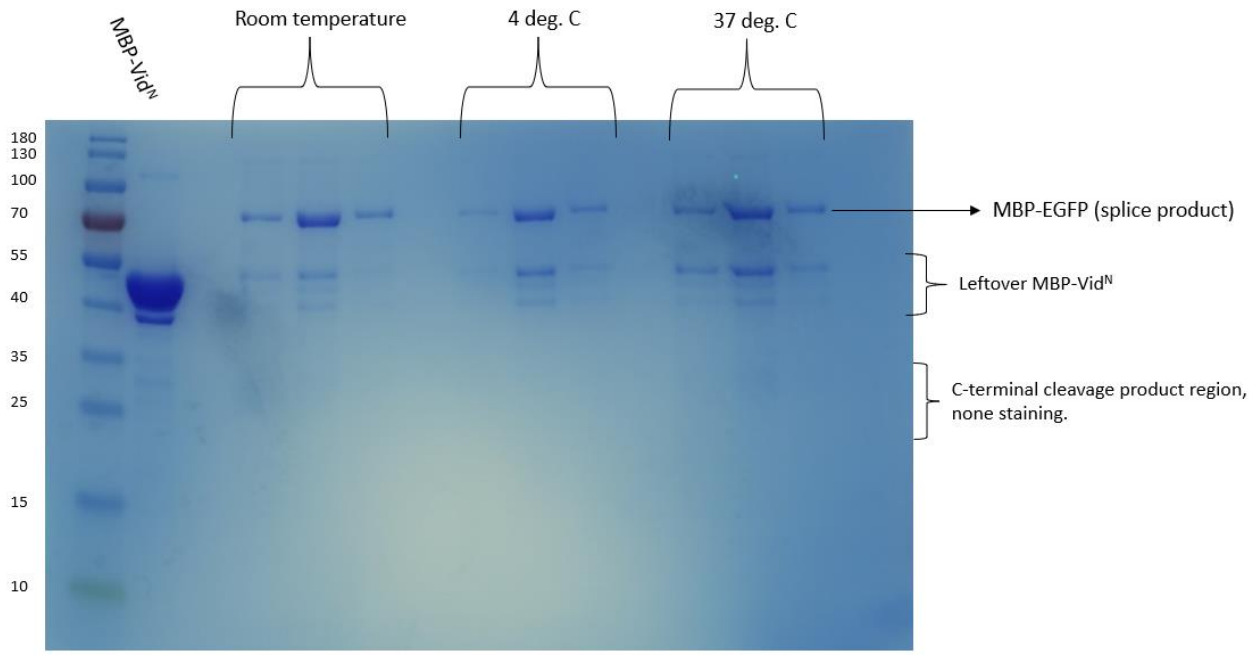

The splicing reaction between Vid^{C}-EGFP and MBP-Vid^{N} results exclusively in the predicted MBP-EGFP splice product and does not lead to any C-terminal cleavage by-product, which should be evidenced by bands corresponding to the MW of EGFP. This absence of cleavage by-products is temperature-independent, as no cleavage of the POI can be observed at RT (25 °C), 4 °C, and 37 °C.

Figure S4.3 SDS-PAGE gels for reaction characterization

SDS-PAGE gels pertaining to on-column splicing characterization and showing the full span of possible MWs are given below:

Time-course analysis of on-resin splicing

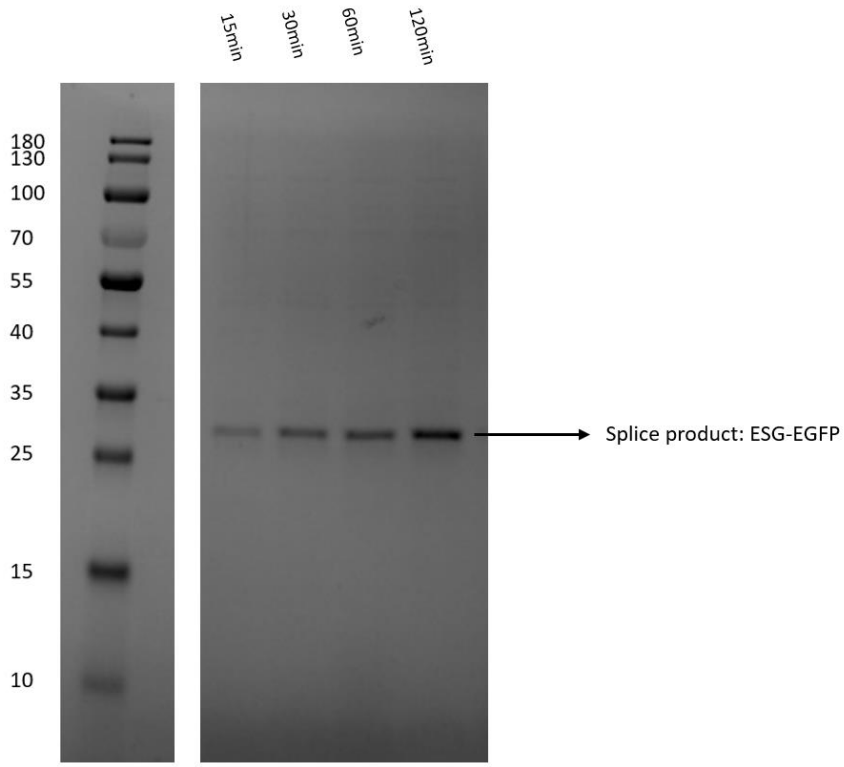

The experiment was repeated 3 times, to similar results.

Temperature dependence analysis of on-resin splicing

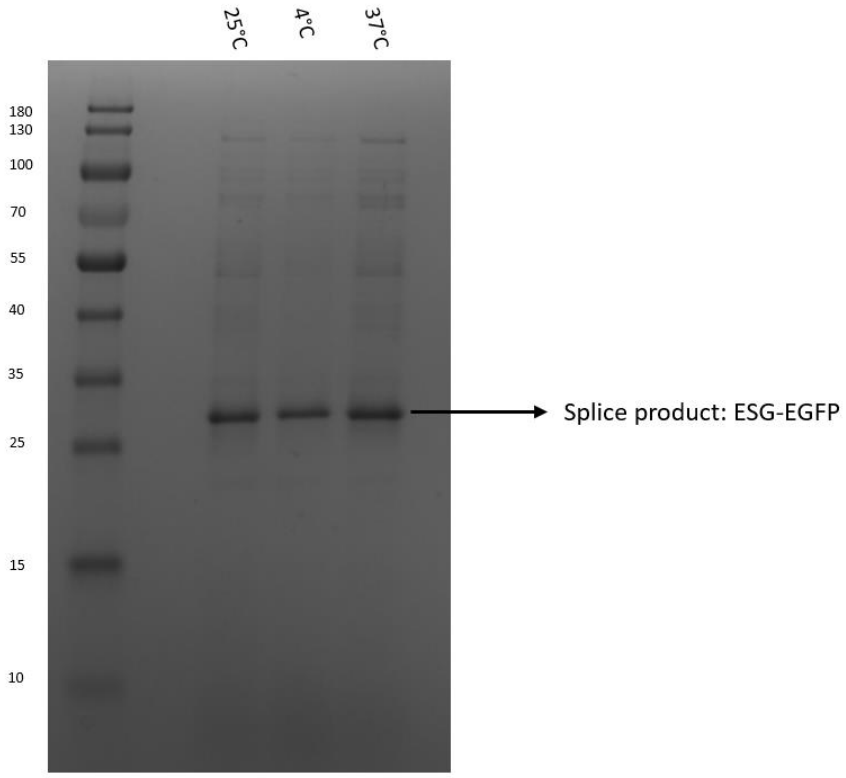

The experiment was repeated 3 times, to similar results.

Stoichiometry analysis of on-resin splicing

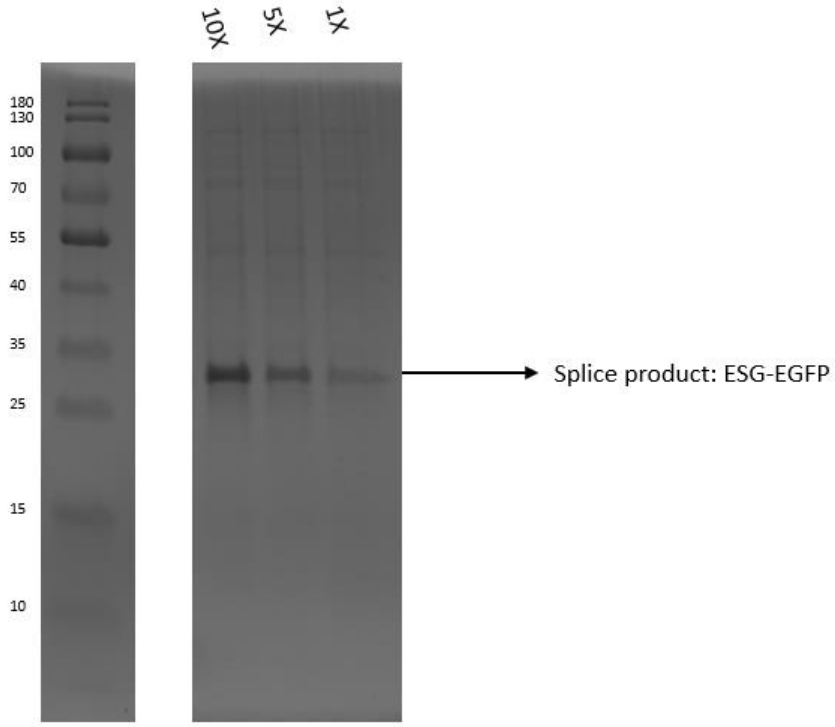

The experiment was repeated 3 times, to similar results.

Figure S4.4 Mass spectrometry for all VEPL-modified species

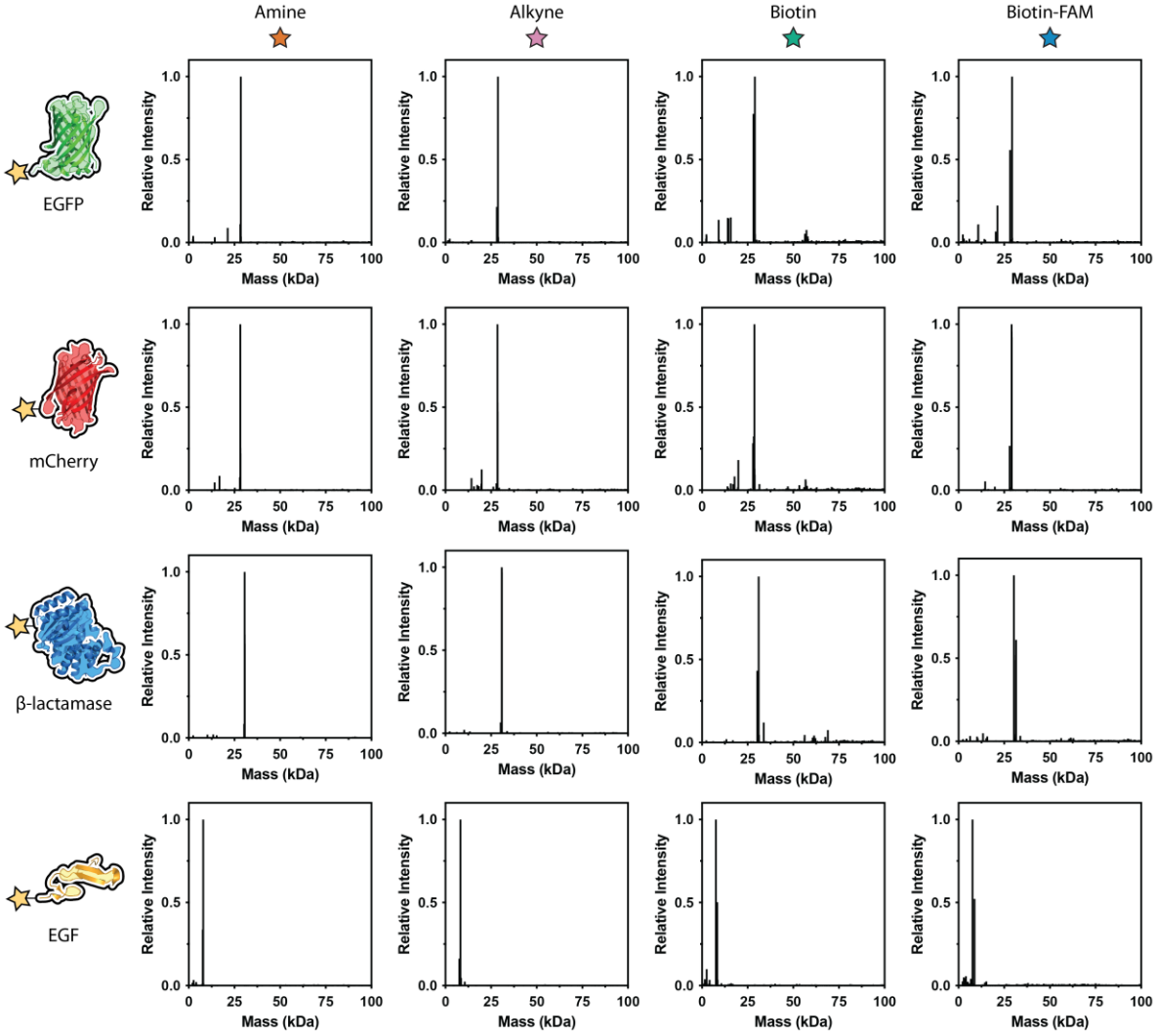

Figure S4.5 SDS-PAGE analysis for VEPL-modified species

SDS-PAGE gels showing on-column splicing of Vid^{C}-POI and ESG-modified Vid^{N} for mCherry, bla, and EGF are given below:

mCherry:

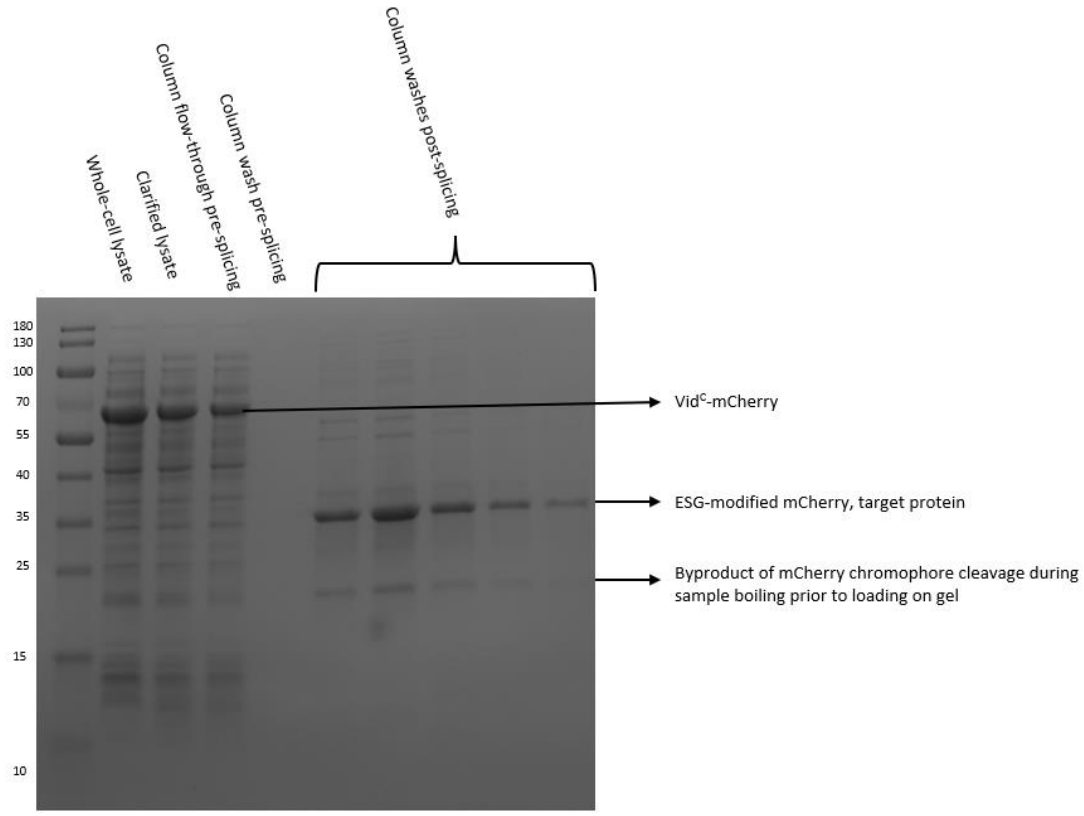

bla:

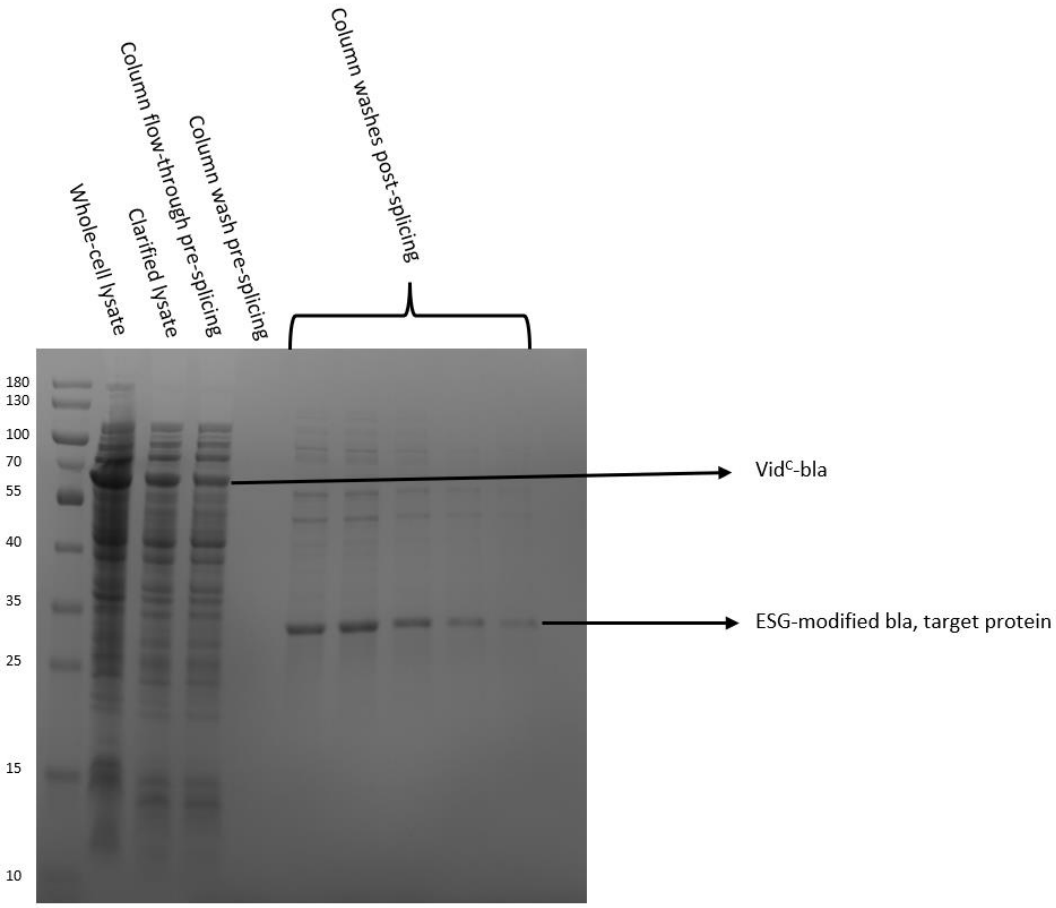
Whole-cell lysate
Clarified lysate
Column flow-through pre-splicing
Column wash pre-splicing
Column washes post-splicing
180
130
100
70
55
40
35
25
15
10
Vid^C-bla
ESG-modified bla, target protein

EGF:

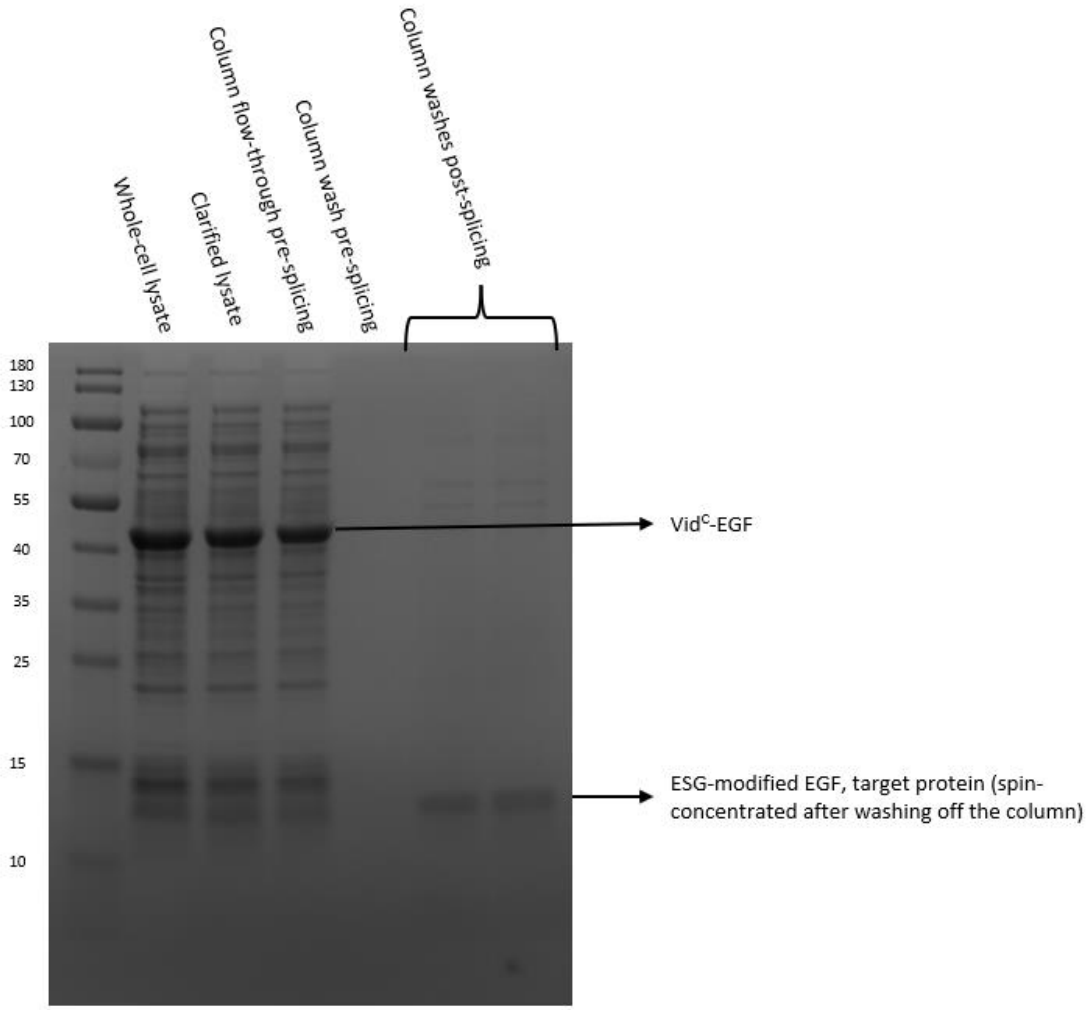
Whole-cell lysate
Clarified lysate
Column flow-through pre-splicing
Column wash pre-splicing
Column washes post-splicing
180
130
100
70
55
40
35
25
15
10
Vid^C-EGF
ESG-modified EGF, target protein (spin-concentrated after washing off the column)

Tables

Table S4.1 Identification codes for all VEPL-modified species

Base Protein	VidN Peptide	N-tagged Protein Identity
EGFP	Amine-Vid^{N}	Amine-EGFP
	Alkyne-Vid^{N}	Alkyne-EGFP
	Biotin-Vid^{N}	Biotin-EGFP
	Biotin-FAM-Vid^{N}	Biotin-FAM-EGFP
mCherry	Amine-Vid^{N}	Amine-mCherry
	Alkyne-Vid^{N}	Alkyne-mCherry
	Biotin-Vid^{N}	Biotin-mCherry
	Biotin-FAM-Vid^{N}	Biotin-FAM-mCherry
bla	Amine-Vid^{N}	Amine-bla
	Alkyne-Vid^{N}	Alkyne-bla
	Biotin-Vid^{N}	Biotin-bla
	Biotin-FAM-Vid^{N}	Biotin-FAM-bla
EGF	Amine-Vid^{N}	Amine-EGF
	Alkyne-Vid^{N}	Alkyne-EGF
	Biotin-Vid^{N}	Biotin-EGF
	Biotin-FAM-Vid^{N}	Biotin-FAM-EGF

Table S4.2 Expected and predicted masses for all VEPL-modified species

N-tagged Protein Identity	Expected Mass (Da)	Observed Mass (Da)
Amine-EGFP	28,461.7	28,462.4
Alkyne-EGFP	28,797.6	28,798.8
Biotin-EGFP	28,943.7	28,944.7
Biotin-FAM-EGFP	29,301.7	29,303.0
Amine-mCherry	28,242.6	28,241.3
Alkyne-mCherry	28,578.6	28,577.6
Biotin-mCherry	28,724.7	28,723.6
Biotin-FAM-mCherry	29,082.7	29,081.9
Amine-bla	30,578.4	30,577.3
Alkyne-bla	30,914.4	30,913.7
Biotin-bla	31,060.4	31,059.2
Biotin-FAM-bla	31,418.5	31,417.2
Amine-EGF	7,891.6	7,891.3
Alkyne-EGF	8,227.5	8,228.7
Biotin-EGF	8,373.6	8,374.7
Biotin-FAM-EGF	8731.6	8,372.9

CHAPTER 5: BOOLEAN LOGIC-GATED PROTEIN PRESENTATION VIA AUTONOMOUSLY COMPILED MOLECULAR TOPOLOGY

Adapted from Gharios, R., Li, A., DeForest, C.A. Boolean Logic-gated Protein Presentation via Autonomously Compiled Molecular Topology (*Submitted*)

Abstract

Stimuli-responsive materials have enabled advanced applications in biosensing, tissue engineering, and therapeutic delivery. Though controlled molecular topology has been demonstrated as an effective route towards creating materials that respond to prespecified input combinations, prior efforts suffer from a reliance on complicated and low-yielding multistep organic syntheses that dramatically limit their utility. Harnessing the power of recombinant expression, we integrate emerging chemical biology tools to create topologically specified protein cargoes that can be site-specifically tethered to and conditionally released from biomaterials following user-programmable Boolean logic. Critically, construct topology is autonomously compiled during expression via spontaneous intramolecular ligations, enabling direct and scalable synthesis of advanced operators. Using this framework, we specify protein release from biomaterials following all 17 possible YES/OR/AND logic outputs from input combinations of three orthogonal protease actuators, multiplexed delivery of 3 distinct biomacromolecules from hydrogels, and 5-input-based conditional cargo liberation. These methods offer unprecedented specificity over biomacromolecule presentation in/from materials.

5.1. Introduction

Programming stimuli-responsiveness into biomaterials and biohybrid constructs represents an exciting frontier poised to galvanize many advanced bioengineering applications.[1–3] For instance, controlled presentation of biomolecules (e.g., proteins, peptides, polysaccharides, nucleic acids) in/from materials holds direct applicability in therapeutic delivery,[4,5] tissue engineering,[6,7] organoid development,[8,9] and the biomanufacturing of value-added chemicals.[10] Co-opting novel methods from organic- and synthetic bio-based chemistries,[11–13] stimuli-responsive material platforms have been reported that sense and act upon diverse inputs including light,[14–17] redox potential,[18] enzyme,[19,20] and pH[21]. While such approaches have largely transformed biomaterials from static to dynamic systems,[22] the overwhelming majority of these platforms exhibits only single-input/single-output-type responses that dramatically limit their scope of use.

Recognizing that next-generation applications, including disease-triggered payload delivery[23,24] and analyte biosensing,[25,26] would benefit tremendously from multi-stimuli-responsiveness, truly "smart" materials have been developed that transduce a set of environmental inputs into a functional output via user-specified Boolean logic.[1] Though logically defined biomolecule release has been accomplished using hydrogel-enzyme hybrids[27], degradable nanoparticles[28], and caged self-immolative polymers[29], existing strategies have been limited in their lack of generalizability, reliance on specific input chemistries, and overall inability to elicit multiplexed operations. Towards more modularly imparting Boolean biocomputability into materials, we recently demonstrated that molecular topology could be used to encode advanced environmental responsiveness[30–32]. Here, the linker between a biomolecule cargo and a stable material serves as an executable YES-gate for programmable release when it

contains a single degradable moiety, an OR-gate (denoted with logic symbol ∨) when two orthogonal cleavable moieties are included in series, and as an AND-gate (denoted by logic symbol ∧) when two orthogonally scissile moieties are present in parallel (**Fig 5.1a-c**). Importantly, logical gates can be expanded hierarchically to create advanced logical circuits responsive to several stimuli via nested YES/OR/AND operations (**Fig 5.1d**). To date, such systems have been obtained exclusively through multistep organic reactions alongside solid/solution-phase peptide synthesis – poorly scalable methods whose inherent complexity and low-yielding nature limit their implementation and potential for higher-ordered logical responses. Given these caveats, (bio)chemical strategies that permit one-step synthesis of logically releasable cargos would be profoundly enabling.

Towards expanding logical complexity and improving synthetic accessibility, we sought to identify generalizable methods that enable the direct and facile assembly of topologically specified Boolean-responsive cargos. In this regard, we were drawn to the benefits of recombinant protein expression, augmented with recent advances in chemical biology. Recombinant polypeptides are intrinsically monodisperse with a sequence defined by its encoding DNA, scalably produced through well-established fermentation processes, and amenable to the introduction of non-natural functionality via semi-synthesis[33] and/or genetic code expansion.[34] Furthermore, judicious use of engineered motifs permits the creation of heterodox protein architectures. For example, proteins can be cyclized head-to-tail auto-catalytically using split inteins (a method referred to as SICLOPPS[35,36], **Fig 5.1f**) or assembled into a variety of bespoke branched structures (e.g., tadpoles, n-armed stars, H-shapes) using Tag/Catcher ligation chemistries (**Fig 5.1g-i**).[37–39] Though these advances can yield diverse

protein topologies starting from simple, singular, plasmid blueprints,[40–44] such methods have not previously been exploited for creation of stimuli-responsive systems.[45]

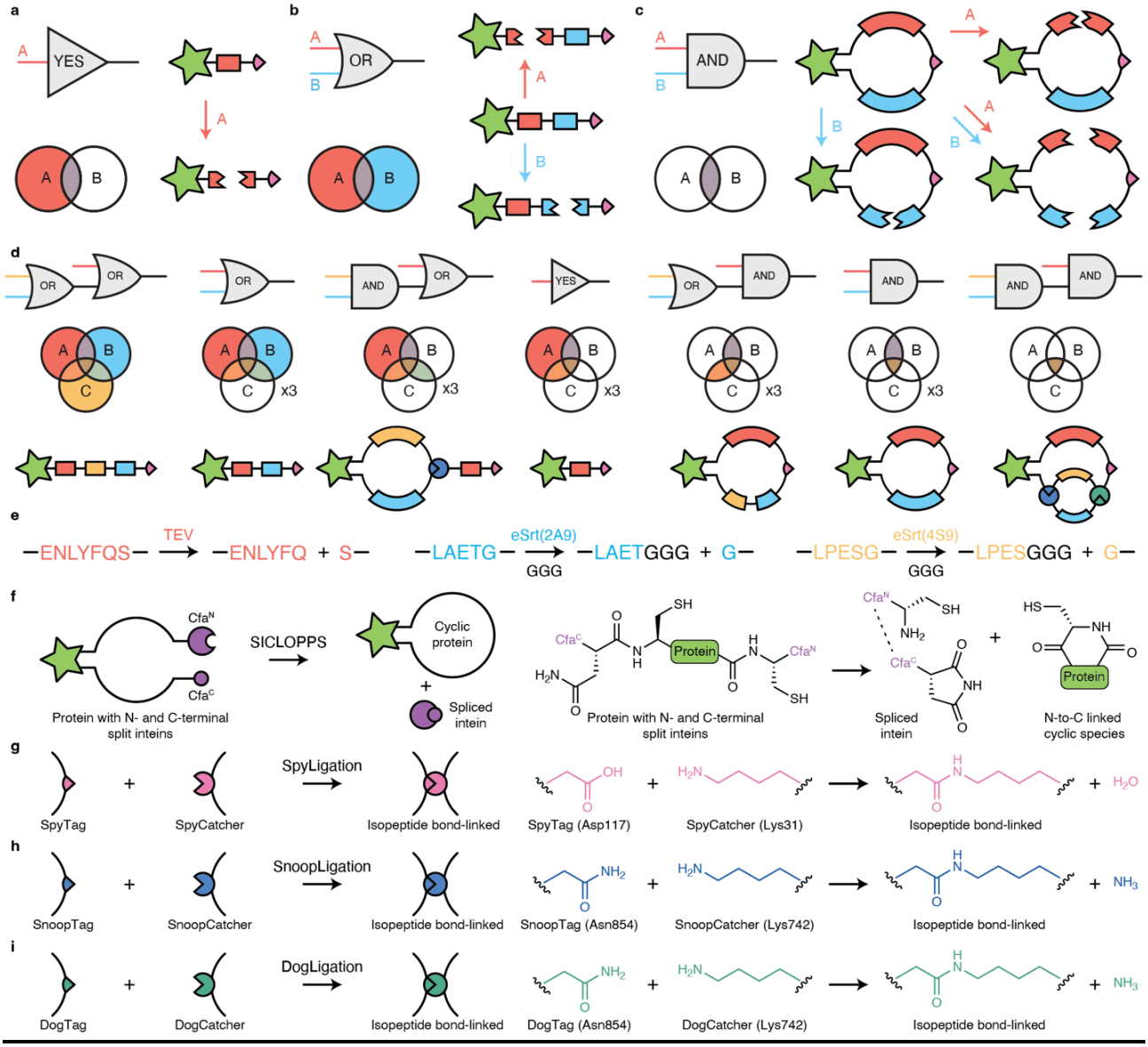

Figure 16: Molecularly compiled topologies enable Boolean logic-based protein presentation

a) The YES-gate tether contains a single protease-responsive sequence (red). Introduction of the cognate protease cleaves this sequence, breaking the covalent linkage between the protein cargo (green star) and tethering motif (pink).

b) The OR-gate tether contains two protease-responsive sequences (red and blue) connected in series. The introduction of either relevant protease cleaves the sequence, resulting in cargo release.

c) The AND-gate tether contains two protease-responsive sequences (red and blue) connected in parallel. The introduction of one cognate protease cleaves one arm but does not fully sever the

cycle. Simultaneous introduction of both proteases cleaves both arms, resulting in protein release.

d) *YES/OR/AND operators can be hierarchically layered to engineer higher-order logical responses. 17 unique protein tethering topologies can be obtained through combination of the three base operations with three distinct actuator-proteases. Each region of the Venn diagrams displayed represents a unique combination of protease inputs and indicates whether the tether is predicted to cleave (colored) or remain intact (white).*
e) *Reactions depicting protease recognition of target sequence and subsequent cleavage: the recognition sequence ENLYFQ↓S is recognized and cleaved by the TEV protease; LAET↓G by eSrt(2A9); LPES↓G by eSrtA(4S9).*
f) *SICLOPPS provides a genetically encoded and near-traceless approach for the N-to-C cyclization of proteins based on intein trans-splicing.*
g) *SpyTag and SpyCatcher spontaneously react and form an isopeptide bond between the Lysine residue on SpyCatcher and Aspartic acid on SpyTag. This reaction is termed "SpyLigation".*
h) *SnoopTag and SnoopCatcher spontaneously react and form an isopeptide bond between the Asparagine residue on SnoopCatcher and Lysine on SnoopTag. This reaction is termed "SnoopLigation".*
i) *DogTag and DogCatcher spontaneously react and form an isopeptide bond between the Lysine residue on DogCatcher and Asparagine on DogTag. This reaction is termed "DogLigation".*

In this work, we introduce a modular chemical biology-based framework to autonomously compile proteins with defined molecular topology that can be site-specifically tethered to and subsequently released from biomaterials via nested Boolean operations. Using this framework, we successfully demonstrate specification of protein release from biomaterials following all 17 possible YES/OR/AND logic outputs from input combinations of three orthogonal protease actuators, as well as the multiplexed delivery of 3 distinct biomacromolecules from a common hydrogel network via distinct logical operations. Further highlighting the expanded logical complexity enabled via these methods, we demonstrate unprecedented control over protein liberation using a system that exercises biocomputation following a 5-input Boolean-responsive operator circuit. Autonomous molecular compilation represents a powerful new framework for biomolecule design and offers high specificity over biomolecule presentation in/from materials.

5.2. Results

5.2.1. Autonomous compilation of logic-gated proteins

Towards establishing design rules that functionally underlie our autonomous molecular compilation, we adopted mGreenLantern[46] – a monomeric GFP variant recently evolved for enhanced brightness and expression levels – as a model protein cargo whose extent of release could be readily quantified via its fluorescence. Seeking to utilize cleavable moieties for protein release that are genetically encoded, we identified three protease actuators that operate on distinct peptide sequence substrates: sortase variants eSrtA(2A9) and eSrtA(4S9) evolved to recognize distinct peptide substrates (LAET↓G and LPES↓G, respectively referred to as A and S),[47,48] alongside an evolved potyviral TEV protease (which acts upon sequence ENLYFQ↓S, referred to as T),[49] reasoning that the trio of actuators would exhibit no undesirable crosstalk (**Fig 5.1e**). Having identified the mGreenLantern cargo and the three stimuli-labile moieties, we sought to recombinantly synthesize the 17 distinct logically responsive systems that exhaustively span all possible hierarchical YES/OR/AND combinations. To enable Ni-NTA-based immobilized metal affinity chromatography (IMAC) purification and covalent anchoring onto SpyCatcher-displaying materials,[50] we installed both a 6x-Histidine tag and a SpyTag motif onto each protein regardless of the targeted logical operation.

With our design criteria established, we assembled the 3 base logical operators as follows: (1) YES gates (i.e., A, S, T) were designed as routine constructs, harboring a protease-specific recognition sequence between the mGreenLantern cargo and the SpyTag anchor (**Fig 5.1a**). (2) OR gates (i.e., A∨S, A∨T, S∨T) followed a similar blueprint, whereby two distinct protease recognition sequences were installed in series between the cargo and anchor-point (**Fig 5.1b**). (3) AND-gates (i.e., A∧S, A∧T, S∧T) were cyclized head-to-tail using a split Cfa intein

(**Fig 5.1c**).[51,52] To further bias the reaction towards complete splicing and eliminate possible by-products, an SsrA tag was installed at the protein C-terminus to mark all un-spliced (i.e., non-cyclized) product for proteasomal degradation and clearance.[53] Plasmids encoding for the 9 possible YES- , OR-, and AND-gated operators were transformed into BL21(DE3) *Escherichia coli*. Following conventional expression, proteins were purified by IMAC; cyclic constructs were further purified via size exclusion chromatography (SEC) to separate the target cyclical constructs from higher-order macrocyclic by-products that can result from SICLOPPS (**Supplementary Methods S5.1-S5.3)**. In each case, desired proteins were obtained with high purity and in good yield (YES and OR operators were produced at 30-50 mg L^{-1} of culture, whereas the AND operators had a final yield of approximately 20 mg L^{-1} of culture), as indicated by sodium dodecyl sulfate-polyacrylamide gel electrophoresis (SDS-PAGE) analysis and liquid chromatography mass spectrometry (LC-MS) (**Extended Data Fig 5.1**, **Supplementary Method S5.4**).

Heartened by our ability to recombinantly produce the base YES-, OR-, and AND-type Boolean gates, each from a singular reading frame, we extended our methods to target higher order logical operators responsive to 3 distinct inputs: (1) AND/(OR)-gated constructs [i.e., A∧(S∨T), S∧(A∨T), T∧(A∨S)] were assembled similarly to the dual-input AND structures, differing in that two of the cleavable sequences were expressed in series to one another and in parallel to the third. (2) OR/(AND)-gated constructs [i.e., A∨(S∧T), S∨(A∧T), T∨(A∧S)] were designed to undergo macrocyclization through SnoopLigation54,55, whereby installation of the SnoopCatcher motif at an internal site in the protein while keeping the SnoopTag at the N-terminus leads to the creation of a bespoke branched structure which faithfully recreates the tadpole-like geometry necessary for the logical operation. Importantly, SnoopLigation and

SpyLigation are fully orthogonal to each other, permitting complete chemical decoupling of payload configuration and anchoring, analogous to the use of orthogonal synthetic "click" chemistries for material synthesis.56 (3) The OR/OR-gated construct [i.e., A∨S∨T] harbors the three protease substrate sequences expressed directly in series. (4) The AND/AND construct [i.e., A∧S∧T] relies on two orthogonal Tag/Catcher ligations occurring in tandem to form a bicyclic protein cargo. Here, SnoopTag is installed at the cargo's N-terminus and a DogTag at the C-terminus, with their concomitant Catchers located internally in the expression frame. Plasmids encoding for these 8 remaining 3-input systems were cloned, transformed into BL21(DE3) cells, expressed, and purified via IMAC/SEC (**Supplementary Methods S5.1-S5.3**). With the exception of the A∧S∧T protein, all species were obtained with the expected molecular weights in good yield and at high purity, as indicated by SDS-PAGE and LC-MS analysis (**Extended Data Fig. 5.1, Supplementary Fig. S5.2, Supplementary Method S5.4**). The A∧S∧T target was correctly identified by whole-protein mass spectrometry, though challenges separating the bicyclic and monocyclic species via SEC limited the final sample purity to ~75%. Notably, the 17 distinct logically responsive proteins were autonomously compiled and obtained from singular plasmids via conventional fermentation/purification and characterized by a single researcher over the course of just a few weeks. In direct contrast to prior efforts reliant on organic synthesis and/or peptide chemistry, the reported approach features a rapid Design-Build-Test-Learn timeline that enables designs to be quickly sequence-optimized, structurally debugged, and scaled up as needed.

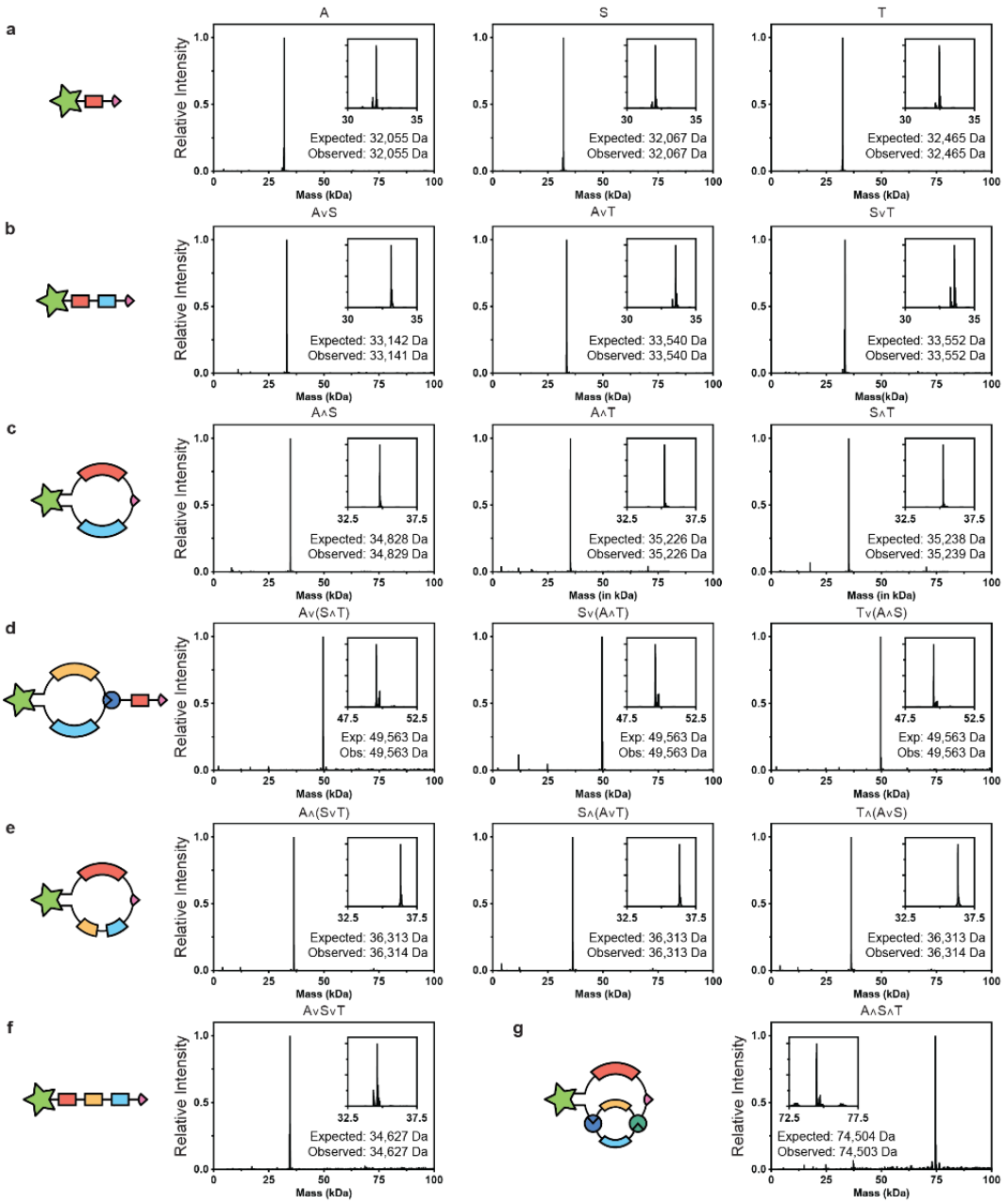

Extended Data 17: Mass spectrometric validation of logically releasable mGreenLantern

a) YES-gated single-input tethers.
*b-c) Two-input OR-gated (**b**) and AND-gated (**c**) tethers.*
*d-g) Three-input (AND)/OR- (**d**), (OR)/AND- (**e**), OR-OR- (**f**), and AND-AND-gated (**g**) tethers.*
Plot titles correspond to the protein tether identity.

5.2.2. Characterization of operator logical response in solution

With our core library in hand, we next sought to assay the 17 constructs' in-solution logical response to each of the 8 possible input combinations of eSrt(2A9) (denoted as $_{A}$), eSrt(4S9) (denoted as $_{S}$), and TEV (denoted as $_{T}$) (**Supplementary Method S5.1-3, Supplementary Fig. S5.1.1-3**) at non-kinetically limited endpoints (**Supplementary Method 5.6**). Following treatment, proteins were electrophoretically separated via SDS-PAGE and visualized using Coomassie staining. As expected, changes in protein mass and/or topology gave rise to altered migration patterns.[57–59] Through gel densitometry, we quantified extent of response for each protein to each input actuator set, demonstrating that our genetically encoded logical operators behaved as expected (**Extended Data Fig 5.2**). Of note, we observed near-perfect responses (infinite signal/noise ratios) for 16 of the 17 operators, attributed to the purity of the starting material and the pristine targeting of orthogonal protease-driven actuation. Owing to impurities present in the A∧S∧T construct, gel densitometry analysis was not performed on the $_{AST}$-releasable cargo. The exhaustive validation of each possible construct demonstrates that complex biocomputation can be achieved with high fidelity through hierarchical nesting of simple YES/OR/AND logic gates.

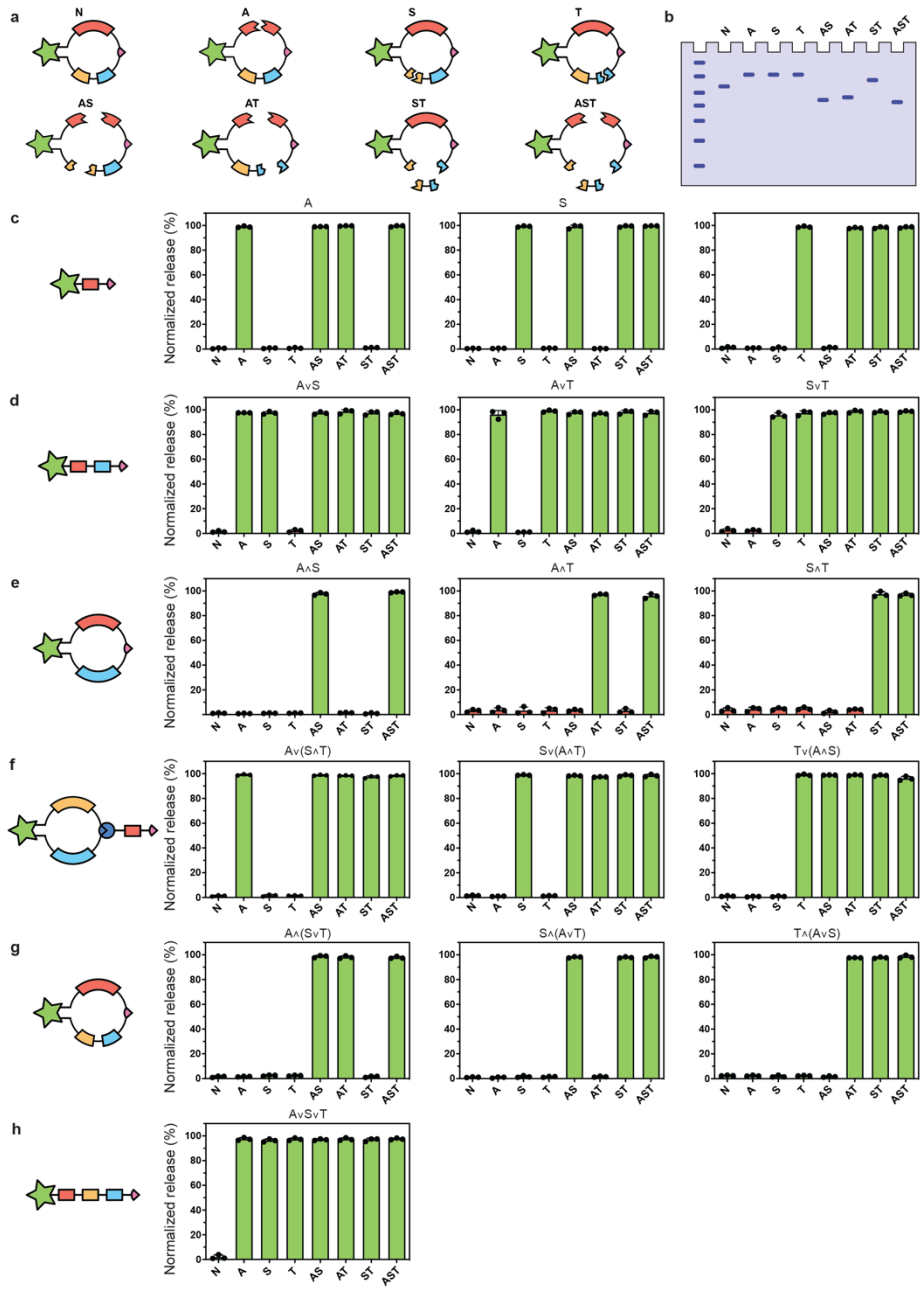

Extended Data 18: SDS-PAGE analysis of in-solution treatment of autonomously compiled mGreenLantern pendants

a) mGreenLantern-[A⋀(S⋁T)] undergoes 8 possible input combinations of $_A$, $_S$, and $_T$. Input conditions {$_A$; $_S$; $_T$; $_{ST}$} are expected to linearize the product but not lead to payload release. Input conditions {$_{AS}$; $_{AT}$; $_{AST}$} are expected to result in payload release.

b) Changes in topology and/or molecular weight in response to a specific set of inputs leads to changes in protein electrophoretic mobility, which can be analyzed through gel densitometry. In the case of mGreenLantern-[A⋀(S⋁T)], input conditions {$_A$; $_S$; $_T$; $_{ST}$} result in construct linearization, but not release, resulting in a band that stains higher than its cyclical counterpart. Input conditions {$_{AS}$; $_{AT}$; $_{AST}$} result in cargo liberation and a substantially reduced MW, leading to a target band that stains lower.

c) The response profiles of the YES-gated single-input tethers.
*d-e) The response profiles of the two-input OR-gated (**b**) and AND-gated (**c**) tethers.*
*f-i) The response profiles of the three-input (**f**) OR/(AND)-, (**g**) AND/(OR)-, and (**h**) OR/OR- -gated tethers.*
Plot titles correspond to the protein tether identity; the y-axis represents extent of cleavage as measured through migration on an SDS-PAGE with gel densitometry analysis; the x-axis indicates treatment conditions, wherein $_N$ indicates no treatment, $_A$ indicates eSrtA(2A9), $_S$ indicates eSrtA(2S9), and $_T$ indicates TEV. Green bars indicate conditions expected to yield tether cleavage, whereas red bars indicate conditions expected to keep the tether non-cleaved. Error bars correspond to ±1 standard deviation about the mean with propagated uncertainties for n=3 experimental replicates.

5.2.3. Characterization of operator logical response from magnetic bead surfaces

After molecularly validating construct behavior, we shifted our focus towards characterizing the stimuli-responsiveness of the species in a materials' context.[60] Here, we developed a magnetic bead-based assay enabling rapid interrogation of each protein's logical response to input actuator combinations, whereby supernatant fluorescence would indicate protease-driven mGreenLantern release from the solid support. Dibenzocyclooctyne (DBCO)-functionalized magnetic beads were uniformly decorated with a monofunctionalized SpyCatcher-azide protein via strain-promoted azide-alkyne cycloaddition (SPAAC).[61] SpyCatcher-azide was obtained using genetic code expansion, wherein azido-phenylalanine was site-specifically installed via amber suppression near the protein's C-terminus (**Supplementary Method S5.7, Supplementary Fig. S5.3**) and served as a linker to immobilize each logic-releasable mGreenLantern protein to the supporting substrate. For each operator type, responsiveness to all eight input combinations involving A, S, and T was evaluated (**Supplementary Method S5.8**). Protein release was quantified by measuring supernatant fluorescence at non-kinetically limited endpoints following treatment (**Fig. 5.2a-b**). Consistent with the in-solution treatment assays, we observed the expected and near-perfect signal-to-noise release profiles for 16 of the 17 logical

operators (**Fig. 5.2c-i**). The A∧S∧T system also yielded the desired response, in that there was significantly higher release accompanying the AST treatment compared to all other conditions, but with ~25% undesired release in two-inputs (i.e., AS, AT, ST) that we attributed to sample impurity. To our knowledge, these computation signatures represent the most logically advanced protein release from materials to date, likely opening new doors for controlled drug delivery and biosensing.

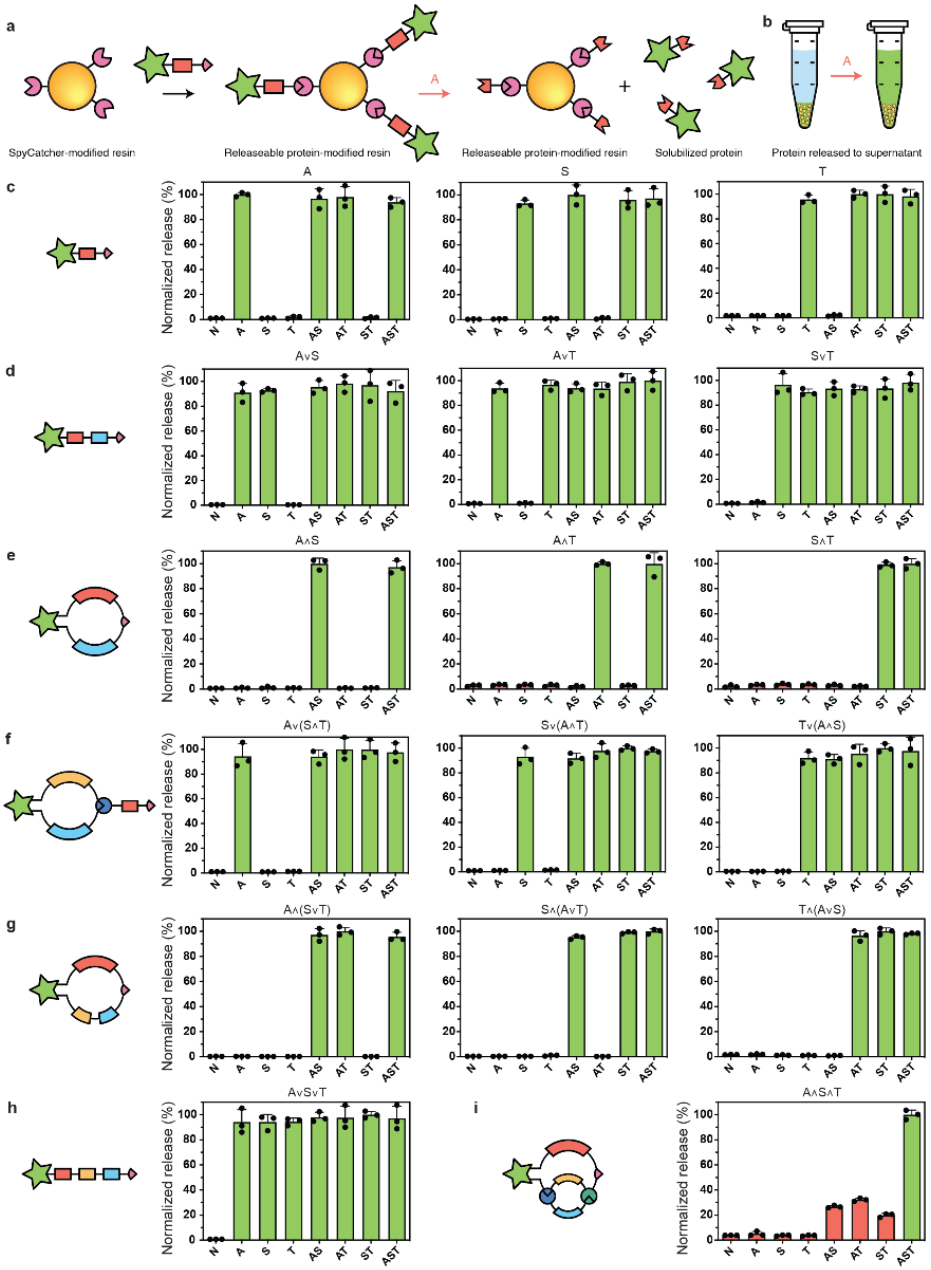

Figure 19: Assembled logic operators undergo pre-programmed cleavages from bead surfaces in response to actuator input combinations

a) SpyCatcher-functionalized magnetic beads can be decorated with different logical operators holding a SpyTag motif through SpyLigation. In this example, an A-releasable mGreenLantern is cleaved from the resin and solubilized in response to an A input.

b) Fluorescent protein release into the supernatant can be used as a surrogate measure to track logical response. In this example, the supernatant in response to input A.

c) The response profiles of the YES-gated single-input tethers.

*b-c) The response profiles of the two-input OR-gated (**b**) and AND-gated (**c**) tethers.*

*d-g) The response profiles of the three-input (AND)/OR- (**d**), (OR)/AND- (**e**), OR-OR- (**f**), and AND-AND-gated (**g**) tethers.*

Plot titles correspond to the protein tether identity; the y-axis represents extent of protein release from bead surfaces as measured via supernatant fluorescence; the x-axis indicates treatment conditions, wherein N indicates no treatment, A indicates eSrtA(2A9), S indicates eSrtA(2S9), and T indicates TEV. Green bars indicate conditions expected to yield tether cleavage, whereas red bars indicate conditions expected to keep the tether non-cleaved. Error bars correspond to ±1 standard deviation about the mean with propagated uncertainties for n=3 experimental replicates.

5.2.4. Characterization of operator logical response from hydrogel matrices

We next sought to further extend the applicability of our method by programming biomacromolecule release from 3D hydrogel networks, thus assessing the ability to trigger and multiplex signals via our autonomously compiled molecular topology-based approach. To do so, we first supplemented our protein toolkit by expressing and purifying two additional YES-gated fluorescent proteins that are spectrally separated from our starting A-releasable mGreenLantern cargo (mGreenLantern-A, λexc.= 495 nm, λem. = 525 nm). Specifically, we constructed and purified an S-releasable mCherry (mCherry-S, λexc.= 580 nm, λem.= 610 nm) and a T-releasable mCerulean (mCerulean-T, λexc.= 433 nm, λem. = 475 nm) (**Supplementary Method S5.9, Supplementary Figs. S5.4-S5.5**) – both also containing a SpyTag motif for material anchoring and 6xHistidine tag for purification. These species responded molecularly as expected to our exhaustive suite of potential inputs, indicated via SDS-PAGE analysis (**Extended Data Fig. 5.3**). Poly(ethylene glycol) (PEG)-based hydrogels were synthesized through the SPAAC-based step-polymerization of a PEG-tetrabicyclononyne (PEG-tetraBCN, Mn ~ 20 kDa) macromer and a triethylene glycol (TEG) diazide[62] in the presence of a small amount of SpyCatcher-azide bound to mGreenLantern-A, mCherry-S, and mCerulean-T via SpyLigation (**Fig. 5.3a**, **Supplementary Method S5.10**). Such tri-functionalized hydrogels were subjected to

each unique input combination involving A, S, and T, and supernatant blue/green/red fluorescence was quantified to determine each individual protein release (**Supplementary Method S5.11**). Gratifyingly, the three proteins were released independently in the manner specified by their preprogrammed YES-gated input (**Extended Data Fig. 5.4**).

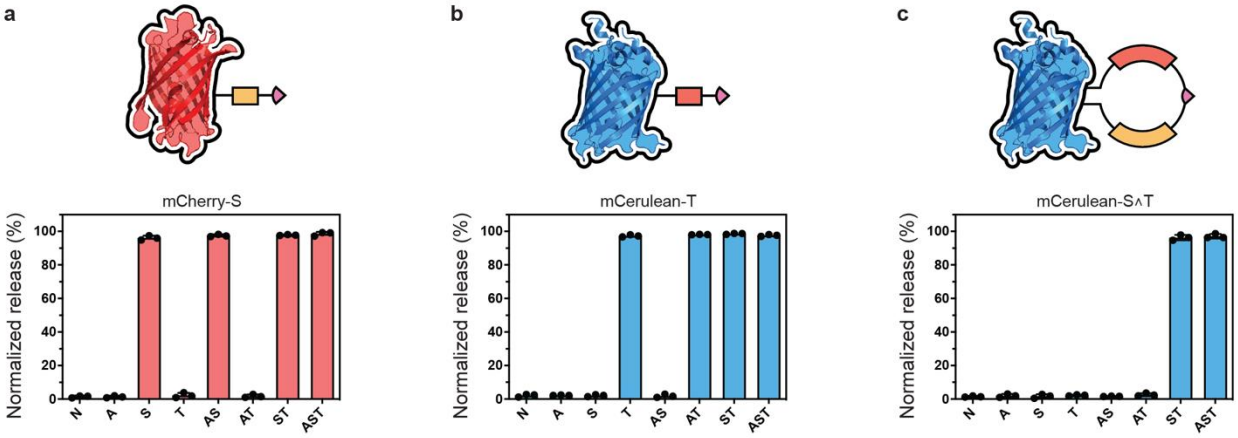

Extended Data 20: SDS-PAGE analysis of in-solution treatment of autonomously compiled mCherry and mCerulean pendants

a-c) Changes in topology and/or molecular weight in response to a specific set of inputs leads to changes in protein electrophoretic mobility, which can be analyzed through gel densitometry. Results are shown for species (a) mCherry-S, (b) mCerulean-T, and (c) mCerulean-S∧T. Plot titles correspond to the protein tether identity; the y-axis represents extent of cleavage as measured through migration on an SDS-PAGE with gel densitometry analysis; the x-axis indicates treatment conditions, wherein $_N$ *indicates no treatment,* $_A$ *indicates eSrtA(2A9),* $_S$ *indicates eSrtA(2S9), and* $_T$ *indicates TEV. Green bars indicate conditions expected to yield tether cleavage, whereas red bars indicate conditions expected to keep the tether non-cleaved. Error bars correspond to ±1 standard deviation about the mean with propagated uncertainties for n=3 experimental replicates.*

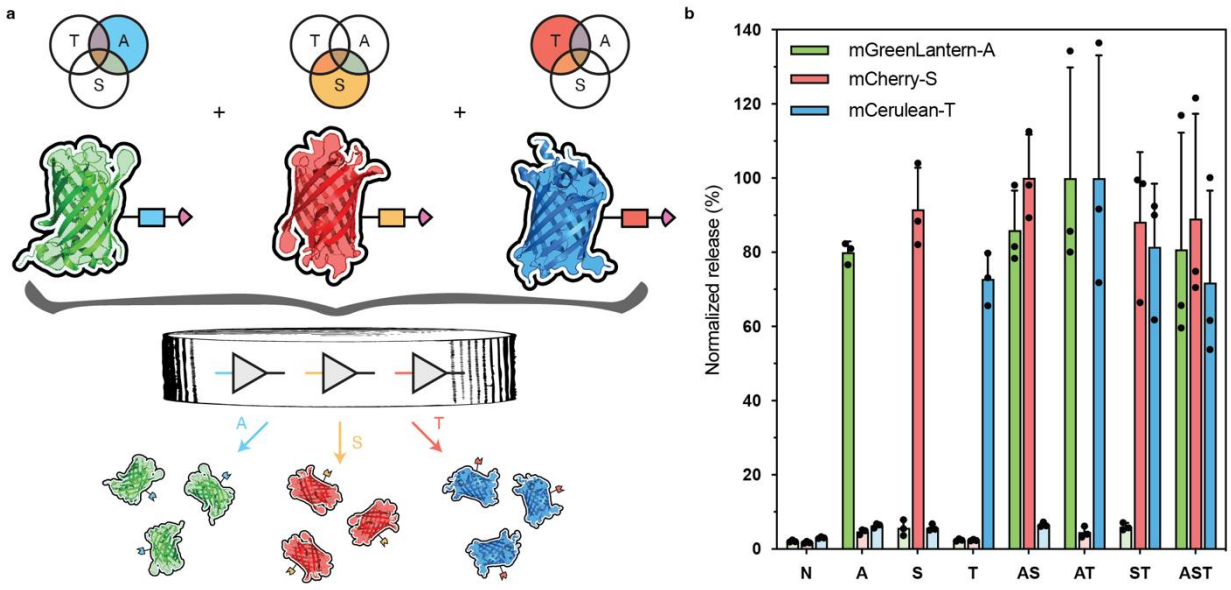

Extended Data 21: Multiplexed YES-gated release of proteins from hydrogel biomaterials

a) *mGreenLantern-A, mCherry-S, and mCerulean-T are tethered homogenously into an underlying PEG network, each exhibiting a different YES-gated response.*
b) *Appropriate protein is released when the correct input combination is present. Fully colored bars (green for mGreenLantern, red for mCherry, blue for mCerulean) indicate conditions expected to yield protein release, whereas opaque colored bars denote conditions not expected to result in release. Error bars correspond to ±1 standard deviation about the mean with propagated uncertainties for n=3 experimental replicates.*

Looking to build on this initial success and benefit from the ease of assembly proffered by our approach, we sought to go beyond the multiplexed release of YES operators and layer in different logical operators into the underlying matrix. Toward this end, we decorated our SpyCatcher-modified PEG hydrogels with mGreenLantern-A∨T, mCherry-S, and a newly designed and solution-characterized mCerulean-S∧T (**Fig. 5.3b**, **Supplementary Method S5.9, Supplementary Figs. S5.4-S5.5, Extended Data Fig. 5.3)**. Following treatment with all possible actuator sets, we observed the release of each target biomacromolecule only in response to the appropriate cues or combinations thereof (**Fig. 5.3c**). Collectively, these studies establish a powerful new route towards the creation of multi-input/multi-output-type materials.

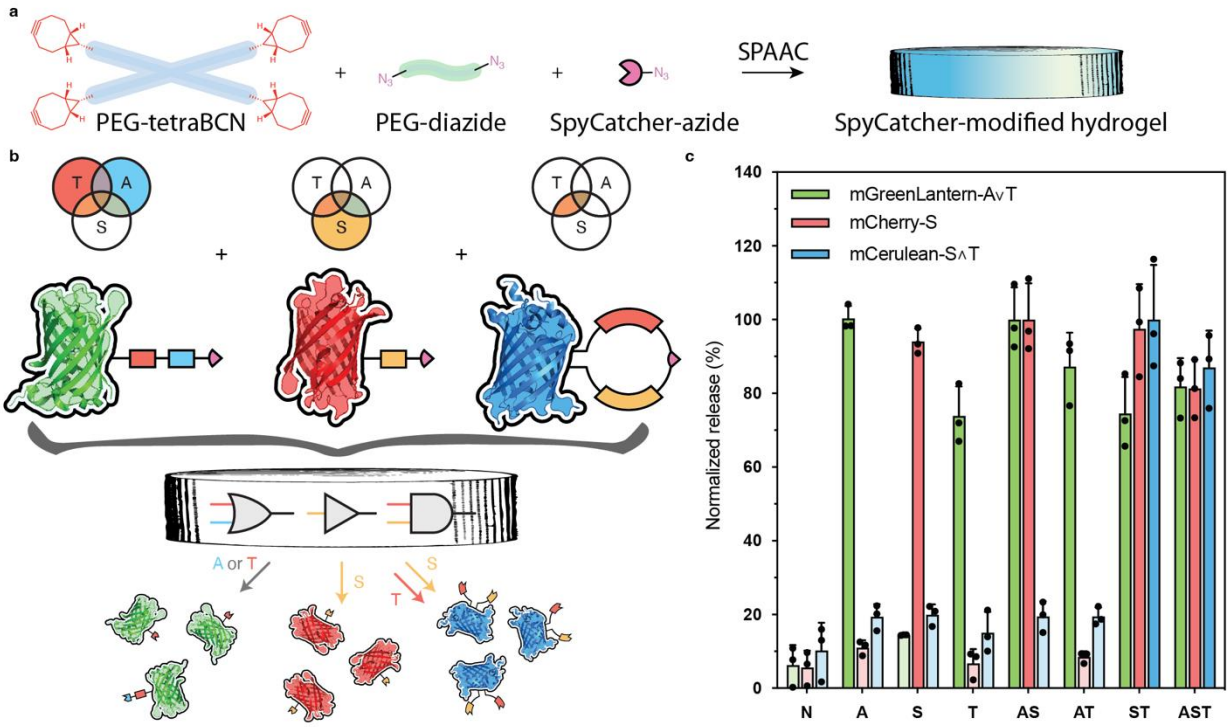

Figure 22: Molecularly compiled topologies enable the multiplexed and independently triggered release of distinct proteins from a hydrogel network

a) PEG-tetraBCN, TEG-diazide, and SpyCatcher-azide react via SPAAC to form hydrogels that can be subsequently functionalized with SpyTagged proteins of interest.

b) mGreenLantern-AVT, mCherry-S, and mCerulean-SΛT are tethered homogenously into an underlying PEG network, each exhibiting a different logical response.

c) Appropriate protein is released when the correct input combination is present. Fully colored bars (green for mGreenLantern, red for mCherry, blue for mCerulean) indicate conditions expected to yield protein release, whereas opaque colored bars denote conditions not expected to result in release. Error bars correspond to ±1 standard deviation about the mean with propagated uncertainties for n=3 experimental replicates.

5.2.5. Seamless scale-up of logical response and complexity through genetic encodability

Having successfully demonstrated the promise of autonomously compiled molecular topologies in three different contexts (i.e., in solution, on surfaces, and within hydrogel networks), we set out to leverage the intrinsic benefits of unsupervised biosynthesis to create a 5-input-responsive [AND/(OR)]OR(AND)-gated system, extending well beyond the biocomputational complexity achievable through other material approaches (**Fig. 5.4a**). Towards this goal, we identified two additional proteases expected to operate orthogonally to our existing set of inputs: the potyviral Tobacco Vein Mottling Virus (TVMV) protease (operating on substrate ETVRFQ↓S, referred to as V)63 and the human rhinovirus-3C (HRV-3C) protease (recognizing LEVLFQ↓GP, denoted as C)64 (**Fig. 5.4b**) (**Supplementary Method S5.5, Supplementary Fig. S5.1**). Having identified our 5 input proteases, we sought to synthesize the mGreenLantern-[(A∨S)∧T]∨(C∧V) protein, a design which would necessitate the compilation of a genetic blueprint into a bi-cyclic protein (**Supplementary Method S5.12**). To achieve such a logical operation, we adopted a recently pioneered "assembly-reaction" synergy approach, where motifs that assemble through fragment dimerization, catenation, or similar mechanisms bring covalent chemistries (e.g., Tag/Catcher ligations) into close proximity that drive reaction completion.[65,66] In our case, we reasoned that deploying SICLOPPS to cyclize a target protein would bring internal Tag and Catcher motifs into physical proximity, promoting complete ligation to create the pinch point-containing bicyclic protein. Employing this methodology, our mGreenLantern-[(A∨S)∧T]∨(C∧V) was generated solubly, in high purity (>95%) (**Supplementary Fig. S5.6**) and yield (5 mg L-1 of culture following IMAC/SEC), and with the expected molecular mass (**Fig. 5.4c**). To validate the response signature of this logical construct, we immobilized mGreenLantern-[(A∨S)∧T]∨(C∧V) onto SpyCatcher-functionalized magnetic

beads (**Supplementary Method S5.13)** and assessed release via supernatant fluorescence following treatment via each of the 32 potential actuator combination sets. We observed the expected anti-interferent penta-input responsiveness, demonstrating protein release only in pre-programmed conditions with near-perfect signal-to-noise ratios (**Fig. 5.4d**). Excitingly, despite its unprecedented functional complexity, this cargo was generated through routine recombinant methods and required no extensive debugging/recoding. Most promisingly, our studies suggest that the potential for even higher-order logical complexity is limited primarily by the number of orthogonally labile peptide motifs and fragment reconstitution chemistries that can be identified.

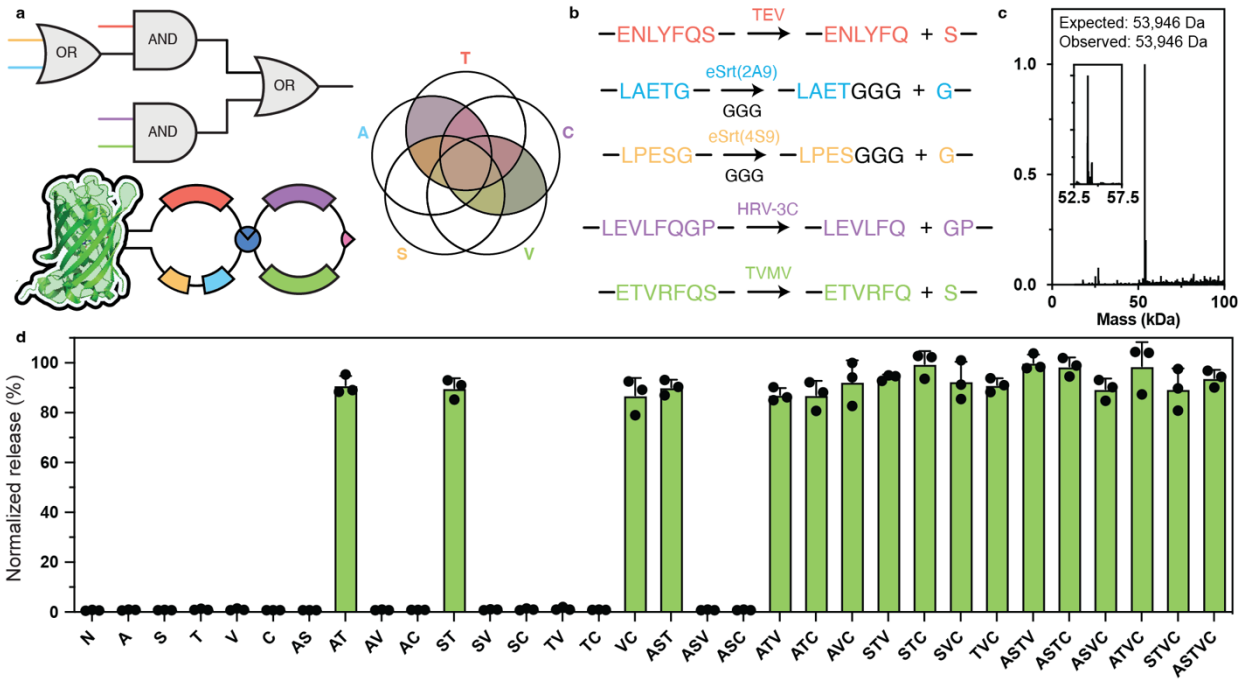

Figure 23: Genetic encodability enables seamless scale-up in logical response complexity

a) *mGreenLantern-[(A∨S)∧T]∨(C∧V) can be assembled on one expression frame and purified rapidly. Each region of the Venn diagrams displayed represents a unique combination of protease inputs and indicates whether the tether is predicted to cleave (colored) or remain intact (white).*

b) *Reactions depicting protease recognition of target sequence and subsequent cleavage: the recognition sequence ENLYFQ↓S is recognized and cleaved by TEV; LAET↓G by eSrt(2A9); LPES↓G by eSrtA(4S9); LEVLFQ↓GP by HRV-3C; ETVRFQ↓S by TVMV.*

c) *mGreenLantern-[(A∨S)∧T]∨(C∧V) is readily purified and obtained with the correct molecular mass.*

d) *The response profiles of the 5-input system. The y-axis represents extent of protein release from bead surfaces as measured via supernatant fluorescence; the x-axis indicates treatment conditions, wherein* $_N$ *indicates no treatment,* $_A$ *indicates eSrtA(2A9),* $_S$ *indicates eSrtA(2S9),* $_T$ *indicates TEV,* $_V$ *indicates TVMV, and* $_C$ *indicates HRV-3C. Green bars indicate conditions expected to yield tether cleavage, whereas red bars indicate conditions expected to keep the tether non-cleaved. Error bars correspond to ±1 standard deviation about the mean with propagated uncertainties for n=3 experimental replicates.*

5.3. Discussion

In this work, we have introduced and harnessed the concept of autonomous macromolecular compilation to create bioactive proteins that can be site-specifically tethered to and conditionally released from biomaterials following user-programmable and hierarchically nested Boolean YES/OR/AND operations. Exploiting the intrinsic modularity and scalability of recombinant expression, we have demonstrated multiplexed and multi-stimuli-triggered protein release from biomaterials, including release through a 5-input-responsive [AND/(OR)]OR(AND)-gated system. Our design rules yield species that are structurally simple, yet functionally complex, all through direct and unsupervised biosynthesis.

The power of the presented approach lies in its modularity. Though we have utilized 5 orthogonal proteases to serve as inputs, polypeptide motifs that sense and respond to other input types (e.g., light[16,67], small molecule[68]) can be readily incorporated to afford additionally engineered programmability. Beyond the fluorescent cargos initially adopted for their ease of characterization, Boolean-actuated release of more exotic bioactive proteins (e.g., enzymes, growth factors, nanobodies) should be easily attained. While we have utilized SpyTag/Catcher ligation to tether proteins to materials, this chemistry can likely be effortlessly swapped for alternative (non)covalent reactions, including those involving de novo designed heterodimer interactions[69] or click-type handle installation via genetic code expansion.[70] Finally, as the systems are fully genetically encoded, opportunities undoubtedly exist to both create and functionally deploy these platforms in cellulo, as well as potentially even in vivo. Owing to its powerful simplicity and plug-and-play potential, we expect that this approach will find a host of applications in highly targeted drug delivery, on-demand biosensor engineering, and next-generation protein architecture development and refinement.

References

1. Badeau, B. A. & DeForest, C. A. Programming Stimuli-Responsive Behavior into Biomaterials. *Annu. Rev. Biomed. Eng.* **21**, 241–265 (2019).
2. Liu, A. P. *et al.* The living interface between synthetic biology and biomaterial design. *Nat. Mater.* **21**, 390–397 (2022).
3. Narkar, A. R., Tong, Z., Soman, P. & Henderson, J. H. Smart biomaterial platforms: Controlling and being controlled by cells. *Biomaterials* **283**, 121450 (2022).
4. Li, J. & Mooney, D. J. Designing hydrogels for controlled drug delivery. *Nat. Rev. Mater.* **1**, (2016).
5. Rizzo, F. & Kehr, N. S. Recent Advances in Injectable Hydrogels for Controlled and Local Drug Delivery. *Adv. Healthc. Mater.* **10**, 2001341 (2021).
6. Drury, J. L. & Mooney, D. J. Hydrogels for tissue engineering: Scaffold design variables and applications. *Biomaterials* **24**, 4337–4351 (2003).
7. Malda, J. *et al.* 25th Anniversary Article: Engineering Hydrogels for Biofabrication. *Adv. Mater.* **25**, 5011–5028 (2013).
8. Aisenbrey, E. A. & Murphy, W. L. Synthetic alternatives to Matrigel. *Nat. Rev. Mater.* **5**, 539–551 (2020).
9. Hofer, M. & Lutolf, M. P. Engineering organoids. *Nat. Rev. Mater.* **6**, 402–420 (2021).
10. Johnston, T. G. *et al.* Compartmentalized microbes and co-cultures in hydrogels for on-demand bioproduction and preservation. *Nat. Commun.* **11**, 563 (2020).
11. Fisher, S. A., Baker, A. E. G. & Shoichet, M. S. Designing Peptide and Protein Modified Hydrogels: Selecting the Optimal Conjugation Strategy. *J. Am. Chem. Soc.* **139**, 7416–7427 (2017).
12. Shadish, J. A. & DeForest, C. A. Site-Selective Protein Modification: From Functionalized Proteins to Functional Biomaterials. *Matter* **2**, 50–77 (2020).
13. Gharios, R., Francis, R. M. & DeForest, C. A. Chemical and biological engineering strategies to make and modify next-generation hydrogel biomaterials. *Matter* **6**, 4195–4244 (2023).
14. Kloxin, A. M., Kasko, A. M., Salinas, C. N. & Anseth, K. S. Photodegradable Hydrogels for Dynamic Tuning of Physical and Chemical Properties. *Science* **324**, 59–63 (2009).
15. Brown, T. E., Marozas, I. A. & Anseth, K. S. Amplified Photodegradation of Cell-Laden Hydrogels via an Addition–Fragmentation Chain Transfer Reaction. *Adv. Mater.* **29**, (2017).
16. Shadish, J. A., Strange, A. C. & Deforest, C. A. Genetically Encoded Photocleavable Linkers for Patterned Protein Release from Biomaterials. *J. Am. Chem. Soc.* **141**, 15619–15625 (2019).
17. Chapla, R., Hammer, J. A. & West, J. L. Adding Dynamic Biomolecule Signaling to Hydrogel Systems via Tethered Photolabile Cell-Adhesive Proteins. *ACS Biomater. Sci. Eng.* **8**, 208–217 (2022).
18. Kilic Boz, R. *et al.* Redox-Responsive Hydrogels for Tunable and "On-Demand" Release of Biomacromolecules. *Bioconjug. Chem.* **33**, 839–847 (2022).
19. Lueckgen, A. *et al.* Enzymatically-degradable alginate hydrogels promote cell spreading and in vivo tissue infiltration. *Biomaterials* **217**, 119294 (2019).

20. Tanimoto, R., Ebara, M. & Uto, K. Tunable enzymatically degradable hydrogels for controlled cargo release with dynamic mechanical properties. *Soft Matter* **19**, 6224–6233 (2023).

21. Ding, H. *et al.* Preparation and application of pH-responsive drug delivery systems. *J. Controlled Release* **348**, 206–238 (2022).

22. Burdick, J. A. & Murphy, W. L. Moving from static to dynamic complexity in hydrogel design. *Nat. Commun.* **3**, 1269 (2012).

23. Zhao, Z., Ukidve, A., Kim, J. & Mitragotri, S. Targeting Strategies for Tissue-Specific Drug Delivery. *Cell* **181**, 151–167 (2020).

24. Manzari, M. T. *et al.* Targeted drug delivery strategies for precision medicines. *Nat. Rev. Mater.* **6**, 351–370 (2021).

25. Culver, H. R., Clegg, J. R. & Peppas, N. A. Analyte-Responsive Hydrogels: Intelligent Materials for Biosensing and Drug Delivery. *Acc. Chem. Res.* **50**, 170–178 (2017).

26. Herrmann, A., Haag, R. & Schedler, U. Hydrogels and Their Role in Biosensing Applications. *Adv. Healthc. Mater.* **10**, 2100062 (2021).

27. Ikeda, M. *et al.* Installing logic-gate responses to a variety of biological substances in supramolecular hydrogel-enzyme hybrids. *Nat. Chem.* **6**, 511–518 (2014).

28. Hou, B. *et al.* Engineering Stimuli-Activatable Boolean Logic Prodrug Nanoparticles for Combination Cancer Immunotherapy. *Adv. Mater.* **32**, 1907210 (2020).

29. Zhang, P. *et al.* A programmable polymer library that enables the construction of stimuli-responsive nanocarriers containing logic gates. *Nat. Chem.* **12**, 381–390 (2020).

30. Badeau, B. A., Comerford, M. P., Arakawa, C. K., Shadish, J. A. & Deforest, C. A. Engineered modular biomaterial logic gates for environmentally triggered therapeutic delivery. *Nat. Chem.* **10**, 251–258 (2018).

31. Gawade, P. M., Shadish, J. A., Badeau, B. A. & DeForest, C. A. Logic-Based Delivery of Site-Specifically Modified Proteins from Environmentally Responsive Hydrogel Biomaterials. *Adv. Mater.* **31**, 1902462 (2019).

32. Ruskowitz, E. R., Comerford, M. P., Badeau, B. A. & Deforest, C. A. Logical stimuli-triggered delivery of small molecules from hydrogel biomaterials. *Biomater. Sci.* **7**, 542–546 (2019).

33. Thompson, R. E. & Muir, T. W. Chemoenzymatic Semisynthesis of Proteins. *Chem. Rev.* **120**, 3051–3126 (2020).

34. de la Torre, D. & Chin, J. W. Reprogramming the genetic code. *Nat. Rev. Genet.* **22**, 169–184 (2021).

35. Scott, C. P., Abel-Santos, E., Wall, M., Wahnon, D. C. & Benkovic, S. J. Production of cyclic peptides and proteins in vivo. *Proc. Natl. Acad. Sci.* **96**, 13638–13643 (1999).

36. Iwai, H., Lingel, A. & Plückthun, A. Cyclic Green Fluorescent Protein Produced in Vivo Using an Artificially Split PI-PfuI Intein from Pyrococcus furiosus *. *J. Biol. Chem.* **276**, 16548–16554 (2001).

37. Zhang, W.-B., Sun, F., Tirrell, D. A. & Arnold, F. H. Controlling Macromolecular Topology with Genetically Encoded SpyTag–SpyCatcher Chemistry. *J. Am. Chem. Soc.* **135**, 13988–13997 (2013).

38. Schoene, C., Bennett, S. P. & Howarth, M. Chapter Seven - SpyRings Declassified: A Blueprint for Using Isopeptide-Mediated Cyclization to Enhance Enzyme Thermal Resilience. in *Methods in Enzymology* (ed. Pecoraro, V. L.) vol. 580 149–167 (Academic Press, 2016).

39. Fan, R. & Aranko, A. S. Catcher/Tag Toolbox: Biomolecular Click-Reactions For Protein Engineering Beyond Genetics. *ChemBioChem* **25**, e202300600 (2024).

40. Qu, Z., Cheng, S. Z. D. & Zhang, W.-B. Macromolecular Topology Engineering. *Trends Chem.* **3**, 402–415 (2021).

41. Liu, Y. *et al.* Mechano-bioconjugation Strategy Empowering Fusion Protein Therapeutics with Aggregation Resistance, Prolonged Circulation, and Enhanced Antitumor Efficacy. *J. Am. Chem. Soc.* **144**, 18387–18396 (2022).

42. Bai, X. *et al.* Cellular synthesis of protein pretzelanes. *Giant* **10**, 100092 (2022).

43. Hou, B., Yan, X., He, J., Zhang, W.-B. & Shao, Y. Self-assembly of three-component bolaform giant surfactants with branched architectures. *Giant* **15**, 100165 (2023).

44. Snoj, J., Lapenta, F. & Jerala, R. Preorganized cyclic modules facilitate the self-assembly of protein nanostructures. *Chem. Sci.* **15**, 3673–3686 (2024).

45. Bressler, E. M. *et al.* Boolean logic in synthetic biology and biomaterials: Towards living materials in mammalian cell therapeutics. *Clin. Transl. Med.* **13**, e1244 (2023).

46. Campbell, B. C. *et al.* mGreenLantern: a bright monomeric fluorescent protein with rapid expression and cell filling properties for neuronal imaging. *Proc. Natl. Acad. Sci.* **117**, 30710–30721 (2020).

47. Dorr, B. M., Ham, H. O., An, C., Chaikof, E. L. & Liu, D. R. Reprogramming the specificity of sortase enzymes. *Proc. Natl. Acad. Sci.* **111**, 13343–13348 (2014).

48. Bretherton, R. C. *et al.* User-Controlled 4D Biomaterial Degradation with Substrate-Selective Sortase Transpeptidases for Single-Cell Biology. *Adv. Mater.* **35**, 2209904 (2023).

49. Keeble, A. H. *et al.* DogCatcher allows loop-friendly protein-protein ligation. *Cell Chem. Biol.* **29**, 339-350.e10 (2022).

50. Zakeri, B. *et al.* Peptide tag forming a rapid covalent bond to a protein, through engineering a bacterial adhesin. *Proc. Natl. Acad. Sci. U. S. A.* **109**, E690–E697 (2012).

51. Stevens, A. J. *et al.* Design of a Split Intein with Exceptional Protein Splicing Activity. *J. Am. Chem. Soc.* **138**, 2162–2165 (2016).

52. Thompson, R. E., Stevens, A. J. & Muir, T. W. Protein engineering through tandem transamidation. *Nat. Chem.* **11**, 737–743 (2019).

53. Townend, J. E. & Tavassoli, A. Traceless Production of Cyclic Peptide Libraries in E. coli. *ACS Chem. Biol.* **11**, 1624–1630 (2016).

54. Veggiani, G. *et al.* Programmable polyproteams built using twin peptide superglues. *Proc. Natl. Acad. Sci.* **113**, 1202–1207 (2016).

55. Xu, Q. *et al.* Catcher/Tag cyclization introduces electrostatic interaction mediated protein-protein interactions to enhance the thermostability of luciferase. *Process Biochem.* **80**, 64–71 (2019).

56. Sun, F. & Zhang, W.-B. Genetically Encoded Click Chemistry†. *Chin. J. Chem.* **38**, 894–896 (2020).

57. Evans, T. C., Benner, J. & Xu, M.-Q. The Cyclization and Polymerization of Bacterially Expressed Proteins Using Modified Self-splicing Inteins *. *J. Biol. Chem.* **274**, 18359–18363 (1999).

58. Siebold, C. & Erni, B. Intein-mediated cyclization of a soluble and a membrane protein in vivo: function and stability. *Biophys. Chem.* **96**, 163–171 (2002).

59. Qi, X. & Xiong, S. Intein-mediated backbone cyclization of VP1 protein enhanced protection of CVB3-induced viral myocarditis. *Sci. Rep.* **7**, 41485 (2017).

60. Oliveira-Silva, R. *et al.* Monitoring Proteolytic Activity in Real Time: A New World of Opportunities for Biosensors. *Trends Biochem. Sci.* **45**, 604–618 (2020).
61. Agard, N. J., Prescher, J. A. & Bertozzi, C. R. A strain-promoted [3 + 2] azide-alkyne cycloaddition for covalent modification of biomolecules in living systems. *J. Am. Chem. Soc.* **126**, 15046–15047 (2004).
62. DeForest, C. A., Polizzotti, B. D. & Anseth, K. S. Sequential click reactions for synthesizing and patterning three-dimensional cell microenvironments. *Nat. Mater.* **8**, 659–664 (2009).
63. Nallamsetty, S. *et al.* Efficient site-specific processing of fusion proteins by tobacco vein mottling virus protease in vivo and in vitro. *Protein Expr. Purif.* **38**, 108–115 (2004).
64. Abdelkader, E. H. & Otting, G. NT*-HRV3CP: An optimized construct of human rhinovirus 14 3C protease for high-yield expression and fast affinity-tag cleavage. *J. Biotechnol.* **325**, 145–151 (2021).
65. Qu, Z. *et al.* A single-domain green fluorescent protein catenane. *Nat. Commun.* **14**, 3480 (2023).
66. Li, T., Zhang, F., Fang, J., Liu, Y. & Zhang, W.-B. Rational Design and Cellular Synthesis of Proteins with Unconventional Chemical Topology. *Chin. J. Chem.* **41**, 2873–2880 (2023).

Acknowledgements

The authors thank R. Francis and A. Garcia for collaborating on designing and validating the SpyCatcher-azide, as well as C. Yang and R. Brady for synthesizing and supplying PEG-tetraBCN. We also acknowledge support from D. Whittington at the University of Washington (UW) Mass Spectrometry Center. This work was supported by a grant (DMR 1807398, C.A.D.) from the National Science Foundation and a Maximizing Investigators' Research Award (R35GM138036, C.A.D.) from the National Institutes of Health. Student support was further provided through a John C. Berg Endowed Fellowship (R.G.), a Goldwater Scholarship (A.L.), Washington NASA Space Grant (A.L), and a University of Washington MEM-C Academic-Year Research Accelerator Fellowship (A.L).

Author Contributions

For this manuscript, R.G. and C.A.D. conceived and designed the experiments; R.G. and A.L. performed the experiments; R.G., A.L., and C.A.D. analyzed the data; C.A.D. prepared the figures with input from R.G.; R.G. and C.A.D. wrote the paper.

Methods

Method S5.1 General method for protein expression

E. Coli BL21.(DE3) cells were transformed with the proper operator construct and grown at 37°C and 220 rpm agitation to an OD of 0.6-0.8 in LB broth supplemented with kanamycin. Isopropyl β-D-1-thiogalactopyranoside (IPTG) was used to induce protein expression (0.5 mM final concentration when for linear constructs, 0.2-0.4 mM when for cyclic constructs), at which point the cultures were moved to a reduced temperature (18°C) for 18 hours. Cells were then harvested via centrifugation (4,000g, 20 minutes, 4°C) and either flash-frozen and stored at -80°C or used directly.

Method S5.2 Protein purification protocol

Method S5.2.1 Immobilized metal-affinity chromatography

Cell pellets were reconstituted in 40 mL of lysis buffer (20 mM Tris, 50 mM NaCl, pH = 7.5). These were then supplemented with phenylmethylsulfonyl fluoride (PMSF) to a final concentration of 1 mM and sonicated on ice (18 minutes at 30% amplitude and 33% duty cycle) (Fisher Scientific; Waltham, MA). After sonication, lysates were centrifuged for 45 minutes at 11,000g to separate soluble from insoluble fractions.

Clarified lysates were loaded onto an Äkta Pure 25L FPLC (Cytiva; Marlborough, MA) equipped with a 5mL HisTrap HP column at a flow rate of 5 mL/min. The HisTrap column was first equilibrated with 5 column volumes of lysis buffer prior to loading. Once all protein was bound, the column was washed with 10+ column volumes of lysis buffer until residual UV read-outs (λ = 280 nm) dropped to 0 absolute units (au). Target protein was then eluted off the column

into a 96-well plate by switching to elution buffer (lysis buffer + 250 mM imidazole). Eluate fractions were assessed for purity by preliminary SDS-PAGE; the purest fractions were then pooled pending further dialysis or SEC.

For linear constructs that had no higher order macro-cycle contaminants, the pooled purified protein was dialyzed (20 mM Tris, 50 mM NaCl, pH = 7.5) to remove imidazole (SnakeSkin™ Dialysis Tubing, 10K MWCO. Fischer Scientific; Waltham, MA). After 4+ dialysis bath changes, proteins were spin-concentrated if needed using an Amicon Ultra 15 centrifugation filter (10 kDa cutoff. Sigma-Alrich; Burlington, MA). The purified solution was supplemented with glycerol (10% of final volume) to act as cryoprotectant, aliquoted into single-use tubes to avoid repeated freeze-thaw cycles, and flash-frozen with liquid nitrogen prior to long-term storage.

Method S5.2.2 Size exclusion chromatography

For cyclized constructs, proteins were loaded again onto an Äkta Pure unit equipped with a HiLoad 26/600 Superdex 75pg SEC column. The column was pre-equilibrated with a high-salt buffer solution (20 mM Tris, 300 mM NaCl, pH = 7.5). Sample injection occurred at a flowrate of 2.6 mL/min. Buffer flowrate through the system occurred at 1.5-1.8 mL/min, depending on the purity of the injected solution. Purified eluates were collected in 96-well tubes. Prior to pooling, preliminary SDS-PAGE was conducted to verify fraction purity. Proteins were then spin-concentrated using an Amicon Ultra 15 centrifugation filter (10 kDa cutoff. Sigma-Alrich; Burlington, MA) and then stocked as described in Method S2.1.

Method S5.3 Plasmid construction for proof-of-concept logical operator expression and ORF sequences

Cloned plasmids [pET-29b(+), with desired sequences inserted between NdeI and XhoI cloning sites] were ordered from GenScript (Piscataway, NJ). The open reading frames (ORFs) of the 17 YES/OR/AND nested logical operators are given below (5' à 3'), with relevant portions color coded for ease of identification. 2A9c, 4S9c, and TEVc respectively denote the recognition sequences for their associated enzymes. All mGreenLantern constructs were designed to contain a SpyTag for material tethering and a 6xHis motif for IMAC-assisted purification.

mGreenLantern – A YES
MGSS-mGreenLantern-GGS(x3)-2A9c-GGS(x3)-SpyTag003-GGS(x3)-6xHis

ATGGGGAGTTCTATGGTATCAAAAGGAGAAGAGTTGTTTACCGGTGTTGTTCCGATTCTGGTCG
AGTTAGATGGCGATGTTAACGGCCACAAGTTCAGCGTTCGTGGTGAGGGTGAAGGCGACGCCAC
CAATGGTAAACTGACCTTGAAGTTCATCTGCACCACGGGTAAGCTGCCTGTTCCGTGGCCGACC
CTGGTAACTACGCTGGGTTATGGTGTTGCATGTTTTGCGCGTTACCCGGACCACATGAAACAAC
ATGATTTCTTTAAGTCTGCAATGCCGGAAGGTTACGTCCAAGAAAGAACAATTAGCTTTAAGGA
CGACGGTACTTACAAAACCCGCGCGGAGGTGAAATTCGAGGGCGACACCCTGGTGAACCGTATT
GTGCTGAAAGGCATCGACTTCAAAGAGGACGGCAACATCCTGGGTCATAAGCTGGAATATAACT
TCAACAGCCACAAAGTTTATATCACCGCCGACAAACAAAAAAACGGGATCAAAGCTAATTTTAA
GACCCGTCATAACGTGGAGGATGGCGGCGTTCAGCTGGCTGACCACTACCAGCAGAACACCCCG
ATTGGTGACGGTCCGGTCTTGCTGCCAGATAATCATTACTTGAGCCATCAGAGCAAGTTGAGCA
AAGATCCGAATGAAAAACGCGATCACATGGTGCTTAAGGAGCGCGTGACGGCGGCGGGTATTAC
CCATGACATGGATGAACTGTATAAGGGCGGCAGCGGCGGCTCCGGCGGCTCTCTGGCGGAAACG
GGTGGTGGAAGCGGCGGTTCGGGTGGTAGTCGTGGTGTGCCGCATATCGTGATGGTTGATGCGT
ATAAGCGTTACAAG GGTGGGTCCGGTGGCTCCGGCGGCTCGCACCACCACCACCACCAC

mGreenLantern – S YES
MGSS-mGreenLantern-GGS(x3)-4S9c-GGS(x3)-SpyTag003-GGS(x3)-6xHis

ATGGGGTCATCTATGGTAAGTAAAGGAGAAGAGCTGTTTACCGGTGTCGTGCCGATTCTGGTTG
AACTGGATGGCGACGTGAACGGTCATAAGTTCAGCGTTCGTGGTGAAGGCGAGGGTGACGCCAC
CAACGGTAAGTTGACCTTGAAGTTCATCTGCACCACGGGTAAGCTTCCGGTTCCGTGGCCGACC
TTGGTGACGACCCTGGGTTATGGTGTCGCGTGTTTTGCCCGTTACCCGGACCACATGAAACAGC
ATGACTTCTTTAAAAGCGCAATGCCGGAAGGCTACGTTCAAGAGCGCACCATTAGCTTTAAGGA
CGACGGAACCTACAAGACGAGAGCGGAAGTGAAATTCGAGGGTGACACCCTGGTCAACCGTATT

GTGCTGAAAGGCATCGATTTCAAAGAGGATGGTAATATTCTGGGCCATAAATTGGAATATAACT
TTAACAGCCACAAGGTGTATATCACGGCTGATAAACAAAAAAACGGCATCAAAGCTAATTTCAA
GACTCGTCATAATGTTGAGGACGGCGGCGTGCAACTGGCAGACCACTACCAGCAGAATACCCCG
ATCGGCGACGGCCCTGTTCTGCTGCCAGACAACCACTACCTGAGCCATCAGAGCAAACTCTCGA
AAGATCCGAATGAAAAACGTGATCACATGGTTTTAAAAGAACGCGTGACTGCGGCGGGTATCAC
CCATGATATGGATGAGCTGTATAAGGGTGGCTCCGGCGGTTCTGGCGGTTCCCTGCCGGAGAGC
GGTGGGGGCTCCGGCGGTTCTGGTGGTAGCCGTGGCGTACCGCATATTGTTATGGTTGATGCGT
ATAAGCGCTACAAG GGCGGTAGTGGCGGTAGCGGTGGTTCTCACCACCACCACCACCAC

mGreenLantern – T YES
MGSS-mGreenLantern-GGS(x3)-TEVc-GGS(x3)-SpyTag003-GGS(x3)-6xHis

ATGGGGTCATCTATGGTAAGTAAAGGAGAAGAGTTGTTTACCGGTGTCGTGCCCATCCTGGTCG
AGTTAGACGGCGACGTTAACGGTCATAAGTTCAGCGTTCGTGGCGAGGGTGAAGGTGACGCCAC
CAACGGCAAACTGACCTTGAAGTTCATCTGCACCACGGGTAAATTACCGGTCCCGTGGCCGACC
TTGGTGACGACCCTTGGTTACGGCGTGGCGTGTTTTGCCCGTTACCCGGACCACATGAAACAGC
ATGACTTCTTCAAAAGCGCAATGCCGGAAGGTTACGTTCAAGAGCGCACCATTAGCTTTAAGGA
TGATGGCACCTATAAAACCCGTGCGGAAGTTAAATTCGAGGGCGACACCCTGGTGAACCGTATT
GTGCTGAAGGGCATCGATTTCAAGGAGGACGGAAACATTCTCGGTCACAAGCTGGAATATAACT
TCAACAGCCACAAGGTGTATATCACTGCGGACAAACAAAAAAATGGCATCAAGGCTAATTTTAA
GACTCGCCATAATGTTGAGGACGGTGGTGTGCAACTGGCTGACCATTACCAGCAGAACACCCCG
ATTGGTGACGGTCCGGTTTTGCTGCCAGATAATCACTACCTGAGCCACCAGAGCAAGCTGAGCA
AAGATCCGAATGAAAAAAGAGATCACATGGTTCTGAAAGAGCGTGTTACGGCGGCAGGCATCAC
CCATGATATGGATGAACTGTACAAGGGCGGCAGCGGCGGCTCGGGTGGTTCGGAAAACCTGTAT
TTTCAGTCAGGTGGCTCCGGTGGTTCTGGCGGTTCTCGTGGTGTTCCGCATATTGTGATGGTAG
ATGCGTATAAGCGCTACAAGGGCGGCTCCGGTGGCTCCGGTGGCTCTCACCACCACCATCACCA
C

mGreenLantern – A v S
MGSS-mGreenLantern-GGS(x3)-2A9c-GGS(x3)-4S9c-GGS(x3)-SpyTag003-GGS(x3)-6xHis

ATGGGGTCAAGTATGGTAAGCAAAGGAGAAGAGTTGTTTACCGGTGTGGTGCCGATTCTGGTTG
AACTGGATGGCGACGTTAACGGTCACAAGTTCAGCGTGCGTGGTGAGGGTGAGGGCGACGCTAC
CAATGGTAAATTGACTTTGAAGTTCATCTGTACCACTGGTAAACTGCCGGTTCCGTGGCCTACG
TTGGTTACCACGCTGGGTTATGGTGTAGCCTGCTTCGCCCGTTACCCGGATCACATGAAACAAC
ACGACTTCTTCAAAAGCGCAATGCCGGAAGGTTACGTGCAAGAACGTACCATTTCTTTTAAGGA
CGACGGCACCTACAAAACCAGAGCGGAGGTTAAATTTGAAGGCGACACCTTGGTCAACCGTATC
GTGCTCAAGGGTATTGATTTTAAAGAGGATGGTAATATTCTGGGTCATAAGCTGGAATATAACT
TTAACAGCCACAAGGTGTATATCACTGCGGACAAACAGAAAAACGGCATCAAAGCAAATTTCAA
GACCCGTCATAACGTGGAGGACGGTGGCGTGCAGCTGGCGGATCACTACCAGCAAAACACCCCG
ATCGGCGACGGTCCGGTTCTGCTGCCGGATAACCATTACCTGAGCCATCAGAGCAAACTGAGCA
AAGATCCGAATGAAAAACGCGACCACATGGTTCTTAAGGAGCGCGTGACCGCGGCGGGTATCAC
GCATGATATGGATGAACTGTATAAGGGTGGTTCCGGCGGCAGCGGCGGAAGCCTGGCTGAAACC
GGTGGCGGCAGCGGTGGGTCCGGCGGCTCGTTACCGGAGTCAGGCGGCGGCTCCGGCGGCAGCG

GTGGTTCTCGTGGTGTCCCACATATTGTTATGGTTGATGCGTATAAGCGCTACAAGGGTGGCTC
CGGAGGTAGTGGTGGTTCTCACCATCACCACCACCAC

mGreenLantern – A ∨ T

MGSS-mGreenLantern-GGS(x3)-2A9c-GGS(x3)-TEVc-GGS(x3)-SpyTag003-GGS(x3)-6xHis

ATGGGGAGTTCTATGGTATCAAAAGGAGAAGAGCTGTTTACCGGTGTTGTTCCAATCTTGGTCG
AGCTGGATGGTGATGTAAATGGCCACAAGTTCAGCGTTCGTGGTGAAGGTGAAGGTGACGCGAC
CAACGGTAAATTGACCCTGAAGTTCATCTGCACCACGGGCAAACTGCCTGTTCCGTGGCCGACC
CTCGTGACCACGCTTGGCTACGGCGTGGCATGTTTTGCCCGTTACCCGGACCACATGAAACAGC
ATGACTTCTTTAAAAGCGCAATGCCGGAAGGCTACGTTCAGGAGAGAACAATTAGCTTTAAGGA
TGATGGCACCTATAAGACCCGTGCGGAAGTTAAATTCGAGGGCGACACCTTGGTGAACCGTATT
GTGTTAAAGGGCATCGATTTCAAAGAGGACGGTAATATTCTGGGTCATAAGTTGGAATATAACT
TTAACAGCCATAAGGTGTATATCACTGCCGATAAACAAAAAAACGGCATCAAAGCTAATTTCAA
GACGCGTCATAACGTTGAGGACGGTGGTGTGCAACTGGCGGACCACTACCAGCAAAACACCCCG
ATTGGTGACGGTCCGGTTCTGCTGCCGGATAATCATTACCTGAGCCACCAGAGCAAACTTAGCA
AGGACCCGAATGAAAAACGCGATCACATGGTCCTGAAAGAGCGCGTGACTGCGGCGGGTATCAC
CCATGACATGGACGAACTGTATAAGGGCGGTAGTGGCGGTTCTGGTGGTTCCCTGGCTGAGACG
GGTGGTGGCTCCGGCGGTTCCGGCGGTTCGGAAAACCTGTACTTCCAGAGCGGGGGTAGCGGTG
GCTCGGGGGGCTCTCGTGGTGTGCCGCATATTGTAATGGTCGATGCGTATAAGCGCTACAAGGG
TGGATCCGGCGGTTCTGGTGGCTCTCACCACCACCACCACCAC

mGreenLantern – S ∨ T

MGSS-mGreenLantern-GGS(x3)-TEVc-GGS(x3)-4S9c-GGS(x3)-SpyTag003-GGS(x3)-6xHis

ATGGGGTCAAGTATGGTAAGCAAAGGAGAAGAGCTGTTTACCGGTGTTGTCCCGATTCTGGTCG
AACTGGATGGCGACGTGAATGGTCATAAGTTCTCCGTGCGTGGTGAGGGCGAGGGTGACGCGAC
CAATGGCAAATTGACCCTTAAGTTCATCTGCACCACGGGTAAACTGCCAGTTCCGTGGCCTACA
TTGGTGACCACCCTGGGTTATGGCGTTGCGTGTTTTGCCCGTTACCCGGACCACATGAAACAGC
ACGACTTTTTCAAGAGCGCAATGCCGGAGGGTTATGTTCAAGAACGCACCATTAGCTTTAAGGA
TGACGGCACCTATAAGACGCGTGCTGAAGTTAAATTCGAAGGCGACACCTTGGTCAACCGTATT
GTTCTGAAAGGGATCGATTTCAAGGAGGATGGTAACATTCTTGGTCACAAATTGGAGTACAACT
TCAACAGCCACAAGGTGTATATCACGGCTGATAAACAAAAAAACGGTATTAAAGCCAATTTTAA
GACCCGTCATAACGTGGAGGACGGTGGCGTGCAGCTGGCAGACCATTACCAGCAAAACACCCCG
ATCGGCGACGGTCCGGTTCTGCTGCCGGATAATCATTACCTGTCCCATCAGAGCAAACTCAGCA
AGGATCCGAATGAAAAAAGAGATCACATGGTTCTGAAGGAGCGCGTGACTGCGGCGGGTATCAC
GCATGATATGGATGAATTATACAAAGGTGGCTCTGGTGGCTCAGGCGGCAGCGAAAACCTGTAC
TTCCAGAGCGGTGGTAGCGGCGGCTCTGGAGGCTCGCTGCCGGAAAGCGGCGGTGGTTCCGGCG
GATCCGGCGGTAGCCGTGGTGTGCCGCATATCGTAATGGTGGACGCGTATAAGCGCTACAAGGG
TGGTTCTGGAGGCTCGGGTGGTAGCCACCACCACCACCACCAC

mGreenLantern – A ∧ S

MGSS-CfaC-GGS(x3)-2A9c-GGS(x3)- mGreenLantern-GGS(x3)-4S9c-GGS(x3)-SpyTag003-GGS(x3)-6xHis-GGS(x3)-CfaN-SsrA

ATGGGAAGTTCAGTAAAAATTATAAGCAGGAAGTCCCTGGGCACCCAAAACGTTTATGACATCG
GCGTCGAGAAAGACCACAACTTCCTGCTGAAGAATGGTCTCGTGGCGAGCAACTGCTTTAACGG
TGGCTCCGGTGGATCGGGTGGTAGCCTGGCGGAGACGGGTGGTGGTTCTGGCGGTTCGGGGGGC
TCAATGGTAAGTAAGGGCGAGGAACTGTTTACCGGAGTCGTGCCGATCTTGGTCGAGCTGGACG
GCGATGTGAACGGCCATAAGTTCAGCGTTCGTGGTGAAGGTGAGGGCGACGCTACCAATGGTAA
GCTCACCTTGAAGTTCATCTGCACCACGGGTAAATTGCCAGTGCCGTGGCCTACCCTGGTGACC
ACCTTAGGCTACGGTGTTGCGTGTTTCGCGCGTTATCCGGACCACATGAAACAACATGACTTCT
TCAAGAGCGCCATGCCGGAAGGCTATGTTCAAGAGAGAACAATTAGCTTTAAGGACGACGGCAC
GTATAAAACCCGTGCGGAAGTTAAATTCGAGGGTGACACGTTGGTTAATCGTATCGTGCTGAAG
GGTATTGATTTTAAAGAGGATGGAAACATCCTGGGTCATAAACTGGAGTACAATTTCAACAGCC
ATAAGGTGTACATTACGGCCGATAAACAAAAAAACGGCATTAAAGCCAACTTCAAGACCCGTCA
CAATGTTGAAGACGGCGGTGTGCAACTGGCCGATCACTACCAGCAGAACACCCCGATCGGCGAC
GGTCCGGTTTTGCTGCCGGATAATCATTACCTGAGCCACCAGAGCAAATTAAGCAAGGACCCGA
ATGAAAAACGTGATCACATGGTTCTCAAAGAGCGCGTGACTGCGGCGGGTATCACCCATGACAT
GGATGAGCTTTACAAAGGTGGTTCGGGGGGCAGCGGTGGTAGCCTGCCAGAAAGCGGCGGCGGT
AGCGGCGGTTCTGGAGGGAGCCGTGGTGTTCCGCATATCGTGATGGTGGACGCTTACAAGCGCT
ATAAAGGTGGCTCCGGTGGTTCAGGTGGTTCTCACCACCACCACCACCACGGCGGTTCTGGCGG
CTCCGGCGGTAGCGCTGAGTATTGCTTGTCCTATGACACCGAAATTCTGACCGTGGAGTACGGT
TTTCTGCCGATTGGTAAGATCGTTGAGGAACGCATTGAATGTACGGTGTACACTGTCGACAAAA
ACGGTTTTGTTTACACCCAGCCGATTGCGCAGTGGCATAATCGTGGTGAACAGGAGGTCTTTGA
ATACTGCCTGGAAGATGGCAGCATTATCCGCGCAACCAAAGACCACAAATTCATGACGACCGAT
GGTCAGATGCTGCCGATCGATGAGATCTTTGAACGTGGTCTGGATCTGAAGCAGGTTGATGGCT
TGCCGGCAGCGAACGATGAAAACTATGCACTGGCTGCG

mGreenLantern – A ∧ T

MGSS-CfaC-GGS(x3)-2A9c-GGS(x3)- mGreenLantern-GGS(x3)-TEVc-GGS(x3)-SpyTag003-GGS(x3)-6xHis-GGS(x3)-CfaN-SsrA

ATGGGAAGTTCAGTAAAAATTATAAGCAGGAAAAGCCTGGGCACCCAGAACGTCTACGACATCG
GTGTGGAAAAAGACCACAACTTCCTGCTCAAGAACGGCTTGGTAGCCAGCAATTGTTTTAATGG
TGGTAGCGGTGGTTCGGGTGGCTCCCTGGCGGAAACCGGCGGTGGTTCTGGTGGCAGCGGCGGA
AGCATGGTCAGCAAGGGTGAGGAACTCTTCACCGGTGTGGTTCCGATCCTGGTCGAGCTGGACG
GCGACGTTAACGGCCACAAGTTCAGCGTTCGTGGTGAGGGCGAAGGTGACGCCACCAATGGTAA
GTTGACCCTAAAGTTCATCTGTACCACGGGAAAGCTGCCGGTGCCGTGGCCTACTTTGGTTACC
ACCCTGGGGTACGGCGTGGCGTGCTTTGCACGTTACCCGGATCACATGAAACAACACGATTTTT
TTAAAAGCGCTATGCCGGAAGGTTACGTGCAAGAGCGTACCATCAGCTTTAAGGATGATGGCAC
CTATAAAACCCGTGCCGAAGTGAAATTCGAGGGCGACACCCTGGTTAATCGTATCGTGTTAAAG
GGCATCGATTTCAAGGAGGACGGTAATATTCTGGGTCATAAATTGGAGTATAACTTCAACAGCC
ATAAAGTTTACATTACCGCAGATAAACAGAAAAACGGCATCAAAGCTAATTTCAAGACTCGCCA
TAACGTGGAGGACGGTGGTGTCCAACTGGCGGATCACTACCAGCAAAACACCCCGATCGGCGAT

GGACCGGTTCTTCTGCCGGACAACCATTATCTGAGTCACCAGTCGAAGTTGAGCAAGGATCCGA
ATGAAAAGCGCGATCACATGGTGCTGAAAGAACGTGTTACGGCTGCTGGTATTACACATGATAT
GGATGAGTTGTACAAGGGTGGCTCCGGCGGTTCTGGTGGTTCGGAAAATCTGTACTTCCAGAGC
GGGGGCTCTGGCGGGTCCGGTGGCAGCCGTGGTGTGCCGCATATTGTGATGGTGGACGCGTATA
AACGTTATAAGGGTGGCTCTGGCGGATCCGGTGGTTCCCATCACCATCACCACCACGGCGGCTC
CGGCGGCTCTGGTGGTTCTGCGGAGTACTGCCTGAGCTATGACACGGAAATTCTGACGGTAGAG
TATGGTTTTCTGCCGATTGGCAAGATCGTTGAGGAACGCATCGAGTGCACGGTTTACACCGTGG
ACAAGAACGGCTTTGTTTATACGCAACCGATTGCGCAGTGGCATAACCGCGGTGAACAAGAAGT
TTTTGAATACTGCTTGGAGGACGGTAGCATTATTCGTGCAACTAAAGACCACAAATTCATGACC
ACCGATGGTCAGATGCTGCCAATCGACGAAATCTTTGAAAGAGGTCTGGACCTGAAACAGGTTG
ATGGCCTGCCAGCAGCGAACGATGAGAACTATGCGCTGGCGGCG

mGreenLantern – S ∧ T

MGSS-CfaC-GGS(x3)-TEVc-GGS(x3)- mGreenLantern-GGS(x3)-4S9c-GGS(x3)-SpyTag003-GGS(x3)-6xHis-GGS(x3)-CfaN-SsrA

ATGGGATCAAGTGTAAAAATTATATCTAGGAAGAGCCTAGGTACCCAAAACGTTTACGATATTG
GTGTGGAAAAAGACCACAACTTTCTGCTTAAGAACGGCCTGGTCGCGAGCAATTGCTTTAATGG
AGGTTCTGGTGGTAGTGGTGGCTCGGAAAATCTGTACTTCCAGAGCGGCGGCTCCGGCGGTAGC
GGCGGTAGCATGGTCAGCAAGGGTGAAGAATTGTTTACCGGTGTTGTACCAATCTTGGTCGAAC
TCGATGGTGATGTTAACGGTCACAAGTTCTCTGTTCGTGGTGAGGGCGAAGGCGATGCGACTAA
CGGTAAGCTGACCTTGAAGTTCATCTGCACGACTGGTAAATTACCGGTTCCATGGCCGACCCTG
GTGACCACGCTGGGCTACGGCGTGGCCTGTTTCGCCCGTTATCCGGATCACATGAAACAGCATG
ACTTTTTTAAATCCGCTATGCCGGAGGGCTACGTGCAAGAGCGCACCATTAGCTTTAAGGACGA
CGGCACCTATAAGACCCGTGCTGAAGTGAAATTCGAGGGCGACACCCTGGTGAACCGCATCGTT
TTGAAGGGCATCGACTTCAAAGAAGACGGTAATATCCTGGGTCACAAACTCGAATACAACTTCA
ACAGCCATAAAGTCTATATTACCGCAGATAAACAAAAAAACGGCATCAAAGCGAACTTCAAGAC
CCGCCATAACGTTGAGGATGGCGGTGTGCAGCTGGCGGATCACTACCAGCAAAACACCCCGATC
GGTGACGGTCCGGTTCTGTTGCCGGACAATCATTACCTGAGCCACCAAAGCAAGTTAAGCAAAG
ACCCGAATGAAAAGCGTGACCACATGGTTCTTAAAGAAAGAGTGACGGCTGCGGGTATTACCCA
TGATATGGATGAGCTGTATAAAGGTGGGTCGGGGGGGGTCCGGTGGCTCCCTGCCGGAGAGCGGT
GGTGGCTCTGGCGGTTCTGGAGGTAGCCGTGGTGTTCCGCATATCGTGATGGTGGATGCCTACA
AGCGTTACAAAGGTGGCAGTGGCGGTTCTGGCGGTTCGCACCATCACCACCATCACGGCGGTAG
CGGTGGTAGCGGTGGTTCAGCGGAATATTGTCTGTCCTATGACACGGAGATCTTGACCGTTGAG
TATGGGTTTCTGCCGATTGGCAAGATCGTCGAGGAGCGTATCGAATGCACCGTGTACACTGTAG
ACAAGAACGGCTTCGTGTATACGCAACCGATCGCGCAGTGGCATAATCGTGGCGAGCAGGAGGT
GTTTGAGTACTGCCTGGAAGATGGCAGCATTATTCGTGCAACGAAAGACCACAAATTCATGACC
ACCGATGGGCAGATGCTGCCTATTGATGAGATTTTCGAACGCGGCTTAGACCTGAAGCAGGTTG
ACGGCTTGCCGGCAGCGAATGATGAGAACTATGCACTGGCTGCG

mGreenLantern – (A ∨ S) ∧ T

MGSS-CfaC-GGS(x3)-2A9c-GGS(x3)-4S9c-GGS(x3)-mGreenLantern-GGS(x3)-TEVc-GGS(x3)- SpyTag003-GGS(x3)-6xHis-GGS(x3)-CfaN-SsrA

ATGGGAAGTTCAGTAAAAATTATAAGCAGGAAGAGCCTGGGTACGCAAAACGTGTACGACATCG
GCGTGGAGAAGGACCACAACTTTCTGTTGAAGAACGGCCTGGTTGCGAGCAACTGCTTCAATGG
CGGCTCCGGTGGATCCGGGGGGTCCCTTGCCGAAACGGGTGGTGGCTCGGGTGGTAGCGGCGGC
TCCTTGCCGGAGAGCGGTGGCGGAAGTGGTGGCAGCGGTGGCTCTATGGTGAGCAAAGGTGAAG
AGTTGTTTACTGGTGTCGTGCCGATATTGGTCGAGCTGGACGGTGACGTAAATGGCCATAAATT
CAGCGTTCGTGGCGAAGGTGAAGGTGACGCCACCAATGGTAAACTGACGTTGAAGTTCATCTGC
ACCACCGGTAAGTTGCCAGTTCCGTGGCCGACCCTGGTTACCACTTTGGGTTATGGCGTTGCGT
GCTTTGCGCGTTATCCGGATCACATGAAACAGCATGATTTTTTTAAAAGCGCAATGCCGGAAGG
CTACGTGCAAGAGCGCACCATCAGTTTTAAGGACGATGGTACATATAAAACCCGTGCAGAAGTG
AAATTCGAAGGTGACACCCTCGTGAACCGCATCGTTCTCAAGGGCATCGACTTCAAAGAGGACG
GCAACATTCTCGGCCACAAGTTGGAATACAATTTCAACAGCCACAAAGTTTACATCACCGCTGA
CAAACAAAAAAACGGGATTAAAGCAAACTTCAAGACCCGTCATAATGTCGAGGACGGTGGTGTG
CAGCTGGCGGACCACTACCAACAAAACACCCCGATTGGCGACGGCCCGGTTCTGTTGCCGGATA
ATCATTACCTGTCCCACCAGAGCAAACTGAGCAAAGATCCGAATGAAAAACGTGATCACATGGT
TCTGAAAGAACGTGTAACTGCGGCCGGTATCACGCATGACATGGATGAACTGTACAAGGGTGGC
AGCGGTGGTTCTGGCGGTTCTGAAAACCTGTACTTCCAGAGCGGCGGCAGCGGCGGCTCCGGTG
GCAGCCGTGGCGTGCCGCATATTGTTATGGTCGACGCGTATAAGCGCTACAAGGGCGGTTCTGG
TGGTTCGGGTGGCTCACATCACCACCACCACCATGGTGGCAGTGGTGGCTCGGGCGGTTCTGCG
GAGTATTGTCTGAGCTATGATACCGAAATCCTGACCGTTGAATATGGTTTCCTGCCAATCGGTA
AGATCGTGGAGGAGCGCATTGAATGTACGGTGTACACCGTTGATAAAAACGGCTTCGTGTATAC
CCAGCCGATTGCTCAGTGGCATAACCGTGGTGAGCAGGAGGTGTTTGAGTACTGCCTTGAGGAC
GGTAGCATTATTCGTGCGACCAAAGACCACAAGTTCATGACCACCGATGGTCAGATGCTGCCGA
TTGATGAGATCTTTGAAAGAGGTCTGGATCTGAAGCAAGTTGATGGCCTGCCGGCAGCTAATGA
TGAGAACTATGCGCTGGCTGCG

mGreenLantern – (A ∨ T) ∧ S

MGSS-CfaC-GGS(x3)-2A9c-GGS(x3)-TEVc-GGS(x3)-mGreenLantern-GGS(x3)-4S9c-GGS(x3)- SpyTag003-GGS(x3)-6xHis-GGS(x3)-CfaN-SsrA

ATGGGAAGTTCAGTAAAAATTATAAGCAGGAAGAGCCTTGGTACACAGAACGTCTACGACATCG
GTGTAGAGAAAGACCACAACTTCCTGCTGAAGAACGGACTGGTGGCCAGCAATTGTTTTAATGG
TGGCTCTGGCGGTTCCGGCGGCAGCCTGGCGGAAACCGGTGGTGGGTCTGGCGGATCCGGCGGA
TCGGAAAACCTGTATTTCCAGAGCGGAGGCAGTGGTGGTAGCGGCGGTTCGATGGTTAGCAAAG
GCGAGGAACTGTTCACCGGTGTCGTGCCGATTCTGGTTGAGCTCGACGGCGACGTTAACGGTCA
TAAGTTCAGCGTTCGTGGTGAGGGTGAGGGTGACGCAACCAATGGCAAGTTGACCCTGAAGTTC
ATCTGCACCACTGGTAAACTGCCGGTTCCGTGGCCGACCTTGGTAACTACGCTGGGCTATGGTG
TAGCCTGCTTTGCCCGTTACCCGGATCACATGAAACAACATGATTTCTTTAAATCCGCTATGCC
GGAAGGTTACGTGCAAGAGCGCACCATTAGCTTTAAGGACGATGGTACGTATAAAACGCGTGCG
GAAGTGAAATTCGAGGGCGACACCCTGGTCAACCGTATTGTTTTAAAGGGCATCGACTTCAAGG

AGGACGGTAATATTTTGGGTCATAAACTGGAGTACAATTTCAACAGCCACAAAGTTTATATTAC
GGCTGATAAACAAAAAAACGGCATCAAAGCCAACTTTAAAACCCGCCATAACGTCGAGGACGGC
GGCGTGCAGTTGGCTGATCACTACCAGCAAAACACCCCGATTGGCGACGGTCCGGTTTTGCTGC
CGGACAATCATTATCTGAGCCATCAGAGCAAGCTCTCCAAGGATCCGAATGAAAAGCGTGATCA
CATGGTGCTTAAGGAGCGTGTTACCGCAGCGGGTATCACGCACGATATGGATGAATTGTACAAA
GGCGGAAGCGGCGGATCCGGTGGCTCTCTCCCAGAAAGCGGCGGTGGTTCTGGCGGCTCCGGCG
GTAGCCGTGGTGTTCCACATATTGTGATGGTGGATGCGTATAAACGTTACAAGGGTGGTAGTGG
CGGTTCTGGTGGCTCGCACCACCATCACCACCACGGTGGTTCCGGCGGCTCTGGTGGTTCAGCG
GAGTATTGCCTGAGCTATGACACCGAAATCTTGACCGTTGAATACGGCTTCCTGCCGATTGGTA
AAATCGTGGAAGAGAGAATCGAATGTACCGTGTACACCGTTGATAAAAACGGCTTTGTCTACAC
TCAACCGATAGCGCAGTGGCATAACCGTGGTGAGCAGGAGGTGTTTGAATACTGCTTAGAGGAC
GGTAGCATTATCCGCGCGACCAAGGACCACAAGTTCATGACCACGGATGGTCAGATGCTGCCGA
TCGATGAGATCTTTGAACGCGGTCTGGATCTGAAGCAAGTTGACGGCCTGCCTGCAGCTAATGA
TGAGAACTATGCGCTGGCGGCA

mGreenLantern – (S ∨ T) ∧ A
MGSS-CfaC-GGS(x3)-4S9c-GGS(x3)-TEVc-GGS(x3)-mGreenLantern-GGS(x3)-2A9c-
GGS(x3)- SpyTag003-GGS(x3)-6xHis-GGS(x3)-CfaN-SsrA

ATGGGAAGTTCAGTAAAAATTATATCTAGGAAGAGCCTCGGTACACAAAACGTGTACGACATCG
GTGTGGAGAAAGACCACAACTTCCTGCTGAAAAACGGCCTGGTCGCCAGCAACTGCTTCAACGG
TGGCTCGGGCGGCTCTGGCGGGTCTCTGCCGGAAAGCGGTGGTGGTTCTGGCGGCTCAGGCGGC
TCAGAAAACCTGTACTTCCAGAGCGGTGGCTCCGGCGGTTCTGGTGGCTCCATGGTGTCCAAGG
GTGAAGAATTGTTTACCGGTGTGGTGCCGATCCTGGTTGAGTTGGACGGCGATGTTAATGGTCA
TAAGTTCAGCGTGCGTGGTGAGGGCGAGGGTGACGCCACCAACGGTAAATTGACCTTGAAGTTC
ATCTGCACGACTGGTAAGCTGCCAGTGCCGTGGCCGACCTTAGTTACCACGTTAGGTTATGGTG
TGGCGTGTTTCGCCCGTTATCCGGACCACATGAAACAGCATGATTTTTTCAAAAGCGCAATGCC
GGAAGGTTATGTTCAAGAGCGCACGATTAGCTTTAAGGATGATGGCACGTACAAGACTCGTGCA
GAGGTGAAATTCGAGGGAGACACCCTGGTCAACCGCATCGTGCTTAAGGGCATTGACTTCAAAG
AGGACGGAAACATTCTTGGCCACAAGTTGGAATACAATTTTAACAGCCATAAGGTGTACATTAC
CGCGGATAAACAAAAAAATGGCATCAAAGCGAATTTCAAGACCCGTCATAATGTTGAAGATGGT
GGTGTGCAGCTGGCGGACCACTACCAGCAGAATACCCCGATCGGCGATGGTCCGGTCTTGCTGC
CGGATAATCATTATCTGAGTCACCAGAGCAAACTGAGCAAGGACCCGAATGAAAAACGCGATCA
CATGGTTCTGAAAGAACGTGTTACCGCAGCTGGTATCACCCATGATATGGATGAATTGTACAAG
GGAGGCAGCGGGGGTAGCGGTGGTTCCCTCGCGGAGACCGGTGGGGGAAGCGGTGGCAGCGGCG
GCTCTCGTGGCGTACCGCATATTGTGATGGTTGACGCGTATAAACGTTATAAAGGCGGTTCGGG
CGGCTCGGGCGGGAGCCACCACCACCACCACCATGGTGGTTCTGGTGGCTCCGGTGGTAGCGCT
GAATACTGCCTGAGCTATGATACCGAGATTTTAACGGTCGAGTACGGCTTTCTGCCGATCGGTA
AGATCGTTGAAGAGCGCATTGAATGCACCGTGTACACGGTTGATAAGAACGGCTTTGTTTACAC
CCAACCGATTGCACAGTGGCATAACCGCGGTGAGCAAGAAGTTTTTGAGTATTGTCTGGAAGAC
GGTTCCATAATTCGTGCGACCAAAGACCACAAGTTCATGACCACCGATGGTCAGATGCTGCCAA
TCGACGAGATCTTTGAGAGAGGCCTGGACCTGAAACAAGTTGACGGGCTGCCTGCAGCGAACGA
TGAGAACTATGCTCTGGCTGCG

mGreenLantern – (A ∧ S) ∨ T

MGSS-SnoopTag-GGS(x3)-2A9c-GGS(x3)-mGreenLantern-GGS(x3)-4S9c-GGS(x3)-SnoopCatcher- GGS(x3)-TEVc-GGS(x3)-SpyTag-GGS(x3)LE-6xHis

ATGGGATCAAGTAAACTAGGGGATATAGAATTCATTAAAGTTAACAAAGGTGGCTCCGGCGGTT
CAGGTGGCTCGCTGGCGGAAACCGGCGGCGGTTCCGGCGGTTCTGGCGGGTCTATGGTCAGCAA
GGGCGAGGAACTCTTCACCGGTGTGGTGCCAATCTTGGTGGAACTGGATGGCGACGTTAATGGT
CACAAGTTCAGCGTTCGCGGTGAGGGTGAGGGTGACGCGACCAACGGCAAGCTTACCCTGAAGT
TCATCTGCACCACCGGTAAATTACCGGTTCCGTGGCCGACGTTGGTTACAACCCTCGGTTACGG
CGTAGCATGTTTTGCGCGTTATCCAGACCACATGAAACAGCACGATTTCTTTAAGTCTGCTATG
CCGGAGGGTTATGTTCAAGAGCGCACCATTTCGTTCAAGGATGATGGCACGTACAAGACTCGCG
CAGAAGTGAAATTCGAGGGCGACACCCTGGTGAACCGTATCGTGCTGAAGGGTATCGACTTCAA
AGAGGACGGAAACATTCTGGGCCACAAACTGGAATATAACTTTAACAGCCACAAGGTGTATATC
ACCGCGGATAAACAAAAGAACGGCATCAAAGCTAATTTTAAAACGCGTCATAACGTGGAAGACG
GCGGCGTGCAACTGGCCGACCATTACCAGCAGAATACCCCGATCGGCGACGGTCCGGTGTTGCT
GCCGGATAATCACTACCTGAGCCATCAGAGCAAGTTGTCCAAGGACCCGAATGAAAAACGTGAT
CACATGGTGTTAAAAGAACGTGTTACTGCGGCAGGTATCACCCATGACATGGATGAACTGTACA
AGGGTGGTTCCGGTGGTAGCGGCGGTAGCCTGCCGGAGAGCGGTGGCGGTTCTGGCGGTTCAGG
TGGTAGCAAGCCGCTGCGTGGTGCCGTTTTTAGCCTGCAGAAACAACATCCGGACTATCCCGAC
ATCTATGGTGCGATTGATCAGAACGGCACCTACCAAAATGTTCGCACCGGTGAAGACGGTAAGT
TGACCTTTAAAAATCTGAGCGATGGTAAATACCGTCTGTTTGAGAACTCGGAGCCGGCTGGTTA
CAAGCCGGTCCAGAACAAGCCGATTGTCGCGTTTCAGATTGTCAACGGTGAGGTTAGAGATGTA
ACCAGCATTGTTCCGCAGGATATCCCGGCGACGTACGAATTTACCAATGGTAAGCACTACATTA
CGAACGAACCGATCCCGCCTAAAGGCGGCTCCGGGGGCAGCGGCGGTAGCGAGAACTTGTATTT
CCAAAGCGGCGGCTCCGGAGGCAGTGGTGGCAGTGCGCATATTGTTATGGTTGATGCCTATAAG
CCGACCAAAGGCGGTTCTGGTGGTTCGGGTGGTTCCCTCGAGCACCACCACCACCACCAC

mGreenLantern – (A ∧ T) ∨ S

MGSS-SnoopTag-GGS(x3)-2A9c-GGS(x3)-mGreenLantern-GGS(x3)- TEVc-GGS(x3)-SnoopCatcher- GGS(x3)-4S9c-GGS(x3)-SpyTag-GGS(x3)LE-6xHis

ATGGGAAGTTCAAAACTAGGGGATATAGAATTCATCAAAGTGAACAAAGGTGGCTCAGGCGGCT
CTGGCGGTAGCTTGGCGGAAACCGGTGGTGGTAGTGGCGGCAGCGGAGGCAGCATGGTTAGCAA
GGGTGAGGAACTGTTCACCGGCGTTGTTCCGATCCTGGTCGAGCTGGATGGCGACGTTAACGGT
CATAAGTTCAGCGTTAGAGGTGAAGGCGAGGGCGACGCGACGAACGGCAAGTTGACCCTGAAGT
TCATCTGCACCACGGGTAAGCTTCCGGTGCCGTGGCCTACCCTGGTGACCACGCTGGGTTACGG
GGTGGCGTGTTTTGCACGTTATCCGGATCACATGAAACAACACGACTTCTTCAAGTCAGCTATG
CCGGAAGGTTATGTTCAAGAACGTACCATTAGCTTTAAGGACGACGGTACCTACAAGACCCGCG
CGGAAGTGAAATTCGAGGGTGACACCTTGGTTAACCGTATTGTGCTGAAGGGGATCGACTTTAA
GGAGGACGGGAATATTTTAGGCCACAAATTGGAATATAACTTCAACAGCCACAAAGTGTATATC
ACTGCTGACAAACAGAAAAACGGGATCAAAGCTAATTTCAAGACGCGTCATAACGTGGAGGATG
GTGGTGTTCAGCTCGCGGATCACTACCAACAGAACACCCCGATCGGTGATGGTCCGGTCCTGCT

GCCGGACAATCATTACCTGTCCCACCAGAGCAAATTAAGCAAAGATCCGAATGAGAAACGTGAC
CACATGGTACTGAAGGAGCGCGTGACTGCGGCAGGCATTACGCATGATATGGATGAACTCTACA
AGGGCGGTAGCGGTGGTAGTGGCGGTTCCGAAAACCTGTATTTCCAAAGCGGTGGTTCCGGCGG
TTCGGGCGGCAGCAAGCCGCTGCGTGGTGCAGTTTTTTCTCTGCAGAAACAACATCCGGACTAC
CCGGACATCTATGGTGCCATTGATCAGAATGGTACATACCAGAACGTACGCACCGGTGAGGACG
GCAAACTTACCTTTAAGAATCTGTCTGATGGCAAGTACCGCCTGTTTGAGAATAGCGAACCGGC
GGGTTACAAACCGGTCCAAAACAAACCGATCGTGGCCTTTCAAATTGTGAATGGCGAGGTTCGT
GATGTTACCAGCATTGTGCCACAGGATATCCCGGCTACCTATGAATTTACCAACGGTAAGCATT
ACATCACGAACGAGCCGATTCCGCCTAAAGGTGGTTCTGGAGGTTCCGGCGGTTCATTGCCAGA
AAGCGGCGGTGGCTCTGGCGGTTCGGGCGGCAGCGCGCACATTGTCATGGTTGATGCATATAAG
CCGACCAAAGGTGGCAGCGGGGGTTCCGGGGGTTCGCTCGAGCACCACCACCACCACCAC

mGreenLantern – (S ∧ T) ∨ A
MGSS-SnoopTag-GGS(x3)-4S9c-GGS(x3)-mGreenLantern-GGS(x3)-TEVc-GGS(x3)-
SnoopCatcher-GGS(x3)-2A9c-GGS(x3)-SpyTag-GGS(x3)LE-6xHis

ATGGGAAGTTCAAAACTAGGGGATATAGAATTCATTAAGGTTAACAAAGGCGGTTCTGGCGGTT
CCGGTGGCAGCCTGCCGGAGAGCGGCGGTGGCTCGGGTGGAAGCGGCGGCTCCATGGTCAGCAA
GGGTGAGGAATTGTTCACCGGTGTCGTACCAATCCTGGTTGAATTAGATGGCGACGTTAACGGC
CACAAGTTCTCCGTGCGCGGTGAGGGTGAGGGTGACGCGACCAACGGCAAATTGACCCTCAAAT
TCATCTGTACCACCGGTAAACTGCCGGTCCCGTGGCCAACTTTGGTGACGACCCTGGGTTATGG
TGTGGCCTGCTTTGCACGTTATCCGGACCACATGAAACAACACGACTTCTTTAAAAGCGCTATG
CCGGAAGGCTATGTTCAAGAGCGCACCATTAGCTTTAAAGATGATGGTACGTACAAGACTCGCG
CAGAAGTTAAATTCGAGGGCGATACCTTGGTGAACCGTATTGTGCTGAAAGGCATCGACTTTAA
AGAGGACGGTAATATTCTGGGTCACAAACTGGAATATAACTTTAATAGCCATAAGGTGTATATC
ACTGCGGACAAACAAAAAAACGGCATTAAAGCTAATTTCAAGACCCGTCATAATGTTGAGGACG
GTGGCGTGCAACTGGCCGATCACTACCAGCAGAACACCCCGATTGGTGACGGCCCGGTTCTCCT
GCCGGATAATCATTACCTGAGCCACCAGAGCAAATTAAGCAAGGACCCGAATGAAAAACGTGAC
CACATGGTCCTGAAAGAACGTGTCACCGCGGCTGGTATCACGCATGATATGGATGAACTGTATA
AGGGTGGCTCAGGCGGCTCAGGTGGCTCCGAGAACCTGTACTTCCAAAGCGGCGGCTCCGGCGG
CTCTGGGGGTTCCAAACCGCTGCGTGGTGCAGTTTTTAGCCTTCAGAAGCAACATCCGGACTAC
CCGGACATCTATGGTGCGATCGATCAGAACGGTACATACCAGAATGTTCGTACCGGCGAGGATG
GTAAGTTGACCTTCAAGAACCTGAGCGATGGTAAGTACCGCCTGTTTGAAAATAGCGAACCGGC
TGGTTACAAGCCGGTGCAAAACAAGCCAATCGTTGCGTTTCAGATTGTCAACGGTGAGGTGAGA
GACGTGACCAGCATTGTTCCGCAGGATATCCCGGCGACCTACGAATTCACCAATGGCAAGCACT
ACATCACGAACGAGCCGATCCCGCCTAAAGGTGGCTCTGGCGGCTCTGGAGGTTCGTTGGCGGA
AACCGGTGGTGGTTCGGGCGGTTCTGGTGGCTCTGCGCATATTGTGATGGTCGATGCGTATAAG
CCGACGAAGGGTGGATCCGGCGGCAGCGGTGGTTCCCTCGAGCACCACCACCACCACCAC

mGreenLantern – A ∨ S ∨ T
MGSS-mGreenLantern-GGS(x3)-2A9c-GGS(x3)-4S9c-GGS(x3)-TEVc-GGS(x3)-SpyTag003-
GGS(x3)-6xHis

ATGGGGTCATCTATGGTAAGTAAAGGAGAAGAGTTGTTTACGGGTGTCGTGCCGATTTTGGTCG
AGCTTGATGGTGACGTGAACGGTCATAAGTTCAGCGTTCGTGGTGAAGGTGAAGGCGACGCTAC

CAATGGTAAACTGACCTTGAAGTTCATCTGCACCACGGGTAAGTTGCCAGTACCGTGGCCGACC
TTGGTCACCACGTTAGGTTATGGTGTGGCGTGTTTTGCCCGTTACCCGGACCACATGAAACAAC
ATGATTTTTTTAAAAGCGCAATGCCGGAAGGTTATGTTCAAGAGCGCACCATTAGCTTTAAGGA
CGATGGCACCTATAAGACTCGCGCAGAGGTGAAATTCGAGGGCGACACCCTCGTTAATCGTATT
GTTCTGAAGGGTATCGATTTCAAGGAGGACGGTAATATTCTGGGTCATAAACTGGAATATAACT
TCAACAGCCACAAGGTGTATATCACAGCCGATAAACAAAAAAACGGCATCAAAGCGAATTTTAA
GACCCGTCATAACGTTGAGGACGGTGGGGTGCAGCTGGCTGACCACTACCAGCAAAACACCCCG
ATCGGTGACGGCCCCGTACTGCTGCCGGACAACCACTACCTGAGCCACCAGAGCAAACTGAGCA
AGGACCCGAATGAAAAACGTGATCACATGGTTCTGAAAGAGCGTGTTACTGCGGCAGGTATTAC
CCATGATATGGATGAACTGTACAAGGGTGGCAGTGGCGGTTCAGGAGGCTCGCTGGCGGAAACC
GGTGGCGGATCCGGCGGTTCTGGCGGGTCGCTGCCGGAGAGCGGTGGCGGCTCCGGGGGCTCTG
GCGGTAGCGAAAACCTGTACTTCCAGAGCGGCGGTTCCGGTGGCTCCGGCGGTTCTAGAGGCGT
GCCGCATATCGTGATGGTTGATGCGTACAAGCGCTACAAAGGTGGCAGCGGTGGCTCTGGCGGC
AGCCACCACCATCACCACCAT

<u>mGreenLantern – A ∧ S ∧ T</u>

MGSS-SnoopTag-GGS(x10)-4S9c-GGS(x10)-DogCatcher-GGS(x10)-SpyTag-GGS(x5)-2A9c-GGS(x5)-mGreenLantern-GGS(x10)-SnoopCatcher-GGS(x10)-TEVc-GGS(x5)-6xHis-GGS(x10)-DogTag

ATGGGAAGTTCAAAACTAGGGGATATAGAATTCATCAAAGTTAACAAGGGTGGTTCGGGAGGTA
GCGGGGGTAGTGGCGGAAGCGGCGGCTCAGGCGGTTCCGGCGGTAGCGGTGGATCTGGTGGTAG
CGGCGGTTCCCTGCCCGAGAGCGGTGGTGGCAGCGGCGGTAGCGGCGGCAGCGGAGGCTCTGGC
GGGTCGGGTGGCTCGGGCGGGTCTGGTGGCAGCGGTGGGAGTGGTGGTAGCAAATTAGGCGAGA
TCGAATTCATCAAGGTGGATAAAACCGATAAAAAACCGCTGCGCGGTGCGGTGTTTAGCCTGCA
GAAGCAACACCCGGATTACCCGGACATCTACGGTGCGATTGACCAGAATGGGACGTACCAGGAT
GTGCGCACTGGTGAGGACGGCAAGTTGACCTTTACCAACCTGTCCGACGGAAAGTATCGTCTTA
TCGAGAACAGCGAGCCGCCGGGTTATAAGCCGGTTCAAAACAAACCAATCGTTAGCTTTCGTAT
TGTGGATGGTGAGGTGCGCGACGTGACCTCGATCGTACCGCAGGGTGGGTCGGGCGGTTCCGGG
GGTAGCGGCGGATCTGGCGGTTCCGGTGGCTCCGGTGGTAGTGGTGGCAGCGGCGGCTCCGGTG
GTTCTGCACATATTGTCATGGTGGACGCATATAAACCGACCAAAGGCGGTAGCGGCGGCTCAGG
GGGTTCTGGGGGTAGCGGCGGATCCCTGGCGGAAACCGGCGGTGGTAGCGGTGGTTCCGGAGGT
TCCGGCGGCAGCGGCGGCTCGATGGTCAGCAAGGGCGAGGAACTGTTTACCGGTGTCGTGCCAA
TCCTGGTGGAACTGGATGGGGACGTGAACGGTCATAAGTTCAGCGTTCGTGGTGAAGGTGAGGG
TGACGCCACAAATGGCAAATTGACCCTCAAGTTTATTTGTACCACCGGCAAGTTACCGGTTCCG
TGGCCGACGTTGGTTACTACGCTGGGTTACGGCGTGGCGTGCTTCGCGCGTTATCCGGACCACA
TGAAACAGCATGATTTCTTTAAAAGCGCTATGCCGGAAGGTTACGTTCAAGAGCGTACCATCAG
CTTTAAGGATGATGGCACCTACAAGACGCGTGCAGAAGTTAAATTCGAAGGCGATACCTTGGTT
AATCGTATCGTTCTGAAGGGCATTGACTTTAAGGAAGACGGCAATATCTTGGGCCACAAACTGG
AATATAACTTCAACAGCCACAAGGTGTACATCACCGCTGACAAACAAAAAAACGGCATCAAAGC
GAACTTCAAGACGCGACATAATGTCGAAGATGGGGGTGTGCAGCTGGCCGATCACTACCAACAG
AACACTCCGATTGGCGACGGTCCGGTTCTCCTCCCGGACAATCACTACCTGTCTCATCAGAGCA
AGCTGTCCAAGGATCCGAATGAAAAACGTGACCACATGGTTCTGAAAGAACGTGTTACTGCTGC
GGGTATTACGCATGATATGGATGAACTGTACAAAGGTGGCTCCGGTGGTTCGGGCGGTTCTGGT
GGCAGCGGTGGTAGCGGGGGGAGCGGAGGCTCCGGTGGTTCCGGCGGCTCGGGCGGTTCCAAGC
CGCTGCGTGGTGCGGTTTTTAGCTTGCAAAAGCAACATCCGGATTATCCGGACATCTATGGTGC

GATCGACCAGAACGGAACCTACCAAAACGTGCGCACCGGCGAGGACGGCAAGTTGACCTTCAAG
AACTTGTCTGATGGAAAGTACCGCCTGTTCGAGAATTCTGAGCCTGCTGGTTACAAACCGGTGC
AAAACAAACCGATTGTGGCATTTCAGATTGTTAATGGTGAGGTCAGAGATGTCACCTCCATTGT
TCCACAGGATATTCCGGCCACCTACGAATTCACCAACGGAAAGCACTATATCACGAACGAACCG
ATTCCGCCGAAAGGTGGCAGTGGTGGTTCTGGCGGTAGCGGCGGCAGCGGAGGCTCCGGGGGTA
GCGGTGGTTCCGGCGGCAGCGGCGGCTCTGGAGGGAGTGAGAACCTGTATTTCCAGTCTGGCGG
CTCCGGTGGCTCTGGCGGCAGCGGTGGTTCGGGTGGTTCCCACCACCATCACCACCATGGTGGC
AGCGGCGGCTCTGGTGGCAGCGGAGGTAGTGGGGGTTCCGGTGGTTCCGGTGGGTCAGGTGGAT
CTGGCGGCTCGGGCGGAAGCGACATTCCGGCGACCTACGAGTTCACCGATGGTAAGCACTATAT
CACCAATGAGCCGATCCCGCCAAAA

Method S5.4 LC-MS collection protocol

Protein identity and purity was confirmed through Liquid Chromatography-Mass Spectrometry (LC-MS). Each sample was filtered (0.22 µm), then injected into an LC-MS (AB-Sciex 5600 QTOF) using an inline polymeric reversed-phase column (PL 1912-1503, Agilent). Protein solutions were separated through over the following 15 minute linear gradient: 10% ACN for 5 minutes, then linear gradient from 10% to 90% ACN over 10 minutes, with mass spectrum scans taken every 1 second in positive mode. The chromatogram was integrated, and the full molecular weight was calculated using Analyst (AB Sciex)

Method S5.5 Plasmid construction for actuator expression and ORF sequences

eSrtA(2A9) ($_A$) and eSrtA(4S9) ($_S$) were gifts from David Liu (Addgene Plasmids #75145 and #75146, respectively), MBP-superTEV ($_T$) from Mark Howarth (Addgene Plasmid #171782), TVMV ($_V$) from David Waugh (Addgene Plasmid #8832), and HRV-3C ($_C$) from Gottfried Otting (Addgene Plasmid #162795). Sequences are given 5’ to 3’ with relevant portions color coded for ease of identification.

eSrtA (2A9) ($_A$)
Srt(2A9)-GS-6xHis

ATGCAGGCGAAACCGCAGATTCCGAAAGATAAAAGCAAAGTGGCGGGTTATATTGAAATTCCGG
ATGCGGATATTAAAGAACCGGTGTATCCGGGCCCGGCGACCCGTGAACAGCTGAACCGGGGCGT
GTGCTTTCATGACGAAAACGAAAGCCTGGATGATCAGAACATTAGCATTGCGGGCCATACCTTT
ATTGATCGTCCGAACTATCAGTTTACCAACCTGAAAGCGGCGAAACCTGGCAGCATGGTGTATT
TTAAAGTGGGCAACGAAACCCGTATATATAAAATGACCAGCATTCGTAAGGTGCATCCGAACGC
GGTGGAAGTGCTGGATGAACAGGAAGGCAAAGATAAACAGTTGACCCTGGTGACCTGCGATGAT
TATAACGAAGAAACCGGCGTGTGGGAATCCCGTAAAATTTTTGTGGCGACCGAAGTGAAAGGAT
CCCACCACCACCACCACCAC

eSrtA (4S9) ($_S$)
Srt(4S9)-GS-6xHis

ATGCAGGCGAAACCGCAGATTCCGAAAGATAAAAGCAAAGTGGCGGGCTATATTGAAATTCCGG
ATGCGGATATTAAAGAACCGGTGTATCCGGGCCCGGCGACCCGTGAACAGCTGGATCGTGGTGT
GTGCTTTGTGGAAGAAAACGAAAGCCTGGATGATCAGAACATTAGCATTACCGGCCATACCGCG
ATTGACCGTCCGAACTATCAGTTTACCAACCTGAGGGCGGCGAAAAAAGGCAGCATGGTGTATC
TTAAAGTGGGCAACGAAACCCGTAAATATAAAATGACCAGCATTCGTAACGTGAAACCGACCGC
GGTGGAAGTGCTGGATGAACAGAAAGGCAAAGATAAACAGCTGACCCTGGTGACCTGCGATGAT
TATAACTTTGAAACCGGCGTGTGGGAAACCCGTAAAATTTTTGTGGCGACCGAAGTGAAAGGAT
CCCACCACCACCACCACCAC

superTEV ($_T$)
MBP-6xHis-superTEV-polyR

ATGGGAATCGAAGAAGGTAAACTGGTAATCTGGATTAACGGCGATAAAGGCTATAACGGTCTCG
CTGAAGTCGGTAAGAAATTCGAGAAAGATACCGGAATTAAAGTCACCGTTGAGCATCCGGATAA
ACTGGAAGAGAAATTCCCACAGGTTGCGGCAACTGGCGATGGCCCTGACATTATCTTCTGGGCA
CACGACCGCTTTGGTGGCTACGCTCAATCTGGCCTGTTGGCTGAAATCACCCCGGACAAAGCGT
TCCAGGACAAGCTGTATCCGTTTACCTGGGATGCCGTACGTTACAACGGCAAGCTGATTGCTTA
CCCGATCGCTGTTGAAGCGTTATCGCTGATTTATAACAAAGATCTGCTGCCGAACCCGCCAAAA
ACCTGGGAAGAGATCCCGGCGCTGGATAAAGAACTGAAAGCGAAAGGTAAGAGCGCGCTGATGT
TCAACCTGCAAGAACCGTACTTCACCTGGCCGCTGATTGCTGCTGACGGGGGTTATGCGTTCAA
GTATGAAAACGGCAAGTACGACATTAAAGACGTGGGCGTGGATAACGCTGGCGCGAAAGCGGGT
CTGACCTTCCTGGTTGACCTGATTAAAAACAAACACATGAATGCAGACACCGATTACTCCATCG
CAGAAGCTGCCTTTAATAAAGGCGAAACAGCGATGACCATCAACGGCCCGTGGGCATGGTCCAA
CATCGACACCAGCAAAGTGAATTATGGTGTAACGGTACTGCCGACCTTCAAGGGTCAACCATCC
AAACCGTTCGTTGGCGTGCTGAGCGCAGGTATTAACGCCGCCAGTCCGAACAAAGAGCTGGCAA
AAGAGTTCCTCGAAAACTATCTGCTGACTGATGAAGGTCTGGAAGCGGTTAATAAAGACAAACC
GCTGGGTGCCGTAGCGCTGAAGTCTTACGAGGAAGAGTTGGCGAAAGATCCACGTATTGCCGCC
ACCATGGAAAACGCCCAGAAAGGTGAAATCATGCCGAACATCCCGCAGATGTCCGCTTTCTGGT
ATGCCGTGCGTACTGCGGTGATCAACGCCGCCAGCGGTCGTCAGACTGTCGATGAAGCCCTGAA
AGACGCGCAGACTAATTCGAGCTCGAACAACAACAACAATAACAATAACAACAACCTCGGGATC

GAGGGAAGGGGAGATTTTGCAGGTCATCATCATCATCATCATCATGGAGAAAGCTTGTTTAAGG
GGCCGCGTGATTACAACCCGATATCGAGCACCATTGTTCATTTGACGAATGAATCTGATGGGCA
CACAACATCGTTGTATGGTATTGGATTTGGTCCCTTCATCATTACAAACAAGCACTTGTTTAGA
AGAAATAATGGAACACTGGTGGTCCAATCACTACATGGTGTATTCAAGGTCAAGAACACCACGA
CTTTGCAACAACACCTCATTGATGGGAGGGACATGATAATTATTCGCATGCCTAAGGATTTCCC
ACCATTTCCTCAAAAGCTGAAATTTAGAGAGCCACAAAGGGAAGAGCGCATAGTCCTTGTGACA
ACCAACTTCCAAACTAAGAGCATGTCTAGCATGGTGTCAGACACTAGTTCGACATTCCCTTCAG
GAGATGGCATATTCTGGAAGCATTGGATTCAAACCAAGGATGGGCAGTGTGGCAGTCCATTAGT
ATCAACTAGAGATGGGTTCATTGTTGGTATACACTCAGCATCGAATTTCACCAACACAAACAAT
TATTTCACAAGCGTGCCGAAAAACTTCATGGAATTGTTGACAAATCAGGAGGCGCAGCAGTGGG
TTAGTGGTTGGCGATTAAATGCTGACTCAGTATTGTGGGGAGGCCATAAAGTTTTCATGGACAA
ACCTGAAGAGCCTTTTCAGCCAGTTAAGGAAGCGACTCAACTCATGAATCGTCGTCGCCGTCGC

HRV-3C (C)
6xHis-NT*-SGGGGS-HRV-3C

ATGCATCATCATCATCACCACAGCCATACCACACCGTGGACCAATCCTGGTCTGGCAGAAAACT
TTATGAATAGCTTTATGCAGGGTCTGAGCAGCATGCCTGGTTTTACCGCAAGCCAGCTGGACAA
AATGAGCACCATTGCACAGAGCATGGTTCAGAGCATTCAGAGCCTGGCAGCACAGGGTCGTACC
AGTCCGAATGATCTGCAGGCACTGAATATGGCATTTGCAAGCAGCATGGCAGAAATTGCAGCAA
GCGAAGAAGGTGGCGGTAGCCTGAGCACCAAAACCAGCAGCATTGCAAGCGCAATGAGCAATGC
ATTTCTGCAGACAACCGGTGTTGTTAATCAGCCGTTTATTAACGAAATTACCCAGCTGGTTAGC
ATGTTTGCACAGGCAGGTATGAATGATGTTAGCGCAGGTAATAGCGGTGGTGGTGGTAGCGGTC
CGAATACCGAATTTGCACTGAGCCTGCTGCGTAAAAACATTATGACCATTACCACCTCCAAAGG
CGAATTTACCGGTCTGGGTATTCATGATCGTGTTTGTGTTATTCCGACACATGCACAACCGGGT
GATGACGTTCTGGTTAATGGTCAGAAAATTCGCGTGAAAGACAAGTATAAACTGGTGGATCCGG
AAAACATTAATCTGGAACTGACCGTTCTGACCCTGGATCGTAATGAAAAATTTCGTGATATCCG
TGGCTTTATCAGCGAAGATCTGGAAGGTGTTGATGCAACCCTGGTTGTTCATAGCAATAACTTT
ACCAACACCATCCTGGAAGTTGGTCCGGTTACCATGGCAGGTCTGATTAATCTGAGCAGTACCC
CGACCAATCGTATGATTCGTTATGATTATGCAACCAAAACCGGTCAGTGTGGTGGTGTTCTGTG
TGCAACCGGTAAAATCTTTGGCATTCATGTTGGTGGCAATGGTCGTCAGGGTTTTAGCGCACAG
CTGAAAAAACAGTATTTCGTGGAAAAGCAG

TVMV (V)
MBP-GS-TVMVc-6xHis-TVMV

ATGAAAATCGAAGAAGGTAAACTGGTAATCTGGATTAACGGCGATAAAGGCTATAACGGTCTCG
CTGAAGTCGGTAAGAAATTCGAGAAAGATACCGGAATTAAAGTCACCGTTGAGCATCCGGATAA
ACTGGAAGAGAAATTCCCACAGGTTGCGGCAACTGGCGATGGCCCTGACATTATCTTCTGGGCA
CACGACCGCTTTGGTGGCTACGCTCAATCTGGCCTGTTGGCTGAAATCACCCCGGACAAAGCGT
TCCAGGACAAGCTGTATCCGTTTACCTGGGATGCCGTACGTTACAACGGCAAGCTGATTGCTTA
CCCGATCGCTGTTGAAGCGTTATCGCTGATTTATAACAAAGATCTGCTGCCGAACCCGCCAAAA
ACCTGGGAAGAGATCCCGGCGCTGGATAAAGAACTGAAAGCGAAAGGTAAGAGCGCGCTGATGT
TCAACCTGCAAGAACCGTACTTCACCTGGCCGCTGATTGCTGCTGACGGGGGTTATGCGTTCAA
GTATGAAAACGGCAAGTACGACATTAAAGACGTGGGCGTGGATAACGCTGGCGCGAAAGCGGGT
CTGACCTTCCTGGTTGACCTGATTAAAAACAAACACATGAATGCAGACACCGATTACTCCATCG

CAGAAGCTGCCTTTAATAAAGGCGAAACAGCGATGACCATCAACGGCCCGTGGGCATGGTCCAA
CATCGACACCAGCAAAGTGAATTATGGTGTAACGGTACTGCCGACCTTCAAGGGTCAACCATCC
AAACCGTTCGTTGGCGTGCTGAGCGCAGGTATTAACGCCGCCAGTCCGAACAAAGAGCTGGCAA
AAGAGTTCCTCGAAAACTATCTGCTGACTGATGAAGGTCTGGAAGCGGTTAATAAAGACAAACC
GCTGGGTGCCGTAGCGCTGAAGTCTTACGAGGAAGAGTTGGCGAAAGATCCACGTATTGCCGCC
ACCATGGAAAACGCCCAGAAAGGTGAAATCATGCCGAACATCCCGCAGATGTCCGCTTTCTGGT
ATGCCGTGCGTACTGCGGTGATCAACGCCGCCAGCGGTCGTCAGACTGTCGATGAAGCCCTGAA
AGACGCGCAGACTAATTCGATCACAAGTTTGTACAAAAAAGCAGGCTCGGAAACCGTGCGTTTC
CAGTCTCACCACCATCATCATCACTCTAAAGCTTTGCTGAAGGGCGTGCGCGATTTTAATCCGA
TCTCTGCTTGCGTATGCCTGCTGGAAAACTCCTCGGATGGTCATAGTGAACGTCTGTTTGGCAT
TGGTTTTGGCCCGTATATCATTGCCAACCAGCATCTGTTTCGTCGTAACAATGGCGAACTGACC
ATCAAAACCATGCATGGTGAATTCAAAGTCAAAAACTCTACCCAGCTGCAGATGAAACCGGTTG
AAGGCCGTGACATTATCGTTATCAAAATGGCTAAAGACTTCCCGCCGTTCCCGCAGAAACTGAA
ATTCCGTCAGCCGACCATCAAAGATCGTGTGTGCATGGTGTCCACCAACTTTCAGCAGAAAAGC
GTCTCGAGCCTGGTGTCTGAATCCTCTCACATTGTGCATAAAGAAGACACTTCTTTCTGGCAGC
ACTGGATCACCACTAAAGATGGCCAGTGTGGCAGCCCACTAGTTTCCATCATTGATGGCAACAT
TCTGGGCATCCACAGCCTGACTCATACCACCAACGGTAGCAACTACTTCGTGGAATTTCCGGAA
AAATTCGTGGCGACTTATCTAGATGCCGCGGATGGTTGGTGCAAAAACTGGAAATTCAACGCGG
ATAAAATCAGCTGGGGTTCCTTTACCCTGGTTGAAGATGCGCCGGAAGATGACTTCATGGCCAA
AAAAACTGTTGCCGCCATCATGGAC

Method S5.6 In-solution treatment of protein library

Each of the 17 mGreenLantern YES/OR/AND nested protein operators were treated with 23 = 8 possible combinations of inputs emanating from A, S, and T. Protease treatments were performed in the following buffer conditions: 20 mM Tris, 50 mM NaCl, pH = 7.5, 1 mM DTT, 1 mM CaCl2, and 18 mM GGG, supplemented with the input-relevant enzymes. Molar ratios of protease to the appropriate mGreenLantern construct were: 1:100, 1:100, and 1:10 for A, S, and T, respectively. Enzymatic treatments were allowed to proceed for 6 hours at 4 °C, non-kinetically limited endpoints determined to yield full cleavage for all constructs. Reactions were quenched by the addition of an equivalent volume of 2x Laemmli buffer containing β-mercaptoethanol and were boiled at 95 °C for 5 min. Samples were then either used directly for loading on SDS-PAGE gels or frozen at -20 °C.

Method S5.7 Expression and purification of SpyCatcher003-Azide

Method S5.7.1. Expression and purification protocol

E. Coli BL21(DE3) cells were co-transformed with two plasmids: one harboring the SpyCatcher003-6xHis construct with an amber STOP codon in a flexible GS loop, and the other encoding for the appropriate amber suppression machinery (pEvol-pAzFRS.2.t1, a gift from Farren Isaacs, Addgene #73546). The cells were then grown at 37 °C and 220 rpm agitation to an OD of 0.6-0.8 in LB broth supplemented with kanamycin and chloramphenicol. Isopropyl β-D-1-thiogalactopyranoside (IPTG) at a final concentration of 0.5 mM and arabinose at a final concentration of 0.1% were used to induce protein expression, at which point the cultures were moved to a reduced temperature (18 °C) for 18 hours. Cells were then harvested via centrifugation (4,000g, 20 min, 4 °C) and either flash-frozen and stored at -80 °C or used directly. Pellets were reconstituted in 40 mL of lysis buffer (20 mM Tris, 50 mM NaCl, pH = 7.5). These were then supplemented with phenylmethylsulfonyl fluoride (PMSF) to a final concentration of 1 mM and sonicated on ice (18 min at 30% amplitude and 33% duty cycle) (Fisher Scientific, Waltham, MA). After sonication, lysates were centrifuged for 45 min at 11,000g to separate soluble from insoluble fractions. Clarified lysates were loaded onto an AKTA Pure 25L FPLC (Cytiva, Marlborough, MA) equipped with a 5mL HisTrap HP column at a flow rate of 5 mL/min. The HisTrap column was first equilibrated with 5 column volumes of lysis buffer prior to loading. Once all protein was bound, the column was washed with 10+ column volumes of lysis buffer until residual UV read-outs ($\lambda = 280$ nm) dropped to 0 absolute units (au). Target protein was then eluted off the column into a 96-well plate by switching to elution buffer (lysis buffer + 250 mM imidazole). The pooled purified protein was dialyzed (20 mM Tris, 50 mM NaCl, pH = 7.5) to remove imidazole (SnakeSkin™ Dialysis Tubing, 3K

MWCO, Fischer Scientific, Waltham, MA). After 4+ dialysis bath changes, proteins were spin-concentrated if needed using an Amicon Ultra 15 centrifugation filter (3 kDa MWCO, Sigma-Aldrich, Burlington, MA). The purified solution was supplemented with glycerol (10% of final volume) to act as cryoprotectant, aliquoted into single-use tubes to avoid repeated freeze-thaw cycles, and flash-frozen with liquid nitrogen prior to long-term storage.

Method S5.7.2. Plasmid construction for SpyCatcher003-Azide

The open reading frames (ORFs) of the plasmids required for the generation of SpyCatcher003-AzF is given below (5' to 3'):

SpyCatcher003-TAG-6xHis

SpyCatcher003-GSGESGS-**AMBER STOP CODON**-GSGESGS-6xHis

ATGGTGACCACCCTTAGCGGCTTGAGCGGTGAACAAGGCCCGTCCGGTGATATGACCACGGAAG
AAGATAGTGCGACCCATATCAAATTCAGCAAACGCGATGAGGACGGCCGGGAGTTAGCTGGTGC
GACGATGGAGCTGCGTGATTCATCTGGGAAAACGATTAGTACATGGATCTCGGATGGACACGTG
AAAGATTTCTACCTGTACCCAGGAAAGTATACATTTGTCGAAACCGCAGCTCCGGACGGCTATG
AAGTGGCAACTGCCATTACCTTTACCGTTAACGAACAGGGTCAGGTTACTGTAAATGGCGAAGC
GACTAAAGGGGACGCCCATACGGGTAGCGGTGAAAGCGGCAGC**TAG**GGCAGCGGTGAAAGCGGT
AGCCACCACCACCACCACCAC

Method S5.8 Development of bead release assay for logical operators

Magnetic beads functionalized with DBCO (Vector Laboratories; Newark, CA) were pre-equilibrated in reaction buffer (20 mM Tris, 50 mM NaCl, pH = 7.5, 1 mM DTT, 1 mM $CaCl_2$, 18 mM GGG) and washed. Bead washes consisted of diluting the working bead slurry volume (50-100 µL) in 1 mL of reaction buffer. The microcentrifuge tube containing the slurry would then be placed in a magnetic separation rack to pull the beads towards the tube wall. While the tube is in the slot, fresh reaction buffer would be added, and the solution is mixed prior to additional washes using the same method (5+ times).

After equilibration, beads are then pre-reacted with 200 µL SpyCatcher-azide (1 mg/mL) for 2 hours at room temperature. Reaction tubes are kept in a stationary tube rotator / mixer throughout the SPAAC conjugation. Afterwards, beads are again washed as described prior to remove any unbound SpyCatcher-azide.

After SpyCatcher conjugation, the appropriate SpyTagged operator (200 µL, 1 mg/mL) is added into the solution to conjugate onto the beads through SpyLigation. Reaction tubes are again kept in a stationary tube rotator / mixer for 2 hours at room temperature. Beads are then thoroughly washed to remove any residual mGreenLantern that remained unbound.

Once beads are washed, all 8 possible input combinations of $_A$, $_S$ and $_T$ are introduced in the same buffer conditions as those used for the in-solution treatments (20 mM Tris, 50 mM NaCl, pH = 7.5, 1 mM DTT, 1 mM $CaCl_2$, 18 mM GGG). Treatments lasted 6 hours at 4°C to allow for full cleavage response. Afterwards, 15 µL is taken from each input condition with a gel-loading pipette and added to a 384 black well plate with a clear bottom. All conditions were performed in at least three technical triplicates. Supernatant fluorescence measurements were taken on a BioTek Synergy Microplate Reader (BioTek; Winooski, VT).

Method S5.9 Plasmid construction for multiplexed release of fluorescent proteins from hydrogel matrices

Cloned plasmids [pET-29b(+), with desired sequences inserted between NdeI and XhoI cloning sites) were ordered from GenScript (Piscataway, NJ). The open reading frames (ORFs) of each]new construct used for multiplexed hydrogel release studies are given below. Sequences are given 5' to 3' with relevant portions color coded for ease of identification. All species were designed to contain a SpyTag003 for material tethering and a 6xHis motif for IMAC-assisted purification.

mCherry – S YES
MGSS-mCherry-GGS(x3)-4S9c-GGS(x3)-SpyTag003-GGS(x3)-6xHis

ATGGGGAGTTCAATGGTGTCCAAAGGGGAAGAGGACAATATGGCTATCATTAAAGAATTTATGC
GTTTCAAAGTACATATGGAAGGAAGCGTTAACGGTCACGAATTCGAGATCGAAGGCGAAGGCGA
GGGTCGCCCATACGAAGGTACGCAGACCGCTAAACTGAAAGTAACCAAAGGCGGACCTTTACCC
TTCGCCTGGGACATTCTAAGTCCGCAATTTATGTATGGTAGCAAGGCGTACGTTAAACACCCGG
CAGATATCCCAGACTATTTAAAGTTGTCGTTTCCTGAGGGTTTTAAATGGGAGCGAGTGATGAA
CTTCGAGGATGGGGGCGTGGTCACAGTCACGCAGGATTCGTCGCTGCAGGATGGGGAATTTATT
TATAAAGTCAAACTGCGCGGGACTAACTTTCCGTCGGACGGCCCGGTCATGCAAAAAAAAACCA
TGGGTTGGGAAGCGTCTAGCGAACGTATGTACCCCGAAGATGGGGCATTGAAAGGGGAAATTAA
ACAACGTCTGAAACTCAAAGATGGCGGACATTATGATGCGGAGGTGAAAACCACTTATAAGGCG
AAAAAACCAGTGCAGCTGCCGGGTGCATATAACGTTAATATTAAACTTGACATCACATCTCATA
ATGAAGATTATACCATAGTGGAACAGTACGAACGTGCCGAAGGTCGCCACTCTACGGGCGGCAT
GGACGAGCTGTACAAGGGCGGTTCCGGCGGTAGTGGTGGAAGCCTGCCGGAAAGCGGCGGAGGT
TCAGGAGGTTCCGGCGGCAGTCGGGGCGTACCGCATATTGTTATGGTTGATGCCTATAAGCGCT
ACAAGGGTGGTTCCGGCGGCAGCGGCGGCTCACACCATCATCACCATCAT

mCerulean – T YES
MGSS-mCerulean-GGS(x3)-TEVc-GGS(x3)-SpyTag003-GGS(x3)-6xHis

ATGGGATCTTCGATGGTCTCCAAAGGCGAAGAACTGTTCACGGGTGTGGTCCCGATTCTGGTGG
AATTGGATGGTGACGTAAATGGCCATAAGTTTTCGGTGAGCGGCGAAGGCGAAGGCGATGCGAC
CTATGGCAAGTTAACCCTGAAATTCATCTGTACCACGGGAAAACTACCGGTGCCGTGGCCAACG
CTGGTGACCACCCTGACGTGGGGCGTACAGTGCTTTGCTCGTTATCCGGATCACATGAAACAGC
ACGACTTCTTTAAAAGCGCTATGCCGGAGGGCTACGTGCAGGAACGGACAATCTTTTTTAAAGA
CGATGGGAATTATAAAACGCGTGCCGAAGTTAAATTTGAGGGTGATACTCTGGTTAATCGTATC
GAACTGAAAGGGATCGATTTCAAAGAGGATGGGAACATACTCGGTCATAAATTGGAGTATAACG
CGATTTCGGATAACGTTTATATTACAGCAGACAAACAGAAGAACGGCATTAAGGCCAACTTTAA

AATCCGCCATAACATTGAAGATGGAAGCGTGCAGCTCGCGGATCACTACCAACAAAATACCCCC
ATCGGCGACGGTCCTGTCCTGCTTCCTGATAATCACTATTTAAGTACTCAAAGTAAACTTTCAA
AGGACCCAAACGAAAAACGCGACCACATGGTGTTGCTGGAGTTCGTCACCGCCGCGGGCATTAC
TTTAGGTATGGATGAACTGTACAAAGGTGGATCAGGTGGTTCCGGGGGCAGCGAAAATCTGTAC
TTTCAGTCAGGCGGCTCCGGGGGGTCTGGAGGCAGCCGCGGTGTACCGCATATTGTTATGGTTG
ATGCATACAAGCGATATAAAGGTGGCAGTGGTGGGTCTGGTGGTAGCCATCATCATCACCATCA
T

mCerulean – S ∧ T

MGSS-CfaC-GGS(x3)-4S9c-GGS(x3)- mCerulean-GGS(x3)-TEVc-GGS(x3)-SpyTag-GGS(x3)-6xHis-GGS(x3)-CfaN-SsrA

ATGGGAAGTTCAGTAAAAATTATAAGCAGGAAGTCCCTCGGCACCCAAAACGTGTACGATATTG
GTGTTGAGAAGGACCACAACTTCTTGTTGAAGAACGGTCTGGTTGCAAGCAATTGTTTCAACGG
TGGTTCAGGCGGTTCTGGCGGTTCCCTGCCGGAAAGCGGTGGCGGCTCTGGTGGCTCCGGTGGC
TCCATGGTGAGCAAAGGCGAGGAATTGTTTACCGGTGTTGTTCCGATCCTGGTCGAGCTGGATG
GCGATGTTAATGGTCACAAGTTCAGCGTGAGCGGTGAAGGTGAGGGTGACGCCACCTATGGCAA
GCTGACCCTGAAATTCATCTGCACTACGGGTAAGTTACCAGTCCCGTGGCCGACGCTGGTGACC
ACCCTGACCTGGGGTGTGCAATGTTTCGCCCGTTATCCGGATCACATGAAACAACATGATTTCT
TTAAGTCTGCCATGCCGGAGGGCTACGTTCAAGAACGTACCATCTTTTTCAAGGACGATGGCAA
CTACAAAACCCGTGCGGAAGTTAAATTTGAAGGTGATACGTTGGTGAACCGTATTGAATTGAAG
GGTATCGACTTCAAAGAAGATGGCAACATTCTGGGTCACAAACTGGAGTACAATGCAATTAGCG
ATAACGTTTACATTACCGCGGATAAACAGAAAAACGGCATCAAAGCGAACTTTAAGATCCGCCA
CAACATTGAGGACGGCAGTGTCCAACTGGCTGACCACTATCAGCAGAATACCCCGATCGGCGAC
GGTCCGGTGTTGCTTCCAGACAATCATTATCTGAGCACCCAGAGCAAGTTGTCGAAGGACCCGA
ATGAAAAACGTGATCACATGGTGCTTTTGGAATTTGTTACCGCGGCGGGTATTACCTTAGGTAT
GGACGAACTGTACAAGGGCGGTTCTGGCGGTTCAGGTGGATCGGAAAATCTGTACTTCCAGAGCG
GAGGTAGCGGCGGTAGCGGGGGAAGTGCGCATATTGTGATGGTTGACGCATATAAACCGACAAAAGGTGGTTCCGGC
GGCAGCGGTGGTTCCCATCATCACCACCATCACGGCGGTTCCGGGGGCAGCGGTGGATCGGCTGAATACTGC
CTGAGCTATGATACCGAAATTCTGACTGTTGAGTACGGTTTTCTGCCTATCGGCAAGATCGTGGAGGAGCGCATCGA
GTGCACCGTCTACACCGTTGATAAAAACGGCTTTGTGTACACTCAGCCGATCGCCCAGTGGCACAACCGCGGTGAAC
AAGAGGTATTTGAATATTGCCTGGAGGACGGTAGCATCATCCGTGCGACGAAAGACCATAAATTCATGACGACCGAT
GGTCAGATGCTGCCGATTGACGAGATCTTCGAGAGAGGCCTCGACCTGAAGCAAGTGGATGGTCTGCCGGCTGCGAA
TGACGAGAACTATGCACTGGCGGCT

Method S5.10 Formation of SPAAC-based hydrogels

Hydrogels (5 μL) were formulated from PEG-tetraBCN (Mn ≈ 20,000 Da, 4 mM), triethylene glycol (TEG) diazide (MW = 200.2 g mol-1, 8 mM), SpyCatcher-azide (15 μM), and the set of SpyTagged fluorescent proteins (2 μM each) in gel buffer (20 mM Tris, 50 mM NaCl, 10 mM CaCl2, pH = 7.5). The fluorescent protein constructs and SpyCatcher-azide were first reacted for 30 min at room temperature before the addition of PEG-tetraBCN. After another 30 min, TEG diazide was also added and the mixture was vortexed. Immediately after the combination of all components, 5 μL volumes of the solution were separated into microcentrifuge tubes (1.5 mL) and centrifuged, resulting in cone-shaped gel solutions about 2 mm tall. After waiting 10 min, 75 μL of gel buffer was added to each tube and the formed hydrogels were washed for 72 hours with 3 buffer changes to remove unconjugated fluorescent protein.

Method S5.11 Multiplexed release from polymeric hydrogels

All treatments were performed at 4 °C in gel buffer (75 μL). Depending on the intended input, samples were treated with a combination of A, S, and T at concentrations of 5 μM, 5 μM, and 7 μM, respectively. DTT (1 mM) was also added to each sample at the same time as the enzymes. After six hours, supernatant fluorescence was measured and used to calculate the corresponding concentrations of released mGreenLantern, mCherry, and mCerulean proteins. mGreenLantern was analyzed with λexc.= 498 nm, λem. = 525 nm; mCherry with λexc.= 580 nm, λem.= 610 nm; mCerulean with λexc.= 433 nm, λem. = 475 nm.

Method S5.12 Plasmid construction for {[(A ∨ S) ∧ T] ∨ (C ∧ V)}-releasable mGreenLantern

A cloned plasmid [pET-29b(+), with desired sequences inserted between NdeI and XhoI cloning sites] was ordered from GenScript (Piscataway, NJ). The open reading frames (ORFs) of plasmid encoding for [(A∨S)∧T]∨(C∧V)-releasable mGreenLantern is given below. Sequences are given 5' to 3' with relevant portions color coded for ease of identification.

MGSS-CfaC-GGS(x3)-mGreenLantern-GGS(x3)-TEVc-GGS(x3)-SnoopTag-GGS(x3)-HRV-3Cc-GGS(x3)-SpyTag-GGS(x3)-TVMVc-GGS(x3)-6xHis-GGS(x3)-SnoopCatcher-GGS(x3)-4S9c-GGS(x3)-2A9c-GGS(x3)-CfaN-SsrA

ATGGGAAGTTCAGTAAAAATTATAAGCAGGAAGAGCCTGGGTACGCAGAATGTGTACGACATCG
GTGTGGAGAAGGACCACAATTTCTTATTGAAGAATGGTCTGGTGGCGAGCAACTGCTTTAACGG
TGGTTCCGGCGGGTCCGGTGGTAGCATGGTTAGCAAAGGCGAGGAACTGTTCACCGGTGTTGTT
CCGATTTTGGTAGAGTTGGACGGCGACGTTAATGGCCATAAGTTCTCTGTTCGTGGTGAGGGCG
AAGGTGACGCTACCAACGGTAAGTTGACGTTGAAGTTTATCTGCACCACCGGTAAATTGCCAGT
TCCGTGGCCGACGTTGGTTACCACGCTGGGCTATGGCGTGGCCTGCTTCGCCCGTTATCCGGAC
CACATGAAACAACATGATTTTTTCAAGTCTGCTATGCCGGAAGGTTACGTGCAAGAGCGTACCA
TTAGCTTTAAAGATGATGGCACCTACAAAACCCGCGCTGAAGTCAAATTCGAGGGTGATACCCT
TGTCAATCGTATCGTTCTGAAGGGCATCGACTTCAAGGAAGATGGTAACATTCTGGGCCACAAG
TTGGAATACAATTTCAACAGCCACAAAGTGTATATTACCGCCGATAAACAAAAAAACGGCATCA
AAGCAAACTTCAAGACCAGACACAACGTCGAGGACGGCGGCGTTCAACTGGCGGATCACTACCA
ACAAAACACCCCGATCGGTGATGGTCCGGTTCTGCTGCCGGACAACCATTACCTGAGCCACCAG
TCCAAGCTCAGCAAAGACCCGAATGAGAAGCGTGATCACATGGTACTTAAGGAGCGCGTCACTG
CGGCTGGTATCACACATGACATGGATGAACTGTACAAGGGCGGCAGTGGCGGCAGCGGCGGTTC
CGAAAATCTGTACTTCCAAAGCGGCGGATCTGGCGGCAGCGGTGGTAGCAAGCTGGGCGACATC
GAGTTCATCAAGGTGAATAAAGGAGGTTCTGGCGGCAGTGGTGGCTCTTTGGAGGTTCTATTCC
AAGGTCCGGGTGGCTCTGGTGGTAGCGGTGGCTCGGCCCATATTGTTATGGTTGATGCGTATAA
GCCCACCAAAGGTGGCTCGGGTGGTAGCGGTGGTTCGGAAACGGTGCGCTTTCAGAGCGGCGGT
TCTGGCGGCAGCGGTGGTAGCCACCACCACCACCATCACGGCGGTAGCGGCGGTTCGGGCGGTT
CAAAACCGCTGCGTGGTGCAGTTTTTAGCCTGCAGAAACAACATCCGGATTATCCGGACATCTA
CGGTGCGATTGACCAGAACGGCACGTACCAGAACGTCCGCACCGGTGAGGACGGTAAACTGACC
TTTAAGAACCTGAGTGATGGTAAATATCGTCTCTTTGAGAACTCAGAGCCGGCGGGTTACAAGC
CGGTGCAGAACAAGCCGATCGTGGCGTTTCAAATTGTGAACGGCGAGGTTCGTGATGTGACTTC
AATTGTCCCGCAGGATATTCCGGCGACCTATGAATTTACTAATGGTAAGCATTACATCACCAAC
GAACCGATCCCGCCTAAAGGTGGGAGCGGTGGTAGCGGCGGTTCCCTGCCTGAAAGCGGCGGTG
GCTCGGGGGGCTCCGGTGGGTCCTTGGCGGAAACCGGTGGTGGCTCCGGGGGAAGCGGGGGCTC
CGCTGAATACTGTCTGAGCTATGACACCGAAATTCTGACGGTGGAGTACGGCTTTCTGCCAATA
GGCAAGATCGTGGAAGAGCGCATTGAATGTACTGTCTATACCGTGGATAAAAACGGCTTCGTGT
ACACCCAGCCGATTGCACAGTGGCATAACCGTGGTGAGCAGGAGGTGTTCGAATACTGCCTGGA
GGACGGTTCTATCATTCGTGCGACGAAAGACCATAAATTCATGACCACAGATGGCCAGATGCTG
CCAATCGACGAGATCTTTGAACGCGGTCTCGACCTGAAACAGGTTGACGGTCTGCCGGCGGCAA
ATGATGAAAACTATGCACTGGCGGCG

Method S5.13 Development of bead release assay for {[(A ∨ S) ∧ T] ∨ (C ∧ V)}-releasable mGreenLantern

Beads were pre-equilibrated in reaction buffer, washed extensively, and functionalized with SpyCatcher-azide and the mGreenLantern cargo as described in **Method S5.8**.

Once beads are washed after mGreenLantern operator tethering, all 32 possible input combinations of $_{A}$, $_{S}$, $_{T}$, $_{V}$, and $_{C}$ are introduced in the same buffer conditions as those used for the in-solution treatments (20 mM Tris, 50 mM NaCl, pH = 7.5, 1 mM DTT, 1 mM $CaCl_2$, 18 mM GGG). Treatments lasted 2 hours at room temperature. Operators $_{A}$ and $_{S}$ were introduced in a 1:25 protease:operator molar ratio, $_{T}$ and $_{V}$ were introduced at 1:10, and $_{C}$ was introduced at 1:20. Afterwards, 15 µL is taken from each input condition with a gel-loading pipette and added to a 384 black well plate with a clear bottom. All conditions were performed in at least three technical triplicates. Supernatant fluorescence measurements were taken on a BioTek Synergy Microplate Reader (BioTek; Winooski, VT).

Supplementary Figures

Figure S5.1 Mass spectrometry characterization of actuators

eSrtA(2A9) ($_A$)

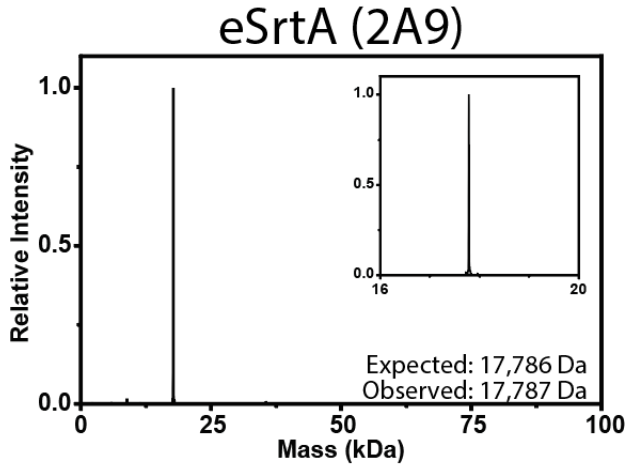

eSrtA(4S9) ($_S$)

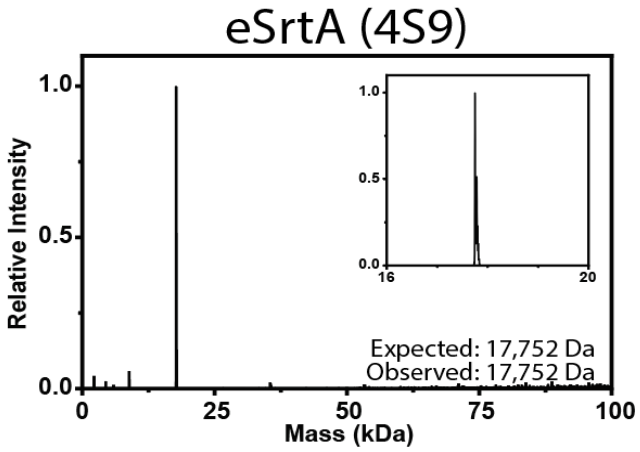

TVMV (V)

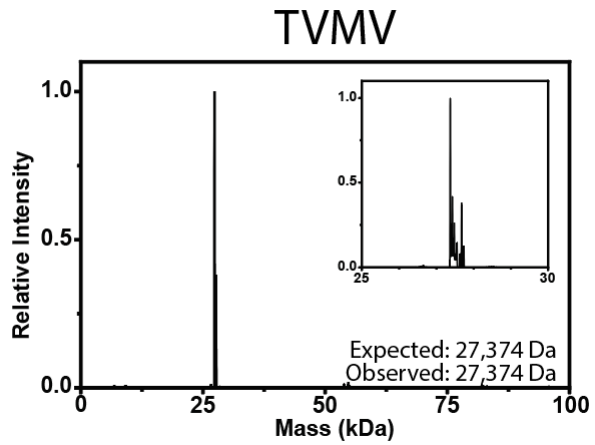

HRV-3C (C)

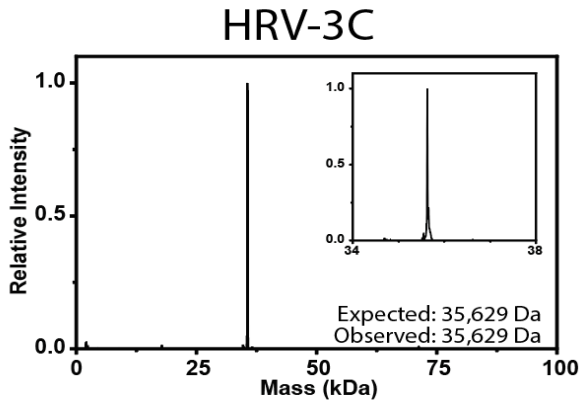

Figure S5.2 SDS-PAGE gels for 17 mGreenLantern logical constructs following in-solution treatment

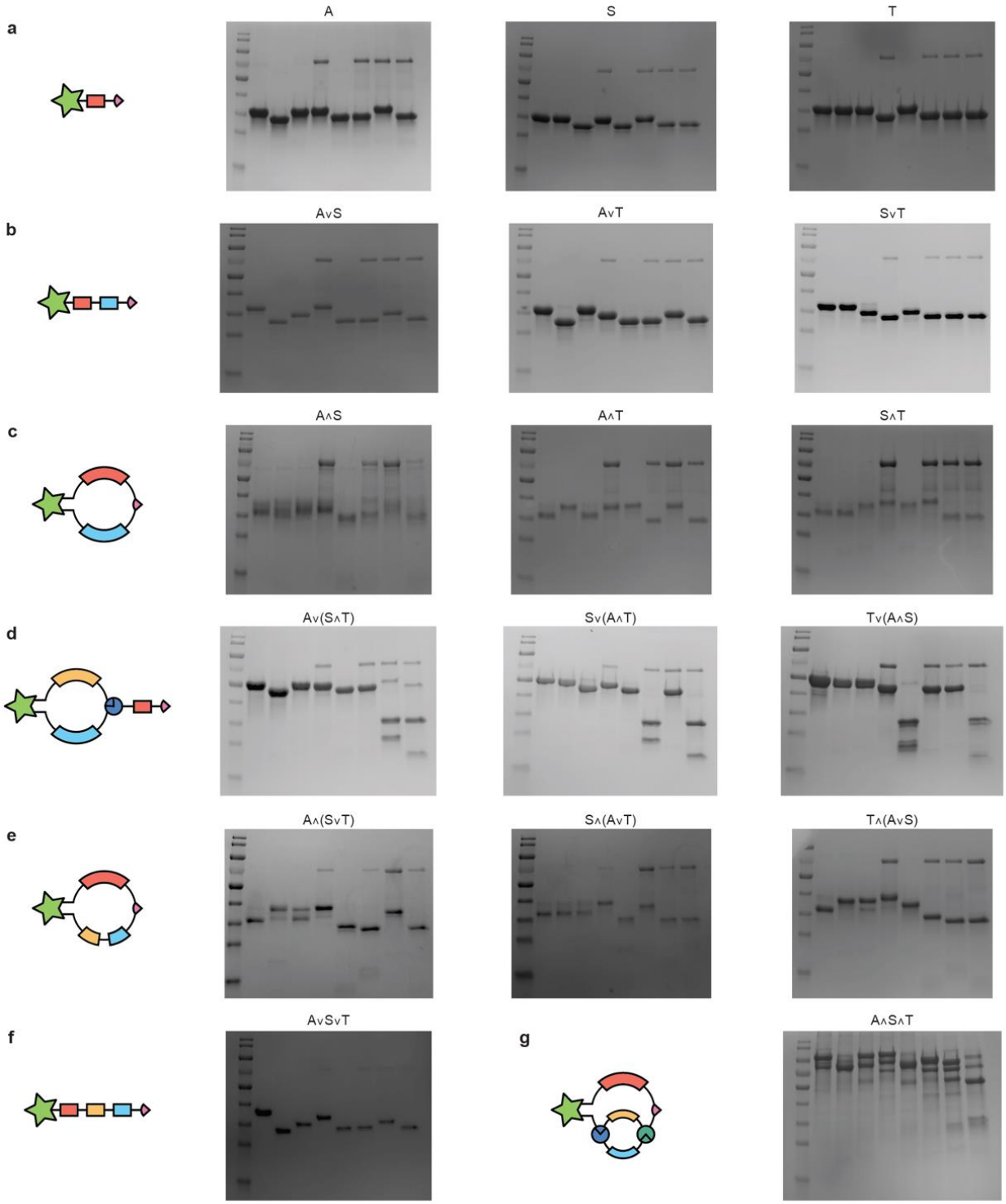

Following in-solution treatment of each of the 17 YES/OR/AND gated mGreenLantern species with A, S, and T, samples were analyzed via SDS-PAGE. Representative uncropped gels for each are given here. **a**) YES-gated single-input tethers. b-c) Two-input (**b**) OR-gated and (**c**) AND-gated tethers. d-g) Three-input (**d**) OR/(AND)-, (**e**) AND/(OR)-, (**f**) OR/OR-, and (**g**)AND/AND-gated tethers. Image titles correspond to the protein tether identity. For each image, lanes from left to right correspond to: ladder, N, A, S, T, AS, AT, ST, AST; N indicates no treatment, A indicates eSrtA(2A9), S indicates eSrtA(2S9), and T indicates TEV. From top to bottom, ladder bands correspond to proteins with molecular weights of 180, 130, 100, 70, 55, 40, 35, 25, and 15 kDa.

Figure S5.3 Mass spectrometry characterization of SpyCatcher-azide

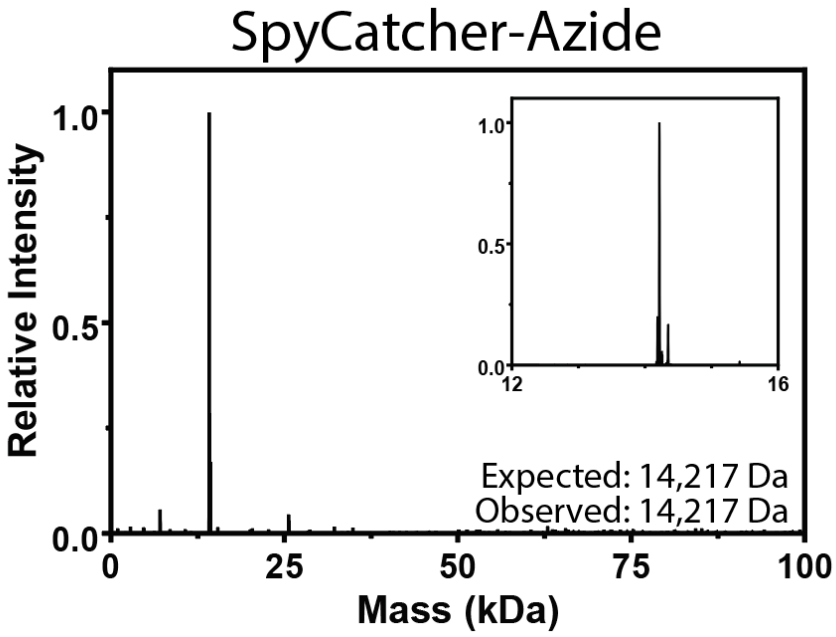

Figure S5.4 Mass spectrometry characterization of mCherry-S, mCerulean-T, and mCerulean – S ∧ T

mCherry – S YES

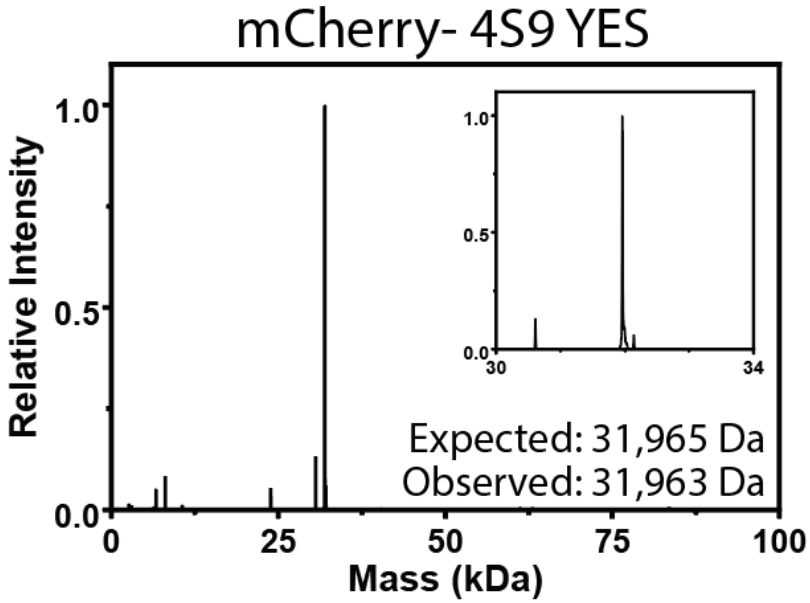

mCerulean – T YES

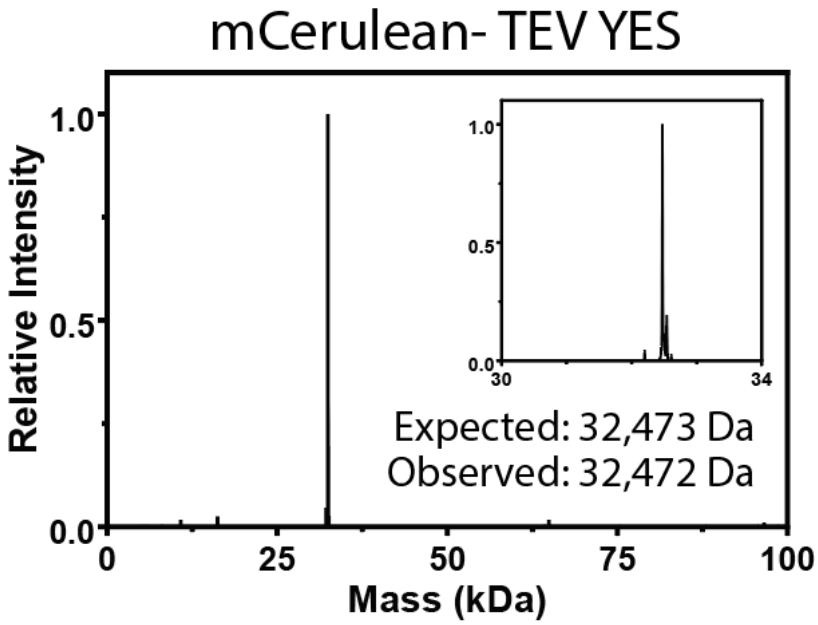

mCerulean – S ∧ T

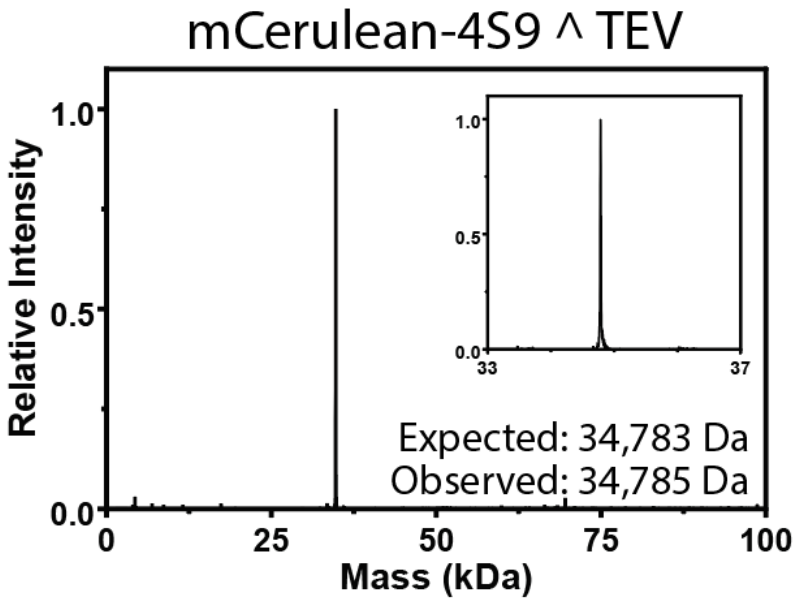

Figure S5.5 SDS-PAGE gels of mCherry-S, mCerulean-T, and mCerulean SΛT following in-solution treatment

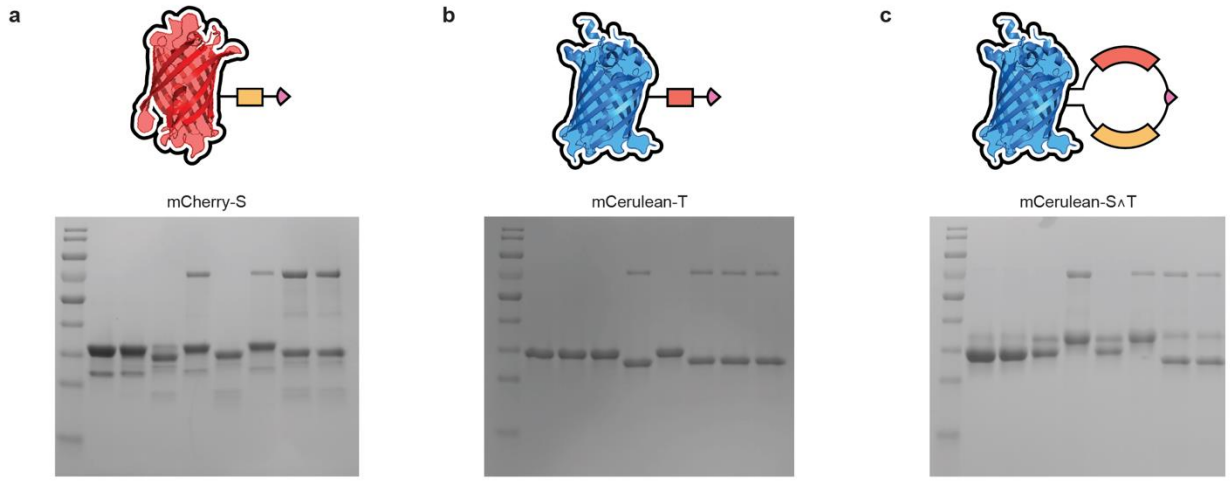

Following in-solution treatment of mCherry-S, mCerulean-T, and mCerulean-AΛT each with A, S, and T, samples were analyzed via SDS-PAGE. Representative uncropped gels for each are given here. **a**) mCherry-S, (**b**) mCerulean-T, and (**c**) mCerulean-AΛT. Image titles correspond to the protein identity. For each image, lanes from left to right correspond to: ladder, N, A, S, T, AS, AT, ST, AST; N indicates no treatment, A indicates eSrtA(2A9), S indicates eSrtA(2S9), and T indicates TEV. From top to bottom, ladder bands correspond to proteins with molecular weights of 180, 130, 100, 70, 55, 40, 35, 25, and 15 kDa.

Figure S5.6 SDS-PAGE analysis of purified mGreenLantern-[(A∨S)∧T]∨(C∧V)

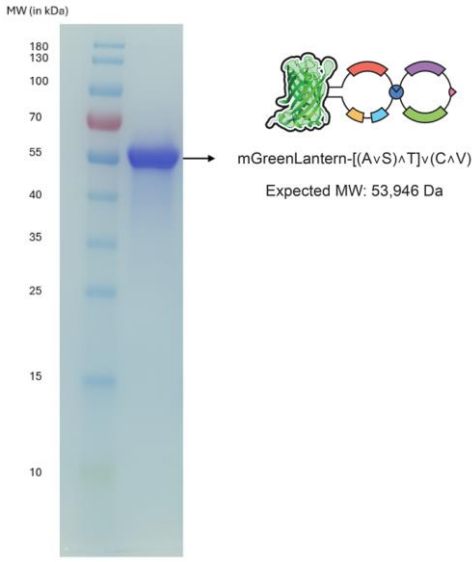

CHAPTER 6: EXPANDING THE SCOPE OF AUTONOMOUSLY COMPILED MOLECULAR TOPOLOGY TO BIOACTIVE PROTEIN RELEASE WITH DIVERSIFIED INPUTS

Adapted from Gharios, R.*, Ross, M.L.*, Li, A.^, Kottantharayil, S.^, DeForest, C.A. (*in preparation*)

*denotes co-first authorship.
^denotes equal contribution.

Abstract

Directing biomolecular topologies has led to the successful engineering of biomaterials endowed with Boolean responsiveness. In this chapter, we seek to extend the applicability of this design framework by assembling all 7 possible logical operations emanating from a YES/AND/OR operator set and applying them to proteins spanning diverse categories: growth factor (epidermal growth factor), model enzymes (β-lactamase, thioredoxin, NanoLuciferase), therapeutic nanobodies (HER2), *de novo*-engineered cytokine (IL-2 mimic Neoleukin 2/15), and fluorescent protein (mGreenLantern). In so doing, we specify biomacromolecule release from material anchors using an input set of three orthogonal protease actuators. Moreover, we also aim to broaden the palette of inputs that are compatible with autonomously compiled topologies. Toward that end, through the successful genetic encoding of a photocleavable protein and a small-molecule responsive motif into our bespoke structures, we demonstrate the seamless purification of proteins endowed with programmable release from biomaterials through Boolean operations that combine photoscission, small-molecule-induced cleavage, as well as protease recognition.

6.1. Introduction

Engineering user control over bio-epitope presentation in/from biomaterials has advanced manifold bioengineering applications such as controlled therapeutic release[1–3] and organoid/tissue engineering.[4,5] Toward this end, state-of-the-art efforts have deployed advances co-opted from disparate disciplines (e.g., chemoenzymatic protein modification, DNA nanotechnology, synthetic chemistry, among others still) and achieved remarkable synergies en route to engineering increasingly "smart" biomaterials and biohybrid constructs.[6,7] However, while these endeavors have been promising, they routinely fall short of attaining a fully generalizable framework that allows for more sophisticated biocomputation. While the broader biomaterials community has indeed found success in developing biomaterials that respond to multiple particular categories of inputs such as light, redox state, and small-molecule actuation,[8–10] these examples often remain case-specific and tightly wound to the specific application at-hand. To date, many of our most promising dynamic biomaterial platforms remain limited to single-input single-output (SISO)-type responses.

To address this unmet need, work in our group has focused on the formalization of methodologies through which we can engineer true biocomputability into biomaterials.[11,12] Rooted in an appreciation for how control over crosslink geometry and topology can scale to form bespoke logical operations, early examples from our group describe the synthetic assembly of an array of molecular structures that recapitulate all 17 possible YES/AND/OR logical operation sets from inputs based on light, enzymatic action, and redox state modulation. This initial thrust was applied successfully for the programming of bulk network degradation,[13] as well as for the release of full-length proteins and small-molecules from hydrogel supports.[14,15]

However, we observed that synthetic avenues very often necessitated protracted multi-step syntheses and led to low material yields, dramatically limiting the potential for material scale-up and technology transfer. Recently, we have shifted our attention to the recombinant expression of user-defined topologies (as described in Chapter 5), reasoning that such an approach would address many of the shortcomings inherent to chemical synthesis-based methodologies. We were inspired by pioneering literature reports that judiciously deploy motifs derived from chemical biology to create a wide array of bespoke protein architectures, often from singular plasmid blueprints. For example, the Zhang group successfully deployed an "assembly-reaction synergy" to create a wide range of architectures such as catenanes[16,17] and rotaxanes,[18] starting from compositionally simple yet information-rich polypeptide motifs. The Jerala group has expertly exploited coiled-coil motifs[19,20] to program multiple aspects of biomolecular assembly and presentation, such as user-directed protein activation,[21] nanostructure formation,[22] and inducible intracellular phase separation.[23] In the same vein, the Dokholyan group has pioneered the incorporation of stimulus-responsive motifs such as photoresponsive or small-molecule responsive domains into larger polypeptides to regulate their activity in a user-directed manner. This allosteric regulation of protein function has been applied successfully for targets such as kinases,[24] GTPases,[25] and transferases.[26] This is in addition to a broad array of work that bridges synthetic biology and material design to form biohybrid constructs endowed with synergistic properties.[27] For example, by incorporating conditional split-protease activation with either a magnetic agarose bead support or hydrogel network, the Weber group successfully engineered binary decoder biohybrids capable of advanced information processing.[28,29]

The rich diversity of these examples points to a rapidly growing armamentarium, which, if codified and deployed properly, can serve as a wellspring of robust biomolecular building blocks and/or motifs for impressive protein-based logical circuits.[30] Taking inspiration from these aforementioned reports, we developed a method for 'autonomously compiled topologies' that allowed us to assemble an exhaustive set of 17 YES/AND/OR operators through genetic encoding from an input set of three orthogonal proteases (Chapter 5). While highly advantageous with regards to material scale-up, improved signal-to-noise ratio (SNR), and ease of layering increasingly complex logical operations, our initial demonstration focused exclusively on the use of fluorescent proteins as model cargos. In efforts presented in this chapter, we seek to expand the scope of our method to gain Boolean control over biomacromolecule presentation for proteins spanning different functional categories (i.e., enzyme, fluorescent, enzyme, growth factor, de novo cytokine). We also assay for their bioactivity upon release from a material support to demonstrate full recapitulation of biological function.

Moreover, our initial demonstration focused exclusively on the use of orthogonal proteases as Boolean inputs. While protease-based actuation is highly enabling across different facets of eukaryotic synthetic biology,[31,32] a major drawback is its lack of spatiotemporal control. Moreover, incorporating a broader palette of potential inputs into our compiled topologies will undoubtedly enable the assembly of even more complex biomaterials. For instance, light as a trigger enables much-improved response dosage as well as theoretically full spatiotemporal control over biological processes.[8] Small-molecule-based actuation may also lead to much-enhanced localized targeting and has proven to be a robust tool for the triggered activation of different classes of proteins.[33] As such, our second objective through this work will be to expand

our framework to include a more comprehensive array of inputs, including light and small molecules.

6.2. Results and Discussion

To demonstrate functional diversity of proteins whose presentation can be controlled via autonomous molecular topology-based compilation, we identified 7 proteins spanning 5 functional classes – growth factor (epidermal growth factor), model enzymes (β-lactamase, thioredoxin, NanoLuciferase), therapeutic nanobodies (HER2), *de novo*-engineered cytokine (IL-2 mimic Neoleukin 2/15), and fluorescent proteins (mGreenLantern) – that will each be engineered as responsive via 1 of the 7 functional response classes (i.e., YES, OR, AND, OR(AND), AND(OR), OR/OR, AND/AND). For instance, EGF follows YES-type logic (EGF-A), bla follows OR (-∨) type logic (bla – A ∨ T), and NanoLuc follows AND (-∧) type logic (NanoLuc – A ∧ T). Having validated that two-input base operators can be recombinantly assembled, we layered these operations hierarchically to access more complex configurations. For instance, Thioredoxin was designed to follow three-input (AND)/OR logic (Trx – (A ∧ C) ∨ T), HER2-NB three-input (OR)/AND logic (HER2-NB (A ∨ T) ∧ C), and Neoleukin 2/15 double-OR logic (Neo A ∨ T ∨ C). For these proofs-of-concept, the proteases deployed were evolved sortase variant (2A9), referred to from hereon as $_{A}$, an evolved variant of the potyviral protease TEV ($_{T}$), and human rhinovirus protease-3C ($_{C}$). ORFs for all aforementioned constructs are provided in **Method S6.1**. All 6 listed operators were successfully recombinantly expressed at high purity as evidenced by LC-MS (**Figure 6.1**) and SDS-PAGE.

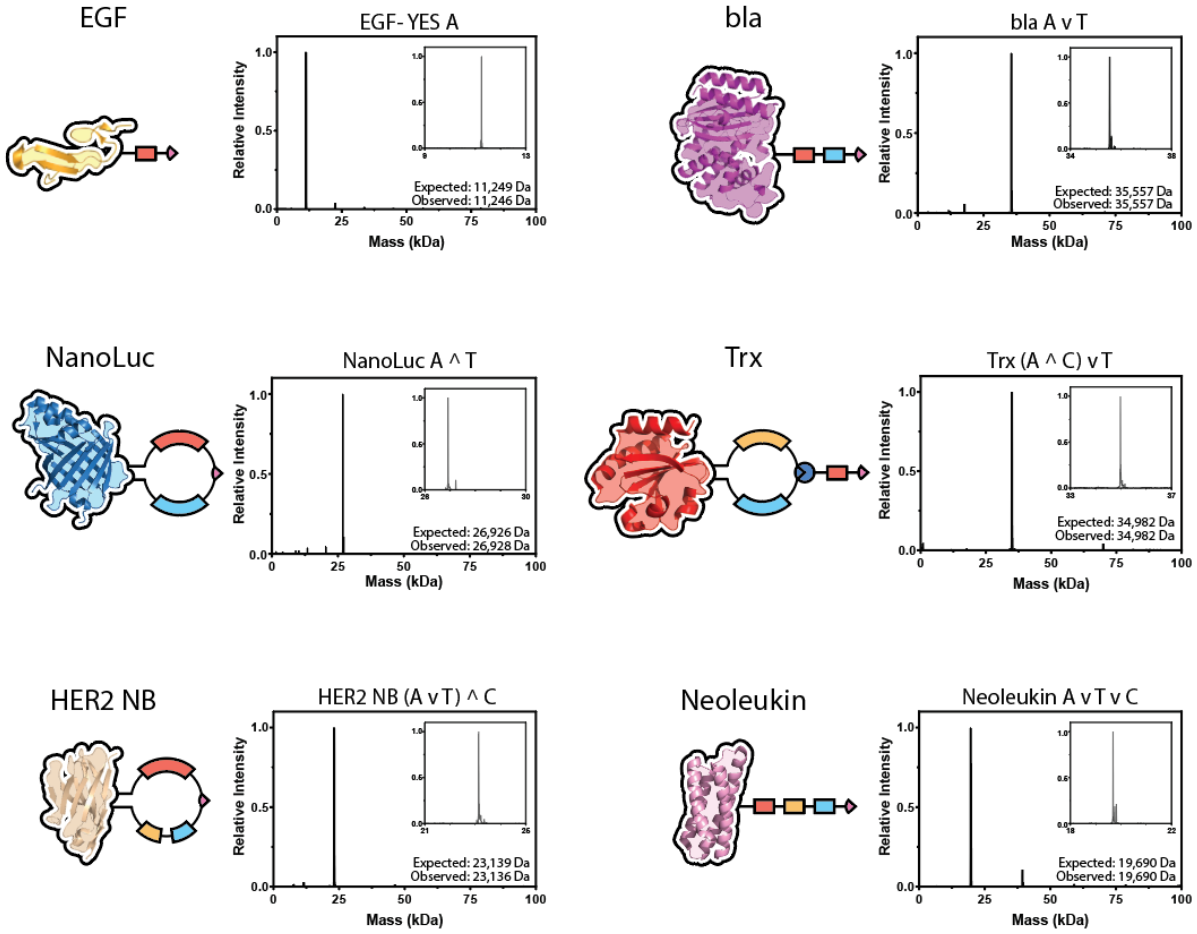

Figure 6.1. Mass spectrometric validation of logically releasable bioactive proteins *EGF-A, bla-A ∨ T, NanoLuc-A ∧ T, Trx-(A ∧ C) ∨ T, HER2-NB-(A ∨ T) ∧ C, and Neoleukin (A ∨ T ∨ C) are all successfully compiled and purified.*

Moreover, we successfully assembled a cyclized Trx construct that is both photochemically (through PhoCl) and proteolytically (through $_{A}$) releasable (**Figure 6.2** & **Method S6.2**).

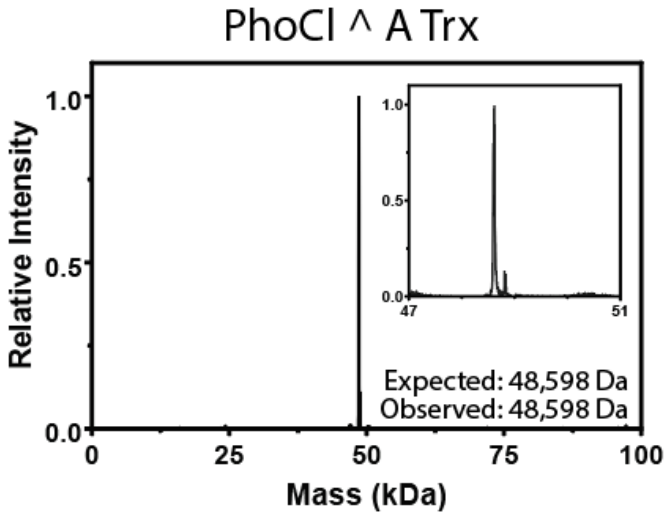

Figure 6.2. Mass spectrometric validation of photo- and A-releasable Trx.

We were then able to successfully validate the design by monitoring cleavage patterns on an SDS-PAGE gel (**Figure 6.3**). Hearteningly, exposure to either light irradiation or $_{A}$ do not yield any payload release, and only light irradiation in tandem with proteolytic action lead to cargo release.

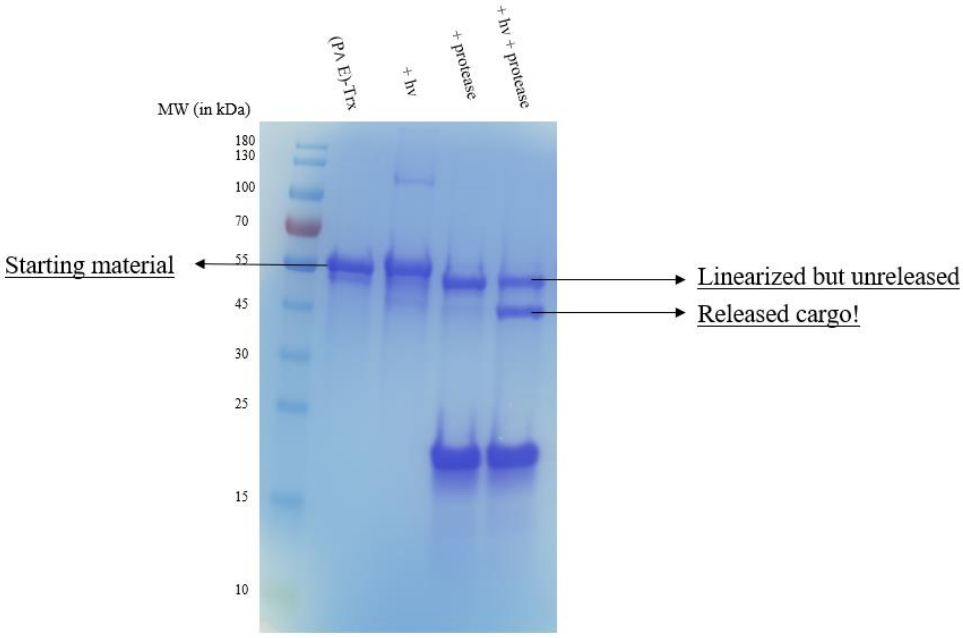

Figure 6.3. Photo- and proteolytically releasable Trx is only released upon exposure to both inputs, in accordance with the designed logical operation.
Light exposure or proteolysis through A alone do not lead to payload release; administration of both stimuli together leads to cargo release in accordance with the logical operation.

6.3. Conclusion

Summarily, we successfully demonstrate the extension of our molecularly compiled topology approach, both by broadening the palette of potential cargos that can be topologically modified to respond to a pre-programmed set of inputs, as well as extending the array of potential inputs that can be administered. These new results now allow us to multiplex input capacities onto bespoke frameworks that are fully genetically encoded and readily portable lab-to-lab. We envision this method to find widespread applicability in the development of next-generation biomaterials geared towards controlled release and regenerative medicine.

References

1. Fenton, O. S., Olafson, K. N., Pillai, P. S., Mitchell, M. J. & Langer, R. Advances in Biomaterials for Drug Delivery. *Adv. Mater.* **30**, 1705328 (2018).
2. Li, J. & Mooney, D. J. Designing hydrogels for controlled drug delivery. *Nat. Rev. Mater.* **1**, (2016).
3. Gao, J., Karp, J. M., Langer, R. & Joshi, N. The Future of Drug Delivery. *Chem. Mater.* **35**, 359–363 (2023).
4. DeForest, C. A. & Anseth, K. S. Advances in Bioactive Hydrogels to Probe and Direct Cell Fate. *Annu. Rev. Chem. Biomol. Eng.* **3**, 421–444 (2012).
5. Hofer, M. & Lutolf, M. P. Engineering organoids. *Nat. Rev. Mater.* **6**, 402–420 (2021).
6. Narkar, A. R., Tong, Z., Soman, P. & Henderson, J. H. Smart biomaterial platforms: Controlling and being controlled by cells. *Biomaterials* **283**, 121450 (2022).
7. Gharios, R., Francis, R. M. & DeForest, C. A. Chemical and biological engineering strategies to make and modify next-generation hydrogel biomaterials. *Matter* **6**, 4195–4244 (2023).
8. Ruskowitz, E. R. & DeForest, C. A. Photoresponsive biomaterials for targeted drug delivery and 4D cell culture. *Nat. Rev. Mater.* **3**, 1–17 (2018).
9. Gelmi, A. & Schutt, C. E. Stimuli-Responsive Biomaterials: Scaffolds for Stem Cell Control. *Adv. Healthc. Mater.* **10**, 2001125 (2021).
10. Fu, Z., Ouyang, L., Xu, R., Yang, Y. & Sun, W. Responsive biomaterials for 3D bioprinting: A review. *Mater. Today* **52**, 112–132 (2022).
11. Badeau, B. A. & Deforest, C. A. Programming Stimuli-Responsive Behavior into Biomaterials. *Annu. Rev. Biomed. Eng.* **21**, 241–265 (2019).
12. Bressler, E. M. *et al.* Boolean logic in synthetic biology and biomaterials: Towards living materials in mammalian cell therapeutics. *Clin. Transl. Med.* **13**, e1244 (2023).
13. Badeau, B. A., Comerford, M. P., Arakawa, C. K., Shadish, J. A. & Deforest, C. A. Engineered modular biomaterial logic gates for environmentally triggered therapeutic delivery. *Nat. Chem.* **10**, 251–258 (2018).
14. Gawade, P. M., Shadish, J. A., Badeau, B. A. & DeForest, C. A. Logic-Based Delivery of Site-Specifically Modified Proteins from Environmentally Responsive Hydrogel Biomaterials. *Adv. Mater.* **31**, 1902462 (2019).
15. Ruskowitz, E. R., Comerford, M. P., Badeau, B. A. & DeForest, C. A. Logical stimuli-triggered delivery of small molecules from hydrogel biomaterials. *Biomater. Sci.* **7**, 542–546 (2019).
16. Liu, D. *et al.* Topology Engineering of Proteins in Vivo Using Genetically Encoded, Mechanically Interlocking SpyX Modules for Enhanced Stability. *ACS Cent. Sci.* **3**, 473–481 (2017).
17. Liu, Y. *et al.* Cellular Synthesis and X-ray Crystal Structure of a Designed Protein Heterocatenane. *Angew. Chem. Int. Ed.* **59**, 16122–16127 (2020).
18. Liu, Y. *et al.* Lasso Proteins: Modular Design, Cellular Synthesis, and Topological Transformation. *Angew. Chem. Int. Ed.* **59**, 19153–19161 (2020).
19. Truebestein, L. & Leonard, T. A. Coiled-coils: The long and short of it. *BioEssays* **38**, 903–916 (2016).
20. Lupas, A. N. & Bassler, J. Coiled Coils – A Model System for the 21st Century. *Trends Biochem. Sci.* **42**, 130–140 (2017).

21. Plaper, T. *et al.* Designed allosteric protein logic. *Cell Discov.* **10**, 1–15 (2024).
22. Snoj, J., Lapenta, F. & Jerala, R. Preorganized cyclic modules facilitate the self-assembly of protein nanostructures. *Chem. Sci.* **15**, 3673–3686 (2024).
23. Ramšak, M. *et al.* Programmable de novo designed coiled coil-mediated phase separation in mammalian cells. *Nat. Commun.* **14**, 7973 (2023).
24. Vishweshwaraiah, Y. L., Chen, J., Chirasani, V. R., Tabdanov, E. D. & Dokholyan, N. V. Two-input protein logic gate for computation in living cells. *Nat. Commun.* **12**, 6615 (2021).
25. Jain, A., Dokholyan, N. V. & Lee, A. L. Allosteric inactivation of an engineered optogenetic GTPase. *Proc. Natl. Acad. Sci.* **120**, e2219254120 (2023).
26. Reynolds, J. A., Vishweshwaraiah, Y. L., Chirasani, V. R., Pritchard, J. R. & Dokholyan, N. V. An engineered N-acyltransferase-LOV2 domain fusion protein enables light-inducible allosteric control of enzymatic activity. *J. Biol. Chem.* **299**, (2023).
27. Burgos-Morales, O. *et al.* Synthetic biology as driver for the biologization of materials sciences. *Mater. Today Bio* **11**, 100115 (2021).
28. Mohsenin, H. *et al.* Design of a Biohybrid Materials Circuit with Binary Decoder Functionality. *Adv. Mater.* **36**, 2308092 (2024).
29. Mohsenin, H. *et al.* PenTag, a Versatile Platform for Synthesizing Protein-Polymer Biohybrid Materials. *Adv. Funct. Mater.* **n/a**, 2308269.
30. Chen, Z. & Elowitz, M. B. Programmable protein circuit design. *Cell* **184**, 2284–2301 (2021).
31. Chung, H. K. & Lin, M. Z. On the cutting edge: protease-based methods for sensing and controlling cell biology. *Nat. Methods* **17**, 885–896 (2020).
32. Fink, T. & Jerala, R. Designed protease-based signaling networks. *Curr. Opin. Chem. Biol.* **68**, 102146 (2022).
33. Liu, P. *et al.* A Bioorthogonal Small-Molecule-Switch System for Controlling Protein Function in Live Cells. *Angew. Chem. Int. Ed.* **53**, 10049–10055 (2014).
34. Dorr, B. M., Ham, H. O., An, C., Chaikof, E. L. & Liu, D. R. Reprogramming the specificity of sortase enzymes. *Proc. Natl. Acad. Sci.* **111**, 13343–13348 (2014).
35. Keeble, A. H. *et al.* DogCatcher allows loop-friendly protein-protein ligation. *Cell Chem. Biol.* **29**, 339-350.e10 (2022).
36. Abdelkader, E. H. & Otting, G. NT*-HRV3CP: An optimized construct of human rhinovirus 14 3C protease for high-yield expression and fast affinity-tag cleavage. *J. Biotechnol.* **325**, 145–151 (2021).
37. Zakeri, B. *et al.* Peptide tag forming a rapid covalent bond to a protein, through engineering a bacterial adhesin. *Proc. Natl. Acad. Sci. U. S. A.* **109**, E690–E697 (2012).
38. Tavassoli, A. & Benkovic, S. J. Split-intein mediated circular ligation used in the synthesis of cyclic peptide libraries in E. coli. *Nat. Protoc.* **2**, 1126–1133 (2007).
39. Veggiani, G. *et al.* Programmable polyproteams built using twin peptide superglues. *Proc. Natl. Acad. Sci. U. S. A.* **113**, 1202–1207 (2016).
40. Kolar, K., Knobloch, C., Stork, H., Žnidarič, M. & Weber, W. OptoBase: A Web Platform for Molecular Optogenetics. *ACS Synth. Biol.* **7**, 1825–1828 (2018).
41. Armbruster, A., Mohamed, A. M., Phan, H. T. & Weber, W. Lighting the way: recent developments and applications in molecular optogenetics. *Curr. Opin. Biotechnol.* **87**, 103126 (2024).
42. Zhang, W. *et al.* Optogenetic control with a photocleavable protein, PhoCl. *Nat. Methods* **14**, 391–394 (2017).

43. Cui, M. *et al.* A single-component, light-assisted uncaging switch for endoproteolytic release. *Nat. Chem. Biol.* **20**, 353–364 (2024).
44. Xiang, D. *et al.* Hydrogels With Tunable Mechanical Properties Based on Photocleavable Proteins. *Front. Chem.* **8**, (2020).
45. Kashyap, P. *et al.* An optogenetic method for the controlled release of single molecules. *Nat. Methods* **21**, 666–672 (2024).
46. Shadish, J. A., Strange, A. C. & Deforest, C. A. Genetically Encoded Photocleavable Linkers for Patterned Protein Release from Biomaterials. *J. Am. Chem. Soc.* **141**, 15619–15625 (2019).
47. Gregorio, N. E. & DeForest, C. A. PhoCoil: An Injectable and Photodegradable Single-component Recombinant Protein Hydrogel for Localized Therapeutic Cell Delivery. 2024.05.07.592971 Preprint at https://doi.org/10.1101/2024.05.07.592971 (2024).
48. Dang, B. *et al.* SNAC-tag for sequence-specific chemical protein cleavage. *Nat. Methods* **16**, 319–322 (2019).

Methods

Method S6.1 Plasmid construction for bioactive protein operators

The open reading frames (ORFs) of the reported logical operators are given below (5' → 3'):

EGF: A – YES
MGSS-hEGF-GGS(x3)-2A9c-GGS(x3)-SpyTag-GGS(x3)LE-6xHis

ATGGGAAGTTCAAATTCTGATAGCGAATGTCCGCTGAGCCATGACGGTTACTGCCTGCACGACG
GCGTCTGTATGTATATCGAGGCGCTGGACAAATACGCCTGCAACTGCGTTGTTGGTTACATTGG
TGAGCGCTGTCAGTATCGTGATTTGAAGTGGTGGGAACTGCGTGGTGGTAGCGGCGGGTCGGGC
GGCAGCCTCGCGGAAACCGGTGGCGGTTCCGGTGGTTCTGGCGGCAGCGCTCACATCGTGATGG
TGGATGCATATAAACCGACGAAGGGTGGCTCCGGCGGTAGCGGTGGCTCTCTCGAGCACCACCA
CCACCACCAC

bla: A ∨ T
MGSS-bla-GGS(x3)-2A9c-GGS(x3)-TEVc-GGS(x3)-SpyTag-GGS(x3)LE-6xHis

ATGGGAAGTTCAATGCACCCCGAAACACTAGTGAAGGTGAAGGACGCGGAGGACCAGCTGGGTG
CGCGTGTGGGCTATATTGAGCTGGATCTGAACAGCGGTAAGATCCTGGAAAGCTTTCGTCCGGA
AGAACGCTTTCCGATGATGAGCACCTTCAAGGTGCTGCTGTGCGGCGCGGTGCTGAGCCGTGTC
GACGCTGGTCAAGAGCAGCTGGGTCGCCGTATCCACTACTCGCAAAACGACTTAGTTGAGTACA
GCCCGGTTACGGAAAAGCACCTGACCGATGGTATGACGGTTCGTGAACTGTGTAGCGCCGCGAT
CACCATGTCTGATAATACCGCAGCGAACCTGTTGCTCACTACAATTGGTGGTCCGAAAGAGTTG
ACGGCGTTTCTGCACAACATGGGTGATCATGTTACCCGTCTGGACCGCTGGGAACCGGAGTTAA
ATGAAGCCATTCCGAATGACGAGCGCGATACCACCATGCCGGCAGCTATGGCTACCACTCTGCG
TAAACTGTTGACCGGCGAGTTGTTGACCCTCGCGAGCCGTCAACAACTCATTGATTGGATGGAA
GCAGACAAGGTCGCAGGCCCACTGTTGCGTTCCGCTCTTCCGGCTGGTTGGTTCATCGCGGATA
AAAGCGGTGCGGGCGAACGTGGTTCAAGAGGCATTATCGCCGCGCTGGGGCCTGACGGTAAGCC
GAGCCGCATCGTTGTAATTTATACCACCGGCTCCCAGGCGACGATGGATGAGCGCAACCGTCAG
ATCGCGGAGATCGGTGCCAGCCTGATTAAACATTGGGGTGGCTCCGGAGGTAGTGGCGGCTCTT
TGGCGGAAACCGGTGGAGGTAGCGGTGGCTCCGGCGGCAGCGAGAACCTGTACTTCCAGAGCGG
TGGCTCCGGTGGCTCTGGTGGCTCTGCGCATATCGTGATGGTTGACGCATATAAACCGACGAAA
GGTGGCTCGGGCGGTTCAGGCGGCTCCCTCGAGCACCACCACCACCACCAC

NanoLuc: A ∧ T

MGSS-CfaC-GGS(x3)-2A9c-GGS(x3)-NanoLuc-GGS(x3)-TEVc-GGS(x3)-SpyTag-GGS(x3)-6xHis-GGS(x3)-CfaN-SsrA

ATGGGAAGTTCAGTAAAAATTATAAGCAGGAAGAGCCTGGGCACACAGAACGTGTACGACATCG
GCGTCGAGAAGGATCACAACTTTCTGCTGAAGAACGGTTTGGTAGCCAGCAATTGTTTTAACGG
CGGGTCTGGCGGTTCTGGCGGCAGCCTGGCTGAAACCGGCGGCGGCAGCGGCGGTTCCGGTGGC
AGCGTTTTCACGCTGGAGGATTTTGTTGGTGACTGGCGCCAGACCGCAGGTTATAACTTGGATC
AGGTCCTGGAACAAGGTGGTGTGTCCAGCTTGTTCCAAAACTTGGGCGTGAGCGTCACTCCGAT
TCAACGTATTGTGCTGTCAGGCGAAAATGGCTTAAAGATCGACATCCACGTGATCATCCCGTAC
GAGGGTCTGAGCGGTGATCAAATGGGTCAGATTGAAAAGATTTTCAAGGTTGTTTACCCGGTTG
ACGACCATCACTTTAAAGTTATCCTGCATTATGGTACCTTGGTTATCGACGGTGTTACTCCGAA
TATGATTGATTACTTTGGTCGTCCGTACGAGGGCATCGCCGTATTCGATGGTAAAAAAATCACC
GTGACGGGTACCTTATGGAATGGAAACAAAATTATTGACGAGCGTCTTATCAACCCGGATGGTT
CCCTCCTGTTTCGTGTTACGATCAATGGCGTCACCGGTTGGCGTCTTTGCGAACGTATCCTGGC
GGGTGGCAGCGGTGGCTCCGGCGGTTCGGAAAACCTGTACTTCCAGAGCGGGGGCTCCGGTGGG
TCGGGTGGTTCTGCACATATTGTGATGGTTGATGCGTATAAACCGACCAAAGGTGGTTCCGGGG
GTAGCGGGGGCAGCCATCACCATCACCACCACGGCGGTTCCGGTGGCAGCGGCGGATCTGCGGA
ATATTGTTTGAGCTATGACACCGAAATCTTGACCGTGGAATACGGCTTTCTGCCTATTGGCAAA
ATCGTGGAAGAACGCATCGAGTGCACCGTGTATACCGTGGATAAGAACGGCTTCGTGTACACCC
AGCCGATTGCGCAGTGGCATAATCGTGGTGAGCAAGAAGTTTTCGAGTACTGCTTGGAGGACGG
TAGCATTATTCGTGCTACCAAGGACCACAAATTCATGACGACCGATGGTCAAATGCTGCCAATC
GACGAGATCTTCGAGCGCGGTCTGGACCTGAAGCAGGTTGACGGCCTGCCGGCAGCTAATGATG
AGAACTATGCGCTGGCGGCG

HER2: (A ∨ T) ∧ C

MGSS-CfaC-GGS(x3)-2A9c-GGS(x6)-TEVc-GGS(x3)-HER2(NB)-GGS(x3)-HRV-3cc-GGS(x3)-SpyTag-GGS(x3)-6xHis-GGS(x3)-CfaN-SsrA

ATGGGAAGTTCAGTAAAAATTATATCTAGGAAGAGCCTGGGTACTCAAAACGTGTACGACATCG
GCGTTGAAAAAGACCATAATTTTTTGCTGAAGAACGGTCTGGTGGCTAGCAATTGTTTCAACGG
TGGCTCGGGCGGTTCTGGCGGCAGCTTGGCGGAAACCGGTGGCGGCTCCGGCGGCAGTGGAGGC
TCCGGCGGCTCCGGCGGGTCGGGTGGTAGCGAAAACCTGTATTTCCAAAGCGGCGGTTCGGGCG
GTAGTGGCGGTTCCGTCCAACTGCAGGAGAGCGGCGGTGGCTTGGTTCAGCCGGGCGGTTCTCT
GAGATTAAGCTGTGCCGCGAGCGGTTTCACGTTTGGTGATAGCGGCATGGGTTGGTATCGTCAG
GCACCGGGAAACGAGTGCGAATTGGTCAGCTCAGTTAGCTCGGATGGTTCCACCTATTACGCGG
ACAGCGTTAAAGGCCGTTTTACCATTAGCCAGGATAATGCGAAAAACACCGTCTACTTGCGTAT
GAATAGCCTTAAGCCGGAAGATACGGCTGTTTACTACTGCGCGGCTGATGATCACAAGTACGAA
CTGGGTACGTGCGAGGCACTGGACTATTGGGGTCGCGGTACACAAGTGACCGTTAGCAGCGGCG
GTAGCGGCGGGTCGGGTGGCTCATTGGAGGTGCTGTTTCAAGGTCCGGGTGGATCCGGTGGATC
TGGCGGTAGCGCGCATATCGTGATGGTGGACGCATATAAACCGACCAAGGGTGGCTCCGGCGGT
TCCGGCGGCAGCCATCACCACCACCACCATGGTGGTTCCGGTGGTAGCGGTGGTTCTGCCGAAT
ACTGCCTGAGCTATGACACTGAAATCCTGACCGTGGAGTATGGTTTCCTGCCAATCGGTAAAAT
CGTAGAGGAACGCATTGAATGTACCGTTTACACCGTGGACAAAAACGGCTTCGTGTACACGCAA
CCGATTGCGCAGTGGCATAACCGCGGTGAACAGGAGGTTTTTGAGTACTGCCTGGAGGACGGCT
CCATTATTCGTGCTACCAAGGACCACAAATTCATGACCACCGATGGTCAGATGCTGCCGATCGA

TGAGATCTTCGAGCGTGGTCTTGACCTGAAGCAGGTTGACGGTCTGCCGGCAGCTAATGATGAG
AACTATGCGCTGGCGGCG

Trx: (A ∧ C) ∨ T

MGSS-SnoopTag-GGS(x3)-2A9c-GGS(x3)-Trx-GGS(x3)-HRV-3cc-GGS(x3)-SnoopCatcher-GGS(x3)-TEVc-GGS(x3)-SpyTag-GGS(x3)LE-6xHis

ATGGGAAGTTCAAAACTAGGGGATATAGAATTCATTAAGGTCAATAAAGGTGGGAGCGGTGGTA
GCGGTGGCTCCTTGGCGGAAACCGGTGGCGGCTCGGGCGGTAGCGGTGGCTCCATGTCCGACAA
GATCATCCATCTGACCGACGATAGCTTTGATACCGACGTGCTGAAAGCGGACGGCGCGATTTTG
GTTGATTTTTGGGCAGAGTGGTGTGGTCCGTGCAAAATGATTGCACCGATCCTGGATGAGATCG
CGGACGAGTACCAGGGTAAGTTAACCGTAGCCAAATTGAATATTGACCAAAACCCGGGTACGGC
TCCGAAGTACGGTATTCGTGGGATCCCGACTCTGTTGCTGTTCAAAAACGGTGAGGTCGCGGCA
ACCAAAGTTGGTGCCCTGAGCAAGGGCCAGCTGAAAGAGTTCCTGGACGCTAACCTGGCGGGTG
GCAGTGGTGGCAGCGGCGGTAGCCTGGAAGTGCTGTTCCAAGGTCCGGGTGGTTCTGGTGGAAG
CGGTGGTAGCAAGCCCCTGCGTGGTGCAGTTTTTAGCCTTCAGAAACAACATCCGGATTACCCG
GACATCTATGGTGCGATCGACCAAAACGGTACGTATCAGAACGTGCGCACCGGTGAAGATGGTA
AACTGACGTTTAAGAACCTCTCAGATGGCAAGTACCGCCTGTTCGAAAACAGCGAACCAGCTGG
TTATAAGCCGGTGCAGAACAAGCCGATCGTGGCGTTTCAAATCGTGAACGGCGAGGTGCGTGAT
GTTACCAGCATCGTTCCGCAGGATATCCCGGCTACCTACGAATTCACTAATGGTAAGCACTACA
TCACCAATGAACCGATTCCACCTAAAGGTGGCTCCGGCGGTTCTGGCGGTTCCGAGAATTTATA
TTTCCAGAGCGGCGGCTCCGGCGGTAGCGGCGGCTCTGCACACATTGTTATGGTTGACGCGTAT
AAGCCGACCAAAGGTGGCTCAGGCGGCTCTGGTGGCTCGCTCGAGCACCACCACCACCACCAC

Neo: A ∨ T ∨ C

MGSS-Neo-GGS(x3)-2A9c-GGS(x3)-TEVc-GGS(x3)-HRV-3cc-GGS(x3)-SpyTag-GGS(x3)LE-6xHis

ATGGGAAGTTCACCCAAAAAGAAAATACAATTGCACGCCGAGCACGCTCTCTATGATGCGCTGA
TGATCTTGAATATTGTGAAAACGAACAGCCCGCCAGCAGAAGAGAAGCTGGAGGACTATGCGTT
TAACTTTGAACTGATTTTGGAAGAGATCGCGCGTCTGTTCGAGAGCGGCGATCAGAAGGACGAA
GCGGAAAAGGCGAAACGTATGAAAGAATGGATGAAGCGCATCAAAACCACCGCTAGCGAAGACG
AGCAGGAGGAAATGGCTAATGCGATTATCACCATCTTACAGAGCTGGATTTTTAGCGGTGGTTC
TGGCGGTTCCGGTGGTTCCCTGGCAGAGACTGGTGGCGGCAGCGGTGGTAGCGGCGGTTCAGAG
AACCTGTACTTCCAAAGCGGAGGCTCTGGGGGTTCGGGCGGCAGCCTGGAAGTTCTGTTCCAAG
GCCCGGGTGGCTCCGGCGGCTCCGGTGGTAGCGCACATATCGTGATGGTTGATGCCTACAAGCC
GACCAAAGGTGGCTCGGGTGGTTCTGGCGGTTCTCTCGAGCACCACCACCACCACCAC

mGreenLantern: A ∧ T ∧ C

MGSS-SnoopTag-GGS(x10)-HRV-3cc-GGS(x10)-DogCatcher-GGS(x10)-SpyTag-GGS(x5)-2A9c-GGS(x5)-mGreenLantern-GGS(x10)-SnoopCatcher-GGS(x10)-TEVc-GGS(x5)-6xHis-GGS(x10)-DogTag

ATGGGAAGTTCAAAACTAGGGGATATAGAATTCATCAAAGTTAACAAGGGTGGTTCGGGAGGTA
GCGGGGGTAGTGGCGGAAGCGGCGGCTCAGGCGGTTCCGGCGGTAGCGGTGGATCTGGTGGTAG
CGGCGGTTCCCTGGAAGTTCTGTTCCAAGGCCCGGGTGGCAGCGGCGGTAGCGGCGGCAGCGGA
GGCTCTGGCGGGTCGGGTGGCTCGGGCGGGTCTGGTGGCAGCGGTGGGAGTGGTGGTAGCAAAT
TAGGCGAGATCGAATTCATCAAGGTGGATAAAACCGATAAAAAACCGCTGCGCGGTGCGGTGTT
TAGCCTGCAGAAGCAACACCCGGATTACCCGGACATCTACGGTGCGATTGACCAGAATGGGACG
TACCAGGATGTGCGCACTGGTGAGGACGGCAAGTTGACCTTTACCAACCTGTCCGACGGAAAGT
ATCGTCTTATCGAGAACAGCGAGCCGCCGGGTTATAAGCCGGTTCAAAACAAACCAATCGTTAG
CTTTCGTATTGTGGATGGTGAGGTGCGCGACGTGACCTCGATCGTACCGCAGGGTGGGTCGGGC
GGTTCCGGGGGTAGCGGCGGATCTGGCGGTTCCGGTGGCTCCGGTGGTAGTGGTGGCAGCGGCG
GCTCCGGTGGTTCTGCACATATTGTCATGGTGGACGCATATAAACCGACCAAAGGCGGTAGCGG
CGGCTCAGGGGGTTCTGGGGGTAGCGGCGGATCCCTGGCGGAAACCGGCGGTGGTAGCGGTGGT
TCCGGAGGTTCCGGCGGCAGCGGCGGCTCGATGGTCAGCAAGGGCGAGGAACTGTTTACCGGTG
TCGTGCCAATCCTGGTGGAACTGGATGGGGACGTGAACGGTCATAAGTTCAGCGTTCGTGGTGA
AGGTGAGGGTGACGCCACAAATGGCAAATTGACCCTCAAGTTTATTTGTACCACCGGCAAGTTA
CCGGTTCCGTGGCCGACGTTGGTTACTACGCTGGGTTACGGCGTGGCGTGCTTCGCGCGTTATC
CGGACCACATGAAACAGCATGATTTCTTTAAAAGCGCTATGCCGGAAGGTTACGTTCAAGAGCG
TACCATCAGCTTTAAGGATGATGGCACCTACAAGACGCGTGCAGAAGTTAAATTCGAAGGCGAT
ACCTTGGTTAATCGTATCGTTCTGAAGGGCATTGACTTTAAGGAAGACGGCAATATCTTGGGCC
ACAAACTGGAATATAACTTCAACAGCCACAAGGTGTACATCACCGCTGACAAACAAAAAAACGG
CATCAAAGCGAACTTCAAGACGCGACATAATGTCGAAGATGGGGGTGTGCAGCTGGCCGATCAC
TACCAACAGAACACTCCGATTGGCGACGGTCCGGTTCTCCTCCCGGACAATCACTACCTGTCTC
ATCAGAGCAAGCTGTCCAAGGATCCGAATGAAAAACGTGACCACATGGTTCTGAAAGAACGTGT
TACTGCTGCGGGTATTACGCATGATATGGATGAACTGTACAAAGGTGGCTCCGGTGGTTCGGGC
GGTTCTGGTGGCAGCGGTGGTAGCGGGGGGAGCGGAGGCTCCGGTGGTTCCGGCGGCTCGGGCG
GTTCCAAGCCGCTGCGTGGTGCGGTTTTTAGCTTGCAAAAGCAACATCCGGATTATCCGGACAT
CTATGGTGCGATCGACCAGAACGGAACCTACCAAAACGTGCGCACCGGCGAGGACGGCAAGTTG
ACCTTCAAGAACTTGTCTGATGGAAAGTACCGCCTGTTCGAGAATTCTGAGCCTGCTGGTTACA
AACCGGTGCAAAACAAACCGATTGTGGCATTTCAGATTGTTAATGGTGAGGTCAGAGATGTCAC
CTCCATTGTTCCACAGGATATTCCGGCCACCTACGAATTCACCAACGGAAAGCACTATATCACG
AACGAACCGATTCCGCCGAAAGGTGGCAGTGGTGGTTCTGGCGGTAGCGGCGGCAGCGGAGGCT
CCGGGGGTAGCGGTGGTTCCGGCGGCAGCGGCGGCTCTGGAGGGAGTGAGAACCTGTATTTCCA
GTCTGGCGGCTCCGGTGGCTCTGGCGGCAGCGGTGGTTCGGGTGGTTCCCACCACCATCACCAC
CATGGTGGCAGCGGCGGCTCTGGTGGCAGCGGAGGTAGTGGGGGTTCCGGTGGTTCCGGTGGGT
CAGGTGGATCTGGCGGCTCGGGCGGAAGCGACATTCCGGCGACCTACGAGTTCACCGATGGTAA
GCACTATATCACCAATGAGCCGATCCCGCCAAAA

Method S6,2 Plasmid construction for Trx variants releasable through diversified inputs

Trx: P ∧ E
MGSS-CfaC-GGS(x3)-2A9c-GGS(x3)-Trx-GGS(x9)-PhoCl2c-GGS(x9)-SpyTag-GGS(x3)-6xHis- GGS(x3)-CfaN-SsrA

ATGGGAAGTTCAGTAAAAATTATATCTAGGAAGAGCCTGGGTACCCAAAATGTTTACGACATCG
GCGTCGAGAAAGACCACAACTTCCTCCTGAAGAACGGTTTGGTGGCTAGCAATTGTTTTAACGG
TGGCTCGGGTGGCTCTGGTGGTTCCCTGGCGGAAACCGGTGGTGGTAGCGGTGGCAGCGGCGGT
TCCATGAGCGATAAAATCATCCATCTGACTGATGATAGCTTCGATACCGACGTTCTTAAGGCTG
ATGGTGCGATTTTAGTGGACTTTTGGGCGGAGTGGTGCGGTCCGTGTAAAATGATTGCGCCAAT
TCTGGACGAAATTGCGGATGAATACCAAGGTAAGTTGACGGTGGCCAAATTAAACATCGACCAG
AATCCGGGTACAGCACCGAAATACGGTATCCGCGGTATTCCGACCCTGCTGCTGTTTAAGAACG
GCGAGGTCGCCGCGACCAAAGTGGGTGCCCTGAGCAAAGGTCAACTGAAGGAGTTTCTGGACGC
CAACCTGGCGGGTGGCAGCGGAGGTAGCGGGGGCAGCGGCGGGAGCGGCGGATCAGGCGGTTCC
GGTGGTTCCGGCGGGAGCGGTGGCAGCGTTATCCCGGATTACTTCAAACAAAGCTTCCCGGAAG
GCTACTCCTGGGAACGTAGCATGACCTATGAAGACGGGGGCATCTGCATTGCGACCAACGATAT
CACCATGGAGGGTGATTCTTTCATTAACAAGATCCACTTCCAGGGTACGAACTTCCCTCCGAAT
GGCCCAGTTATGCAGAAACGTACCGTTGGTTGGGAAGCAAGCACCGAGAAGATGTATGAGCGTG
ATGGTGTTCTGAAAGGTGACGTGAAAATGAAATTGCTGCTTAAGGGCGGCGGTCACTACCGTGG
TGACTACCGCACCACGTACAAAGTTAAGCAAAAACCGGTTAAGCTGCCGGACTGTCATTTTGTG
GATCACCGCATCGAGATATTGTCCCATGATAAGGACTATAACAAGGTGAAGCTGTATGAACATG
CTGTGGCTAAGACCTCGACCGATAGCATGGATGAGCTGTATAAGGGTGGTTCCGGCGGTATGGT
GAGCAAAGGTGAGGAGACGATTACCAGCGTCATCAAACCAGATATGAAAAATAAGCTGCGTATG
GAAGGCAACGTCAATGGTCACGCATTCGTCATCGAAGGTGAGGGGTCTGGGAAACCGTTCGAGG
GAATCCAGACCATTGACCTGGAAGTTAAAGAAGGTGCGCCGCTGCCTTTCGCCTATGATATCTT
GACAACTGCGTTTCATTACGGCAATCGTGTTTTCACCAAGTATCCGCGTGGCGGCTCAGGCGGC
TCTGGCGGCAGCGGTGGCAGTGGCGGCTCTGGCGGCTCTGGCGGCTCCGGCGGATCGGGCGGTA
GCGCGCACATTGTTATGGTTGACGCATACAAGCCGACGAAAGGCGGTAGCGGAGGTTCCGGTGG
CAGCCATCATCACCACCACCACGGGGGCTCCGGTGGTTCTGGTGGTTCTGCGGAGTATTGCCTG
AGCTATGACACCGAGATCTTGACCGTGGAATATGGTTTTCTACCGATTGGTAAAATCGTGGAAG
AGCGCATCGAGTGCACCGTCTACACCGTAGACAAGAACGGCTTCGTGTACACGCAGCCGATCGC
GCAGTGGCATAACCGTGGTGAGCAGGAAGTGTTTGAGTACTGCCTGGAGGACGGAAGTATTATT
AGAGCGACGAAGGACCACAAATTCATGACCACTGACGGTCAGATGCTGCCGATCGATGAAATTT
TTGAACGCGGCTTGGACTTGAAGCAAGTTGATGGCCTTCCGGCAGCGAATGACGAGAACTATGC
ACTGGCTGCT

CHAPTER 7: NEW AVENUES FOR AUTONOMOUSLY COMPILED MOLECULAR TOPOLOGIES

Adapted from Gharios, R.*, Ross, M.L.*, Li, A.^, Kottantharayil, S.^, DeForest, C.A. (*in preparation*)

*denotes co-first authorship.
^denotes equal contribution.

7.1. Engineering User Control over Bulk Material Degradation

7.1.1. Background

Having successfully demonstrated the deployment of an autonomously compiled topology approach for the generation of a suite of releasable tethers from material supports, we sought to leverage many of the benefits inherent to our method (e.g., scalability, ease of debugging, rapid DBTL cycles, etc.) to expand its applicability further. A direct extension of our approach requiring minimal sequence re-engineering and optimization would be to re-purpose our current array of plasmids, which spans all 17 possible combinations of YES/AND/OR operators using three orthogonal proteases as inputs, into an exhaustive suite of material crosslinks. Functionally, this would enable us to switch from controlling biomacromolecule release from underlying material anchors such as hydrogel matrices or functionalized beads, and instead program bulk material degradation using similar designs.

7.1.2. Approach

7.1.2.1. Crosslink sequence design

While previous tether-based plasmid sequences necessitated the inclusion of one “anchor” point for covalent tethering into a material support, a crosslink design would require two such anchors

at a minimum. For our two previous reports, we had elected to use SpyTag to covalently anchor biomacromolecules into SpyCatcher-presenting materials through SpyLigation. Thus, in order to engineer polypeptides as crosslinks, I incorporated two SpyTags around our fluorescent mGreenLantern. This strategy holds several benefits: 1) the protein is large enough to be analyzed via SDS-PAGE, and 2) the crosslinker's intrinsic fluorescence can be exploited to quantify material degradation. All proteins were purified as described previously (refer to Chapters 5 and 6) and were verified through LC-MS (**Figure 1**) and SDS-PAGE analysis.

7.1.2.2. Base material sequence design

With our engineered crosslinks in hand, we sought to identify a suitable base material for our proof-of-concept hydrogel networks. The broad utility of SpyLigation enables us to theoretically select any material based on the requirements of the application at hand. For example, we could envision a synthetic backbone (e.g., PEG) consisting of a multi-armed structure (where the valency is greater than or equal to 3) end-capped with strained alkynes (e.g., DBCO). We could then "click" in our pre-validated SpyCatcher-azide through SPAAC, thereby enabling us to crosslink these materials through SpyLigation. However, for the purposes of this work, we elected to adopt a purely genetically encoded route, reasoning that this would allow us to pre-program and, if needed, screen through different material properties through facile sequence modification.

Toward this end, I reviewed some prior literature that reports the synthesis of fully protein-based hydrogel networks. Deciding to avoid globular folds as backbone sequences, I gravitated in the direction of telechelic chains, reasoning that these would express better, particularly when interspaced by a minimum of 3 SpyCatcher motifs. Elastin-like polypeptides (ELPs) in specific

are a workhorse material that have been used for the preparation of fully recombinant protein-based networks by multiple groups over the years, and lend themselves well to purification through routine IMAC as well as potentially faster alternative methods such as heat cycling. In the same vein, our group has pioneered the use of XTEN – a repeat peptide sequence first deployed as a genetically encoded alternative to PEG for the extension of therapeutic half-life – as a backbone sequence for hydrogel biomaterials. Having decided to test both putative directions, I designed two backbone sequences that use either ELP or XTEN as telechelic chain. Both sequences are otherwise similar, as they incorporate the use of GS spacers to separate the telechelic chain from the incorporated SpyCatcher motifs. Furthermore, both designs contain a total of 3 SpyCatchers since this is the theoretical minimum of covalent anchoring points that would enable us to form a gel with our dually SpyTagged crosslinkers. We refer to the backbone sequence plasmids as "TriCatcher-X" where X refers to the specific telechelic chain adopted. Moreover, the crosslinks had been designed similarly to the tethers (**Chapter 5**), in that they harbored a fluorescent protein payload (rendering longitudinal tracking of gel degradation possible) and a 6xHistidine tag for IMAC purification. Differently from the tethered cargos, however, these sequences harbor two SpyTags that flank the protein instead of one; this design change theoretically enables us to form covalently linked networks thanks to the final Tag/Catcher valency.

7.1.3. Methods

The sequences designed for the suite of crosslinks is provided below, along with their corresponding annotation.

YES Gates

mGreenLantern – A YES

MGSS-SpyTag-GGS(x3)-mGreenLantern-GGS(x3)-2A9c-GGS(x3)-SpyTag-GGS(x3)-6xHis

```
ATGGGATCAAGTGCTCACATAGTAATGGTTGACGCGTACAAGCCGACGAAGGGTGGTAGCGGTG
GCTCTGGTGGCTCCATGGTCAGCAAGGGTGAGGAATTGTTTACCGGTGTTGTGCCGATCCTGGT
GGAGCTGGATGGCGACGTGAACGGCCACAAGTTCAGCGTTCGTGGTGAAGGTGAGGGCGACGCG
ACCAACGGTAAATTGACCCTGAAGTTCATCTGCACCACGGGTAAGCTGCCGGTGCCGTGGCCGA
CTTTGGTGACCACGCTTGGTTACGGCGTGGCATGTTTTGCACGTTATCCGGACCACATGAAACA
GCACGACTTCTTTAAGAGCGCTATGCCGGAAGGTTATGTGCAAGAACGTACCATTAGCTTTAAG
GACGACGGCACCTACAAGACCCGCGCGGAGGTCAAATTCGAGGGCGACACCTTGGTAAACAGAA
TCGTGTTAAAGGGCATCGATTTCAAGGAGGATGGTAATATTCTGGGTCATAAGCTGGAATATAA
CTTTAACAGCCATAAAGTTTATATCACGGCTGATAAACAAAAAAACGGTATCAAAGCCAATTTC
AAGACCCGTCATAACGTGGAAGATGGTGGTGTCCAGCTGGCGGACCACTACCAGCAAAACACCC
CGATTGGTGACGGCCCTGTTTTGCTGCCAGATAATCATTACCTGAGCCACCAGAGCAAACTCTC
GAAGGACCCGAATGAGAAACGTGATCACATGGTTCTGAAAGAGCGCGTTACTGCCGCGGGTATT
ACCCATGATATGGATGAACTGTATAAAGGCGGATCTGGTGGGTCCGGCGGAAGCCTGGCGGAAA
CGGGTGGCGGTAGCGGCGGTTCTGGCGGTAGTGCACATATTGTTATGGTTGATGCGTACAAACC
GACCAAGGGTGGTTCCGGCGGCTCGGGCGGCTCCCATCACCACCACCACCAC
```

mGreenLantern – T YES

MGSS-SpyTag-GGS(x3)-mGreenLantern-GGS(x3)-TEVc -GGS(x3)-SpyTag-GGS(x3)-6xHis

```
ATGGGATCAAGTGCTCACATAGTAATGGTTGACGCCTACAAGCCAACGAAAGGTGGTTCAGGTG
GTTCCGGTGGCTCCATGGTCAGCAAGGGTGAGGAATTGTTTACCGGTGTCGTGCCGATCCTGGT
AGAGCTGGATGGCGACGTTAACGGTCACAAGTTCAGCGTTCGTGGTGAGGGCGAGGGCGACGCT
ACCAATGGCAAACTGACCCTGAAATTCATCTGCACCACCGGTAAGCTGCCGGTGCCGTGGCCTA
CGCTCGTGACAACCCTGGGTTACGGCGTGGCGTGTTTTGCCCGTTATCCGGACCACATGAAACA
ACACGACTTCTTTAAAAGCGCTATGCCGGAAGGTTATGTTCAAGAGCGCACCATTAGCTTTAAG
GACGACGGCACCTATAAGACCCGTGCGGAAGTTAAATTTGAAGGCGACACCCTGGTGAACCGCA
TTGTTTTGAAGGGAATCGATTTCAAGGAGGATGGAAACATTCTGGGTCATAAGTTGGAATACAA
CTTCAACAGCCATAAGGTCTATATCACTGCGGATAAACAGAAAAACGGTATCAAAGCAAATTTC
AAGACTCGCCATAATGTTGAGGACGGTGGCGTGCAACTGGCAGATCACTACCAGCAGAACACCC
CGATTGGTGACGGACCGGTGTTGCTGCCGGATAATCATTACCTGAGCCATCAGAGCAAGCTTAG
CAAAGATCCGAATGAAAAACGTGATCACATGGTCCTGAAAGAGCGTGTTACCGCGGCAGGTATC
```

ACGCACGACATGGATGAATTATATAAGGGTGGTTCGGGCGGCAGCGGCGGCTCTGAAAACCTGT
ACTTCCAGTCGGGAGGCAGCGGTGGCTCCGGTGGCTCTGCGCATATTGTGATGGTTGATGCGTA
CAAGCCGACGAAAGGTGGTTCCGGCGGCAGTGGTGGTAGCCACCACCACCACCACCAT

mGreenLantern – C YES

MGSS-SpyTag-GGS(x3)-mGreenLantern-GGS(x3)-HRV-3Cc-GGS(x3)-SpyTag-GGS(x3)-6xHis

ATGGGATCAAGTGCTCACATAGTAATGGTTGACGCGTACAAGCCGACGAAGGGTGGTAGCGGTG
GCTCTGGTGGCTCCATGGTCAGCAAGGGTGAGGAATTGTTTACCGGTGTTGTGCCGATCCTGGT
GGAGCTGGATGGCGACGTGAACGGCCACAAGTTCAGCGTTCGTGGTGAAGGTGAGGGCGACGCG
ACCAACGGTAAATTGACCCTGAAGTTCATCTGCACCACGGGTAAGCTGCCGGTGCCGTGGCCGA
CTTTGGTGACCACGCTTGGTTACGGCGTGGCATGTTTTGCACGTTATCCGGACCACATGAAACA
GCACGACTTCTTTAAGAGCGCTATGCCGGAAGGTTATGTGCAAGAACGTACCATTAGCTTTAAG
GACGACGGCACCTACAAGACCCGCGCGGAGGTCAAATTCGAGGGCGACACCTTGGTAAACAGAA
TCGTGTTAAAGGGCATCGATTTCAAGGAGGATGGTAATATTCTGGGTCATAAGCTGGAATATAA
CTTTAACAGCCATAAAGTTTATATCACGGCTGATAAACAAAAAAACGGTATCAAAGCCAATTTC
AAGACCCGTCATAACGTGGAAGATGGTGGTGTCCAGCTGGCGGACCACTACCAGCAAAACACCC
CGATTGGTGACGGCCCTGTTTTGCTGCCAGATAATCATTACCTGAGCCACCAGAGCAAACTCTC
GAAGGACCCGAATGAGAAACGTGATCACATGGTTCTGAAAGAGCGCGTTACTGCCGCGGGTATT
ACCCATGATATGGATGAACTGTATAAAGGCGGATCTGGTGGGTCCGGCGGAAGCCTAGAAGTAT
TATTTCAAGGACCCGGCGGTAGCGGCGGTTCTGGCGGTAGTGCACATATTGTTATGGTTGATGC
GTACAAACCGACCAAGGGTGGTTCCGGCGGCTCGGGCGGCTCCCATCACCACCACCACCAC

OR Gates

mGreenLantern – A ∨ T

MGSS-SpyTag-GGS(x3)-mGreenLantern-GGS(x3)-2A9c-GGS(x3)-TEVc-GGS(x3)-SpyTag-GGS(x3)-6xHis

ATGGGATCAAGTGCTCACATAGTAATGGTTGACGCCTACAAACCGACGAAAGGTGGCAGCGGCG
GTAGCGGAGGCAGCGTCAGCAAGGGTGAGGAACTGTTCACCGGTGTTGTTCCGATTCTGGTAGA
GCTGGATGGCGACGTTAACGGTCACAAGTTCAGCGTTCGTGGTGAGGGTGAAGGTGACGCGACC
AATGGCAAACTGACCCTGAAATTTATCTGCACCACCGGTAAACTCCCTGTGCCGTGGCCGACTC
TTGTGACCACTTTAGGTTATGGTGTCGCGTGTTTTGCACGTTATCCGGATCACATGAAACAACA
TGACTTTTTTAAGAGCGCTATGCCGGAAGGTTACGTGCAAGAAAGAACCATTAGCTTTAAGGAT
GATGGTACGTACAAGACCCGTGCAGAGGTTAAATTCGAGGGCGATACCCTGGTTAATCGTATTG
TGTTGAAGGGCATCGATTTCAAGGAGGACGGCAACATTCTGGGTCACAAGTTAGAATATAACTT
CAACAGCCACAAGGTGTATATCACCGCGGATAAACAGAAAAACGGCATCAAAGCCAATTTCAAA
ACCCGCCATAATGTTGAGGACGGTGGCGTGCAGCTGGCTGACCACTATCAGCAAAACACCCCGA
TCGGGGACGGTCCGGTTTTGCTGCCAGACAACCACTACTTGAGCCACCAGAGCAAGTTGAGCAA
GGACCCGAATGAAAAACGTGATCACATGGTGCTGAAAGAGCGCGTGACGGCGGCAGGTATCACC
CATGACATGGATGAATTGTACAAGGGCGGTTCGGGCGGTTCTGGTGGGTCGCTGGCGGAGACAG

GTGGCGGCTCCGGCGGCTCCGGCGGCTCCGAAAACCTGTACTTCCAGAGCGGCGGTTCCGGAGG
CAGCGGTGGTTCTGCGCATATTGTAATGGTCGATGCGTACAAGCCGACGAAGGGTGGTTCCGGT
GGCTCTGGCGGTTCTCACCACCATCACCACCAT

mGreenLantern – A ∨ C

MGSS-SpyTag-GGS(x3)-mGreenLantern-GGS(x3)-2A9c-GGS(x3)-HRV-3Cc-GGS(x3)-SpyTag-GGS(x3)-6xHis

ATGGGATCAAGTGCTCACATAGTAATGGTTGATGCGTACAAGCCAACCAAGGGGGGCTCCGGGG
GTTCCGGCGGCTCGGTGAGCAAGGGTGAGGAATTGTTCACCGGTGTGGTGCCTATTTTAGTAGA
GCTGGATGGCGACGTTAATGGTCACAAGTTCAGCGTTCGTGGCGAGGGCGAAGGTGACGCGACC
AACGGTAAACTGACCCTGAAATTCATCTGCACCACGGGCAAATTGCCGGTGCCGTGGCCGACGC
TTGTGACGACGCTCGGTTACGGCGTCGCTTGTTTTGCCCGTTATCCGGATCACATGAAACAACA
TGATTTCTTTAAAAGCGCTATGCCGGAGGGTTATGTTCAGGAGCGTACCATTAGCTTTAAGGAT
GACGGCACCTACAAGACCCGCGCAGAAGTTAAATTTGAAGGCGATACCTTGGTCAACCGTATTG
TGCTGAAGGGCATCGACTTTAAAGAAGACGGCAACATTCTGGGTCATAAGCTTGAGTATAACTT
CAACAGCCACAAGGTGTATATCACCGCAGACAAACAGAAGAACGGCATCAAAGCTAATTTCAAA
ACTCGCCATAACGTGGAGGACGGTGGTGTTCAACTGGCCGACCACTACCAGCAGAATACCCCGA
TCGGTGACGGTCCGGTTTTGCTGCCGGATAACCATTACCTGAGCCACCAGAGCAAACTGAGCAA
GGACCCGAATGAAAAACGTGATCACATGGTCCTCAAAGAGCGCGTTACTGCGGCGGGTATTACC
CATGACATGGATGAACTGTATAAGGGTGGTTCAGGTGGTAGCGGCGGTAGTCTGGCGGAAACCG
GTGGCGGTAGCGGTGGTTCTGGCGGGTCTGCGCATATCGTGATGGTTGATGCCTACAAGCCGAC
CAAAGGTGGCTCGGGCGGCTCCGGTGGTAGCCACCATCACCACCACCAT

mGreenLantern – T ∨ C

MGSS-SpyTag-GGS(x3)-mGreenLantern-GGS(x3)- TEVc-GGS(x3)-HRV-3Cc-GGS(x3)-SpyTag-GGS(x3)-6xHis

ATGGGAAGTTCAGCTCACATAGTAATGGTTGACGCGTACAAGCCGACGAAAGGTGGGTCTGGAG
GTTCGGGCGGTAGCGTGTCCAAAGGCGAGGAACTGTTCACCGGTGTTGTTCCGATCCTAGTCGA
GCTGGATGGTGATGTCAACGGCCACAAATTTAGCGTTCGTGGTGAAGGCGAGGGCGACGCGACC
AATGGTAAATTGACCCTTAAGTTTATTTGTACGACCGGTAAACTTCCGGTTCCGTGGCCGACCC
TGGTAACTACGCTGGGTTATGGTGTGGCCTGCTTTGCACGTTACCCGGACCACATGAAACAACA
TGACTTCTTCAAGAGCGCTATGCCGGAAGGTTATGTTCAGGAGCGCACCATTAGCTTTAAGGAC
GACGGCACCTATAAGACCAGAGCGGAAGTGAAATTCGAGGGCGATACGCTGGTGAACCGTATTG
TGCTGAAGGGTATTGATTTTAAAGAGGATGGAAACATTTTAGGTCATAAGTTGGAATACAATTT
TAACAGCCACAAGGTTTATATCACTGCGGATAAACAGAAAAACGGTATCAAAGCGAATTTCAAG
ACTCGCCATAACGTGGAGGACGGTGGCGTTCAGCTGGCAGACCACTACCAGCAAAACACCCCGA
TCGGCGACGGTCCTGTGCTGCTGCCGGACAACCATTACCTGTCCCACCAGAGCAAGTTGTCTAA
GGATCCGAATGAAAAACGTGATCACATGGTTCTCAAGGAGCGTGTTACCGCTGCTGGTATCACC
CATGACATGGATGAACTGTACAAGGGTGGCTCCGGCGGCAGCGGCGGGAGCGAAAATCTGTATT

TCCAAAGCGGCGGATCAGGCGGTAGCGGTGGCAGCCTGGAGGTCTTGTTCCAAGGTCCGGGTGG
GTCCGGCGGCTCCGGTGGTTCGGCGCATATCGTGATGGTGGATGCCTACAAACCAACCAAGGGT
GGCTCAGGGGGTAGTGGTGGCAGCCATCACCACCACCACCAC

AND Gates

mGreenLantern – A ∧ T

MGSS-CfaC-GGS(x3)-SpyTag-GGS(x3)-2A9c-GGS(x3)- mGreenLantern-GGS(x3)-SpyTag-
GGS(x3)- TEVc-GGS(x3)-6xHis-GGS(x3)-CfaN-SsrA

ATGGGAAGTTCAGTAAAAATTATATCTAGGAAGTCCCTGGGCACCCAAAACGTTTACGACATTG
GCGTAGAGAAGGACCACAACTTTTTGCTTAAGAACGGCTTAGTGGCTTCTAACTGCTTTAACGG
TGGCTCTGGTGGCTCTGGTGGCTCTGCCCACATCGTTATGGTGGACGCGTATAAACCGACGAAA
GGTGGGAGCGGCGGTAGCGGTGGTTCCCTGGCGGAAACGGGCGGCGGTTCCGGCGGCAGCGGTG
GTTCCGTGAGCAAGGGTGAGGAACTGTTCACCGGTGTTGTTCCGATCCTGGTCGAACTTGATGG
TGATGTTAACGGCCATAAATTCAGCGTTCGTGGTGAGGGCGAGGGTGATGCCACCAATGGTAAG
TTGACCCTGAAGTTCATCTGCACCACGGGTAAACTGCCGGTGCCGTGGCCTACCCTGGTGACCA
CTTTGGGCTATGGCGTAGCGTGTTTTGCACGTTATCCGGATCACATGAAACAACATGACTTCTT
TAAGAGCGCTATGCCGGAAGGCTATGTACAAGAAAGAACAATTAGCTTTAAGGACGATGGTACG
TACAAGACGCGTGCGGAGGTGAAATTCGAGGGTGACACCTTGGTTAATCGCATCGTCCTCAAGG
GCATCGACTTCAAAGAAGACGGAAACATTCTGGGTCACAAACTGGAATACAATTTCAACAGCCA
CAAGGTGTACATTACCGCGGACAAGCAAAAAAACGGCATTAAAGCAAACTTCAAGACCCGTCAT
AATGTCGAGGACGGTGGCGTGCAGCTGGCGGACCACTACCAGCAGAACACCCCGATCGGCGACG
GACCGGTGTTGTTGCCAGATAATCATTATCTGAGCCATCAGAGCAAATTAAGCAAAGACCCGAA
TGAAAAACGTGATCACATGGTGTTGAAGGAGCGTGTTACTGCGGCTGGTATCACGCATGATATG
GATGAATTATACAAGGGTGGTTCCGGCGGCTCGGGCGGTAGCGCCCATATTGTTATGGTTGACG
CGTATAAGCCGACGAAGGGTGGCTCAGGTGGTTCTGGTGGGTCTGAAAATCTGTACTTCCAGAG
CGGCGGGAGCGGTGGTAGTGGCGGCTCCCACCATCACCACCACCACGGTGGCTCCGGTGGCTCG
GGAGGCAGCGCGGAATACTGCCTGAGCTATGATACCGAAATTCTGACCGTCGAGTACGGTTTTC
TGCCGATCGGCAAAATCGTGGAGGAACGCATTGAATGTACCGTTTACACCGTGGACAAGAACGG
TTTTGTTTATACCCAACCGATCGCCCAGTGGCATAACCGCGGTGAGCAGGAGGTGTTTGAGTAC
TGCCTGGAAGACGGTAGCATTATTCGTGCAACCAAAGATCACAAATTCATGACCACCGATGGTC
AAATGCTGCCGATCGATGAGATCTTTGAGCGCGGTCTGGATCTGAAACAGGTTGACGGCCTGCC
AGCAGCTAATGATGAGAACTATGCACTGGCGGCG

mGreenLantern – A ∧ C

MGSS-CfaC-GGS(x3)-SpyTag-GGS(x3)-2A9c-GGS(x3)- mGreenLantern-GGS(x3)-SpyTag-
GGS(x3)- HRV-3Cc-GGS(x3)-6xHis-GGS(x3)-CfaN-SsrA

ATGGGAAGTTCAGTAAAAATTATAAGCAGGAAGTCCCTTGGTACGCAGAACGTGTACGACATCG
GCGTGGAGAAAGACCACAACTTCCTGCTCAAGAATGGTCTGGTGGCGAGCAATTGTTTTAACGG
TGGTTCGGGCGGCAGCGGGGGCTCCGCTCACATTGTGATGGTTGACGCGTACAAGCCGACGAAA
GGTGGCAGTGGTGGTTCCGGTGGTAGTCTGGCCGAGACGGGTGGTGGTTCTGGTGGCTCCGGCG

GATCCGTGAGCAAGGGCGAAGAACTCTTCACTGGTGTTGTTCCGATCTTGGTCGAGTTAGATGG
TGACGTTAATGGTCATAAATTCAGCGTTAGAGGTGAAGGTGAGGGCGACGCGACCAATGGTAAA
CTGACCTTGAAGTTCATCTGCACCACCGGAAAGTTGCCAGTGCCGTGGCCGACACTAGTCACCA
CCCTGGGCTATGGTGTGGCGTGTTTCGCCCGTTATCCGGATCACATGAAACAGCATGATTTTTT
CAAGAGCGCAATGCCGGAAGGTTATGTTCAAGAGCGCACCATTAGCTTTAAGGACGACGGCACC
TATAAAACTCGCGCGGAAGTAAAATTCGAAGGTGACACCCTGGTAAATCGTATTGTGTTGAAAG
GCATCGATTTCAAAGAAGATGGAAACATTTTGGGCCACAAACTGGAATACAATTTCAACAGCCA
TAAAGTTTACATTACCGCTGATAAGCAAAAAAACGGGATTAAAGCAAACTTCAAGACCCGTCAC
AATGTTGAGGACGGTGGTGTGCAACTGGCGGACCACTATCAGCAAAACACCCCGATCGGCGACG
GTCCGGTTTTGCTGCCGGATAACCATTATCTGAGCCATCAGAGCAAGCTTTCTAAAGACCCGAA
CGAAAAACGTGATCACATGGTGTTGAAGGAGCGTGTTACGGCTGCCGGTATCACCCATGACATG
GATGAACTGTACAAGGGGGGTTCTGGTGGCTCTGGCGGCAGCGCGCACATCGTGATGGTTGACG
CGTACAAACCAACGAAGGGCGGTAGCGGAGGCAGCGGTGGCTCTCTGGAAGTTTTATTTCAGGG
TCCGGGTGGTAGCGGTGGCTCTGGGGGTAGCCATCACCACCACCACCATGGTGGCAGCGGCGGT
TCCGGCGGCTCAGCGGAGTACTGCCTGAGCTATGATACCGAAATTTTGACCGTCGAGTACGGCT
TTCTGCCGATTGGTAAGATCGTTGAGGAGCGCATCGAGTGCACGGTCTACACCGTTGATAAAAA
CGGCTTCGTCTACACCCAGCCGATTGCACAATGGCATAATCGTGGTGAGCAGGAGGTGTTTGAA
TACTGCCTGGAAGACGGCTCGATCATTCGTGCTACCAAGGATCACAAGTTTATGACCACAGATG
GCCAGATGCTGCCCATCGACGAGATCTTTGAACGCGGTCTGGATCTGAAACAAGTGGACGGCCT
GCCGGCAGCGAACGATGAGAACTATGCCCTGGCCGCG

mGreenLantern – T ∧ C

MGSS-CfaC-GGS(x3)-SpyTag-GGS(x3)-TEVc-GGS(x3)- mGreenLantern-GGS(x3)-SpyTag-GGS(x3)-HRV-3Cc-GGS(x3)-6xHis-GGS(x3)-CfaN-SsrA

ATGGGAAGTTCAGTAAAAATTATATCTAGGAAGAGCCTGGGTACACAAAACGTGTACGACATCG
GTGTCGAGAAGGACCACAACTTTCTGCTCAAGAACGGCTTGGTGGCCTCCAACTGCTTTAACGG
TGGCTCAGGTGGCTCTGGTGGTAGCGCGCACATCGTGATGGTGGACGCGTACAAGCCAACGAAA
GGCGGTTCTGGCGGTTCCGGTGGTTCCGAGAACCTGTACTTCCAAAGCGGCGGCTCTGGCGGCT
CGGGCGGAAGTGTCAGCAAAGGTGAAGAACTGTTCACCGGTGTTGTTCCGATTCTGGTCGAGTT
AGATGGTGACGTTAATGGCCATAAGTTCAGCGTGAGAGGTGAGGGCGAAGGTGATGCCACCAAT
GGCAAATTGACCTTGAAGTTCATCTGCACCACGGGTAAACTTCCGGTTCCGTGGCCGACTTTGG
TTACTACGCTGGGTTATGGCGTTGCATGTTTTGCGCGTTACCCGGACCACATGAAACAACATGA
CTTCTTTAAAAGCGCTATGCCGGAAGGTTATGTTCAAGAACGCACCATTAGCTTTAAGGACGAT
GGCACCTATAAAACCCGTGCTGAAGTGAAGTTCGAAGGCGACACCCTGGTGAACCGCATCGTGC
TTAAGGGGATCGACTTCAAAGAGGACGGTAATATTCTGGGCCACAAGTTGGAGTACAATTTCAA
CAGCCATAAAGTTTACATTACTGCGGATAAACAAAAAAACGGCATCAAAGCAAATTTTAAGACC
CGTCATAACGTGGAGGATGGTGGCGTGCAGCTGGCAGATCACTACCAGCAGAATACCCCGATTG
GTGACGGTCCGGTGCTGTTGCCAGACAACCATTATCTGAGCCATCAGAGCAAATTGAGCAAGGA
TCCGAATGAAAAGCGCGATCACATGGTTCTGAAAGAACGTGTTACCGCTGCGGGTATTACCCAC
GATATGGATGAATTATATAAGGGCGGTTCGGGTGGAAGCGGTGGTTCCGCGCACATCGTGATGG
TGGACGCCTACAAACCGACGAAAGGTGGCTCCGGCGGTAGCGGTGGTTCGTTGGAGGTTTTATT
CCAAGGACCGGGTGGGTCTGGCGGCTCTGGTGGCTCCCACCACCACCACCACCACGGCGGTAGC
GGCGGTTCCGGTGGCTCGGCGGAATACTGCCTGAGCTACGACACCGAAATCCTGACCGTAGAAT

ACGGTTTTCTGCCTATCGGCAAGATCGTCGAGGAGCGTATTGAGTGCACCGTTTACACCGTTGA
CAAAAACGGCTTCGTGTATACGCAGCCGATCGCCCAGTGGCATAACCGTGGTGAGCAGGAGGTT
TTTGAATATTGTCTGGAAGATGGTAGCATTATTCGTGCGACCAAGGACCACAAGTTCATGACCA
CCGATGGTCAGATGCTGCCGATTGATGAGATCTTTGAGCGCGGTCTGGACCTGAAGCAGGTAGA
CGGTCTGCCGGCAGCGAATGATGAGAACTATGCACTGGCTGCG

(OR) AND Gates

mGreenLantern – (A ∨ T) ∧ C

MGSS-CfaC-GGS(x3)-SpyTag-GGS(x3)-2A9c-GGS(x3)-TEVc-GGS(x3)-mGreenLantern-
GGS(x3)-SpyTag-GGS(x3)-HRV-3Cc-GGS(x3)-6xHis-GGS(x3)-CfaN-SsrA

ATGGGAAGTTCAGTAAAAATTATATCTAGGAAGAGCCTCGGTACTCAAAACGTATATGATATCG
GTGTCGAGAAGGACCACAACTTTCTGCTGAAGAACGGTCTGGTAGCTAGCAACTGCTTCAACGG
TGGCTCCGGCGGTAGCGGGGGCTCAGCCCACATCGTTATGGTGGACGCGTACAAGCCGACAAAA
GGCGGTTCTGGCGGATCTGGTGGTTCTTTAGCCGAAACCGGCGGCGGATCGGGCGGCTCGGGCG
GCTCTGAAAACCTGTACTTCCAAAGCGGAGGTTCGGGTGGTTCTGGCGGCTCCGTCAGCAAAGG
TGAAGAGCTGTTTACGGGTGTGGTGCCTATCCTGGTCGAGCTGGATGGTGATGTTAATGGCCAC
AAGTTCAGCGTTCGTGGTGAGGGTGAAGGTGACGCTACCAATGGCAAGTTGACCTTGAAATTCA
TTTGTACCACGGGCAAACTGCCAGTGCCGTGGCCGACCTTGGTGACTACGCTGGGTTATGGTGT
GGCGTGTTTTGCGCGTTATCCGGATCACATGAAACAACATGACTTCTTCAAGAGCGCCATGCCG
GAAGGTTATGTTCAAGAGCGTACCATCAGCTTTAAGGATGATGGCACCTATAAAACTAGAGCTG
AAGTCAAATTCGAGGGTGACACCTTGGTCAATCGTATTGTGCTGAAGGGCATCGACTTTAAAGA
AGATGGTAACATCTTGGGTCATAAGCTGGAATACAATTTTAACAGCCACAAAGTTTACATCACC
GCAGATAAACAAAAAAACGGGATCAAAGCGAACTTCAAGACCCGCCACAACGTGGAGGACGGTG
GCGTTCAGCTGGCGGACCACTATCAGCAGAACACCCCGATTGGTGACGGCCCGGTCCTTTTGCC
GGATAATCATTATCTGTCTCACCAGAGCAAACTGAGCAAGGATCCGAATGAGAAACGTGACCAC
ATGGTGTTAAAAGAACGTGTTACGGCAGCGGGTATCACGCACGACATGGATGAGCTGTACAAAG
GTGGCTCGGGCGGCAGCGGTGGCTCCGCGCATATTGTGATGGTTGACGCCTATAAGCCGACCAA
AGGCGGCTCCGGCGGGAGCGGCGGTAGCTTGGAGGTGCTGTTCCAGGGTCCAGGTGGTTCCGGC
GGTAGCGGTGGCAGCCATCACCACCACCATCATGGTGGGTCCGGCGGTAGCGGAGGTTCCGCGG
AATACTGCCTCAGCTATGACACCGAAATTTTGACCGTTGAGTACGGCTTCTTACCGATTGGTAA
GATCGTGGAGGAACGCATCGAATGCACCGTTTACACCGTGGACAAGAACGGTTTTGTTTACACC
CAGCCGATTGCGCAATGGCATAACCGCGGTGAGCAGGAGGTTTTTGAATACTGCCTGGAAGATG
GAAGTATTATACGTGCGACCAAGGACCACAAGTTCATGACCACGGATGGGCAGATGCTGCCGAT
CGACGAGATTTTTGAACGCGGTCTGGATCTGAAACAGGTTGACGGCCTGCCGGCAGCGAATGAT
GAGAATTACGCTTTGGCAGCA

mGreenLantern – (A ∨ C) ∧ T

MGSS-CfaC-GGS(x3)-SpyTag-GGS(x3)-2A9c-GGS(x3)-HRV-3Cc-GGS(x3)-mGreenLantern-
GGS(x3)-SpyTag-GGS(x3)-TEVc-GGS(x3)-6xHis-GGS(x3)-CfaN-SsrA

ATGGGAAGTTCAGTAAAAATTATAAGCAGGAAGAGCCTGGGCACCCAGAATGTTTACGACATCG
GTGTCGAGAAGGACCACAACTTCCTGCTGAAGAACGGTTTGGTCGCGAGCAATTGCTTTAACGG
TGGAAGCGGCGGCTCTGGGGGCAGCGCCCACATCGTGATGGTGGACGCGTATAAGCCAACGAAG
GGCGGCTCGGGCGGTAGCGGCGGTTCCTTGGCGGAGACTGGTGGCGGCAGCGGAGGTTCTGGTG
GTTCTTTGGAGGTGCTGTTTCAAGGTCCGGGTGGTTCCGGTGGCTCTGGCGGTTCCGTGAGCAA
AGGTGAGGAATTGTTCACCGGTGTTGTTCCGATCCTGGTGGAACTGGATGGTGACGTGAACGGT
CACAAGTTCAGCGTTCGTGGTGAGGGTGAGGGTGATGCGACCAATGGCAAGCTGACCCTTAAGT
TCATCTGCACTACGGGTAAACTTCCAGTCCCGTGGCCTACCCTGGTTACCACCTTAGGCTACGG
CGTGGCATGTTTTGCACGTTATCCGGATCACATGAAACAGCATGACTTTTTCAAATCCGCTATG
CCGGAAGGTTATGTTCAAGAGCGCACCATTAGCTTTAAAGACGATGGTACGTACAAGACGAGAG
CGGAAGTTAAATTCGAGGGCGACACCCTGGTTAACCGCATCGTTCTGAAGGGTATCGACTTCAA
AGAGGATGGTAATATTCTCGGTCATAAATTAGAATACAATTTCAACAGCCACAAGGTGTATATC
ACTGCGGATAAACAAAAAAACGGCATCAAAGCAAACTTTAAGACCCGTCATAACGTGGAAGATG
GCGGCGTACAATTGGCTGATCACTATCAGCAAAACACCCCGATCGGCGACGGTCCGGTTTTGCT
GCCGGACAACCATTACCTGAGCCATCAGAGCAAGCTGAGCAAAGATCCGAATGAAAAACGTGAC
CACATGGTGCTGAAAGAGCGTGTTACGGCTGCGGGTATTACCCATGATATGGATGAGTTGTACA
AGGGCGGCTCAGGTGGTTCCGGCGGTTCAGCCCATATTGTGATGGTCGACGCCTACAAGCCGAC
GAAAGGTGGCTCTGGTGGTTCCGGCGGCTCTGAAAATCTGTACTTCCAAAGCGGGGGCAGCGGA
GGCTCGGGTGGCAGCCACCACCACCACCACCATGGTGGTTCCGGCGGGAGCGGTGGCTCCGCGG
AATACTGCCTATCGTATGATACGGAAATCCTGACCGTAGAGTATGGTTTCCTGCCGATTGGTAA
GATCGTGGAAGAGCGCATTGAATGTACCGTGTACACCGTGGACAAAAACGGTTTTGTCTATACT
CAGCCGATTGCACAGTGGCATAACCGCGGTGAGCAGGAGGTTTTTGAATACTGCCTGGAAGACG
GCAGCATTATTCGTGCTACCAAGGACCACAAATTCATGACCACCGATGGTCAGATGCTGCCGAT
CGACGAAATTTTTGAACGTGGCCTGGATCTGAAGCAGGTTGACGGCCTCCCGGCAGCGAATGAT
GAAAACTATGCCCTGGCGGCG

mGreenLantern – (T ∨ C) ∧ A

MGSS-CfaC-GGS(x3)-SpyTag-GGS(x3)-TEVc-GGS(x3)-HRV-3Cc-GGS(x3)-mGreenLantern-
GGS(x3)-SpyTag-GGS(x3)-2A9c-GGS(x3)-6xHis-GGS(x3)-CfaN-SsrA

ATGGGAAGTTCAGTAAAAATTATATCTAGGAAGAGCCTGGGCACCCAAAACGTGTACGATATTG
GTGTTGAGAAAGACCACAACTTCCTGCTGAAGAACGGATTGGTTGCGAGCAATTGTTTTAACGG
CGGTTCTGGCGGATCCGGCGGTTCTGCACATATTGTTATGGTTGACGCTTACAAGCCGACGAAA
GGTGGCTCTGGCGGTAGCGGTGGCTCTGAAAACCTGTACTTCCAGAGCGGAGGTTCTGGTGGTT
CCGGTGGCAGCTTAGAGGTGTTGTTTCAAGGTCCGGGTGGTTCCGGCGGTAGCGGGGGTAGCGT
GAGCAAGGGCGAAGAGCTGTTCACCGGTGTTGTTCCGATCCTGGTCGAGCTGGACGGTGACGTT
AACGGTCACAAATTTAGCGTCCGTGGTGAAGGTGAGGGTGACGCGACCAATGGCAAACTGACCC
TCAAGTTCATCTGCACGACTGGTAAGCTGCCGGTACCGTGGCCAACGTTGGTCACCACCCTTGG
TTATGGTGTGGCCTGCTTCGCCCGTTATCCGGATCACATGAAACAGCATGATTTTTTTAAGAGC
GCTATGCCGGAAGGTTATGTTCAAGAGCGCACCATCAGCTTTAAGGACGACGGCACCTATAAGA
CCCGTGCAGAGGTGAAATTCGAGGGCGACACCCTGGTGAACCGTATTGTTTTGAAGGGCATCGA
CTTCAAAGAAGATGGTAATATTCTGGGTCATAAATTGGAATACAATTTCAACAGCCACAAGGTG
TACATTACCGCGGATAAACAAAAAAACGGCATCAAGGCTAATTTCAAAACCCGTCATAACGTTG
AGGACGGTGGGGTGCAACTGGCCGATCACTATCAGCAGAACACCCCGATTGGTGACGGCCCAGT
TTTGTTGCCGGATAACCATTACCTGAGCCACCAGAGCAAACTCAGCAAGGACCCGAATGAAAAA

CGTGATCACATGGTGCTGAAGGAGCGCGTGACTGCGGCTGGTATCACCCATGATATGGATGAAC
TGTATAAGGGCGGGTCGGGCGGTAGTGGCGGTTCCGCGCATATCGTCATGGTTGATGCGTATAA
ACCGACCAAAGGTGGGTCCGGCGGTTCCGGCGGCTCGCTGGCGGAGACCGGTGGCGGTTCAGGC
GGCAGCGGTGGTAGCCACCACCACCACCACCATGGAGGTAGCGGCGGGTCTGGCGGCTCGGCGG
AATACTGCCTCTCCTATGATACGGAAATTTTAACCGTGGAGTACGGCTTTCTGCCGATTGGCAA
GATCGTTGAGGAACGCATTGAATGTACCGTTTACACTGTCGATAAAAACGGTTTCGTGTACACG
CAACCGATCGCTCAGTGGCATAACCGCGGTGAGCAGGAGGTATTTGAATACTGCCTGGAAGATG
GCAGCATTATCCGTGCGACCAAGGACCACAAATTCATGACCACAGATGGTCAGATGCTGCCGAT
CGACGAGATCTTTGAAAGAGGCCTGGACCTGAAGCAGGTTGACGGCCTGCCTGCGGCGAATGAT
GAGAACTATGCACTGGCAGCT

(AND) OR Gates

mGreenLantern – (A ∧ T) ∨ C

MGSS-SnoopTag-GGS(x3)-2A9c-GGS(x3)-mGreenLantern-GGS(x3)-SpyTag-GGS(x3)-TEVc-GGS(x3)-SnoopCatcher- GGS(x3)-HRV-3Cc-GGS(x3)-SpyTag-GGS(x3)-6xHis

ATGGGAAGTTCAAAACTAGGGGATATAGAATTCATCAAAGTGAACAAAGGTGGCTCAGGCGGCT
CTGGCGGTAGCTTGGCGGAAACCGGTGGTGGTAGTGGCGGCAGCGGAGGCAGC
ATGGTTAGCAAGGGTGAGGAACTGTTCACCGGCGTTGTTCCGATCCTGGTCGAGCTGGATGGCG
ACGTTAACGGTCATAAGTTCAGCGTTAGAGGTGAAGGCGAGGGCGACGCGACGAACGGCAAGTT
GACCCTGAAGTTCATCTGCACCACGGGTAAGCTTCCGGTGCCGTGGCCTACCCTGGTGACCACG
CTGGGTTACGGGGTGGCGTGTTTTGCACGTTATCCGGATCACATGAAACAACACGACTTCTTCA
AGTCAGCTATGCCGGAAGGTTATGTTCAAGAACGTACCATTAGCTTTAAGGACGACGGTACCTA
CAAGACCCGCGCGGAAGTGAAATTCGAGGGTGACACCTTGGTTAACCGTATTGTGCTGAAGGGG
ATCGACTTTAAGGAGGACGGGAATATTTTAGGCCACAAATTGGAATATAACTTCAACAGCCACA
AAGTGTATATCACTGCTGACAAACAGAAAAACGGGATCAAAGCTAATTTCAAGACGCGTCATAA
CGTGGAGGATGGTGGTGTTCAGCTCGCGGATCACTACCAACAGAACACCCCGATCGGTGATGGT
CCGGTCCTGCTGCCGGACAATCATTACCTGTCCCACCAGAGCAAATTAAGCAAAGATCCGAATG
AGAAACGTGACCACATGGTACTGAAGGAGCGCGTGACTGCGGCAGGCATTACGCATGATATGGA
TGAACTCTACAAGGGCGGTAGCGGTGGTAGTGGCGGTTCCGCTCACATAGTAATGGTTGATGCA
TATAAACCAACGAAAGGTGGCAGCGGCGGTAGCGGTGGCTCCGAGAACCTCTACTTCCAAAGCG
GCGGTTCTGGCGGCTCAGGCGGATCGAAACCGCTGCGTGGTGCGGTTTTCAGCTTGCAAAAACA
GCATCCGGACTACCCGGACATCTATGGTGCAATTGATCAGAATGGCACCTACCAGAACGTGCGC
ACCGGTGAAGATGGTAAGCTGACCTTTAAAAACCTGAGCGACGGCAAGTATCGTCTGTTCGAGA
ACAGCGAGCCGGCAGGTTACAAACCGGTTCAGAACAAGCCGATCGTGGCGTTTCAAATTGTCAA
TGGTGAGGTTCGTGATGTTACCAGCATTGTGCCGCAGGACATCCCGGCTACCTACGAATTTACG
AACGGCAAGCATTATATCACCAATGAACCGATCCCGCCTAAAGGTGGTAGTGGTGGCAGCGGTG
GCTCCTTGGAAGTGCTGTTCCAAGGTCCGGGTGGGTCCGGGGGCAGCGGAGGCTCTGCCCATAT
TGTCATGGTTGATGCGTATAAGCCGACTAAGGGTGGTTCTGGCGGTTCCGGTGGCAGCCATCAC
CACCACCACCAC

mGreenLantern – (A ∧ C) ∨ T

MGSS-SnoopTag-GGS(x3)-2A9c-GGS(x3)-mGreenLantern-GGS(x3)-SpyTag-GGS(x3)-HRV-3Cc-GGS(x3)-SnoopCatcher- GGS(x3)-TEVc-GGS(x3)-SpyTag-GGS(x3)-6xHis

ATGGGAAGTTCAAAACTAGGGGATATAGAATTCATCAAAGTGAACAAAGGTGGCTCAGGCGGCT
CTGGCGGTAGCTTGGCGGAAACCGGTGGTGGTAGTGGCGGCAGCGGAGGCAGCATGGTTAGCAA
GGGTGAGGAACTGTTCACCGGCGTTGTTCCGATCCTGGTCGAGCTGGATGGCGACGTTAACGGT
CATAAGTTCAGCGTTAGAGGTGAAGGCGAGGGCGACGCGACGAACGGCAAGTTGACCCTGAAGT
TCATCTGCACCACGGGTAAGCTTCCGGTGCCGTGGCCTACCCTGGTGACCACGCTGGGTTACGG
GGTGGCGTGTTTTGCACGTTATCCGGATCACATGAAACAACACGACTTCTTCAAGTCAGCTATG
CCGGAAGGTTATGTTCAAGAACGTACCATTAGCTTTAAGGACGACGGTACCTACAAGACCCGCG
CGGAAGTGAAATTCGAGGGTGACACCTTGGTTAACCGTATTGTGCTGAAGGGGATCGACTTTAA
GGAGGACGGGAATATTTTAGGCCACAAATTGGAATATAACTTCAACAGCCACAAAGTGTATATC
ACTGCTGACAAACAGAAAAACGGGATCAAAGCTAATTTCAAGACGCGTCATAACGTGGAGGATG
GTGGTGTTCAGCTCGCGGATCACTACCAACAGAACACCCCGATCGGTGATGGTCCGGTCCTGCT
GCCGGACAATCATTACCTGTCCCACCAGAGCAAATTAAGCAAAGATCCGAATGAGAAACGTGAC
CACATGGTACTGAAGGAGCGCGTGACTGCGGCAGGCATTACGCATGATATGGATGAACTCTACA
AGGGCGGTAGCGGTGGTAGTGGCGGTTCCGCTCACATAGTAATGGTTGATGCATATAAACCAAC
GAAGGGCGGGTCAGGTGGCAGCGGCGGATCTCTGGAAGTGCTGTTCCAAGGTCCGGGTGGCTCT
GGCGGTTCGGGCGGCTCCAAACCGCTGCGTGGCGCGGTGTTTAGCCTGCAGAAACAACATCCGG
ACTACCCAGACATCTATGGTGCAATTGACCAGAATGGAACCTACCAGAACGTGCGCACTGGTGA
GGACGGTAAGTTGACCTTCAAGAACTTGTCGGATGGTAAATATCGTCTGTTTGAAAACAGCGAG
CCGGCTGGTTATAAGCCGGTTCAGAACAAACCGATCGTGGCGTTTCAAATTGTTAATGGCGAAG
TTCGTGATGTTACCAGCATTGTGCCGCAGGATATCCCGGCGACCTACGAGTTCACCAACGGTAA
GCATTACATCACCAATGAACCGATCCCTCCGAAAGGCGGTTCCGGCGGTTCTGGTGGTTCCGAG
AACCTCTACTTCCAATCCGGTGGTAGCGGTGGTAGCGGCGGCAGCGCACATATTGTCATGGTTG
ATGCCTATAAACCGACGAAGGGTGGCAGCGGCGGTAGCGGTGGCAGCCATCACCACCACCACCA
C

mGreenLantern – (T ∧ C) ∨ A

MGSS-SnoopTag-GGS(x3)-TEVc-GGS(x3)-mGreenLantern-GGS(x3)-SpyTag-GGS(x3)-HRV-3Cc-GGS(x3)-SnoopCatcher- GGS(x3)-2A9c-GGS(x3)-SpyTag-GGS(x3)-6xHis

ATGGGATCAAGTAAACTAGGGGATATAGAATTCATTAAGGTGAATAAAGGTGGCAGCGGTGGCT
CCGGCGGCAGCGAGAACCTGTACTTCCAATCTGGTGGGTCCGGCGGCTCCGGTGGTAGTATGGT
TAGCAAGGGCGAGGAACTGTTCACGGGTGTTGTCCCGATCCTGGTCGAGCTTGACGGCGACGTT
AACGGCCACAAGTTCAGCGTGCGTGGTGAGGGCGAGGGTGACGCGACCAATGGCAAGCTGACCC
TCAAGTTCATCTGCACAACCGGTAAACTGCCGGTACCCTGGCCGACCTTGGTTACCACGCTGGG
CTACGGCGTCGCGTGTTTTGCGCGTTATCCGGACCACATGAAGCAGCACGACTTTTTTAAAAGC
GCCATGCCGGAAGGCTACGTGCAAGAACGCACCATTAGCTTTAAGGATGATGGCACCTACAAGA
CCCGTGCAGAAGTTAAATTCGAGGGCGACACCCTGGTGAACCGTATTGTCCTGAAAGGTATCGA
CTTCAAAGAGGACGGCAATATTCTGGGTCATAAGTTGGAGTATAACTTCAACAGCCACAAGGTG
TATATCACCGCGGATAAACAGAAGAACGGCATCAAAGCTAATTTCAAAACTCGCCATAATGTTG
AAGACGGTGGTGTGCAACTGGCTGACCACTATCAGCAGAATACCCCGATCGGTGACGGTCCGGT
TTTGTTGCCTGACAACCATTACCTGTCCCATCAGAGCAAGCTGAGCAAAGATCCGAATGAAAAA
CGTGATCACATGGTCTTAAAAGAGCGTGTTACTGCCGCAGGTATTACCCATGACATGGATGAAC

TGTATAAAGGCGGCAGCGGTGGTTCTGGCGGTTCTGCCCACATTGTTATGGTTGATGCGTACAA
GCCGACCAAAGGTGGCTCTGGTGGATCGGGTGGCAGCCTTGAGGTATTGTTCCAAGGTCCTGGT
GGTAGCGGTGGCAGCGGCGGTTCCAAGCCGCTGAGAGGTGCAGTTTTTAGCTTACAGAAACAAC
ATCCGGATTACCCGGACATCTATGGTGCGATTGATCAGAACGGCACCTACCAGAATGTTCGCAC
CGGTGAGGACGGCAAACTGACGTTTAAAAACCTGTCGGATGGCAAGTATCGTCTGTTTGAAAAC
AGCGAACCGGCGGGTTACAAGCCGGTGCAAAACAAACCGATCGTGGCATTTCAAATTGTGAACG
GTGAGGTGCGCGACGTGACGAGCATTGTGCCACAGGATATCCCGGCTACCTATGAATTTACCAA
CGGCAAACATTACATCACGAACGAGCCGATCCCACCGAAAGGAGGCTCCGGCGGTTCTGGGGGT
TCTCTAGCGGAAACCGGTGGTGGTAGCGGTGGATCGGGTGGTAGCGCGCATATCGTTATGGTGG
ATGCCTACAAGCCGACCAAGGGTGGTTCCGGCGGTAGCGGCGGTTCCCACCATCACCACCACCA
C

OR OR Gate

mGreenLantern – 2A9 ∨ TEV ∨ HRV-3C

MGSS-SpyTag-GGS(x3)-mGreenLantern-GGS(x3)-2A9c-GGS(x3)-TEVc-GGS(x3)-HRV-3Cc-GGS(x3)-SpyTag-GGS(x3)-6xHis

ATGGGAAGTTCAGCTCACATAGTAATGGTTGATGCTTACAAGCCAACGAAAGGAGGTAGCGGCG
GGTCCGGTGGTTCCATGGTTAGCAAGGGTGAAGAACTGTTCACCGGTGTTGTTCCGATTCTGGT
CGAGCTTGACGGCGACGTGAACGGCCACAAGTTCTCTGTTCGTGGTGAGGGTGAGGGTGACGCT
ACCAATGGTAAATTGACCTTGAAGTTCATCTGCACCACTGGTAAACTGCCTGTTCCGTGGCCGA
CGCTCGTGACCACCTTAGGTTATGGTGTCGCGTGTTTTGCCCGTTATCCGGATCACATGAAACA
GCATGACTTTTTTAAAAGCGCTATGCCGGAAGGTTACGTGCAAGAGCGCACCATTTCCTTTAAG
GACGACGGAACCTACAAGACACGCGCAGAAGTCAAATTCGAGGGCGATACCCTGGTGAATCGTA
TTGTCCTGAAAGGCATCGACTTCAAGGAGGACGGAAACATTCTGGGTCATAAGTTAGAGTATAA
CTTCAACAGCCATAAGGTGTATATCACCGCGGATAAACAGAAAAACGGCATTAAAGCAAATTTT
AAGACGCGTCACAACGTGGAAGACGGTGGCGTGCAACTGGCCGATCACTATCAGCAGAATACCC
CGATCGGTGATGGCCCGGTTTTGCTGCCGGATAACCACTACCTGAGCCATCAGAGCAAGCTGAG
CAAAGACCCGAATGAAAAACGTGATCACATGGTTCTGAAAGAGCGCGTTACTGCAGCGGGTATC
ACCCATGACATGGATGAATTGTACAAGGGTGGCTCTGGCGGCTCCGGCGGTTCTCTGGCGGAAA
CCGGTGGTGGTTCCGGCGGTTCCGGTGGATCGGAGAACCTGTACTTCCAAAGCGGTGGTTCTGG
TGGAAGCGGCGGCAGCTTGGAAGTTCTGTTTCAAGGTCCGGGCGGCAGCGGCGGTTCCGGCGGC
AGTGCGCATATCGTGATGGTAGATGCGTACAAGCCGACGAAAGGTGGCTCAGGCGGCTCGGGGG
GCAGCCACCACCATCACCACCAC

Material Backbone

TriCatcher-ELP

MGSS-SpyCatcher003-GGS(x3)-ELP-GGS(x3)-SpyCatcher003-GGS(x3)-ELP-GGS(x3)-SpyCatcher003-GGS(x3)-6xHis

ATGGGAAGTTCAATGGTAACTACACTATCTGGCCTGAGCGGCGAGCAGGGTCCAAGCGGTGATA
TGACCACAGAGGAAGACTCTGCCACTCACATCAAATTTAGCAAACGTGATGAAGACGGCCGTGA
ACTGGCTGGTGCTACCATGGAATTACGTGACTCCAGCGGTAAGACCATCAGCACCTGGATTTCT
GACGGCCATGTTAAGGACTTCTATCTGTATCCGGGCAAATACACCTTTGTTGAAACCGCTGCGC
CGGACGGTTACGAAGTTGCGACTGCGATCACCTTCACTGTGAACGAGCAAGGTCAGGTTACAGT
TAACGGTGAGGCCACGAAGGGTGATGCGCACACCGGTGGTTCGGGTGGTTCGGGTGGCTCCGTT
GGCGTTCCGGGTGTTGGGGTTCCGGGTGTGGGCGTGCCGGGCGAGGGCGTTCCTGGGGTTGGTG
TCCCGGGTGTGGGCGTTCCGGGCGTAGGTGTGCCGGGTGTTGGAGTTCCAGGCGAGGGCGTCCC
GGGCGTTGGCGTGCCGGGCGTCGGTGTCCCAGGGGTTGGCGTGCCGGGCGTGGGTGTACCGGGC
GAGGGAGTGCCGGGTGTGGGCGTGCCGGGGGTAGGCGAGGGCGGCGGTAGCGGCGGTTCTGGTG
GTTCTATGGTTACCACGCTGAGCGGTCTGAGCGGTGAGCAAGGTCCGAGCGGGGACATGACTAC
CGAAGAAGATTCCGCGACGCATATCAAATTCAGCAAGCGCGATGAAGACGGCCGCGAATTGGCG
GGTGCGACGATGGAACTTAGAGACAGCAGCGGCAAGACCATTAGCACCTGGATTAGCGACGGCC
ATGTTAAAGATTTCTATCTGTATCCGGGGAAGTACACGTTCGTGGAAACCGCTGCGCCGGATGG
TTACGAGGTGGCCACCGCGATTACCTTTACCGTCAATGAACAGGGTCAGGTTACCGTTAACGGT
GAGGCAACAAAAGGTGACGCACACACCGGTGGTAGCGGCGGAAGCGGCGGTAGTGTTCCGGGTG
TTGGGGTGCCGGGTGTTGGTGTCCCGGGCGAGGGTGTGCCGGGCGTGGGTGTGCCAGGTGTTGG
TGTGCCGGGCGTTGGTGTGCCAGGCGTGGGAGTGCCGGGTGAGGGTGTGCCGGGTGTCGGCGTG
CCTGGCGTCGGCGTGCCGGGCGTTGGTGTACCGGGTGTCGGAGTGCCGGGCGAGGGTGTGCCGG
GTGTTGGCGTACCGGGCGTTGGTGTTCCGGGCGGCGGCTCCGGTGGCTCTGGCGGTTCCATGGT
TACGACCTTGTCAGGTCTCAGCGGCGAACAAGGACCGAGCGGCGACATGACCACCGAAGAGGAT
AGCGCAACCCACATCAAGTTTTCCAAGCGCGACGAGGACGGACGTGAACTGGCGGGAGCAACGA
TGGAATTGCGTGATAGCAGCGGAAAAACCATTTCTACCTGGATCTCTGATGGCCACGTGAAGGA
TTTCTACCTGTACCCGGGTAAATACACCTTCGTGGAAACGGCGGCGCCTGATGGCTATGAAGTG
GCAACGGCCATCACCTTTACTGTGAATGAGCAGGGCCAAGTGACCGTCAACGGCGAGGCAACCA
AAGGTGATGCGCATACCGGTGGCTCCGGTGGTAGTGGCGGCTCCCATCACCATCACCACCAC

TriCatcher-XTEN

MGSS-SpyCatcher003-GGS(x3)-XTEN-GGS(x3)-SpyCatcher003-GGS(x3)-XTEN-GGS(x3)-SpyCatcher003-GGS(x3)-6xHis

ATGGGAAGTTCAATGGTAACTACACTATCTGGCCTGTCCGGCGAACAAGGTCCATCGGGGGACA
TGACCACCGAGGAAGACTCGGCGACCCACATCAAATTTAGCAAGCGCGACGAAGACGGCCGTGA
ACTTGCCGGTGCCACCATGGAATTGCGCGATAGCAGCGGCAAAACCATCTCCACCTGGATCAGC
GATGGTCACGTAAAAGATTTTTACCTGTATCCGGGCAAATACACCTTTGTTGAAACGGCGGCAC
CGGATGGCTATGAAGTCGCGACTGCGATTACCTTCACCGTCAACGAACAGGGTCAAGTTACCGT
TAATGGTGAAGCAACAAAAGGTGACGCACACACCGGTGGCAGCGGCGGTAGCGGTGGTTCCGGT
TCTCCTGCCGGTTCGCCGACATCTACGGAGGAGGGCACCTCCGAGTCAGCGACGCCGGAAAGCG
GTCCAGGAACGTCTACTGAGCCGAGCGAGGGTAGCGCGCCAGGGAGCCCGGCTGGCTCGCCGAC
GAGCACCGAGGAGGGCACCAGTACCGAGCCGAGCGAGGGTAGCGCTCCTGGCACCTCCACAGAG
CCGTCCGAAGGCTCAGCCCCAGGTACCAGCGAAAGCGCGACTCCGGAGAGCGGTCCGGGCAGTG
AACCGGCGACCTCCGGTAGCGAGACCCCCGGCTCTGAGCCGGCTACCAGCGGTAGTGAGACTCC
GGGATCCCCGGCTGGTAGCCCGACCTCTACCGAGGAAGGTACGTCTGAAAGCGCGACCCCGGAA
TCAGGCCCTGGCACCTCCACTGAGCCGTCTGAAGGTAGCGCGCCGGGTGGCAGCGGTGGTAGCG
GCGGCTCTATGGTGACCACCCTGAGTGGCCTGTCCGGTGAACAGGGTCCGTCGGGAGATATGAC
CACAGAAGAGGACAGCGCGACCCATATTAAATTCAGCAAACGTGACGAAGATGGCAGAGAACTG

GCAGGTGCAACGATGGAACTGCGTGACAGCAGCGGTAAGACGATCAGCACCTGGATTAGCGATG
GTCACGTTAAAGATTTCTACTTATATCCGGGCAAGTACACCTTCGTGGAAACCGCGGCACCGGA
TGGCTACGAAGTCGCCACCGCCATTACCTTTACCGTGAACGAGCAGGGCCAAGTGACCGTGAAC
GGTGAAGCAACGAAGGGCGATGCACATACCGGTGGTAGCGGGGGTTCCGGAGGTAGCGGCACCT
CCACCGAACCGAGTGAGGGCTCCGCGCCGGGTAGCCCGGCAGGCTCCCCGACCAGCACCGAAGA
GGGTACTTCAACAGAGCCGAGCGAGGGTAGCGCTCCAGGCACCTCTACTGAACCGTCTGAGGGC
TCAGCTCCGGGGACGTCAGAGAGCGCGACGCCAGAGAGCGGTCCGGGTACGTCTACCGAGCCGT
CCGAGGGTTCCGCTCCGGGCACCTCCGAATCGGCGACCCCGGAGTCAGGTCCGGGCTCCGAGCC
GGCGACGAGCGGCTCAGAGACACCGGGTACAAGCACGGAGCCGTCCGAGGGTTCTGCGCCCGGT
ACATCTACCGAACCGTCAGAGGGCAGCGCGCCGGGTACCTCTGAGTCTGCGACACCGGAGTCCG
GTCCGGGCACTTCTGAAAGCGCGACCCCAGAAAGCGGTCCGGGCGGCTCTGGAGGTTCGGGTGG
TTCTATGGTTACCACCCTGTCCGGCTTGTCTGGTGAACAAGGCCCTAGCGGCGACATGACCACC
GAGGAAGACAGCGCTACCCATATCAAGTTCAGCAAACGTGATGAAGACGGTCGCGAACTCGCGG
GCGCAACGATGGAACTGCGTGACAGTAGCGGTAAGACGATCAGCACGTGGATTAGCGACGGCCA
CGTGAAGGACTTCTATTTGTACCCGGGTAAGTACACCTTCGTGGAAACGGCTGCCCCAGATGGT
TATGAAGTGGCCACTGCGATCACCTTTACCGTTAATGAACAGGGTCAGGTTACTGTTAACGGTG
AGGCGACCAAGGGTGATGCACATACCGGTGGCTCTGGCGGCTCCGGTGGTAGCCATCATCACCA
CCACCAC

7.1.4. Results

We have so far been able to successfully recombinantly express and purify 16/17 crosslinkers and both backbone sequence variants. These successes are corroborated by both LC-MS (**Figure 7.1**) as well as SDS-PAGE evincing high construct purity.

Moreover, we have identified TriCatcher-ELP as the backbone material of choice for downstream hydrogel studies given its higher expression yields as compared to TriCatcher-XTEN. We have also been able to successfully formulate a gel at a concentration of 10 wt% by reacting TriCatcher-ELP and a (TVC)-cleavable mGreenLantern. Studies are currently underway to verify that the pristine logical response seen in our work on controlled release is faithfully recapitulated in a bulk material degradation context.

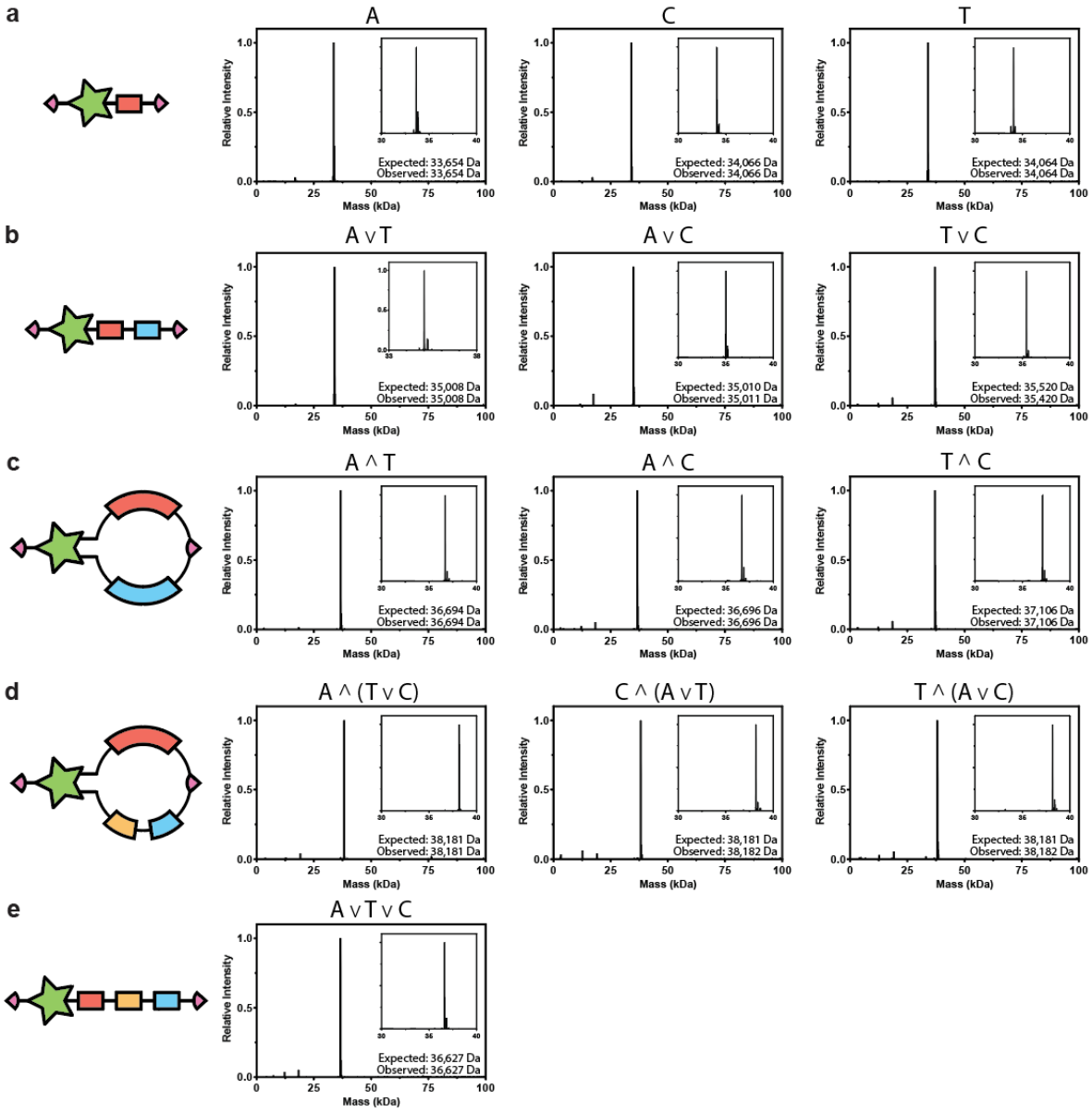

Figure 24. Mass spectrometric validation of logically releasable mGreenLantern crosslinks

a) YES-gated single-input crosslinks.
*b-c) Two-input OR-gated (**b**) and AND-gated (**c**) crosslinks.*
d) Three-input (OR)/AND-gated crosslinks.
e) Three-input OR-OR crosslink.
Plot titles correspond to the protein tether identity.

7.1.5. Future work

Downstream experiments involve an exhaustive validation equivalent to that which we conducted for protein release studies. They also involve a concomitant demonstration of the controlled release of a model therapeutic that is either passively encapsulated in the network or covalently tethered. This work will be continued by Murial L. Ross.

7.2. Deploying Autonomously Compiled Molecular Topologies for the Engineering of Next-Generation Biosensors

7.2.1. Background

A main observation from our work on engineering bespoke protein circuits as logical operators was the relative ease with which we could deploy workhorse organisms such as *E.Coli* to engineer complex architectures. In fact, our method allowed us to construct highly nuanced topologies into diverse categories of proteins (e.g., fluorescent proteins, model enzymes, growth factor, cytokines, therapeutic nanobodies) while requiring minimal purification steps. We looked to expand the scope of molecularly compiled topologies further still by identifying areas where straightforward generation of difficult protein architectures would prove highly advantageous. One such avenue that we deem underserved is that of biosensor engineering. Specifically, we seek to engineer biosensors based on Förster resonance energy transfer (FRET) rapidly and straightforwardly.

Having identified through our previous results that SICLOPPS can reliably cyclize proteins with proximal termini, we hypothesized that this advantage could be exploited to bring two spectrally overlapping fluorescent proteins into proximity with each other, causing a baseline amount of FRET. Their relative distance can then be modulated through sequential proteolytic cleavage events, which would enable us to establish a differential response (**Figure 7.2**).

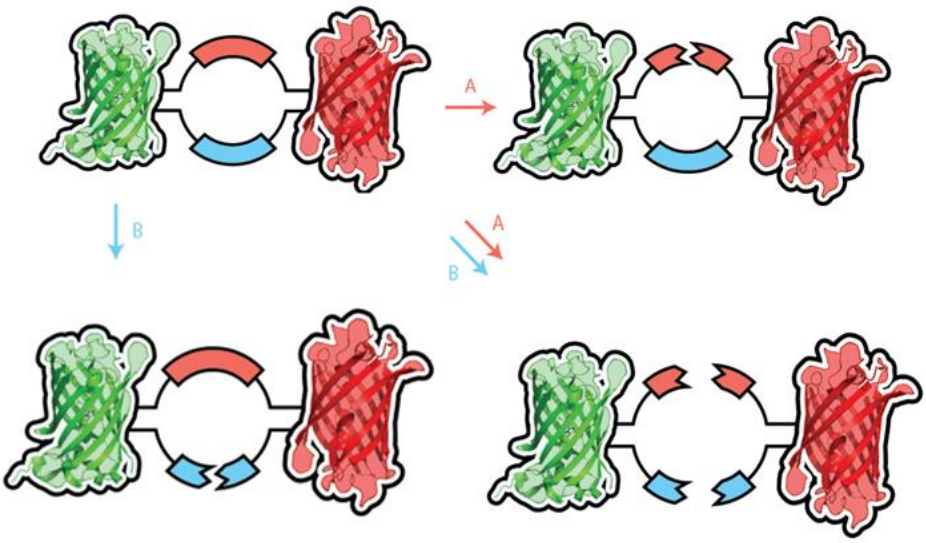

Figure 7.2. FRET reporters can be recombinantly expressed as two fluorescent proteins linked by proteolytic cleavage sequences engineered in parallel.
FRET biosensors can be assembled as AND-type operations wherein the donor and acceptor are engineered to harbor two cleavage sequences in parallel.

7.2.2. Approach

In addition to physical proximity, another design consideration when engineering a FRET module is the identification of proteins that are spectrally overlapping, i.e. the absorption spectrum of the acceptor should overlap with the emission spectrum of the donor. I gravitated towards the following pair: EGFP ($\lambda_{exc.}$= 488 nm, $\lambda_{em.}$= 507 nm) and mScarlet3 ($\lambda_{exc.}$= 569 nm, $\lambda_{em.}$= 592 nm) given recent reports that demonstrate successful FRET biosensor engineering in mammalian cells.

Broadly, our design consists of these two fluorescent proteins that are ligated at their respective termini with GS repeats through SICLOPPS, with two proteolytic recognition sequences (A and T) encoded into the linkers. Given the positioning of the cut sites, our reported design is

effectively an “AND”-gated operation. In its purified state, EGFP and mScarlet3 are in close proximity owing to intein *trans*-splicing and subsequent cyclization. Upon the introduction of either protease (A or T), we predict the macro-structure to be linearized but still present some quantifiable FRET signal in spite of the increased distance between EGFP and mScarlet3. Upon the introduction of both proteases together (A and T), we expect the two fluorescent proteins to be completely released from each other, leading to complete loss of the FRET signal. The ORF for the preliminary sequence that I designed is given in the **Methods** section below.

7.2.3. Results

The putative biosensor construct was purified successfully through IMAC and an additional round of SEC. This was corroborated by both LC-MS and SDS-PAGE (**Figure 7.3.**).

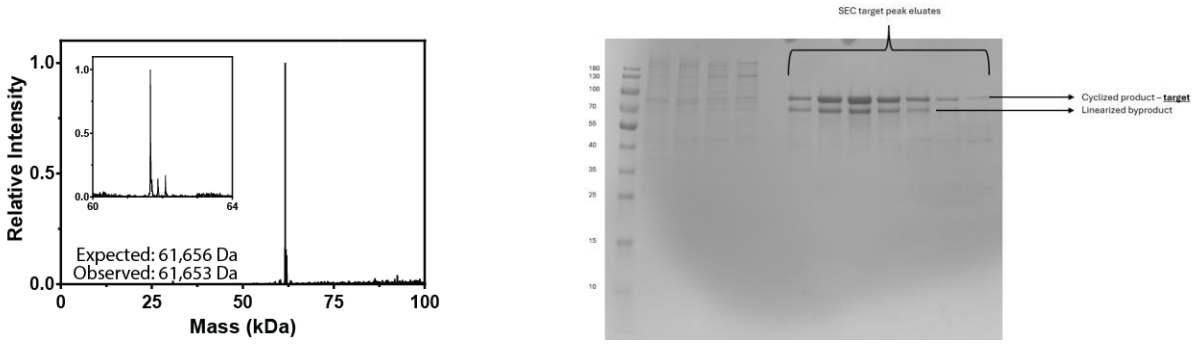

Figure 7.3. Mass spectrometric and SDS-PAGE validation of EGFP-mScarlet3 (A∧T). *FRET biosensors, designed as AND-type logical operations, can be autonomously compiled from single expression frames.*

Upon administration of an exhaustive suite of inputs to validate the design, we obtained molecular signatures consistent with stepwise control over fluorescent protein proximity (**Figure 7.4**). This validates that our approach holds translational promise, as more complex proteolytic

signatures can now be engineered into FRET biosensor designs in order to afford a portable method for the early detection of different disease states.

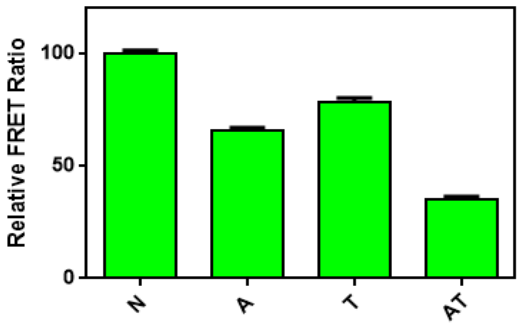

Figure 7.4. FRET can be modulated based on the type / number of inputs. *Introducing single inputs ({A}, {T}) leads to a linearized construct that separates the two fluorescent proteins relative to their starting conformation, leading to less total FRET. Introduction of both inputs together fully cleaves both linkers, leading to near-abrogation of FRET relative to the starting amount.*

7.2.3. Methods

MGSS-CfaC-GGS(x5)-EGFP-GGS(x5)-2A9c-GGS(x5)-mScarlet3-GGS(x5)-TEVc-GGS(x5)-6xHis-GGS(x5)-CfaN-SsrA

ATGGGAAGTTCAGTAAAAATTATATCTAGGAAGAGTCTGGGTACGCAAAACGTTTACGACATCG
GGGTCGAGAAGGACCACAACTTCCTGCTGAAGAACGGCCTGGTCGCGAGCAACTGCTTCAACGG
TGGTTCGGGTGGTAGCGGTGGTTCCGGTGGTAGCGGCGGTTCCATGGTGAGCAAGGGTGAGGAG
CTGTTTACCGGTGTGGTGCCGATCCTGGTCGAGCTGGATGGCGATGTTAACGGCCACAAATTCT
CCGTGAGCGGTGAGGGCGAAGGTGATGCAACGTACGGCAAACTCACCCTCAAGTTCATTTGTAC
CACCGGCAAACTGCCGGTTCCGTGGCCGACTCTGGTCACCACATTGACTTATGGTGTTCAATGT
TTTAGTCGTTATCCAGACCACATGAAACAGCATGATTTCTTCAAGAGCGCTATGCCGGAAGGTT
ATGTTCAAGAACGTACCATTTTTTTCAAAGATGATGGTAATTACAAGACCCGTGCTGAGGTGAA
GTTCGAGGGCGACACCTTGGTCAACCGCATCGAACTGAAGGGCATCGACTTCAAGGAGGACGGC
AACATCCTGGGTCATAAGTTAGAGTACAACTACAATAGCCATAACGTGTACATCATGGCGGACA
AGCAAAAAAATGGCATCAAAGTTAACTTCAAGATCCGCCATAACATTGAGGACGGTAGTGTCCA
ACTGGCGGACCACTATCAGCAAAATACCCCGATCGGCGACGGCCCAGTGTTGCTCCCAGATAAT
CATTACCTGAGCACGCAGTCAGCCTTGAGCAAAGACCCGAATGAAAAACGTGATCACATGGTTC
TCTTGGAGTTCGTGACTGCGGCCGGTATTACCTTGGGCATGGATGAATTATATAAAGGCGGTTC
GGGCGGAAGCGGTGGCTCTGGCGGTTCAGGTGGTAGCCTGGCGGAGACGGGCGGCGGTAGCGGG

GGTTCCGGCGGCAGCGGGGGTTCCGGCGGCTCGATGGACAGCACCGAAGCAGTTATTAAAGAAT
TCATGCGTTTTAAAGTGCACATGGAAGGTTCAATGAACGGTCATGAATTCGAGATCGAGGGTGA
AGGTGAGGGTAGACCTTATGAAGGTACACAGACCGCTAAACTGCGCGTTACCAAGGGGGGTCCG
CTGCCGTTCAGCTGGGATATCCTAAGCCCGCAGTTTATGTATGGTTCTCGTGCGTTTACCAAAC
ATCCGGCAGATATCCCGGACTATTGGAAACAGAGCTTTCCGGAGGGCTTCAAGTGGGAACGCGT
GATGAATTTTGAGGACGGCGGTGCGGTGTCCGTGGCCCAGGATACGAGCCTTGAGGACGGTACT
CTAATTTATAAGGTGAAACTTAGAGGTACGAACTTCCCGCCTGATGGTCCGGTTATGCAGAAGA
AAACCATGGGTTGGGAAGCGTCCACTGAGCGTCTGTACCCGGAAGACGTGGTACTGAAGGGCGA
CATCAAGATGGCGCTGCGCCTGAAAGACGGCGGACGTTACCTGGCGGACTTTAAGACCACGTAT
CGTGCGAAAAAACCGGTGCAAATGCCGGGTGCATTTAATATTGATCGTAAACTTGACATTACTA
GCCACAACGAAGACTACACGGTTGTCGAGCAGTATGAACGTAGCGTAGCCCGTCATAGCACCGG
TGGCTCCGGCGGCTCTGGGGGCTCTGGTGGTAGCGGCGGTAGCGGTGGTTCCGGCGGTTCTGAA
AACCTGTATTTCCAGTCGGGCGGGTCCGGTGGCTCTGGTGGTAGCGGCGGGAGCGGGGGTAGCC
ATCACCACCACCACCACGGCGGCTCCGGCGGCTCTGGTGGTAGCGGCGGTTCCGGCGGCTCTGC
GGAATACTGCTTGAGCTATGATACCGAAATTCTGACCGTGGAATACGGTTTCCTGCCGATCGGT
AAAATTGTTGAGGAACGCATTGAGTGCACCGTTTACACCGTTGATAAAAACGGCTTTGTTTACA
CCCAACCGATCGCCCAATGGCACAATCGTGGTGAACAGGAGGTTTTTGAGTACTGCTTGGAGGA
CGGCAGCATCATTCGTGCGACGAAGGACCACAAATTTATGACCACCGATGGTCAGATGCTGCCG
ATCGACGAGATCTTTGAACGCGGTCTGGATCTGAAGCAGGTTGACGGGTTGCCGGCTGCTAATG
ATGAGAACTACGCACTGGCAGCC

7.2.4. Potential pitfalls

The likelihood of success for this design is largely dependent on the purity of the starting construct. However, we detected the formation of a linearized byproduct (approx.. 20%), i.e. product that underwent N- and C-terminal cleavages rather than intein *trans*-splicing (**Figure 7.3**). The presence of such a byproduct may lead to a confounding result, such that one of the proteolytic treatments leads to consistently significantly less total FRET than the other owing to the higher proportion of linear material. While no final conclusions can be made until reliable testing data are produced, a relatively easy workaround should this design fail is the adoption of a Tag/Catcher platform for the cyclization of this biosensor rather than SICLOPPS. Tag/Catcher chemistries have resulted in quantitative cyclization yields in our hands; their main disadvantage, however, relative to the adoption of inteins, is the bulky fragment that is left behind on the final

construct which is likely to result in some distance between the two fluorescent proteins and may obviate FRET detection.

CHAPTER 8: FUTURE DIRECTIONS IN SMART BIOMATERIALS

Throughout this document, I have presented different advances made in the engineering of next-generation biomaterials, all of which adopt chemical biology as framework of choice. Specifically, in **Chapter 1**, I reviewed developments in the engineering of next-generation hydrogel biomaterials, with emphasis placed on the promise of reaction platforms derived from chemical biology. **Chapter 2** drew parallels between synthetic biology on the one hand and biomaterial science on the other; I take this analogy as a springboard to inspire discussion into the engineering of biomaterials that are endowed with true biocomputational promise. In **Chapter 4**, I presented a generalizable semisynthesis-based approach for the engineering of N-terminally functionalized proteins in a single step. Later, in **Chapters 5-7**, I discussed different facets of our autonomous molecular compilation-based strategy. Specifically, **Chapter 5** covered the recombinant expression of bespoke topologies – corresponding to complex logical operations – geared towards biomolecule release from hydrogel networks and other solid supports. **Chapter 6** went over the extension of this strategy to a diverse palette of bioactive protein cargos and to a broader set of inputs. Lastly, **Chapter 7** discussed future frontiers for this autonomous compilation thrust, with emphasis placed on the engineering of bespoke topologies as crosslinks for the engineering of biomaterials capable of programmable network degradation, as well as the demonstration of a facile strategy for the engineering of next-generation biosensors.

Overall, this thesis showcases the promise of chemical biology-derived tools for the engineering of next-generation biomaterials and biohybrid constructs. I believe these efforts will inform and inspire future work that deploys a number of these motifs in tandem toward the development of

ever-more sophisticated biomaterials that are straightforwardly assembled and compiled, evince true translational promise, and remain portable between different laboratory settings.